

Georg-August-Universität Göttingen
INSTITUT FÜR NUMERISCHE UND ANGEWANDTE MATHEMATIK

**Stabilized Finite Element Methods for Coupled
Incompressible Flow Problems**

Dissertation
zur Erlangung des
mathematisch-naturwissenschaftlichen Doktorgrades
“Doctor rerum naturalium”
an der Georg-August-Universität Göttingen

im Promotionsprogramm Mathematik
der Georg-August University School of Science (GAUSS)

vorgelegt von
Daniel Arndt
aus
Hildesheim

Göttingen, 2015

Betreuungsausschuss

- Prof. Dr. Gert Lube,
Institut für Numerische und Angewandte Mathematik,
Georg-August-Universität Göttingen
- Prof. Dr. rer. nat. Dr.-Ing. habil Andreas Dillmann,
Institut für Aerodynamik und Strömungstechnik,
Deutsches Zentrum für Luft- und Raumfahrt

Prüfungskommission

- Referent:
Prof. Dr. Gert Lube,
Institut für Numerische und Angewandte Mathematik,
Georg-August-Universität Göttingen
- Korreferent:
Prof. Dr. rer. nat. Dr.-Ing. habil Andreas Dillmann,
Institut für Aerodynamik und Strömungstechnik,
Deutsches Zentrum für Luft- und Raumfahrt
- Externer Gutachter:
Prof. Dr. Guido Kanschat,
Interdisziplinäres Zentrum für Wissenschaftliches Rechnen,
Ruprecht-Karls-Universität Heidelberg

Weitere Mitglieder der Prüfungskommission:

- Prof. Dr. Andreas Tilgner,
Institut für Geophysik,
Georg-August-Universität Göttingen
- Prof. Dr. Anja Sturm,
Institut für Mathematische Stochastik,
Georg-August-Universität Göttingen
- Prof. Dr. Max Wardetzky,
Institut für Numerische und Angewandte Mathematik,
Georg-August-Universität Göttingen
- Prof. Dr. Ingo Witt,
Mathematisches Institut,
Georg-August-Universität Göttingen

Tag der mündlichen Prüfung: 19.01.2016

Acknowledgements

First and for most, I would like to thank my supervisor Prof. Dr. Gert Lube for his continuous and unexhaustible support throughout the preparation of this thesis. He encouraged my interest in numerical mathematics from the beginning of my studies and takes a great share in my interest in Computational Fluid Dynamics. He always took the time for helpful discussions and has always been a source of motivation. I can hardly imagine a better supervisor.

Further thanks go to Prof. Dr. rer. nat. Dr.-Ing. habil Andreas Dillmann who supported me as co-advisor and co-referee in my thesis.

I want to thank Dr. Helene Dallmann for the great collaboration in the past few years. Sharing the office with her resulted in a good working atmosphere and many insightful discussions on various topics.

I am also thankful for the collaboration with Dr. Benjamin Wacker and his willingness to proof-read parts of this document.

Furthermore, I want to thank all the members of the workgroup “Discrete Differential Geometry” for sharing insights in many other research topics and in life in general during the lunch breaks. Special consideration deserves Andrew Sageman-Furnas for his support in the final phase of this project and proof-reading parts of this thesis.

For the financial support I would like to thank the “CRC 963 Astrophysical Flow Instabilities and Turbulence”, the Cusanuswerk and the Institute for Numerical and Applied Mathematics.

Furthermore, I thank Dr.-Ing. Markus Rütten for the opportunity to use the SCART cluster of the DLR in Göttingen for conducting various of the numerical simulations presented in this document.

Finally, I would like to express my gratitude to all my friends for all the helpful distraction when it was needed and for the great support in many aspects. I am deeply grateful for my parents who were always there for me throughout my studies and the PhD program. Without their support this thesis would not have been possible.

Contents

1	Introduction	1
1.1	Outline	2
1.2	Overview of Publications and Contributions	3
2	Mathematical Model	7
2.1	Description of the Problem	7
2.1.1	Non-Isothermal Flow	7
2.1.2	Electrically Conducting Fluids	8
2.1.3	The Full Model	9
2.2	Weak Formulation	11
2.3	Discretization	12
2.4	Finite Element Spaces	14
2.5	Stabilization and Assumptions	15
2.5.1	Local Projection Stabilization	15
2.5.2	Interpolation	18
3	Semi-Discrete Error Estimates	21
3.1	The Oseen and the Navier-Stokes Problem	21
3.1.1	Stability	22
3.1.2	Quasi-Optimal Error Estimates	23
3.2	Directional Do-Nothing Boundary Conditions	29
3.2.1	Description of the Model	29
3.2.2	Stability	30
3.2.3	Error Estimates	31
3.3	Non-Isothermal Flow	32
3.3.1	Stability	32
3.3.2	Quasi-Optimal Semi-Discrete Error Estimates	33
3.3.3	Parameter Choice	36
3.4	Incompressible Resistive Magnetohydrodynamics	37
3.4.1	Stability	38
3.4.2	Quasi-Optimal Error Estimates	40

3.5	Summary	44
4	Error Estimates for the Fully Discretized Equations	47
4.1	Description of the Time Discretization	47
4.2	On the Regularity of the Maxwell Problem	50
4.3	Stability Estimates	52
4.4	Estimates of the Discretization Errors	57
4.4.1	The Momentum Equation	57
4.4.2	The Fourier Equation	61
4.4.3	The Induction Equation	63
4.4.4	Summary	68
4.5	Convergence Results	70
5	Numerical Results	83
5.1	Isothermal Insulating Flow	84
5.1.1	The No-Flow Problem	84
5.1.2	Outflow Boundary Conditions	86
5.1.3	Time Discretization	88
5.1.4	Flow Over a Horizontal Plate	91
5.1.5	Taylor-Green Vortex	95
5.1.6	Rotating Poiseuille Flow	97
5.2	Non-Isothermal Insulating Flow	100
5.2.1	Traveling Wave	100
5.2.2	Rayleigh-Bénard Convection	102
5.3	Isothermal Electrically Conducting Flow	107
5.3.1	Singular Solution	109
5.3.2	Magnetic Field Expulsion	110
5.4	Non-Isothermal Electrically Conducting Flow	116
6	Discussion and Conclusions	119
6.1	Discussion of the Analytical Results	119
6.2	Discussion of the Numerical Results	122
6.3	Conclusions	124
6.4	Outlook	125
	Bibliography	127

1 Introduction

Due to the ubiquity of fluids, the simulations of flow problem is of great importance in many applications: Examples include the design process of new aircraft or cars, simulations of air flow in the interior of buildings, simulation of the natural convection in the earth's mantle, simulation of fusion reactors or understanding the dynamo effect in astrophysical bodies. The simulation of all these phenomena in experiments is often very complicated and expensive. Hence, there is an increasing desire to perform numerical simulations be it to complement the experiments or to replace them.

The goal of Computational Fluid Dynamics is the derivation of proper mathematical modeling and the efficient implementation of the derived algorithms. From a mathematical point of view the description of flow problems is based on the Navier-Stokes equations. Finding a proper discretization of these equations is subject to research and exhibits many difficulties. Due to the fact that physical phenomena occur on many different scales all of these have to be considered to obtain sensible solutions. Resolving all scales is in most cases by far too expensive, especially when turbulence comes into play. Therefore the behavior on small scales has to be modeled. Apart from that also other difficulties arise in a finite element simulation. With vanishing viscosity, i.e. dominating convection, control over mass conservation is lost and this as well as internal shear or boundary layers lead to unphysical oscillations in the solution.

To account for that using feasible computational costs various stabilization techniques have been considered. Unfortunately, there is no approach that leads to accurate, efficient and robust results for all problems and applications.

In this thesis, a finite element discretization of the incompressible Navier-Stokes equations for a non-isothermal and electrically conducting fluid in a possibly rotating frame of reference is considered. In order to account for instabilities and to diminish unphysical oscillations a stabilization for the incompressibility constraint as well as a local projection approach for various terms is considered. Within this model the goal is to derive parameter bounds and suitable ansatz spaces such that quasi-optimality and semi-robustness of the resulting method can be shown both analytically and numerically. Furthermore, the efficient implementation of the numerical solver is considered.

1.1 Outline

In Chapter 2 the mathematical model used throughout this thesis is given. After stating and describing the equations that govern the fluid behavior in the considered physical model in Section 2.1, a suitable variational form is derived in Section 2.2. Afterwards, the finite element semi-discretization in space in combination with the stabilizations is introduced and all the assumptions that are used throughout this thesis with respect to ansatz spaces are stated in Sections 2.3-2.5.

Chapter 3 is devoted to the investigation of the semi-discrete problems. The analytical results in this section originate from the publications this thesis is based on. In Section 3.1 first the model without any coupling quantities is considered. First, stability considerations give the existence and uniqueness of the discrete solutions. Afterwards, the convergence behavior for various choices of inf-sup stable ansatz pairs is considered. In particular, a suitable choice of parameter bounds is derived and it is shown how a local mesh width restriction can be avoided. In Section 3.2 it is investigated how the results can be transferred to the case of different boundary conditions. In particular, an outflow boundary condition that gives stability for the discrete solution is considered. Section 3.3 is devoted to non-isothermal flow. In particular, we consider how the estimates due to the coupling of the Navier-Stokes equations with the Fourier equation for the temperature changes. Compared to the observations in 3.1 another approach to circumvent a mesh size restriction is introduced. Finally, in Section 3.4, the combination of the Navier-Stokes equations with the induction equation for electrically conducting fluids is investigated. For a stationary and linearized model stability and convergence results are given. Opposed to standard approaches, the performed analysis is not restricted to curl conforming ansatz spaces but allows for nodal-based approaches. In comparison to the previous sections, also the case of solution with reduced regularity is considered. For this case as well as for the case of sufficiently regular continuous solutions, suitable parameter bounds are investigated.

Chapter 4 aims to combine all the results for the semi-discretized equations into the consideration of the fully discretized and fully coupled model. For the time-discretization a pressure-correction splitting scheme based on BDF2 is considered. In particular, we try to extend results for the fully discretized Navier-Stokes equations to non-isothermal and electrically conducting fluids. In comparison to the semi-discretization for the induction equation, a slightly different stabilization approach that requires sufficient regularity is chosen and justified in Section 4.2. After stability considerations for the proposed algorithm in Section 4.3, the discretization errors for all steps in the approach are estimated and finally combined in Section 4.4. These results are used to obtain convergence of the

full algorithm in Section 4.5 where also suitable parameter choices and restrictions with respect to the mesh size width and the time step are stated.

Chapter 5 is devoted to the numerical investigation of the full algorithm for flow that might be non-isothermal or electrically conducting in a possibly rotating frame of reference. This Chapter is a combination of results that were obtained in previous publications and some new extensions with respect to more complex flow behavior. With respect to the structure, in Section 5.1 first non-isothermal and electrically insulating fluids are considered. After validating the theoretical convergence results with respect to spatial temporal discretization, the influence of the stabilization model for boundary layer flow and turbulent flow is considered. In particular, it is examined if a combined model of grad-div stabilization and LPS-SU can serve as an implicit turbulence model. In Section 5.2 non-isothermal fluids are investigated. After the theoretical rates of convergence are confirmed in a first example, Rayleigh-Bénard convection is considered both with respect to a rotating and non-rotating boundary and in a parameter regime from laminar to transient and possibly turbulent flow. Section 5.3 is dedicated to electrically conducting flow. In two examples, the difference in the stabilization parameter design for a sufficiently regular continuous solution and a continuous solution with reduced regularity is investigated. Finally, in Section 5.4 the scaling behavior of the fully coupled algorithm is examined.

1.2 Overview of Publications and Contributions

The present thesis is based on the following publications:

- [ABL15] D. Arndt, M. Braack, and G. Lube, “Finite elements for the Navier-Stokes problem with outflow condition”, in *Proceedings ENUMATH 2015*, submitted, 2015.
- [AD15] D. Arndt and H. Dallmann, “Error Estimates for the Fully Discretized Incompressible Navier-Stokes Problem with LPS Stabilization”, Institute for Numerical and Applied Mathematics, Tech. Rep., 2015, Nr. 2015-08.
- [ADL15a] D. Arndt, H. Dallmann, and G. Lube, “Local projection FEM stabilization for the time-dependent incompressible Navier–Stokes problem”, *Numerical Methods for Partial Differential Equations*, vol. 31, no. 4, pp. 1224–1250, 2015.
- [ADL15b] —, “Quasi-Optimal Error Estimates for the Fully Discretized Stabilized Incompressible Navier-Stokes Problem”, *ESAIM: Mathematical Modelling and Numerical Analysis*, 2015, under review.

- [AL15] D. Arndt and G. Lube, “FEM with Local Projection Stabilization for Incompressible Flows in Rotating Frames”, NAM-Preprint, 2015.
- [DA15] H. Dallmann and D. Arndt, “Stabilized Finite Element Methods for the Oberbeck-Boussinesq Model”, *Journal of Scientific Computing*, 2015, in revision.
- [DAL15] H. Dallmann, D. Arndt, and G. Lube, “Local projection stabilization for the Oseen problem”, *IMA Journal of Numerical Analysis*, 2015. DOI: [10.1093/imanum/drv032](https://doi.org/10.1093/imanum/drv032).
- [LAD15] G. Lube, D. Arndt, and H. Dallmann, “Understanding the limits of inf-sup stable Galerkin-FEM for incompressible flows”, in *Boundary and Interior Layers, Computational and Asymptotic Methods - BAIL 2014*, P. Knobloch, Ed., ser. Lecture Notes in Computational Science and Engineering, vol. 108, Springer International Publishing, 2015. DOI: [10.1007/978-3-319-25727-3](https://doi.org/10.1007/978-3-319-25727-3).
- [WAL15] B. Wacker, D. Arndt, and G. Lube, “Nodal-based Finite Element Methods with Local Projection Stabilization for Linearized Incompressible Magneto-hydrodynamics”, *Computer Methods in Applied Mechanics and Engineering*, 2015, accepted for publication. DOI: [10.1016/j.cma.2016.01.004](https://doi.org/10.1016/j.cma.2016.01.004).

The goal of the present work has been to analytically and numerically analyze the discretized Navier-Stokes equations for a non-isothermal, electrically conducting fluid in a rotating frame of reference with as few stabilizations as possible. In particular, we considered the suitability of the pressure-correction method for the time-discretization and an efficient implementation of the scheme.

We started in [DAL15] with a semi-discretized analysis for the time-dependent Oseen problem improving results by Matthies/Tobiska in [MT15]. In particular, we were able to state (quasi-optimal) error estimates that do not depend on the Reynolds number explicitly. Local mesh size restrictions could be removed when considering a compatibility condition between fine and coarse spaces.

These results were transferred to the nonlinear Navier-Stokes equations in [ADL15a]. Carefully estimating the convective term, we were able to obtain the same quasi-optimal estimates as for the Oseen case. Numerical examples supported the theory that grad-div stabilization alone is able to remove unphysical oscillations for a wide range of Reynolds numbers.

The recent observations for the Stokes, the Oseen and the Navier-Stokes problem were summarized in [LAD15] with major contribution for the numerical analysis by Gert Lube. In this work we first considered the scalability of the implemented pressure-correction based solver.

In [ABL15] we were then able to combine considerations of Braack et al. for outflow boundary conditions [BMZ14] with our results for the stabilized Navier-Stokes equations with homogeneous boundary conditions. It turned out that apart from a different Gronwall constant the results remain the same. This modification breaks the semi-robustness of the estimate although numerically no such problems have been observed.

Next, we considered non-isothermal flow based on the previous experience with isothermal flow in [DA15] using the Oberbeck-Boussinesq model. The analytical part of this work is based on Helene Dallmann's PhD thesis [Dal15]. In summary, we encountered no major difficulties while extending the numerical analysis. For the numerical part we mainly considered Rayleigh-Bénard convection and were able to approximate DNS results for the Nusselt number with minimal stabilization. In particular, we extended the numerical experiments from [Dal15] to show that even the scaling of the boundary layers is simulated correctly and that we can reproduce the Nusselt number results for a DNS simulation with a hundred times fewer degrees of freedom.

For the case of an electrically conducting (but isothermal) fluid we considered a stationary and linearized model mode in [WAL15]. This work is based on Benjamin Wacker's PhD thesis [Wac15]. The circumstance that the magnetic field might have less regularity in comparison to the velocity and the kinematic pressure posed some difficulties here. Nevertheless, the suggested parameter design for velocity and kinematic pressure remains the same. Just for the induction equation we needed to include stabilization for the magnetic pseudo-pressure and were restricted to a much weaker control for the incompressibility constraint similar to the parameter design suggested by Badia and Codina [BC12].

With respect to time discretization and implementation, a fully coupled solver for Navier-Stokes simulations proved to be too less robust and to have unacceptable CPU times, mostly for Large-Eddy simulations of weakly turbulent flows. Due to these reasons, the author implemented a massively parallel solver based on a pressure-correction splitting algorithm that decouples all considered quantities. For the analysis we first considered the Navier-Stokes case for a non-isothermal, electrically non-conducting fluid. Preliminary considerations in [ABL15] show how to extend the semi-discrete estimates to fully discretized ones. Unfortunately, it turned out that both this way and by first discretizing in

time and then in space lead to suboptimal results and severe restrictions on mesh size and time step size.

Based on an approach by Guermond in [Gue99], we considered in [ADL15b] a discretization in space and time at the same time without any intermediate steps. This way semi-robust and quasi-optimal estimates both with respect to spatial and temporal discretization can be proven. In particular, there is essentially no time step size restriction with respect to error estimates in the energy norm.

In [AL15] we observe that these results extend to the case of a rotating frame of reference. The additional Coriolis term and its stabilization pose no further problems.

This dissertation now combines the semi-discrete results with respect to non-isothermal and electrically conducting flow with the results for the fully discretized Navier-Stokes equations in a (possibly) rotating frame of reference. In the following, this model is investigated both numerically and analytically. Furthermore, the efficient implementation of the approach has been a major part of this thesis and is considered in one numerical example.

During the preparation of this thesis various contributions to the finite element library `deal.II`, on which the implementation is based, have been made. Besides the introduction of bubble enriched finite elements, in particular periodic boundary condition on distributed meshes has been considered and resulted in a joint work with Matthias Maier in the tutorial program `step-45` [AM15].

2 Mathematical Model

This chapter is devoted to the mathematical framework we want to consider throughout this thesis. First, a mathematical description of the model for a nonisothermal and electrically conducting fluid in a rotating frame of reference is given. Then we derive a weak formulation from it and motivate the choice of stabilization terms in the discretization. Finally, we state the assumptions on the ansatz spaces that we make throughout this thesis.

2.1 Description of the Problem

The description of the model is divided in three parts: We first state the model that we are going to use for non-isothermal flow. Afterwards we shortly consider the form that is used for the Maxwell equations. Finally, we state the combined form that we will investigate throughout this thesis.

2.1.1 Non-Isothermal Flow

In [FN09] the general Navier-Stokes-Fourier model is described:

Non-isothermal flow for Newtonian fluids in an inertial frame of reference can be described by:

- The continuity equation $\partial_t \varrho + \nabla \cdot (\varrho \mathbf{u}) = 0,$
- the momentum equation $\partial_t (\varrho \mathbf{u}) + \nabla \cdot (\varrho \mathbf{u} \otimes \mathbf{u}) + \nabla \cdot p = \nabla \cdot \mathbb{S} + \mathbf{f},$
- the entropy balance $\partial_t (\varrho s) + \nabla \cdot (\varrho s \mathbf{u}) - \kappa \nabla \cdot \frac{\nabla \vartheta}{\vartheta} = \sigma + \varrho \frac{Q}{\vartheta},$
- the total energy balance $\frac{d}{dt} \int_{\Omega} (\varrho |\mathbf{u}|^2 + \varrho e) dx = \int_{\Omega} (\varrho \mathbf{f} \cdot \mathbf{u} + \varrho Q) dx,$
- Gibbs' equation $\vartheta Ds = De + pD \left(\frac{1}{\rho} \right).$

where

$$\mathbb{S} = \mu \left(\nabla \mathbf{u} + (\nabla \mathbf{u})^T - \frac{2}{3} \nabla \cdot \mathbf{u} \mathbb{I} \right) + \eta \nabla \cdot \mathbf{u} \mathbb{I}, \quad (2.1)$$

$$\sigma = \frac{1}{\vartheta} \left(\mathbb{S} : \nabla \mathbf{u} + \kappa \frac{|\nabla \vartheta|^2}{\vartheta} \right). \quad (2.2)$$

The remaining physical quantities are given by

Symbol	Unit	Name
\mathbf{u}	m s^{-1}	velocity
ϱ	kg m^{-3}	density
p	$\text{kg m}^{-1} \text{s}^{-2}$	kinematic pressure
ϑ	K	temperature
Q	$\text{m}^2 \text{s}^{-3}$	production of the internal energy
s	$\text{m}^2 \text{s}^{-2} \text{K}^{-1}$	specific entropy
e	$\text{m}^2 \text{s}^{-2}$	specific energy
\mathbf{f}	$\text{kg m}^{-2} \text{s}^{-2}$	density of body forces

and the physical parameters by

Symbol	Unit	Description
μ	$\text{kg m}^{-1} \text{s}^{-1}$	shear viscosity coefficient
η	$\text{kg m}^{-1} \text{s}^{-1}$	bulk viscosity coefficient
κ	$\text{m kg s}^{-3} \text{K}$	heat conductivity coefficient.

In case the Mach number $\text{Ma} := U_{ref}/\sqrt{p_{ref}\varrho_{ref}}$ tends to zero, the Froude number $\text{Fr} := U_{ref}/\sqrt{L_{ref}f_{ref}}$ behaves as $\text{Fr} \approx \sqrt{\text{Ma}}$ and there are only small temperature differences, the Oberbeck-Boussinesq approximation [Obe79; Bou03] states that the above equations simplify to

$$\begin{aligned} \rho(\partial_t \mathbf{u} + \nabla \cdot (\mathbf{u} \otimes \mathbf{u})) + \nabla p &= \nabla \cdot \mathbb{S} - \rho \alpha \theta \mathbf{g} + \mathbf{f}_{ext}, \\ \nabla \cdot \mathbf{u} &= 0, \\ \rho c_p (\partial_t \theta + \nabla \cdot (\theta \mathbf{u})) - \nabla \cdot (\kappa \nabla \theta) &= f_\theta. \end{aligned}$$

with the *specific heat at constant pressure* c_p and the *coefficient of thermal expansion* α . The force term \mathbf{g} is often used as the gravitational force.

2.1.2 Electrically Conducting Fluids

For the magnetic field and its influence on the fluid we follow the description in [Dav01]. For materials that are neither magnetic nor dielectric, Maxwell's equations give

$$\begin{aligned} \nabla \times \mathbf{b} &= \mu \mathbf{j}, & \nabla \cdot \mathbf{j} &= 0, \\ \partial_t \mathbf{b} + \nabla \times \mathbf{E} &= \mathbf{f}_b, & \nabla \cdot \mathbf{b} &= 0, \end{aligned}$$

$$\mathbf{j} = \sigma(\mathbf{E} + \mathbf{u} \times \mathbf{b}), \quad \mathbf{f}_{Ind} = \mathbf{j} \times \mathbf{b}.$$

if displacement currents and charge density are neglected. The remaining physical quantities and parameters are given by

Symbol	Unit	Name
\mathbf{b}	V s m^{-2}	magnetic field
\mathbf{j}	A m^{-2}	current density
\mathbf{E}	V m^{-1}	electric field
μ	$\text{V s A}^{-1} \text{m}^{-1}$	permeability
σ	$\text{A V}^{-1} \text{m}^{-1}$	electrical conductivity

These equations can be combined to give for the magnetic field the equation

$$\begin{aligned} \mathbf{f}_b &= \partial_t \mathbf{b} + \nabla \times \mathbf{E} \\ &= \partial_t \mathbf{b} + \nabla \times \left(\frac{\mathbf{j}}{\sigma} - \mathbf{u} \times \mathbf{b} \right) \\ &= \partial_t \mathbf{b} - \nabla \times (\mathbf{u} \times \mathbf{b}) + \nabla \times \left(\frac{\mathbf{b}}{\mu\sigma} \right) \\ &= \partial_t \mathbf{b} - \nabla \times (\mathbf{u} \times \mathbf{b}) + \lambda \nabla \times (\nabla \times \mathbf{b}) \end{aligned}$$

with the magnetic diffusivity $\lambda := (\mu\sigma)^{-1}$. Additionally, we obtain the force term

$$\mathbf{f}_{Ind} = \mathbf{j} \times \mathbf{b} = \frac{1}{\mu} \nabla \times \mathbf{b} \times \mathbf{b}.$$

2.1.3 The Full Model

The model that we are going to consider in the following is a combination of the Maxwell model and the Oberbeck-Boussinesq approximation. The momentum equation is given by

$$\begin{aligned} \partial_t \mathbf{u} + (\mathbf{u} \cdot \nabla) \mathbf{u} + 2\boldsymbol{\omega} \times \mathbf{u} - \nu \Delta \mathbf{u} \\ + \nabla p + \beta \theta \mathbf{g} - (\nabla \times \mathbf{b}) \times \mathbf{b} = \mathbf{f}_u \quad \text{in } (t_0, T) \times \Omega \\ \nabla \cdot \mathbf{u} = 0 \quad \text{in } (t_0, T) \times \Omega \\ \mathbf{u}(t_0, \cdot) = \mathbf{u}_0(\cdot) \quad \text{in } \Omega \end{aligned} \tag{2.3}$$

for a frame of reference rotating with angular velocity $\boldsymbol{\omega}$. The additional centrifugal force term $\boldsymbol{\omega} \times (\boldsymbol{\omega} \times \mathbf{r}) = -\frac{1}{2} \nabla |\boldsymbol{\omega} \times \mathbf{r}|^2$ is absorbed in the pressure being a gradient force. In particular, $p = \tilde{p} - \frac{1}{2} |\boldsymbol{\omega} \times \mathbf{r}|^2$ if \tilde{p} is the pressure in an inertial frame of reference. The term $\beta \theta \mathbf{g}$ accounts for the effects of the temperature on the density in the Oberbeck-Boussinesq

model and $(\nabla \times \mathbf{b}) \times \mathbf{b}$ for the coupling with the magnetic field.

The magnetic field \mathbf{b} has to satisfy the induction equation

$$\begin{aligned} \partial_t \mathbf{b} - \nabla \times (\mathbf{u} \times \mathbf{b}) + \lambda \nabla \times (\nabla \times \mathbf{b}) + \nabla r &= \mathbf{f}_b & \text{in } (t_0, T) \times \Omega \\ \nabla \cdot \mathbf{b} &= 0 & \text{in } (t_0, T) \times \Omega \\ \mathbf{b}(t_0, \cdot) &= \mathbf{b}_0(\cdot) & \text{in } \Omega \end{aligned} \quad (2.4)$$

and the temperature θ has to fulfill

$$\begin{aligned} \partial_t \theta - \alpha \Delta \theta + (\mathbf{u} \cdot \nabla) \theta &= f_\theta & \text{in } (t_0, T) \times \Omega, \\ \theta(t_0, \cdot) &= \theta_0(\cdot) & \text{in } \Omega. \end{aligned} \quad (2.5)$$

Here, $\Omega \subset \mathbb{R}^d$ is a bounded polyhedral Lipschitz domain with boundary $\partial\Omega$.

If not differently stated, we use homogeneous boundary conditions according to

$$\mathbf{u}|_{\partial\Omega} = \mathbf{0}, \quad \mathbf{n} \times \mathbf{b}|_{\partial\Omega} = 0, \quad \theta|_{\partial\Omega} = 0. \quad (2.6)$$

Remark 2.1.1 (Notation). In the following, we will consider the usual Sobolev spaces $W^{m,p}(G)$ with norm $\|\cdot\|_{W^{m,p}(G)}$ and semi-norm $|\cdot|_{W^{m,p}(G)}$ for a measurable subset G of Ω where $m \in \mathbb{N}_0$, $p \geq 1$. In particular, we have $L^p(G) = W^{0,p}(G)$. In the case $p = 2$, we set $H^m(G) = W^{m,2}(G)$. Moreover, we define closed subspaces by

$$\begin{aligned} W_0^{1,2}(\Omega) &:= \{u \in W^{1,2}(\Omega) : u|_{\partial\Omega} = 0\}, \\ L_0^2(\Omega) &:= \{u \in L^2(\Omega) : \int_{\Omega} u \, dx = 0\}, \\ H^{curl}(\Omega) &:= \{\mathbf{u} \in [L^2(\Omega)]^d : \nabla \times \mathbf{u} \in [L^2(\Omega)]^d\}, \\ H_0^{curl} &:= \{\mathbf{u} \in H^{curl}(\Omega) : \mathbf{n} \times \mathbf{u}|_{\partial\Omega} = 0\}, \\ H^{div}(\Omega) &:= \{\mathbf{u} \in [L^2(\Omega)]^d : \nabla \cdot \mathbf{u} \in L^2(\Omega)\}, \\ H_0^{div} &:= \{\mathbf{u} \in H^{div}(\Omega) : \nabla \cdot \mathbf{u} = 0\}. \end{aligned}$$

and for the norms and semi-norms by

$$\begin{aligned} \|u\|_{W^{m,p}(\Omega)} &:= \left(\sum_{0 \leq |\alpha| \leq m} \|D^\alpha u\|_{L^p(\Omega)}^p \right)^{1/p}, & |u|_{W^{m,p}(\Omega)} &:= \|D^m u\|_{L^p(\Omega)}, \\ \|u\|_{W^{m,\infty}(\Omega)} &:= \max_{0 \leq |\alpha| \leq m} \|D^\alpha u\|_{L^\infty(\Omega)}, & |u|_{W^{m,\infty}(\Omega)} &:= \|D^m u\|_{L^\infty(\Omega)}, \\ \|u\|_{H^{curl}(\Omega)} &:= \|\nabla \times u\|_{L^2(\Omega)} + \|u\|_{L^2(\Omega)}, & |u|_{H^{curl}(\Omega)} &:= \|\nabla \times u\|_{L^2(\Omega)}. \end{aligned} \quad (2.7)$$

where $p \in [1, \infty)$. The L^2 inner product on G is denoted by $(\cdot, \cdot)_G$. For $G = \Omega$ we will usually omit the index G . This notation of norms, semi-norms and inner products is also applied in the vector-valued case. For time-dependent problems we use the notation $L^p(t_0, T; X)$ for vector-valued functions in the Sobolev space X with bounded norm $(\int_{t_0}^T \|\cdot(s)\|_X^p ds)^{\frac{1}{p}}$, $1 \leq p < \infty$ and standard modification for $p = \infty$.

2.2 Weak Formulation

We now introduce a weak formulation for the equations (2.3)-(2.5). For well-posedness, we consider the function spaces

$$\begin{aligned} \mathbf{V} &:= [W_0^{1,2}(\Omega)]^d, & Q &:= L_0^2(\Omega), \\ \mathbf{C} &:= H_0^{\text{curl}}(\Omega), & S &:= W_0^{1,2}(\Omega), & \Theta &:= W_0^{1,2}(\Omega). \end{aligned} \quad (2.8)$$

With these definitions we seek for continuous solutions according to

$$\begin{aligned} \mathbf{u} &\in L^2(t_0, T; \mathbf{V}) \cap L^\infty(t_0, T; [L^2(\Omega)]^d), \\ p &\in L^2(t_0, T; Q), \\ \mathbf{b} &\in L^2(t_0, T; \mathbf{C}) \cap L^\infty(t_0, T; [L^2(\Omega)]^d), \\ \theta &\in L^2(t_0, T; \Theta) \cap L^\infty(t_0, T; L^2(\Omega)). \end{aligned}$$

For the external force terms, we assume $\mathbf{f}_u \in L^2(t_0, T; [L^2(\Omega)]^d) \cap C(t_0, T; [L^2(\Omega)]^d)$, $\mathbf{f}_b \in L^2(t_0, T; H_0^{\text{div}}(\Omega))$ and $f_\theta \in L^2(t_0, T; L^2(\Omega)) \cap C(t_0, T; L^2(\Omega))$. For convenience, we often drop the explicit time dependence, e.g. we write \mathbf{u} instead of $\mathbf{u}(t)$.

The equations (2.3)-(2.5) are now multiplied with test functions from the respective space and integrated over the domain Ω . Using the boundary conditions (2.6), integration by parts yields the weak formulation:

Find $(\mathbf{u}, p): (t_0, T) \rightarrow \mathbf{V} \times Q$ such that

$$\begin{aligned} (\partial_t \mathbf{u}, \mathbf{v}) + c_u(\mathbf{u}; \mathbf{u}, \mathbf{v}) + (2\boldsymbol{\omega} \times \mathbf{u}, \mathbf{v}) + \nu(\nabla \mathbf{u}, \nabla \mathbf{v}) \\ - (p, \nabla \cdot \mathbf{v}) + (\beta \mathbf{g} \theta, \mathbf{v}) - ((\nabla \times \mathbf{b}) \times \mathbf{b}, \mathbf{v}) = (\mathbf{f}_u, \mathbf{v}), \\ (\nabla \cdot \mathbf{u}, q) = 0 \end{aligned} \quad (2.9)$$

holds for all $(\mathbf{v}, q) \in \mathbf{V} \times Q$ for $t \in (t_0, T)$ a.e.

Find $\mathbf{b}: (t_0, T) \rightarrow \mathbf{C}$ such that

$$\begin{aligned} (\partial_t \mathbf{b}, \mathbf{c}) - (\nabla \times (\mathbf{u} \times \mathbf{b}), \mathbf{c}) + \lambda(\nabla \times \mathbf{b}, \nabla \times \mathbf{c}) + (\nabla r, \mathbf{c}) = (\mathbf{f}_b, \mathbf{c}), \\ (\mathbf{b}, \nabla s) = 0 \end{aligned} \quad (2.10)$$

holds for all $(\mathbf{c}, s) \in \mathbf{C} \times S$ for $t \in (t_0, T)$ a.e.

Find $\theta \in \Theta$ such that

$$(\partial_t \theta, \psi) + \alpha(\nabla \theta, \nabla \psi) + c_\theta(\mathbf{u}; \theta, \psi) = (f_\theta, \psi) \quad (2.11)$$

holds for all $(\mathbf{v}, q, \psi) \in \mathbf{V} \times Q \times \Theta$ for $t \in (t_0, T)$ a.e.

The convective terms

$$\begin{aligned} c_u(\mathbf{w}; \mathbf{u}, \mathbf{v}) &:= \frac{1}{2} [((\mathbf{w} \cdot \nabla) \mathbf{u}, \mathbf{v}) - ((\mathbf{w} \cdot \nabla) \mathbf{v}, \mathbf{u})], \\ c_\theta(\mathbf{w}; \theta, \psi) &:= \frac{1}{2} [((\mathbf{w} \cdot \nabla) \theta, \psi) - ((\mathbf{w} \cdot \nabla) \psi, \theta)]. \end{aligned}$$

have been chosen in a skew-symmetric form due to stability purposes in the discretization.

Remark 2.2.1. The ansatz spaces with respect to velocity and kinematic pressure satisfy the compatibility condition

$$\exists \beta_u > 0 : \inf_{q \in Q \setminus \{0\}} \sup_{\mathbf{v} \in \mathbf{V} \setminus \{0\}} \frac{(q, \nabla \cdot \mathbf{v})}{\|q\|_Q \|\mathbf{v}\|_{\mathbf{V}}} \geq \beta_u \quad (2.12)$$

and similarly for the ansatz spaces with respect to magnetic field and magnetic pseudo-pressure it holds

$$\exists \beta_b > 0 : \inf_{s \in S \setminus \{0\}} \sup_{\mathbf{c} \in \mathbf{C} \setminus \{0\}} \frac{(\nabla s, \mathbf{c})}{\|s\|_S \|\mathbf{c}\|_{\mathbf{C}}} \geq \beta_b. \quad (2.13)$$

In particular, by the closed range theorem this means that the spaces of weakly solenoidal functions are not trivial:

$$\begin{aligned} \mathbf{V}^{div} &:= \{\mathbf{u} \in \mathbf{V} : (\nabla \cdot \mathbf{u}, q) = 0 \quad \forall q \in Q\} \neq \{0\}, \\ \mathbf{C}^{div} &:= \{\mathbf{c} \in \mathbf{C} : (\mathbf{u}, \nabla s) = 0 \quad \forall s \in S\} \neq \{0\}. \end{aligned}$$

2.3 Discretization

For the discretization of the above equations (2.9)-(2.11) we try to mimic properties of the continuous formulation. Therefore we consider a family of conforming finite-dimensional ansatz spaces

$$\mathbf{V}_h \subset \mathbf{V}, \quad Q_h \subset Q, \quad \mathbf{C}_h \subset \mathbf{C}, \quad S_h \subset S, \quad \Theta_h \subset \Theta$$

such that the sequences of discrete subspaces are dense in their continuous counterparts. The discretized equations then read:

Find $(\mathbf{u}_h, p_h): (t_0, T) \rightarrow \mathbf{V}_h \times Q_h$ such that

$$\begin{aligned} (\partial_t \mathbf{u}_h, \mathbf{v}_h) + c_u(\mathbf{u}_h; \mathbf{u}_h, \mathbf{v}_h) + (2\boldsymbol{\omega} \times \mathbf{u}_h, \mathbf{v}_h) + \nu(\nabla \mathbf{u}_h, \nabla \mathbf{v}_h) \\ - (p_h, \nabla \cdot \mathbf{v}_h) + (\beta \mathbf{g} \theta_h, \mathbf{v}_h) - ((\nabla \times \mathbf{b}_h) \times \mathbf{b}_h, \mathbf{v}_h) = (\mathbf{f}_u, \mathbf{v}_h), \\ (\nabla \cdot \mathbf{u}_h, q_h) = 0 \end{aligned} \quad (2.14)$$

holds for all $(\mathbf{v}_h, q_h) \in \mathbf{V}_h \times Q_h$ for $t \in (t_0, T)$ a.e.

Find $(\mathbf{b}_h, r_h): (t_0, T) \rightarrow \mathbf{C}_h \times S_h$ such that

$$\begin{aligned} (\partial_t \mathbf{b}_h, \mathbf{v}_h) - (\nabla \times (\mathbf{u}_h \times \mathbf{b}_h), \mathbf{c}_h) \\ + \lambda(\nabla \times \mathbf{b}_h, \nabla \times \mathbf{c}_h) + (\nabla r, \mathbf{c}_h) = (\mathbf{f}_b, \mathbf{c}_h), \\ (\mathbf{b}_h, \nabla s_h) = 0 \end{aligned} \quad (2.15)$$

holds for all $(\mathbf{c}_h, s_h) \in \mathbf{C}_h \times S_h$ for $t \in (t_0, T)$ a.e.

Find $\theta_h: (t_0, T) \rightarrow \Theta_h$ such that

$$(\partial_t \theta_h, \psi_h) + \alpha(\nabla \theta_h, \nabla \psi_h) + c_\theta(\mathbf{u}_h; \theta_h, \psi_h) = (f_\theta, \psi_h) \quad (2.16)$$

holds for all $\psi_h \in \Theta_h$ for $t \in (t_0, T)$ a.e.

Analogously to the continuous case, we define the spaces of discretely divergence-free solutions according to

$$\begin{aligned} \mathbf{V}_h^{div} &:= \{\mathbf{v}_h \in \mathbf{V}_h : (\nabla \cdot \mathbf{v}_h, q_h) = 0 \quad \forall q_h \in Q_h\}, \\ \mathbf{C}_h^{div} &:= \{\mathbf{c}_h \in \mathbf{C}_h : (\nabla \cdot \mathbf{c}_h, s_h) = 0 \quad \forall s_h \in S_h\} \end{aligned}$$

and equations (2.14) and (2.15) imply $\mathbf{u}_h \in \mathbf{V}_h^{div}$ and $\mathbf{b}_h \in \mathbf{C}_h^{div}$.

Unfortunately, the continuous inf-sup conditions (2.12) and (2.13) do not imply a discrete counterpart and in particular

$$\mathbf{V}_h^{div} \not\subset \mathbf{V}^{div}, \quad \mathbf{C}_h^{div} \not\subset \mathbf{C}^{div}.$$

In this thesis we impose this compatibility between velocity and kinematic pressure ansatz space and between the ansatz space for the magnetic field and the magnetic pseudo-pressure explicitly:

Assumption 2.3.1.

The ansatz spaces \mathbf{V}_h and Q_h satisfy

$$\exists \beta_{u,h} > 0 : \inf_{q_h \in Q_h \setminus \{0\}} \sup_{\mathbf{v}_h \in \mathbf{V}_h \setminus \{0\}} \frac{(q_h, \nabla \cdot \mathbf{v}_h)}{\|q_h\|_Q \|\mathbf{v}_h\|_{\mathbf{V}}} \geq \beta_{u,h}$$

with a constant $\beta_{u,h}$ independent of h .

Assumption 2.3.2.

The ansatz spaces \mathbf{C}_h and S_h satisfy

$$\exists \beta_{b,h} > 0 : \inf_{s_h \in S_h \setminus \{0\}} \sup_{\mathbf{c}_h \in \mathbf{C}_h \setminus \{0\}} \frac{(s_h, \nabla \cdot \mathbf{c}_h)}{\|s_h\|_S \|\mathbf{c}_h\|_C} \geq \beta_{b,h}$$

with a constant $\beta_{b,h}$ independent of h .

Remark 2.3.3. Provided these conditions are fulfilled, it holds

$$\mathbf{V}_h^{div} \neq \{0\} \quad \mathbf{C}_h^{div} \neq \{0\}.$$

due to the closed range theorem.

2.4 Finite Element Spaces

For a simplex $T \in \mathcal{T}_h$ or a quadrilateral/hexahedron T in \mathbb{R}^d , let \hat{T} be the reference unit simplex or the unit cube $(-1, 1)^d$. The reference mapping $F_T: \hat{T} \rightarrow T$ is affine for simplices and multi-linear for quadrilaterals/ hexahedra. We require that F_T is bijective and its Jacobian is bounded for a family of triangulations according to

$$\exists c_1, c_2 > 0 : \quad c_1 h_T^d \leq |\det DF_T(\hat{\mathbf{x}})| \leq c_2 h_T^d \quad \forall \hat{\mathbf{x}} \in \hat{T} \quad (2.17)$$

with constants $c_1, c_2 > 0$ independent of the cell diameter h_T . This in particular implies that the aspect ratio of each cell is uniformly bounded.

Let $\hat{\mathbb{P}}_l$ and $\hat{\mathbb{Q}}_l$ with $l \in \mathbb{N}_0$ be the set of polynomials of degree $\leq l$ and of polynomials of degree $\leq l$ in each variable separately. Moreover, we set

$$\mathbb{R}_l(\hat{T}) := \begin{cases} \mathbb{P}_l(\hat{T}) & \text{on simplices } \hat{T} \\ \mathbb{Q}_l(\hat{T}) & \text{on quadrilaterals/hexahedra } \hat{T}. \end{cases}$$

Bubble-enriched spaces are

$$\mathbb{P}_l^+(\hat{T}) := \mathbb{P}_l(\hat{T}) + b_{\hat{T}} \cdot \mathbb{P}_{l-2}(\hat{T}), \quad \mathbb{Q}_l^+(\hat{T}) := \mathbb{Q}_l(\hat{T}) + \psi \cdot \text{span}\{\hat{x}_i^{r-1}, i = 1, \dots, d\}$$

with polynomial bubble function $b_{\hat{T}} := \prod_{i=0}^d \hat{\lambda}_i \in \hat{\mathbb{P}}_{d+1}$ on the reference simplex \hat{T} with barycentric coordinates $\hat{\lambda}_i$ and with d -quadratic function $\psi(\hat{\mathbf{x}}) := \prod_{i=1}^d (1 - \hat{x}_i^2)$ on the reference cube. Define

$$Y_{h,-l} := \{v_h \in L^2(\Omega) : v_h|_T \circ F_T \in \mathbb{R}_l(\hat{T}) \quad \forall T \in \mathcal{T}_h\},$$

$$Y_{h,l} := Y_{h,-l} \cap W^{1,2}(\Omega)$$

and bubble-enriched spaces $Y_{h,\pm l}^+$ analogously. For convenience, we write $\mathbf{V}_h = \mathbb{R}_k$ instead of $\mathbf{V}_h := [Y_{h,k}]^d \cap V$ for the velocity (with obvious modifications for \mathbb{R}_k^+) and similarly for kinematic pressure, temperature, magnetic field and magnetic pseudo-pressure.

2.5 Stabilization and Assumptions

Testing our weak discretized formulation symmetrically, we find

$$\begin{aligned} & \partial_t \|\mathbf{u}_h\|_0^2 + \nu \|\nabla \mathbf{u}_h\|_0^2 + \partial_t \|\mathbf{b}_h\|_0^2 + \lambda \|\nabla \times \mathbf{b}\|_0^2 + \partial_t \|\theta_h\|_0^2 + \alpha \|\nabla \theta_h\|_0^2 \\ & = (\mathbf{f}_u, \mathbf{u}_h) + (\mathbf{f}_b, \mathbf{b}_h) + (f_\theta, \theta_h) - (\beta \mathbf{g} \theta_h, \mathbf{u}_h). \end{aligned}$$

This means that for vanishing viscosities $\nu \rightarrow 0$, $\lambda \rightarrow 0$, $\alpha \rightarrow 0$ we lose control over

- the divergence of the velocity $\nabla \cdot \mathbf{v}_h$,
- the divergence of the magnetic field $\nabla \cdot \mathbf{b}_h$,
- the convection $(\mathbf{u}_h \cdot \nabla) \mathbf{u}_h$ in the momentum equation,
- the Coriolis term $2\boldsymbol{\omega} \times \mathbf{u}_h$ in the momentum equation,
- the convection $(\mathbf{u}_h \cdot \nabla) \theta_h$ in the temperature equation and
- the coupling between velocity and magnetic field $\nabla \times (\mathbf{u}_h \times \mathbf{b}_h)$ and $(\nabla \times \mathbf{b}_h) \times \mathbf{b}_h$.

All of these losses can lead to unphysical oscillations in the discrete solutions. Our aim is to remove these and to regain control over these terms while still approximating the continuous solutions suitably. Therefore, we want to stabilize each of these terms separately. Due to the fact that the continuous velocity and the continuous magnetic field are enforced to be solenoidal, there is no harm in simply adding divergence constraints according to

$$\tau_{u,gd}(\nabla \cdot \mathbf{u}_h, \nabla \cdot \mathbf{v}_h) \quad \text{and} \quad \tau_{b,gd}(\nabla \cdot \mathbf{b}_h, \nabla \cdot \mathbf{c}_h) \quad (2.18)$$

to the respective equations.

2.5.1 Local Projection Stabilization

The remaining terms do not vanish for a continuous solution. Residual-based methods aim to provide stabilization by penalizing the residuum in the strong formulation. Drawbacks of such an approach are additional non-symmetric terms and the occurrence of higher

order derivatives. For an overview compare [RST08]. Here, we want to pursue another approach called local projection stabilization (LPS). We suppose that unphysical oscillations that arise due to the vanishing control over the described terms are located on small scales and therefore only these have to be stabilized.

Let $\{\mathcal{M}_h\}$ be a family of shape-regular macro decompositions of Ω . In the one-level LPS-approach, one has $\mathcal{M}_h = \mathcal{T}_h$ and chooses a coarser ansatz space. In the two-level LPS-approach, the decomposition \mathcal{T}_h is derived from refinement. We denote by h_T and h_M the diameter of cells $T \in \mathcal{T}_h$ and $M \in \mathcal{M}_h$. It holds $h_T \leq h_M \leq Ch_T$ for all $T \subset M$ and $M \in \mathcal{M}_h$.

Assumption 2.5.1.

Let the ansatz spaces \mathbf{V}_h and \mathbf{C}_h satisfy the local inverse inequalities

$$\|\nabla \mathbf{v}_h\|_{L^2(M)} \leq Ch_M^{-1} \|\mathbf{v}_h\|_{L^2(M)} \quad \forall \mathbf{v}_h \in \mathbf{V}_h, M \in \mathcal{M}_h, \quad (2.19)$$

$$\|\nabla \mathbf{c}_h\|_{L^2(M)} \leq Ch_M^{-1} \|\mathbf{c}_h\|_{L^2(M)} \quad \forall \mathbf{c}_h \in \mathbf{C}_h, M \in \mathcal{M}_h. \quad (2.20)$$

Let $D_M^{u/b/\theta} \subset [L^\infty(M)]^d$ denote coarse ansatz spaces on $M \in \mathcal{M}_h$ for \mathbf{u}_h resp. \mathbf{b}_h resp. θ_h . For each $M \in \mathcal{M}_h$, let $\pi_M: [L^2(M)]^d \rightarrow D_M^{u/b/\theta}$ be the orthogonal L^2 -projection. Moreover, we denote by $\kappa_M^{u/b/\theta} := id - \pi_M^{u/b/\theta}$ the so-called fluctuation operator.

Assumption 2.5.2.

The fluctuation operators $\kappa_M^{u/b/\theta}$ provide the approximation property

$$\|\kappa_M^{u/b/\theta} \mathbf{w}\|_{L^2(M)} \leq Ch_M^l \|\mathbf{w}\|_{W^{l,2}(M)}, \quad \forall \mathbf{w} \in W^{l,2}(M), M \in \mathcal{M}_h, l = 0, \dots, s_{u/b/\theta}. \quad (2.21)$$

A sufficient condition for Assumption 2.5.2 is $\mathbb{P}_{s_{u/b/\theta}-1} \subset D_M^{u/b/\theta}$.

For each macro element $M \in \mathcal{M}_h$, we denote elementwise averaged streamline directions $\mathbf{u}_M, \mathbf{b}_M \in \mathbb{R}^d$ as approximations to \mathbf{u}_h and \mathbf{b}_h satisfying

$$|\mathbf{u}_M| \leq C \|\mathbf{u}\|_{\infty, M}, \quad |\mathbf{b}_M| \leq C \|\mathbf{b}\|_{\infty, M}.$$

Possible choices are

$$\mathbf{u}_M := \frac{1}{|M|} \int_M \mathbf{u}_h(x) dx, \quad \mathbf{b}_M := \frac{1}{|M|} \int_M \mathbf{b}_h(x) dx. \quad (2.22)$$

With these preparations we can define the stabilizations

$$s_{u,gd}(\mathbf{u}, \mathbf{v}) := \sum_{M \in \mathcal{M}_h} \tau_{u,gd,M} (\nabla \cdot \mathbf{u}, \nabla \cdot \mathbf{v})_M$$

$$\begin{aligned}
s_{u,SU}(\mathbf{w}; \mathbf{u}, \mathbf{v}) &:= \sum_{M \in \mathcal{M}_h} \tau_{u,SU,M}(\kappa((\mathbf{w}_M \cdot \nabla)\mathbf{u}), \kappa(\mathbf{w}_M \cdot \nabla\mathbf{v}))_M \\
s_{u,Cor}(\boldsymbol{\omega}; \mathbf{u}, \mathbf{v}) &:= \sum_{M \in \mathcal{M}_h} \tau_{u,Cor,M}(\kappa(\boldsymbol{\omega} \times \mathbf{u}), \kappa(\boldsymbol{\omega} \times \mathbf{v}))_M \\
\tilde{s}_{u,Lor}(\mathbf{d}; \mathbf{u}, \mathbf{v}) &:= \sum_{M \in \mathcal{M}_h} \tilde{\tau}_{u,Lor,M}(\kappa(\nabla \times (\mathbf{u} \times \mathbf{d}_M)), \kappa(\nabla \times (\mathbf{v} \times \mathbf{d}_M)))_M \\
s_{b,gd}(\mathbf{b}, \mathbf{c}) &:= \sum_{M \in \mathcal{M}_h} \tau_{b,gd,M}(\nabla \cdot \mathbf{b}_h, \nabla \cdot \mathbf{c}_h)_M \\
s_{b,Lor}(\mathbf{w}; \mathbf{b}, \mathbf{c}) &:= \sum_{M \in \mathcal{M}_h} \tau_{b,Lor,M}(\kappa(\nabla \times (\mathbf{w}_M \times \mathbf{b})), \kappa(\nabla \times (\mathbf{w}_M \times \mathbf{c})))_M \\
s_{b,Ind}(\mathbf{d}; \mathbf{b}, \mathbf{c}) &:= \sum_{M \in \mathcal{M}_h} \tau_{b,Ind,M}(\kappa((\nabla \times \mathbf{b}) \times \mathbf{d}_M), \kappa((\nabla \times \mathbf{c}) \times \mathbf{d}_M))_M \\
s_{\theta,SU}(\mathbf{w}; \theta, \psi) &:= \sum_{M \in \mathcal{M}_h} \tau_{\theta,SU,M}(\kappa((\mathbf{w}_M \cdot \nabla)\theta), \kappa((\mathbf{w}_M \cdot \nabla)\psi))_M \\
s_{r,PSPG}(r, s) &:= \sum_{M \in \mathcal{M}_h} \tau_{r,PSPG,M}(\nabla \mathbf{r}, \nabla \mathbf{s})_M
\end{aligned}$$

where $\mathbf{w} \in \mathbf{V}_h$ and $\mathbf{d} \in \mathbf{C}_h$ with piecewise constant approximations \mathbf{w}_M and \mathbf{d}_M .

We are now able to state the stabilized semi-discretization in space:

Find $(\mathbf{u}_h, p_h): (t_0, T) \rightarrow \mathbf{V}_h \times Q_h$ such that

$$\begin{aligned}
&(\partial_t \mathbf{u}_h, \mathbf{v}_h) + c_u(\mathbf{u}_h; \mathbf{u}_h, \mathbf{v}_h) + (2\boldsymbol{\omega} \times \mathbf{u}_h, \mathbf{v}_h) + \nu(\nabla \mathbf{u}_h, \nabla \mathbf{v}_h) - (p_h, \nabla \cdot \mathbf{v}_h) \\
&\quad + \tau_{u,gd}(\nabla \cdot \mathbf{u}_h, \nabla \cdot \mathbf{v}_h) + s_{u,SU}(\mathbf{u}_h; \mathbf{u}_h, \mathbf{v}_h) + s_{u,Cor}(\boldsymbol{\omega}; \mathbf{u}_h, \mathbf{v}_h) \\
&\quad + \tilde{s}_{u,Lor}(\mathbf{b}_h; \mathbf{u}_h, \mathbf{v}_h) + (\beta \mathbf{g} \theta_h, \mathbf{v}_h) - ((\nabla \times \mathbf{b}_h) \times \mathbf{b}_h, \mathbf{v}_h) = (\mathbf{f}_u, \mathbf{v}_h), \\
&\quad (\nabla \cdot \mathbf{u}_h, q_h) = 0
\end{aligned} \tag{2.23}$$

holds for all $(\mathbf{v}_h, q_h) \in \mathbf{V}_h \times Q_h$ for $t \in (t_0, T)$ a.e.

Find $(\mathbf{b}_h, r_h): (t_0, T) \rightarrow \mathbf{C}_h \times S_h$ such that

$$\begin{aligned}
&(\partial_t \mathbf{b}_h, \mathbf{c}_h) - (\nabla \times (\mathbf{u}_h \times \mathbf{b}_h), \mathbf{c}_h) + \lambda(\nabla \times \mathbf{b}_h, \nabla \times \mathbf{c}_h) - (\nabla r_h, \mathbf{c}_h) \\
&\quad + \tau_{b,gd}(\nabla \cdot \mathbf{b}_h, \nabla \cdot \mathbf{c}_h) + s_{b,Lor}(\mathbf{u}_h; \mathbf{b}_h, \mathbf{c}_h) + s_{b,Ind}(\mathbf{b}_h; \mathbf{b}_h, \mathbf{c}_h) = (\mathbf{f}_b, \mathbf{c}_h), \\
&\quad (\mathbf{b}_h, \nabla s_h) + s_{r,PSPG}(r_h, s_h) = 0
\end{aligned} \tag{2.24}$$

holds for all $(\mathbf{c}_h, s_h) \in \mathbf{C}_h \times S_h$ for $t \in (t_0, T)$ a.e.

Find $\theta_h: (t_0, T) \rightarrow \Theta_h$ such that

$$(\partial_t \theta_h, \psi_h) + \alpha(\nabla \theta_h, \nabla \psi_h) + c_\theta(\mathbf{u}_h; \theta_h, \psi_h) + s_{\theta,SU}(\mathbf{u}_h; \theta_h, \psi_h) = (f_\theta, \psi_h) \tag{2.25}$$

holds for all $(\mathbf{v}_h, q_h, \psi_h) \in \mathbf{V}_h \times Q_h \times \Theta_h$ for $t \in (t_0, T)$ a.e.

2.5.2 Interpolation

Additionally, we require that suitable interpolation operators exist:

Assumption 2.5.3.

There are (quasi-)interpolation operators $j_u: \mathbf{V} \rightarrow \mathbf{V}_h$ and $j_p: Q \rightarrow Q_h$ such that for all $M \in \mathcal{M}_h$, for all $\mathbf{w} \in \mathbf{V} \cap [W^{l,2}(\Omega)]^d$ with $1 \leq l \leq k_u + 1$

$$\|\mathbf{w} - j_u \mathbf{w}\|_{L^2(M)} + h_M \|\nabla(\mathbf{w} - j_u \mathbf{w})\|_{L^2(M)} \leq Ch_M^l \|\mathbf{w}\|_{W^{l,2}(\omega_M)} \quad (2.26)$$

and for all $q \in Q \cap H^l(M)$ with $1 \leq l \leq k_p + 1$

$$\|q - j_p q\|_{L^2(M)} + h_M \|\nabla(q - j_p q)\|_{L^2(M)} \leq Ch_M^l \|q\|_{W^{l,2}(\omega_M)}. \quad (2.27)$$

on a suitable patch $\omega_M \supset M$ holds. Moreover, let

$$\|\mathbf{v} - j_u \mathbf{v}\|_{L^\infty(M)} \leq Ch_M \|\mathbf{v}\|_{W^{1,\infty}(\omega_M)} \quad \forall \mathbf{v} \in [W^{1,\infty}(\omega_M)]^d.$$

Assumption 2.5.4.

There are (quasi-)interpolation operators $j_b: \mathbf{C} \rightarrow \mathbf{C}_h$ and $j_r: S \rightarrow S_h$ such that for all $M \in \mathcal{M}_h$, for all $\mathbf{c} \in \mathbf{C} \cap [W^{l,2}(\Omega)]^d$ with $1 \leq l \leq k_b + 1$

$$\|\mathbf{c} - j_b \mathbf{c}\|_{L^2(M)} + h_M \|\nabla(\mathbf{c} - j_b \mathbf{c})\|_{L^2(M)} \leq Ch_M^l \|\mathbf{c}\|_{W^{l,2}(\omega_M)} \quad (2.28)$$

and for all $s \in S \cap H^l(M)$ with $1 \leq l \leq k_r + 1$

$$\|s - j_r s\|_{L^2(M)} + h_M \|\nabla(s - j_r s)\|_{L^2(M)} \leq Ch_M^l \|s\|_{W^{l,2}(\omega_M)}. \quad (2.29)$$

on a suitable patch $\omega_M \supset M$ holds. Moreover, let

$$\|\mathbf{b} - j_b \mathbf{b}\|_{L^\infty(M)} \leq Ch_M \|\mathbf{b}\|_{W^{1,\infty}(\omega_M)} \quad \forall \mathbf{b} \in [W^{1,\infty}(\omega_M)]^d.$$

Assumption 2.5.5.

There is a (quasi-)interpolation operator $j_\theta: \Theta \rightarrow \Theta_h$ such that for all $M \in \mathcal{M}_h$, for all $\psi \in \Theta \cap W^{l,2}(\Omega)$ with $1 \leq l \leq k_\theta + 1$

$$\|\psi - j_\theta \psi\|_{L^2(M)} + h_M \|\nabla(\psi - j_\theta \psi)\|_{L^2(M)} \leq Ch_M^l \|\psi\|_{W^{l,2}(\omega_M)} \quad (2.30)$$

on a suitable patch $\omega_M \supset M$ holds. Moreover, let

$$\|\theta - j_\theta \theta\|_{L^\infty(M)} \leq Ch_M \|\theta\|_{W^{1,\infty}(\omega_M)} \quad \forall \theta \in W^{1,\infty}(\omega_M).$$

Remark 2.5.6. We often require that an interpolation operator is divergence-preserving. According to Girault & Scott [GS03], such an operator satisfying the above interpolation assumptions 2.5.3 resp. 2.5.4 exists provided $k \geq 2$ for $d = 2$ and $k \geq 3$ for $d = 3$. It is argued in [GS03] that the restriction $k \geq 3$ can be lifted for quadrilateral/hexahedral meshes to $k \geq 2$.

With these preparations, we consider a splitting of the total error:

Definition 2.5.7 (Notation).

We define the interpolation errors $\boldsymbol{\eta}_u, \boldsymbol{\eta}_b, \eta_\theta, \eta_p, \eta_r$ by

$$\boldsymbol{\eta}_u := \mathbf{u} - j_u \mathbf{u}, \quad \boldsymbol{\eta}_b := \mathbf{b} - j_b \mathbf{b}, \quad \eta_p := p - j_p p, \quad \eta_r := r - j_r r, \quad \eta_\theta := \theta - j_\theta \theta$$

and the discretization errors $\mathbf{e}_u, \mathbf{e}_b, e_\theta, e_p, e_r$ by

$$\mathbf{e}_u := j_u \mathbf{u} - \mathbf{u}_h, \quad \mathbf{e}_b := j_b \mathbf{b} - \mathbf{b}_h, \quad e_p := j_p p - p_h, \quad e_r := j_r r - r_h, \quad e_\theta := j_\theta \theta - \theta_h.$$

This gives for the total errors $\boldsymbol{\xi}_u, \boldsymbol{\xi}_b, \xi_\theta, \xi_p, \xi_r$

$$\begin{aligned} \boldsymbol{\xi}_u &:= \mathbf{u} - \mathbf{u}_h = \boldsymbol{\eta}_u + \mathbf{e}_u, & \boldsymbol{\xi}_b &:= \mathbf{b} - \mathbf{b}_h = \boldsymbol{\eta}_b + \mathbf{e}_b, & \xi_p &:= p - p_h = \eta_p + e_p, \\ \xi_r &:= r - r_h = \eta_r + e_r, & \xi_\theta &:= \theta - \theta_h = \eta_\theta + e_\theta & . \end{aligned}$$

3 Semi-Discrete Error Estimates

In the following, we summarize semi-discrete error estimates that we obtained for various forms of the coupled Navier-Stokes equations. Here we restrict ourselves to the above described discrete formulation. In particular, we use for the summary no edge stabilization and just one common coarse space.

We begin with the Oseen equations [DAL15] and proceed to the uncoupled Navier-Stokes equations [ADL15a]. Next, the analysis is extended to outflow boundary conditions instead of the homogeneous Dirichlet boundary conditions [ABL15]. Finally, we consider the temperature coupling and the coupling with the induction equation separately.

In the following, we will call an error estimate to be *semi-robust* if the coefficients multiplying the corresponding Sobolev norms of the solutions in the upper bound do not depend on the problem parameters. We will call an error estimate *quasi-optimal* if the order of convergence is the same as for the interpolation errors.

3.1 The Oseen and the Navier-Stokes Problem

We first neglect the coupling with the temperature and the induction equation and consider the time-dependent Oseen equations as well as the Navier-Stokes equations in an inertial frame of reference. The Oseen equations differ from the Navier-Stokes equations by replacing the convective term $c(\mathbf{u}; \mathbf{u}; \mathbf{v})$ by $c(\mathbf{a}; \mathbf{u}; \mathbf{v})$ with $\mathbf{a} \in L^\infty(t_0, T; W^{1,\infty}(\Omega))$ and $\nabla \cdot \mathbf{a} = 0$ in the continuous formulation (2.9):

Find $(\mathbf{u}, p): (t_0, T) \rightarrow \mathbf{V} \times Q$ such that

$$\begin{aligned} (\partial_t \mathbf{u}, \mathbf{v}) + c_u(\mathbf{a}; \mathbf{u}, \mathbf{v}) + \nu(\nabla \mathbf{u}, \nabla \mathbf{v}) - (p, \nabla \cdot \mathbf{v}) &= (\mathbf{f}_u, \mathbf{v}), \\ (\nabla \cdot \mathbf{u}, q) &= 0 \end{aligned} \tag{3.1}$$

holds for all $(\mathbf{v}, q) \in \mathbf{V} \times Q$ for $t \in (t_0, T)$ a.e..

Similarly, $c(\mathbf{u}_h; \mathbf{u}_h; \mathbf{v}_h)$ is replaced by $c(\mathbf{a}; \mathbf{u}_h; \mathbf{v}_h)$ in the discretized formulation (2.23):

Find $(\mathbf{u}_h, p_h): (t_0, T) \rightarrow \mathbf{V}_h \times Q_h$ such that

$$\begin{aligned} (\partial_t \mathbf{u}_h, \mathbf{v}_h) + c_u(\mathbf{a}; \mathbf{u}_h, \mathbf{v}_h) + \nu(\nabla \mathbf{u}_h, \nabla \mathbf{v}_h) - (p_h, \nabla \cdot \mathbf{v}_h) \\ + s_{u,gd}(\mathbf{u}_h, \mathbf{v}_h) + s_{u,SU}(\mathbf{u}_h; \mathbf{u}_h, \mathbf{v}_h) = (\mathbf{f}_u, \mathbf{v}_h), \\ (\nabla \cdot \mathbf{u}_h, q_h) = 0 \end{aligned} \quad (3.2)$$

holds for all $(\mathbf{v}_h, q_h) \in \mathbf{V}_h \times Q_h$ for $t \in (t_0, T)$ a.e..

For the analysis, let us define the mesh-dependent expression $||| \cdot |||_{LPS_u}$ via symmetric testing by

$$||| \mathbf{v} |||_{LPS_u}^2 := \nu \|\nabla \mathbf{v}\|_0^2 + s_{u,gd}(\mathbf{v}, \mathbf{v}) + s_{u,SU}(\mathbf{a}; \mathbf{v}, \mathbf{v}) \quad \forall \mathbf{v} \in \mathbf{V}.$$

For the Navier-Stokes problem, we choose $\mathbf{a} = \mathbf{u}_h$.

The approach here improves some results by Matthies/Tobiska in [MT15].

3.1.1 Stability

We can first state a common result:

Lemma 3.1.1.

Let $\mathbf{f}_u \in L^1(t_0, T; L^2(\Omega))$ and $\mathbf{u}_0 \in L^2(\Omega)$. Then there exists a discrete solution $\mathbf{u}_h \in \mathbf{V}_h^{div}$ of the LPS-model (3.2). For $t_0 \leq t \leq T$ we obtain

$$\frac{1}{2} \|\mathbf{u}_h\|_0^2 + \int_{t_0}^t |||(\mathbf{u}_h(s), 0)|||_{LPS_u}^2 ds \leq \|\mathbf{u}_h(t_0)\|_0^2 + \frac{3}{2} \|\mathbf{f}_u\|_{L^1(t_0, t; L^2(\Omega))}^2. \quad (3.3)$$

Proof. [DAL15, Lemma 3.1] and [ADL15a, Lemma 3.1] □

For the Oseen problem, we can also bound the time derivative:

Lemma 3.1.2.

Let $\mathbf{f}_u \in L^2(t_0, T; L^2(\Omega))$. Then there holds

$$\begin{aligned} \|\partial_t \mathbf{u}_h\|_{L^2(t_0, t; L^2(\Omega))}^2 + |||\mathbf{u}_h|||_{LPS_u}^2 \\ \leq |||\mathbf{u}_h(t_0)|||_{LPS_u}^2 + \frac{2}{\nu} \|\mathbf{a}\|_{L^\infty(t_0, t; L^\infty(\Omega))}^2 \|\mathbf{u}_h(t_0)\|_0^2 \\ + 2 \|\mathbf{f}_u\|_{L^2(t_0, t; L^2(\Omega))}^2 + \frac{3}{\nu} \|\mathbf{a}\|_{L^\infty(t_0, t; L^\infty(\Omega))}^2 \|\mathbf{f}\|_{L^1(t_0, t; L^2(\Omega))}. \end{aligned} \quad (3.4)$$

Proof. [DAL15, Lemma 3.1] □

Remark 3.1.3. If we assume Lipschitz continuity in time for \mathbf{f}_u , the Picard-Lindelöf theorem yields uniqueness of the solution.

Lemma 3.1.4.

If $\mathbf{f}_u \in L^2(t_0, T; L^2(\Omega))$ and $\mathbf{u}_h \in H^1(t_0, T; [L^2(\Omega)]^d)$, there exists a unique discrete kinematic pressure p_h in a solution $\mathbf{U}_h = (\mathbf{u}_h, p_h) \in \mathbf{V}_h^{div} \times Q_h$ of (3.2). Moreover, for $t_0 \leq t \leq T$, we obtain

$$\begin{aligned} \|p_h\|_{L^2(t_0, t; L^2(\Omega))}^2 &\leq \frac{3}{\beta_{u,h}^2} \left[C_P^2 (\|\mathbf{f}_u\|_{L^2(t_0, t; L^2(\Omega))}^2 + \|\partial_t \mathbf{u}_h\|_{L^2(t_0, t; L^2(\Omega))}^2) \right. \\ &\quad \left. + K^2 \int_{t_0}^t \|\mathbf{u}_h(s)\|_{LPS_u}^2 ds \right] \end{aligned}$$

with $K := \sqrt{\nu} + \frac{C_P \|\mathbf{a}\|_{L^\infty(t_0, t; L^\infty(\Omega))}}{\sqrt{\nu}} + \max_{M \in \mathcal{M}_h} \sqrt{\tau_{u, SU, M} \|\mathbf{a}_M\|_{L^\infty(t_0, t; L^\infty(M))}^2 + d\tau_{u, gd, M}}$.

Proof. [DAL15, Lemma 3.1] and [ADL15a, Remark 3.2] □

3.1.2 Quasi-Optimal Error Estimates

As in [MT15], we are interested in semi-robust methods of order k , i.e., there exists a constant $C > 0$, independent on critical data (like ν and h) such that for $0 \leq t \leq T$

$$\begin{aligned} \|\mathbf{e}_u\|_{L^\infty(t_0, t; L^2(\Omega))}^2 + \int_{t_0}^t \|\mathbf{e}_u\|_{LPS_u}^2 ds \\ \leq Ch^{2k} \left(\|\mathbf{u}\|_{L^2(t_0, t; W^{k+1, 2}(\Omega))}^2 + \|\partial_t \mathbf{u}\|_{L^2(t_0, t; W^{k, 2}(\Omega))}^2 + |p|_{L^2(t_0, t; W^{k, 2}(\Omega))}^2 \right) \end{aligned} \quad (3.5)$$

where $h := \max_M h_M$.

In a first step, we improved the results of Matthies & Tobiska [MT15] for vanishing reaction-type term $\sigma \mathbf{u}$. The basic tool is to work in the space \mathbf{V}_h^{div} . In a second step, a (mild) mesh restriction is removed. Finally, we identified methods of order $k + \frac{1}{2}$ for $\nu \leq Ch$.

Remark 3.1.5. We restrict ourselves here to velocity estimates. Using the discrete inf-sup condition, we can recover convergence results rates for the kinematic pressure afterwards.

In the following, we assume stricter regularity according to

$$\mathbf{u} \in [L^2(t_0, T; V) \cap L^\infty(t_0, T; L^2(\Omega)) \cap L^\infty(t_0, T; W^{1, \infty}(\Omega))]^d.$$

Methods of order k without compatibility condition

In the following, we assume that Assumptions 2.3.1, 2.5.2, 2.5.1 and 2.5.3 are valid with a divergence-preserving interpolation operator j_u . Furthermore, we consider $k := k_u = k_p + 1$. Then we can give a discretization error result for the velocity:

Theorem 3.1.6.

Assume for the initialization that $\mathbf{u}_h(t_0) = j_u \mathbf{u}_0$. We obtain for the discrete velocity approximation $\mathbf{e}_u \in L^\infty(t_0, T; L^2(\Omega)) \cap L^2(t_0, T; \mathbf{V}_h^{div})$ of the LPS-method (3.2):

$$\begin{aligned}
& \|\mathbf{e}_u\|_{L^\infty(t_0, T; L^2(\Omega))}^2 + \int_{t_0}^t \|\mathbf{e}_u(\tau)\|_{LPS_u}^2 d\tau \\
& \leq \sum_{M \in \mathcal{M}_h} \int_{t_0}^t e^{C_G(\mathbf{u})(t-\tau)} \left((\nu + \tau_{u, SU, M} |\mathbf{a}_M|^2 + d\tau_{u, gd, M}) \|\nabla \boldsymbol{\eta}_u(\tau)\|_{0, M}^2 \right. \\
& \quad \left. + \frac{\|\mathbf{a}\|_{L^\infty(M)}^2}{\nu} \|\boldsymbol{\eta}_u(\tau)\|_{0, M}^2 + \min \left\{ \frac{d}{\nu}, \frac{1}{\tau_{u, gd, M}} \right\} \|\eta_p(\tau)\|_{0, M}^2 \right. \\
& \quad \left. + \|\partial_t \boldsymbol{\eta}_u(\tau)\|_{0, M}^2 + \tau_{u, SU, M} |\mathbf{a}_M|^2 \|\kappa_M(\nabla \mathbf{u})(\tau)\|_{0, M}^2 \right) d\tau
\end{aligned} \tag{3.6}$$

where $\mathbf{a} := \mathbf{u}_h$ in the Navier-Stokes case. Furthermore, the Gronwall constant can be chosen as $C_G^{Oseen}(\mathbf{u}) = 1$ for the Oseen problem and

$$C_G^{NSE}(\mathbf{u}) = 1 + C \|\mathbf{u}\|_{L^\infty(t_0, T; W^{1, \infty}(\Omega))} + C \max_{M \in \mathcal{M}_h} \left\{ \frac{h_M^2}{\tau_{u, gd, M}} \right\} \|\mathbf{u}\|_{L^\infty(t_0, T; W^{1, \infty}(\Omega))}$$

for the Navier-Stokes problem.

Proof. [DAL15, Theorem 4.1] and [ADL15a, Theorem 4.1] □

Corollary 3.1.7.

Let $\mathbf{u} \in L^\infty(t_0, T; L^2(\Omega)) \cap L^2(t_0, T; V)$, $p \in L^2(t_0, T; L^2(\Omega))$ and $\partial_t \mathbf{u} \in L^2(t_0, T; L^2(\Omega))$. Then estimate (3.6) implies strong velocity convergence of the semi-discrete LPS-method in $L^\infty(t_0, T; L^2(\Omega)) \cap L^2(t_0, T; V)$.

Proof. [DAL15, Corollary 4.3] and [ADL15a, Corollary 4.1] □

Corollary 3.1.8.

Assume additionally a smooth solution of the time-dependent (Oseen or Navier-Stokes) problem according to

$$\mathbf{u} \in L^2(t_0, T; [W^{k+1, 2}(\Omega)]^d), \quad \partial_t \mathbf{u} \in L^2(t_0, T; [W^{k, 2}(\Omega)]^d), \quad p \in L^2(t_0, T; W^{k, 2}(\Omega)).$$

Provided $\mathbf{u}_h(t_0) = j_u \mathbf{u}_0$, we obtain for $t_0 \leq t \leq T$ the semi-discrete a priori estimate for the approximation $\mathbf{e}_u = \mathbf{u}_h - j_u \mathbf{u}$ of the LPS-method (3.2):

$$\begin{aligned}
& \|\mathbf{e}_u\|_{L^\infty(t_0, t; L^2(\Omega))}^2 + \int_{t_0}^t \|\mathbf{e}_u(\tau)\|_{LPS_u}^2 d\tau \\
& \leq C \sum_{M \in \mathcal{M}_h} h_M^{2k} \int_{t_0}^t e^{C_G(\mathbf{u})(t-\tau)} \left((\nu(1 + Re_M^2) + \tau_{u, SU, M} |\mathbf{a}_M|^2 + d\tau_{u, gd, M}) |\mathbf{u}(\tau)|_{W^{k+1, 2}(\omega_M)}^2 \right. \\
& \quad + \tau_{u, SU, M} |\mathbf{a}_M|^2 h_M^{2(s-k)} |\mathbf{u}(\tau)|_{W^{s+1, 2}(\omega_M)}^2 + \|\partial_t \mathbf{u}(\tau)\|_{W^{k, 2}(\omega_M)}^2 \\
& \quad \left. + \min \left\{ \frac{d}{\nu}, \frac{1}{\tau_{u, gd, M}} \right\} |p(\tau)|_{W^{k, 2}(\omega_M)}^2 \right) d\tau
\end{aligned} \tag{3.7}$$

with the previously defined Gronwall constant $C_G(\mathbf{u})$, the mesh Reynolds number $Re_M := \frac{h_M \|\mathbf{a}\|_{L^\infty(M)}}{\nu}$ and $s \in \{0, \dots, k\}$.

Proof. [DAL15, Corollary 4.4] and [ADL15a, Corollary 4.2] □

Remark 3.1.9. With a parameter choice according to

$$\tau_{u, gd, M} = \tau_{u, gd, 0}, \quad \tau_{u, SU, M} \leq \tau_0 \frac{h_M^{2(k-s)}}{|\mathbf{a}_M|^2} \tag{3.8}$$

(where $\mathbf{a} = \mathbf{u}_h$ in the Navier-Stokes case) we obtain a semi-robust method of order k in the sense of (3.5) provided that it holds

$$Re_M = \frac{h_M \|\mathbf{a}\|_{L^\infty(M)}}{\nu} \leq \frac{1}{\sqrt{\nu}}. \tag{3.9}$$

In particular, the bound for the discretization error does not depend on ν and the estimate is semi-robust. For the Navier-Stokes problem, this result strongly depends on the following estimate of the convective term.

Lemma 3.1.10.

For the difference of the convective terms, we obtain

$$\begin{aligned}
& c(\mathbf{u}; \mathbf{u}, \mathbf{e}_h) - c(\mathbf{u}_h; \mathbf{u}_h, \mathbf{e}_h) \\
& \leq \frac{1}{4\varepsilon} \sum_{M \in \mathcal{M}_h} \frac{1 + \nu Re_M^2}{h_M^2} \|\boldsymbol{\eta}_u\|_{L^2(M)}^2 + 3\varepsilon \|\boldsymbol{\eta}_u\|_{LPS}^2 + 4\varepsilon \|\mathbf{e}_h\|_{LPS}^2 \\
& \quad + \left[\|\mathbf{u}\|_{W^{1, \infty}(\Omega)} + \left(\varepsilon h^2 + \frac{C}{\varepsilon} \max_{M \in \mathcal{M}_h} \frac{h^2}{\gamma_M} \right) \|\mathbf{u}\|_{W^{1, \infty}(\Omega)} \right] \|\mathbf{e}_h\|_{L^2(\Omega)}^2
\end{aligned}$$

with the local Reynolds number $Re_M := h_M \|\mathbf{u}\|_{L^\infty(M)} / \nu$.

Proof. [ADL15a, Lemma 7.1] □

Remark 3.1.11. Possible variants of the triples $\mathbf{V}_h/Q_h/D_M$ are

- One-level methods:

$$\mathbb{P}_k/\mathbb{P}_{k-1}/\mathbb{P}_s, \quad \mathbb{Q}_k/\mathbb{Q}_{k-1}/\mathbb{Q}_s, \quad \mathbb{P}_k^+/\mathbb{P}_{-(k-1)}/\mathbb{P}_s, \quad \mathbb{Q}_k/\mathbb{P}_{-(k-1)}/\mathbb{P}_s$$

- Two-level methods:

$$\mathbb{P}_k/\mathbb{P}_{k-1}/\mathbb{P}_s, \quad \mathbb{Q}_k/\mathbb{Q}_{k-1}/\mathbb{Q}_s, \quad \mathbb{P}_k^+/\mathbb{P}_{-(k-1)}/\mathbb{P}_s, \quad \mathbb{Q}_k/\mathbb{P}_{-(k-1)}/\mathbb{P}_s$$

with $s \in \{0, 1, \dots, k-1\}$.

Methods of order k with compatibility condition

In order to avoid the mesh size restriction $Re_M \leq \frac{1}{\sqrt{\nu}}$ in (3.9), we need to improve the estimate of the convective term. First, we want to state another assumption with respect to the streamline approximation of the velocity in the Navier-Stokes case:

Assumption 3.1.12.

The streamline direction \mathbf{u}_M satisfies

$$\|\mathbf{u}_M - \mathbf{u}\|_{\infty, M} \leq Ch_M \|\mathbf{u}\|_{1, \infty} \quad \forall M \in \mathcal{M}_h.$$

Furthermore, we consider special choices of coarse and fine spaces that fulfill the following compatibility condition.

Assumption 3.1.13.

For $Y_{h,k}(M) = \{\mathbf{v}_h|_M : \mathbf{v}_h \in Y_{h,k}, \mathbf{v}_h = 0 \text{ on } \Omega \setminus M\}$ there exists $\tilde{\beta}_{u,h} > 0$ such that

$$\inf_{\mathbf{w}_h \in D_M} \sup_{\mathbf{v}_h \in Y_{h,k}(M)} \frac{(\mathbf{v}_h, \mathbf{w}_h)_M}{\|\mathbf{v}_h\|_{0, M} \|\mathbf{w}_h\|_{0, M}} \geq \tilde{\beta}_{u,h}. \quad (3.10)$$

Sufficient conditions on the meshes $\mathcal{T}_h, \mathcal{M}_h$, the fine and coarse spaces can be found in [MST07]. In particular, for the one-level approach with $\mathcal{T}_h = \mathcal{M}_h$, one has to enrich the velocity space by local bubble functions.

Lemma 3.1.14.

Let Assumption 3.1.13 be valid. Then there is an interpolation operator $i: \mathbf{V} \rightarrow \mathbf{V}_h$ such that for $1 \leq l \leq k+1$

$$\begin{aligned} (\mathbf{v} - i\mathbf{v}, \mathbf{w}_h) &= 0 & \forall \mathbf{w}_h \in D_h^u &:= \bigoplus D_M, \quad \mathbf{v} \in \mathbf{V}, \\ \|\mathbf{v} - i\mathbf{v}\|_{0, M} + h_M \|\mathbf{v} - i\mathbf{v}\|_{W^{1,2}(M)} &\leq Ch_M^l \|\mathbf{v}\|_{W^{l,2}(\omega_M)} & \forall \mathbf{v} \in \mathbf{V} \cap [H^l(\Omega)]^d. \end{aligned} \quad (3.11)$$

Proof. See Matthies et al. [MST07]. \square

In consequence, the interpolation operator $j_u: \mathbf{V} \rightarrow \mathbf{V}_h$ does in general not act in \mathbf{V}_h^{div} and the previously presented analysis leading to Theorem 3.1.6 has to be modified. In particular, the term $(\nabla \cdot \boldsymbol{\eta}_u, \eta_p)$ has to be handled. In case the discrete ansatz space for the kinematic pressure is discontinuous, we need to include an additional edge stabilization. For consistency we do not consider that in the following and just restrict ourselves to continuous kinematic pressure ansatz spaces.

Theorem 3.1.15.

With the additional Assumption 3.1.13 we obtain for $t_0 \leq t \leq T$ and $Q_h \supset \mathbb{P}_{k-1}$ the semi-discrete error estimate

$$\begin{aligned}
& \| \mathbf{e}_u \|_{L^\infty(t_0, t; L^2(\Omega))}^2 + \int_{t_0}^t \| |(\mathbf{e}_u, e_p)(\tau)| \|_{LPS_u}^2 d\tau \\
& \leq \sum_{M \in \mathcal{M}_h} \int_{t_0}^t e^{C_G(\mathbf{u})(t-\tau)} \left((\nu + \tau_{u, SU, M} |\mathbf{a}_M|^2 + d\tau_{u, gd, M}) \| \nabla \boldsymbol{\eta}_u(\tau) \|_{0, M}^2 + \frac{\| \boldsymbol{\eta}_u(\tau) \|_{0, M}^2}{\tau_{u, SU, M}} \right. \\
& \quad \left. + \tau_{u, SU, M} |\mathbf{a}_M|^2 \| \kappa_M(\nabla \mathbf{u})(\tau) \|_{0, M}^2 \right. \\
& \quad \left. + \min \left\{ \frac{d}{\nu}, \frac{1}{\tau_{u, gd, M}} \right\} \| \eta_p(\tau) \|_{0, M}^2 + \| \partial_t \boldsymbol{\eta}_u(\tau) \|_{0, M}^2 \right) d\tau
\end{aligned} \tag{3.12}$$

with the Gronwall constants

$$\begin{aligned}
C_G^{Oseen}(\mathbf{u}) &= 1 + C \max_{M \in \mathcal{M}_h} \tau_{u, SU, M} \| \mathbf{a} \|_{L^\infty(t_0, t; W^{1, \infty}(M))}^2 \\
C_G^{NSE}(\mathbf{u}) &= 1 + C \| \mathbf{u} \|_{L^\infty(t_0, T; W^{1, \infty}(\Omega))} \\
& \quad + C \max_{M \in \mathcal{M}_h} \left\{ \left(\frac{h_M^2}{\tau_{u, gd, M}} + \tau_{u, SU, M} \right) \| \mathbf{u} \|_{L^\infty(t_0, t; W^{1, \infty}(M))}^2 \right\}.
\end{aligned}$$

Proof. [DAL15, Theorem 4.8] and [ADL15a, Theorem 4.2] \square

Remark 3.1.16. Assumption 3.1.12 can be replaced by one corresponding to the discrete solution:

Assumption 3.1.17.

The streamline direction \mathbf{u}_M satisfies

$$\| \mathbf{u}_h - \mathbf{u}_M \|_{\infty, M} \leq Ch_M \| \mathbf{u}_h \|_{1, \infty} \quad \forall M \in \mathcal{M}_h.$$

Then the Gronwall constant in the Navier-Stokes case changes to

$$C_G^{NSE}(\mathbf{u}) = 1 + C|\mathbf{u}|_{L^\infty(t_0, T; W^{1, \infty}(\Omega))} + C \max_{M \in \mathcal{M}_h} \left\{ \frac{h_M^2}{\tau_{u, gd, M}} \|\mathbf{u}\|_{L^\infty(t_0, t; W^{1, \infty}(M))}^2 \right\} \\ + C \max_{M \in \mathcal{M}_h} \{ \tau_{u, SU, M} \|\mathbf{u}_h\|_{L^\infty(t_0, t; W^{1, \infty}(M))}^2 \}.$$

In this case, the above estimate is no longer a priori.

Corollary 3.1.18.

For the discretization error, it holds the estimate

$$\|e_u\|_{L^\infty(t_0, T); L^2(\Omega)}^2 + \int_{t_0}^t \| |(e_u, e_p)(\tau)| \|_{LPS_u}^2 d\tau \\ \leq C \sum_{M \in \mathcal{M}_h} h_M^{2k} \int_{t_0}^t e^{C_G(\mathbf{u})(t-\tau)} \left((\nu + \tau_{u, SU, M} |\mathbf{a}_M|^2 + d\tau_{u, gd, M} + \frac{h_M^2}{\tau_{u, SU, M}}) |\mathbf{u}(\tau)|_{W^{k+1, 2}(\omega_M)}^2 \right. \\ \left. + \tau_{u, SU, M} |\mathbf{a}_M|^2 h_M^{2(s-k)} |\mathbf{u}(\tau)|_{W^{s+1, 2}(\omega_M)} + \|\partial_t \mathbf{u}(\tau)\|_{W^{k, 2}(\omega_M)}^2 \right. \\ \left. + \min \left\{ \frac{d}{\nu}, \frac{1}{\tau_{u, gd, M}} \right\} |p(\tau)|_{W^{k, 2}(\omega_M)}^2 \right) d\tau \quad (3.13)$$

with the previously defined Gronwall constant $C_G(\mathbf{u})$.

Proof. [DAL15, Corollary 4.9] and [ADL15a, Corollary 4.3] □

Remark 3.1.19. Regarding the stabilization parameters, we obtain from formula (3.13) that a method of order k results from

$$\tau_{u, gd, M} = \tau_{u, gd, 0}, \quad \underline{\tau}_0 h_M^2 \leq \tau_{u, SU, M} \leq \bar{\tau}_0 \frac{h_M^{2(k-s)}}{|\mathbf{a}_M|^2} \quad (3.14)$$

with $s \in \{k-1, k\}$ and tuning constants $\tau_{u, gd, 0}, \underline{\tau}_0, \bar{\tau}_0 = \mathcal{O}(1)$.

Remark 3.1.20. According to [MST07; MT15], the following choices of ansatz spaces satisfy the critical Assumption 3.1.13:

- One-level methods:

$$\mathbb{P}_k^+ / \mathbb{P}_{k-1} / \mathbb{P}_{k-1}, \quad \mathbb{P}_k^+ / \mathbb{P}_{-(k-1)} / \mathbb{P}_{k-1}, \quad \mathbb{Q}_k / \mathbb{P}_{-(k-1)} / \mathbb{P}_{k-1}$$

- Two-level methods:

$$\mathbb{P}_k / \mathbb{P}_{k-1} / \mathbb{P}_{k-1}, \quad \mathbb{Q}_k / \mathbb{Q}_{k-1} / \mathbb{P}_{k-1}, \quad \mathbb{P}_k^+ / \mathbb{P}_{-(k-1)} / \mathbb{P}_{k-1}, \quad \mathbb{Q}_k / \mathbb{P}_{-(k-1)} / \mathbb{P}_{k-1}$$

Methods of order $k + \frac{1}{2}$ with compatibility condition

We now restrict ourselves to one-level methods ($\mathcal{M}_h = \mathcal{T}_h$) with $\mathbf{V}_h = \mathbb{P}_k^+$, $Q_h = \mathbb{P}_k$, $D_M = \mathbb{P}_{k-1}$ and $k \geq 1$ and assume $\nu \leq Ch$.

Corollary 3.1.21.

For $t \in [t_0, T]$ the error estimate

$$\begin{aligned} & \|e_u\|_{L^\infty(t_0, t); L^2(\Omega)}^2 + \int_{t_0}^t \|(\mathbf{e}_u, e_p)(\tau)\|_{LPS_u}^2 d\tau \\ & \leq C \sum_{M \in \mathcal{M}_h} h_M^{2k} \int_{t_0}^t e^{C_G(\mathbf{u})(t-\tau)} \left((\nu + \tau_{u, SU, M} |\mathbf{a}_M|^2 + d\tau_{u, gd, M} + \frac{h_M^2}{\tau_{u, SU, M}}) |\mathbf{u}(\tau)|_{W^{k+1, 2}(\omega_M)}^2 \right. \\ & \quad \left. + h_M^2 \|\partial_t \mathbf{u}(\tau)\|_{W^{k+1, 2}(\omega_M)}^2 + h_M^2 \left(\min \left\{ \frac{d}{\nu}, \frac{1}{\tau_{u, gd, M}} \right\} \right) |p(\tau)|_{W^{k+1, 2}(\omega_M)}^2 \right) d\tau \end{aligned} \quad (3.15)$$

holds with the same Gronwall as in Corollary 3.1.15.

Proof. [DAL15, Corollary 4.11] and [ADL15a, Corollary 4.4] □

Remark 3.1.22. Choosing the stabilization parameters according to

$$\tau_{u, SU, M} = \tau_{u, SU, 0} h_M, \quad \tau_{u, gd, M} = \tau_{u, gd, 0} h_M \quad (3.16)$$

with tuning constants $\tau_0, \tau_{u, gd, 0} = \mathcal{O}(1)$, we obtain a method of order $k + \frac{1}{2}$ in the sense of [MST07]. This means that the discretization error estimates are superconvergent with respect to the assumptions on the interpolation error estimates in $H^1(\Omega)$.

3.2 Directional Do-Nothing Boundary Conditions

So far we only considered the case of homogeneous boundary conditions. In [ABL15], we were able to extend the results from the previous section for the grad-div and LPS-SU stabilized model to outflow boundaries.

3.2.1 Description of the Model

In case there is a boundary $\Gamma_{out} \subset \partial\Omega$ on which we do not prescribe Dirichlet boundary, the continuous model (2.9) implies that the so called ‘‘do-nothing condition’’

$$\nu \nabla \mathbf{u} \cdot \mathbf{n} - p \mathbf{n} = 0 \quad \text{at } \Gamma_{out}$$

holds. This is a common way to deal with the situation in which one wants to model the flow in a domain that is much larger than Ω under the assumption that the influence from the unmodeled larger part is negligible.

A typical case is a channel in which an object is placed. We specify the inflow profile and assume homogeneous Dirichlet boundary conditions on the side walls of the channel. In flow direction, we assume that the channel is infinitely long. For numerical simulations, we want to consider a bounded domain and hence need to cut the channel at a face Γ_{out} . Unfortunately, the missing control over inflow at Γ_{out} leads to problems when proving existence and stability of weak solutions for the Navier-Stokes equations, see [HRT96]. These stability issues can also be observed numerically.

In order to circumvent this disadvantage, we consider here the so-called “directional-do-nothing condition” [Bra15] that is given by

$$\nu \nabla \mathbf{u} \cdot \mathbf{n} - p \mathbf{n} - \beta (\mathbf{u} \cdot \mathbf{n})_- \mathbf{u} = 0 \quad \text{at } \Gamma_{out} \quad (3.17)$$

where $\beta > 0$. If there is no inflow at Γ_{out} ($\mathbf{u} \cdot \mathbf{n} \geq 0$), the additional term $\beta (\mathbf{u} \cdot \mathbf{n})_-$ vanishes and this condition reduces to the “do-nothing condition”. For this approach, existence of weak solutions is proved in [BMZ14].

The weak formulation that arises differs only by the formulation of the convective term

$$c_u^{DDN}(\mathbf{w}; \mathbf{u}, \mathbf{v}) := c_u(\mathbf{w}; \mathbf{u}, \mathbf{v}) + \int_{\Gamma_{out}} \left(\frac{1}{2} (\mathbf{w} \cdot \mathbf{n}) - \beta (\mathbf{w} \cdot \mathbf{n})_- \right) \mathbf{u} \cdot \mathbf{v} \, ds$$

that is not skew-symmetric anymore. Due to the different boundary condition the ansatz space, the ansatz space for the velocity changes to

$$\mathbf{V}^{DDN} := \{ \mathbf{u} \in H^1(\Omega)^d : \mathbf{u}|_{\partial\Omega \setminus \Gamma_{out}} = 0 \}.$$

The stabilized discrete problem also just differs by the convective term from the case of homogeneous boundary conditions.

3.2.2 Stability

If we test the weak discrete formulation symmetrically, we observe

$$\begin{aligned} & \frac{1}{2} \partial_t \|\mathbf{u}\|_0^2 + \nu \|\mathbf{u}\|_0^2 + s_{u,SU}(\mathbf{u}_h; \mathbf{u}_h, \mathbf{u}_h) + s_{u,gd}(\mathbf{u}_h, \mathbf{u}_h) \\ & + \int_{\Gamma_{out}} \|\mathbf{u}_h\|^2 \left(\frac{1}{2} (\mathbf{u}_h \cdot \mathbf{n})_+ + \left(\frac{1}{2} - \beta \right) (\mathbf{u}_h \cdot \mathbf{n})_- \right) \, ds \leq \|\mathbf{f}_u\|_0 \|\mathbf{u}_h\|_0. \end{aligned}$$

In particular, for $\beta \geq \frac{1}{2}$ we achieve stability of the discrete solution proceeding as in the proof of Lemma 3.1.1. For the continuous solution, the analogon to the above estimate gives existence of weak solutions, see [BMZ14], and uniqueness in case of small data, see [Bra15].

3.2.3 Error Estimates

We have seen that symmetric testing gives us some more control compared to the case of homogeneous Dirichlet boundary conditions and we define the stability norm here by

$$\begin{aligned} \|\mathbf{v}\|_{LPS_u}^2 &:= \nu \|\nabla \mathbf{v}\|_0^2 + s_{u,gd}(\mathbf{v}, \mathbf{v}) + s_{u,SU}(\mathbf{u}_h; \mathbf{v}, \mathbf{v}) \\ &\quad + \int_{\Gamma_{out}} \|\mathbf{u}_h\|^2 \left(\frac{1}{2} (\mathbf{u}_h \cdot \mathbf{n})_+ + \left(\frac{1}{2} - \beta \right) (\mathbf{u}_h \cdot \mathbf{n})_- \right) ds \quad \forall \mathbf{v} \in \mathbf{V}. \end{aligned}$$

With these preparations, assuming that the assumptions 2.5.2, 2.5.1 and 2.5.3 hold true with an divergence-preserving interpolation operator j_u , a convergence result can be derived for this case, too:

Theorem 3.2.1.

For sufficiently regular continuous solution \mathbf{u} , p and $\beta > 1/2$, it holds for the discretization error:

$$\|\mathbf{e}_u\|_{L^\infty(t_0, T; L^2(\Omega))}^2 + \int_{t_0}^T \|\mathbf{e}_u(t)\|_{LPS_u}^2 dt \leq C \int_{t_0}^T e^{C_G(\mathbf{u})(t-\tau)} \sum_{M \in \mathcal{M}_h} \phi_M(\tau) d\tau$$

with the Gronwall constant

$$C_G := c(1 + \|\mathbf{u}\|_{L^\infty(t_0, T; W^{1, \infty}(\Omega))} + h \|\mathbf{u}\|_{L^\infty(t_0, T; W^{1, \infty}(\Omega))}^2 + (1 + \nu^{-1}) \|\mathbf{u}\|_{L^\infty(\Gamma_{out})})$$

and the quantity ϕ_M depending on \mathbf{u} and on the interpolation errors $\boldsymbol{\eta}_u$, η_p

$$\phi_M := \|\partial_t \boldsymbol{\eta}_u\|_M^2 + (c_1 + c_3) \|\nabla \boldsymbol{\eta}_u\|_M^2 + c_2 \|\boldsymbol{\eta}_u\|_M^2 + c_3 \|\kappa_M(\nabla \mathbf{u})\|_M^2 + c_4 \|\eta_p\|_M^2$$

and coefficients c_1, \dots, c_4 :

$$c_1 = \nu + \tau_{u,gd,M}, \quad c_2 = h_M^{-2} + \nu^{-1} \|\mathbf{u}\|_{L^\infty(M)}, \quad c_3 = \tau_{u,SU,M} |\mathbf{u}|_M^2, \quad c_4 = (\nu + \tau_{u,gd,M})^{-1}.$$

Proof. [ABL15, Theorem 2] □

This estimate just differs from Corollary 3.1.8 by the additional term $\nu^{-1} \|\mathbf{u}\|_{L^\infty(\Gamma_{out})}$ in the Gronwall constant. In consequence, the estimate is no longer semi-robust and the error might deteriorate quickly in time for small ν . However, this estimate might not be sharp as we have never experienced such a behavior in our numerical results.

For the ansatz spaces, Theorem 3.2.1 suggests an equilibration of $\|\nabla \boldsymbol{\eta}_u\|_M^2$ and $\|\eta_p\|_M^2$. In view of Assumption 2.5.3, this means $k_u = k_{p+1}$. Finally, note that the resulting parameter bounds are the same as for homogeneous Dirichlet boundary conditions.

3.3 Non-Isothermal Flow

Now, we give up the assumption that the flow is isothermal and consider heat transport within the Oberbeck-Boussinesq model [Bou03; Obe79]. The semi-discretized approach in [DA15] allows for different coarse space for the velocity SU and the temperature SU stabilization. For simplicity, we here restrict ourselves to one coarse space \mathcal{M}_h .

For $\mathbf{v} \in \mathbf{V}$ and $\theta \in \Theta$, we define

$$\begin{aligned} \|\mathbf{v}\|_{LPS_u}^2 &:= \nu \|\nabla \mathbf{v}\|_0^2 + s_{u,SU}(\mathbf{u}_h; \mathbf{v}, \mathbf{v}) + s_{u,gd}(\mathbf{v}, \mathbf{v}), \\ \|\theta\|_{LPS_\theta}^2 &:= \alpha \|\nabla \theta\|_0^2 + s_{\theta,SU}(\mathbf{u}_h; \theta, \theta) \end{aligned}$$

similar to the previous sections.

3.3.1 Stability

We again start with a stability result that gives existence and uniqueness of the discrete solutions. The following result states the desired stability:

Theorem 3.3.1.

Assume $(\mathbf{u}_h, p_h, \theta_h) \in \mathbf{V}_h^{div} \times Q_h \times \Theta_h$ is a solution of (2.23), (2.25) with initial data $\mathbf{u}_h(t_0) \in [L^2(\Omega)]^d$, $\theta_h(t_0) \in L^2(\Omega)$ and $\mathbf{f}_u, f_\theta \in L^1(t_0, T; L^2(\Omega))$. For $t_0 \leq t \leq T$, we obtain

$$\begin{aligned} \|\theta_h\|_{L^\infty(t_0, t; L^2(\Omega))} &\leq \|\theta_h(t_0)\|_0 + \|f_\theta\|_{L^1(t_0, T; L^2(\Omega))} =: C_\theta(T, \theta_h(t_0), f_\theta), \\ \|\mathbf{u}_h\|_{L^\infty(t_0, t; L^2(\Omega))} &\leq \|\mathbf{u}_h(t_0)\|_0 + \|\mathbf{f}_u\|_{L^1(t_0, T; L^2(\Omega))} \\ &\quad + \beta \|\mathbf{g}\|_{L^1(t_0, T; L^\infty(\Omega))} \left(\|\theta_h(t_0)\|_0 + \|f_\theta\|_{L^1(t_0, T; L^2(\Omega))} \right) \\ &=: C_u(T, \mathbf{u}_h(t_0), \theta_h(t_0), \mathbf{f}_u, f_\theta), \\ \|\theta_h\|_{L^2(t_0, t; LPS)} &\leq C_\theta(T, \theta_h(t_0), f_\theta), \\ \|\mathbf{u}_h\|_{L^2(t_0, t; LPS)} &\leq C_u(T, \mathbf{u}_h(t_0), \theta_h(t_0), \mathbf{f}_u, f_\theta). \end{aligned}$$

Proof. [DA15, Theorem 1] □

Remark 3.3.2. The discrete inf-sup stability again yields a stability estimate of the kinematic pressure as well. The above theorem gives us existence of the semi-discrete quantities

due to Carathéodory's Existence Theorem. If we assume Lipschitz continuity in time for \mathbf{f}_u , f_θ and \mathbf{g} , the Picard-Lindelöf Theorem yields uniqueness of the solution.

3.3.2 Quasi-Optimal Semi-Discrete Error Estimates

In this section, we present quasi-optimal error estimates in the finite element setting introduced above.

Theorem 3.3.3.

Let $(\mathbf{u}, p, \theta): [t_0, T] \rightarrow \mathbf{V}^{div} \times Q \times \Theta$, $(\mathbf{u}_h, p_h, \theta_h): [t_0, T] \rightarrow \mathbf{V}_h^{div} \times Q_h \times \Theta_h$ be solutions of (2.9), (2.11) and (2.23), (2.25) satisfying

$$\begin{aligned} \mathbf{u} &\in L^\infty(t_0, T; [W^{1,\infty}(\Omega)]^d), & \partial_t \mathbf{u} &\in L^2(t_0, T; [L^2(\Omega)]^d), & p &\in L^2(t_0, T; Q \cap C(\Omega)), \\ \theta &\in L^\infty(t_0, T; W^{1,\infty}(\Omega)), & \partial_t \theta &\in L^2(t_0, T; L^2(\Omega)), & \mathbf{u}_h &\in L^\infty(t_0, T; [L^\infty(\Omega)]^d). \end{aligned}$$

Let Assumptions 2.5.1, 2.5.3, 2.5.5 be valid and $\mathbf{u}_h(t_0) = j_u \mathbf{u}_0$, $\theta_h(t_0) = j_\theta \theta_0$. We obtain for all $t_0 \leq t \leq T$ for the discretization errors:

$$\begin{aligned} &\|\mathbf{e}_{u,h}\|_{L^\infty(t_0,t;L^2(\Omega))}^2 + \|e_{\theta,h}\|_{L^\infty(t_0,t;L^2(\Omega))}^2 \\ &\quad + \int_{t_0}^t \left(\|\mathbf{e}_{u,h}(\tau)\|_{LPS}^2 + \|e_{\theta,h}(\tau)\|_{LPS}^2 \right) d\tau \\ &\lesssim \int_{t_0}^t e^{C_G(\mathbf{u},\theta,\mathbf{u}_h)(t-\tau)} \left\{ \sum_{M \in \mathcal{M}_h} \left[(\nu + \tau_{u,SU,M} |\mathbf{u}_M|^2 + \tau_{u,gd,M} d) \|\nabla \boldsymbol{\eta}_u(\tau)\|_{0,M}^2 \right. \right. \\ &\quad + h_M^{-2} \|\boldsymbol{\eta}_u(\tau)\|_{0,M}^2 + \|\partial_t \boldsymbol{\eta}_u(\tau)\|_{0,M}^2 \\ &\quad + \tau_{u,SU,M} |\mathbf{u}_M|^2 \|\kappa_M^u(\nabla \mathbf{u})(\tau)\|_{0,M}^2 + \min \left\{ \frac{d}{\nu}, \frac{1}{\tau_{u,gd,M}} \right\} \|\eta_p(\tau)\|_{0,M}^2 \Big] \\ &\quad + \sum_{M \in \mathcal{M}_h} \left[\|\partial_t \eta_\theta(\tau)\|_0^2 + \left(h_M^{-2} + \beta \|\mathbf{g}\|_{\infty,M} \right) \|\eta_\theta(\tau)\|_{0,M}^2 \right. \\ &\quad \left. \left. + (\alpha + \tau_{\theta,SU,M} |\mathbf{u}_M|^2) \|\nabla \eta_\theta(\tau)\|_{0,M}^2 + \tau_{\theta,SU,M} |\mathbf{u}_M|^2 \|\kappa_M^\theta(\nabla \theta)(\tau)\|_{0,M}^2 \right] \right\} d\tau \end{aligned}$$

with the Gronwall constant

$$\begin{aligned} C_G(\mathbf{u}, \theta, \mathbf{u}_h) &= 1 + \beta \|\mathbf{g}\|_\infty + |\mathbf{u}|_{W^{1,\infty}(\Omega)} + |\theta|_{W^{1,\infty}(\Omega)} + \|\mathbf{u}_h\|_\infty \\ &\quad + \max_{M \in \mathcal{M}_h} \{h_M^2 |\mathbf{u}|_{W^{1,\infty}(M)}^2\} + \max_{M \in \mathcal{M}_h} \left\{ \frac{h_M^2}{\tau_{u,gd,M}} |\mathbf{u}|_{W^{1,\infty}(M)}^2 \right\} \\ &\quad + \max_{M \in \mathcal{M}_h} \{\tau_{u,gd,M}^{-1} \|\mathbf{u}\|_{\infty,M}^2\} + \max_{M \in \mathcal{M}_h} \{h_M^2 |\theta|_{W^{1,\infty}(M)}^2\} \\ &\quad + \max_{M \in \mathcal{M}_h} \left\{ \frac{h_M^2}{\tau_{u,gd,M}} |\theta|_{W^{1,\infty}(M)}^2 \right\} + \max_{M \in \mathcal{M}_h} \{\tau_{u,gd,M}^{-1} \|\theta\|_{\infty,M}^2\}. \end{aligned} \tag{3.18}$$

Proof. [DA15, Theorem 2] □

This result can be used to obtain convergence results provided the continuous solutions are sufficiently smooth:

Corollary 3.3.4.

Consider a solution $(\mathbf{u}, p, \theta): [t_0, T] \rightarrow \mathbf{V}^{div} \times Q \times \Theta$ of (2.9), (2.11) satisfying

$$\begin{aligned} \mathbf{u} &\in L^\infty(t_0, T; [W^{1,\infty}(\Omega)]^d) \cap L^2(t_0, T; [W^{k_u+1,2}(\Omega)]^d), \\ \partial_t \mathbf{u} &\in L^2(t_0, T; [W^{k_u,2}(\Omega)]^d), \\ p &\in L^2(t_0, T; W^{k_p+1,2}(\Omega) \cap C(\Omega)), \\ \theta &\in L^\infty(t_0, T; W^{1,\infty}(\Omega)) \cap L^2(t_0, T; W^{k_\theta+1,2}(\Omega)), \\ \partial_t \theta &\in L^2(t_0, T; W^{k_\theta,2}(\Omega)) \end{aligned}$$

and a solution $(\mathbf{u}_h, p_h, \theta_h): [t_0, T] \rightarrow \mathbf{V}_h^{div} \times Q_h \times \Theta_h$ of (2.23), (2.25) satisfying $\mathbf{u}_h \in L^\infty(t_0, T; [L^\infty(\Omega)]^d)$. Let Assumptions 2.5.1, 2.5.3, 2.5.5 be valid as well as $\mathbf{u}_h(t_0) = j_u \mathbf{u}_0$, $\theta_h(t_0) = j_\theta \theta_0$ hold. For $t_0 \leq t \leq T$, we obtain the estimate for the semi-discrete error $\boldsymbol{\xi}_{u,h} = \mathbf{u} - \mathbf{u}_h$, $\xi_{\theta,h} = \theta - \theta_h$:

$$\begin{aligned} &\|\boldsymbol{\xi}_{u,h}\|_{L^\infty(t_0,t;L^2(\Omega))}^2 + \|\xi_{\theta,h}\|_{L^\infty(t_0,t;L^2(\Omega))}^2 \\ &\quad + \int_{t_0}^t \left(\|\boldsymbol{\xi}_{u,h}(\tau)\|_{LPS}^2 + \|\xi_{\theta,h}(\tau)\|_{LPS}^2 \right) d\tau \\ &\lesssim \int_{t_0}^t e^{C_G(\mathbf{u},\theta)(t-\tau)} \left\{ \sum_{M \in \mathcal{M}_h} h_M^{2(k_p+1)} \min \left\{ \frac{d}{\nu}, \frac{1}{\tau_{u,gd,M}} \right\} \|p(\tau)\|_{W^{k_p+1,2}(\omega_M)}^2 \right. \\ &\quad + \sum_{M \in \mathcal{M}_h} h_M^{2k_u} \left[(1 + \nu + \tau_{u,SU,M} |\mathbf{u}_M|^2 + \tau_{u,gd,M} d) \|\mathbf{u}(\tau)\|_{W^{k_u+1,2}(\omega_M)}^2 \right. \\ &\quad \quad \left. \left. + \|\partial_t \mathbf{u}(\tau)\|_{W^{k_u,2}(\omega_M)}^2 + \tau_{u,SU,M} |\mathbf{u}_M|^2 h_M^{2(s_u-k_u)} \|\mathbf{u}(\tau)\|_{W^{s_u+1,2}(\omega_M)}^2 \right] \right. \\ &\quad + \sum_{M \in \mathcal{M}_h} h_M^{2k_\theta} \left[\|\partial_t \theta(\tau)\|_{W^{k_\theta,2}(\omega_M)}^2 + \tau_{\theta,SU,M} |\mathbf{u}_M|^2 h_M^{2(s_\theta-k_\theta)} \|\theta(\tau)\|_{W^{s_\theta+1,2}(\omega_M)}^2 \right] \\ &\quad \left. + \left(1 + h_M^2 \beta \|\mathbf{g}\|_{\infty,M} + \alpha + \tau_{\theta,SU,M} |\mathbf{u}_M|^2 \right) \|\theta(\tau)\|_{W^{k_\theta+1,2}(\omega_M)}^2 \right\} d\tau \end{aligned} \tag{3.19}$$

with $s_u \in \{0, \dots, k_u\}$, $s_\theta \in \{0, \dots, k_\theta\}$ and a Gronwall constant as defined in Theorem 3.3.3.

Proof. [DA15, Corollary 1] □

Remark 3.3.5. Note that the above results do not provide a priori bounds since the Gronwall constant depends on $\|\mathbf{u}_h\|_\infty$. This allows us to prevent mesh width restrictions of the form

$$Re_M = \frac{h_M \|\mathbf{u}_h\|_{\infty, M}}{\nu} \leq \frac{1}{\sqrt{\nu}}, \quad Pe_M = \frac{h_M \|\mathbf{u}_h\|_{\infty, M}}{\alpha} \leq \frac{1}{\sqrt{\alpha}}$$

similar to the ones obtained in [ADL15a]. This is due to a different estimate of the convective terms. Namely, Lemma 3.1.10 is replaced by the following Lemma.

Lemma 3.3.6.

We can estimate the difference of the convective terms in the momentum equation for arbitrary $\varepsilon > 0$ by

$$\begin{aligned} & c_u(\mathbf{u}; \mathbf{u}, \mathbf{e}_{u,h}) - c_u(\mathbf{u}_h; \mathbf{u}_h, \mathbf{e}_{u,h}) \\ & \leq \frac{C}{\varepsilon} \sum_{M \in \mathcal{M}_h} \frac{1}{h_M^2} \|\boldsymbol{\eta}_u\|_{0,M}^2 + 3\varepsilon \|\boldsymbol{\eta}_u\|_{LPS}^2 + 3\varepsilon \|\mathbf{e}_{u,h}\|_{LPS}^2 \\ & \quad + \left[\|\mathbf{u}\|_{W^{1,\infty}(\Omega)} + \varepsilon \max_{M \in \mathcal{M}_h} \{h_M^2 |\mathbf{u}|_{W^{1,\infty}(M)}^2\} + \frac{C}{\varepsilon} \max_{M \in \mathcal{M}_h} \left\{ \frac{h_M^2}{\tau_{u,gd,M}} |\mathbf{u}|_{W^{1,\infty}(M)}^2 \right\} \right. \\ & \quad \left. + \frac{C}{\varepsilon} \max_{M \in \mathcal{M}_h} \{\tau_{u,gd,M}^{-1} \|\mathbf{u}\|_{\infty, M}^2 + \varepsilon \|\mathbf{u}_h\|_\infty^2\} \right] \|\mathbf{e}_{u,h}\|_0^2 \end{aligned}$$

with C independent of h_M , ε , the problem parameters and the solutions.

Proof. [DA15, Lemma 1] □

Remark 3.3.7. Provided a certain compatibility condition between fine and coarse ansatz spaces holds true (according to [MST07]), we can improve the above results similarly to the consideration in [ADL15a]. In particular, we obtain

$$\begin{aligned} & \|\mathbf{e}_{u,h}\|_{L^\infty(t_0,t;L^2(\Omega))}^2 + \|e_{\theta,h}\|_{L^\infty(t_0,t;L^2(\Omega))}^2 \\ & \quad + \int_{t_0}^t \left(\|\mathbf{e}_{u,h}(\tau)\|_{LPS}^2 + \|e_{\theta,h}(\tau)\|_{LPS}^2 \right) d\tau \\ & \leq C \int_{t_0}^t e^{C'_G(\mathbf{u},\theta,\mathbf{u}_h)(t-\tau)} \left\{ \sum_{M \in \mathcal{M}_h} \min \left\{ \frac{d}{\nu}, \frac{1}{\tau_{u,gd,M}} \right\} \|\boldsymbol{\eta}_p(\tau)\|_{0,M}^2 \right. \\ & \quad + \sum_{M \in \mathcal{M}_h} \left[(\nu + \tau_{u,SU,M} |\mathbf{u}_M|^2 + \tau_{u,gd,M} d) \|\nabla \boldsymbol{\eta}_u(\tau)\|_{0,M}^2 + \left(\frac{1}{h_M^2} + \frac{1}{\tau_{u,SU,M}} \right) \|\boldsymbol{\eta}_u(\tau)\|_{0,M}^2 \right. \\ & \quad \left. \left. + \|\partial_t \boldsymbol{\eta}_u(\tau)\|_{0,M}^2 + \tau_{u,SU,M} |\mathbf{u}_M|^2 \|\kappa_M^u(\nabla \mathbf{u})(\tau)\|_{0,M}^2 \right] \right. \\ & \quad \left. + \sum_{M \in \mathcal{M}_h} \left[(\alpha + \tau_{\theta,SU,M} |\mathbf{u}_M|^2) \|\nabla \eta_\theta(\tau)\|_{0,M}^2 + \left(\frac{1}{\tau_{\theta,SU,M}} + \beta \|\mathbf{g}\|_{\infty, M} \right) \|\eta_\theta(\tau)\|_{0,M}^2 \right] \right\} \end{aligned}$$

$$+ \tau_{\theta, SU, M} |\mathbf{u}_M|^2 \left[\kappa_M^\theta (\nabla \theta)(\tau) \|_{0, M}^2 + \|\partial_t \eta_\theta(\tau)\|_{0, M}^2 \right] \Big\} d\tau$$

with Gronwall constant

$$\begin{aligned} C'_G(\mathbf{u}, \theta, \mathbf{u}_h) &= 1 + \beta \|\mathbf{g}\|_\infty + |\mathbf{u}|_{W^{1, \infty}(\Omega)} + |\theta|_{W^{1, \infty}(\Omega)} \\ &+ \max_{M \in \mathcal{M}_h} \{h_M^2 |\mathbf{u}|_{W^{1, \infty}(M)}^2\} + \max_{M \in \mathcal{M}_h} \left\{ \frac{h_M^2}{\tau_{u, gd, M}} |\mathbf{u}|_{W^{1, \infty}(M)}^2 \right\} \\ &+ \max_{M \in \mathcal{M}_h} \{\tau_{u, gd, M}^{-1} \|\mathbf{u}\|_{\infty, M}^2\} + \max_{M \in \mathcal{M}_h} \{h_M^2 |\theta|_{W^{1, \infty}(M)}^2\} \\ &+ \max_{M \in \mathcal{M}_h} \left\{ \frac{h_M^2}{\tau_{u, gd, M}} |\theta|_{W^{1, \infty}(M)}^2 \right\} + \max_{M \in \mathcal{M}_h} \{\tau_{u, gd, M}^{-1} \|\theta\|_{\infty, M}^2\} \\ &+ \max_{M \in \mathcal{M}_h} \left\{ \tau_{u, SU, M} |\mathbf{u}_h|_{W^{1, \infty}(M)}^2 \right\} + \max_{M \in \mathcal{M}_h} \left\{ \tau_{\theta, SU, M} |\mathbf{u}_h|_{W^{1, \infty}(L)}^2 \right\}. \end{aligned}$$

The details for this can be found in [Dal15].

Remark 3.3.8. Again, the above estimates give us the possibility to derive an error estimate for the kinematic pressure via the discrete inf-sup condition. If

$$\mathbf{u} \in L^\infty(t_0, T; [W^{1, \infty}(\Omega)]^d), \quad \mathbf{u}_h \in L^\infty(t_0, T; [L^\infty(\Omega)]^d),$$

we obtain the estimate for the semi-discrete kinematic pressure error $\xi_{p, h} = p - p_h$ for $t_0 \leq t \leq T$

$$\begin{aligned} &\|\xi_{p, h}\|_{L^2(t_0, t; L^2(\Omega))}^2 \\ &\leq \frac{C}{\beta_d^2} \left\{ \|\partial_t \xi_{u, h}\|_{L^2(t_0, t; H^{-1}(\Omega))}^2 + \beta^2 \|\mathbf{g}\|_{L^\infty(t_0, t; L^\infty(\Omega))}^2 \|\xi_{\theta, h}\|_{L^2(t_0, t; L^2(\Omega))}^2 \right. \\ &\quad + (\|\mathbf{u}\|_{L^2(t_0, t; L^\infty(\Omega))}^2 + \|\mathbf{u}_h\|_{L^2(t_0, t; L^\infty(\Omega))}^2) \|\xi_{u, h}\|_{L^\infty(t_0, t; L^2(\Omega))}^2 \\ &\quad + \int_{t_0}^t \left(\nu + \max_{M \in \mathcal{M}_h} \{\tau_{u, gd, M}^{-1} \|\mathbf{u}_h\|_{\infty, M}^2\} \right. \\ &\quad \quad \left. + \max_{M \in \mathcal{M}_h} \{\tau_{u, SU, M} |\mathbf{u}_M|^2\} + \max_{M \in \mathcal{M}_h} \{\tau_{u, gd, M} d\} \right) \|\xi_{u, h}\|_{LPS}^2 d\tau \\ &\quad \left. + \int_{t_0}^t \max_{M \in \mathcal{M}_h} \{\tau_{u, SU, M} |\mathbf{u}_M|^2\} \sum_{M \in \mathcal{M}_h} \tau_{u, SU, M} |\mathbf{u}_M|^2 \|\kappa_M^u (\nabla \mathbf{u})\|_{0, M}^2 d\tau \right\} \end{aligned}$$

with a constant $C > 0$ independent of the problem parameters, h_M and the solutions.

3.3.3 Parameter Choice

For the ansatz spaces (3.19), suggests to choose

$$k := k_u = k_\theta = k_p + 1.$$

This is for example fulfilled if we choose Taylor-Hood elements $\mathbf{V}_h = \mathbb{Q}_k$, $Q_h = \mathbb{Q}_{k-1}$ and $\Theta_h = \mathbb{Q}_k$.

The presented error estimates motivate a parameter choice as

$$\begin{aligned} \tau_{u,gd,M} &= \tau_{u,gd,0}, \\ 0 \leq \tau_{u,SU,M} &\leq \tau_{u,SU,0} \frac{h_M^{2(k_u-s_u)}}{|\mathbf{u}_M|^2}, \\ 0 \leq \tau_{\theta,SU,M} &\leq \tau_{\theta,SU,0} \frac{h_M^{2(k_\theta-s_\theta)}}{|\mathbf{u}_M|^2} \end{aligned} \quad (3.20)$$

for $M \in \mathcal{M}_h$, where $\tau_{u,gd,0}, \tau_{u,SU,0}, \tau_{\theta,SU,0} = \mathcal{O}(1)$ denote non-negative tuning constants. For $\theta \equiv 0$ this reduces to the parameter bounds that we obtained for the Navier-Stokes equations.

Comparing the physical dimensions in the momentum equation (2.23) and the Fourier equation (2.25), we obtain

$$\begin{aligned} [\tau_{u,SU,M}] \frac{m^2}{s^4} &= [s_{u,SU}(\mathbf{u}_h; \mathbf{u}_h, \mathbf{u}_h)] = \left[\left(\frac{\partial \mathbf{u}_h}{\partial t}, \mathbf{u}_h \right) \right] = \frac{m^2}{s^3}, \\ [\tau_{\theta,SU,M}] \frac{K^2}{s^2} &= [s_{\theta,SU}(\mathbf{u}_h; \theta_h, \theta_h)] = \left[\left(\frac{\partial \theta_h}{\partial t}, \theta_h \right) \right] = \frac{K^2}{s}. \end{aligned}$$

This suggests a parameter design as

$$\tau_{\theta,SU,M} \sim h_M/|\mathbf{u}_M|, \quad \tau_{u,SU,M} \sim h_M/|\mathbf{u}_M|, \quad (3.21)$$

that is within the above (theoretical) parameter bounds. We will consider this choice in the numerical examples.

3.4 Incompressible Resistive Magnetohydrodynamics

Finally, we assume that the flow is isothermal again and consider the coupling with the Maxwell problem for an electrically conducting fluid [WAL15]. Here, we consider a linearized and stationary version of formulation (2.9), (2.10):

Find $\mathbf{U} := (\mathbf{u}, \mathbf{b}, p, r) \in \mathbf{V} \times \mathbf{C} \times Q \times S$ such that

$$\begin{aligned}
\mathcal{A}_G(\mathbf{U}, \mathbf{V}) &= \mathcal{F}_G(\mathbf{V}), \\
\mathcal{A}_G(\mathbf{U}, \mathbf{V}) &:= \nu(\nabla \mathbf{u}, \nabla \mathbf{v}) + c_u(\mathbf{a}; \mathbf{u}, \mathbf{v}) - (p, \nabla \cdot \mathbf{v}) - ((\nabla \times \mathbf{b}) \times \mathbf{d}, \mathbf{v}) \\
&\quad + (\nabla \cdot \mathbf{u}, q) - (\mathbf{b}, \nabla s) \\
&\quad + \lambda(\nabla \times \mathbf{b}, \nabla \times \mathbf{c}) + (\nabla r, \mathbf{c}) - (\nabla \times (\mathbf{u} \times \mathbf{d}), \mathbf{c}), \\
\mathcal{F}_G(\mathbf{V}) &:= (\mathbf{f}_u, \mathbf{v}) + (\mathbf{f}_b, \mathbf{c})
\end{aligned} \tag{3.22}$$

holds for all $\mathbf{V} := (\mathbf{v}, \mathbf{c}, q, s) \in \mathbf{V} \times \mathbf{C} \times Q \times S$. The quantities $\nabla \cdot \mathbf{a} = 0$, $\mathbf{a} \in L^\infty(\Omega)^d \cap H^1(\Omega)^d$ and $\mathbf{d} \in W^{1,\infty}(\Omega)^d \cap H^{curl}(\Omega)$ are prescribed approximations to the velocity and the magnetic field.

Remark 3.4.1. We can consider these equations as a problem that arises after time discretization with time step size Δt for an extrapolated velocity field \mathbf{a} and an extrapolated magnetic field \mathbf{b} in the limit $\Delta t \rightarrow \infty$.

Opposed to the considerations in [WAL15], we here restrict ourselves to inf-sup stable ansatz spaces for the fluid part that does not require any stabilization for the kinematic pressure. With the previous notations for the stabilization terms, we get here in summary

$$\begin{aligned}
\mathcal{S}_{lps}(\mathbf{U}_h, \mathbf{V}_h) &= s_{u,SU}(\mathbf{a}; \mathbf{u}_h, \mathbf{v}_h) + s_{u,gd}(\mathbf{u}_h, \mathbf{v}_h) + \tilde{s}_{u,Lor}(\mathbf{d}; \mathbf{u}_h, \mathbf{v}_h) \\
&\quad + s_{b,Ind}(\mathbf{d}; \mathbf{b}_h, \mathbf{c}_h) + s_{b,gd}(\mathbf{b}_h, \mathbf{c}_h) + s_{r,PSPG}(\nabla r_h, \nabla s_h)
\end{aligned} \tag{3.23}$$

for the stabilizations. The discretized formulation then reads:

Find $\mathbf{U}_h \in \mathbf{V}_h \times \mathbf{C}_h \times Q_h \times S_h$ such that

$$\mathcal{A}_{Stab}(\mathbf{U}_h, \mathbf{V}_h) := \mathcal{A}_G(\mathbf{U}_h, \mathbf{V}_h) + \mathcal{S}_{lps}(\mathbf{U}_h, \mathbf{V}_h) = \mathcal{F}_G(\mathbf{V}_h) \tag{3.24}$$

holds for all $\mathbf{V}_h \in \mathbf{V}_h \times \mathbf{C}_h \times Q_h \times S_h$.

3.4.1 Stability

As usual, we first consider the stability of the discretized solution that is going to give us existence and uniqueness.

The norm we want to control is again motivated by testing the discrete formulation symmetrically. In particular, we define for all $\mathbf{V} \in \mathbf{V} \times \mathbf{C} \times Q \times S$ the (weak) semi-norms

$$\begin{aligned}
\|\mathbf{V}\|_G &:= \left(\nu \|\nabla \mathbf{v}\|_0^2 + \lambda \|\nabla \times \mathbf{c}\|_0^2 \right)^{1/2}, \\
\|\mathbf{V}\|_{Stab} &:= \mathcal{S}_{lps}(\mathbf{V}, \mathbf{V})^{1/2}, \\
\|\mathbf{V}\|_w &:= \left(\|\mathbf{V}\|_G^2 + \|\mathbf{V}\|_{Stab}^2 \right)^{1/2}
\end{aligned}$$

and note $\mathcal{A}_{Stab}(\mathbf{v}, \mathbf{v}) = \|\mathbf{v}\|_w^2$ due to

$$((\nabla \times \mathbf{b}) \times \mathbf{d}, \mathbf{v}) = -(\nabla \times (\mathbf{v} \times \mathbf{d}), \mathbf{b})$$

and the skew-symmetry of the convective term $c_u(\mathbf{a}, \cdot, \cdot)$.

We introduce a problem length scale L_0 and define the following norms

$$\begin{aligned} \|\mathbf{v}\|_V &:= \frac{\sqrt{\nu}}{L_0} \|\mathbf{v}\|_0 + \sqrt{\nu} \|\nabla \mathbf{v}\|_0, & \|\mathbf{c}\|_C &:= \frac{\sqrt{\lambda}}{L_0} \|\mathbf{c}\|_0 + \sqrt{\lambda} \|\nabla \times \mathbf{c}\|_0, \\ \|q\|_Q &:= \frac{1}{\sqrt{\nu}} \|q\|_0, & \|s\|_S &:= \frac{1}{\sqrt{\lambda}} \|s\|_0 + \frac{L_0}{\sqrt{\lambda}} \|\nabla s\|_0 \end{aligned}$$

in the sense of consistent units and introduce the Galerkin norm

$$\|\mathbf{v}\|_{Gal} := (\|\mathbf{v}\|_V + \|\mathbf{c}\|_C + \|q\|_Q + \|s\|_S)^{1/2} \quad (3.25)$$

for the continuous problem. Finally, we consider a (strong) stabilized norm that combines the weak semi-norm with the L^2 parts of the Galerkin norm:

$$\|\|\mathbf{v}\|\|_s := \left(\|\|\mathbf{v}\|\|_w^2 + \frac{\nu}{L_0^2} \|\mathbf{v}\|_0^2 + \frac{\lambda}{L_0^2} \|\mathbf{c}\|_0^2 + \frac{1}{\nu} \|q\|_0^2 \right)^{1/2}.$$

Now, we can show stability for all considered quantities:

Corollary 3.4.2.

From the definition of the weak semi-norm, it follows immediately

$$\|\|\mathbf{u}_h\|\|_w \leq \sup_{\mathbf{v}_h \in \mathbf{V}_h \times \mathbf{C}_h \times Q_h \times S_h} \frac{\mathcal{F}_G(\mathbf{v}_h)}{\|\|\mathbf{v}_h\|\|_w}. \quad (3.26)$$

for the solution $\mathbf{u}_h \in \mathbf{V}_h \times \mathbf{C}_h \times Q_h \times S_h$ of the stabilized discrete problem.

Proof. [WAL15, Corollary 4.9] □

Remark 3.4.3. For the continuous problem a Poincaré type inequality

$$\|\mathbf{c}\|_0^2 \leq C(\|\nabla \times \mathbf{c}\|_0^2 + \|\mathbf{n} \times \mathbf{c}\|_{0, \partial\Omega}^2) \quad \forall \mathbf{c} \in H_0^{curl}(\Omega) \cap H_0^{div}(\Omega)$$

can be shown, cf. [Mon03, Corollary 3.51]. Hence, stability in the weak semi-norm implies stability with respect to $H^{curl}(\Omega)$ for the continuous problem.

Unfortunately, the discrete magnetic field is only weakly solenoidal and therefore this inequality is not applicable. In fact, we need to rely on proper estimates for the stabilization parameters:

Theorem 3.4.4.

For the solution $\mathbf{u}_h \in \mathbf{V}_h \times \mathbf{C}_h \times Q_h \times S_h$ of the stabilized discrete problem it holds in the strong norm

$$\|\mathbf{u}_h\|_s \leq C_1 \|\mathbf{u}_h\|_w + C_2 \sup_{(\mathbf{v}_h, s_h) \in \mathbf{V}_h \times S_h} \frac{|\mathcal{F}_G((\mathbf{v}_h, \mathbf{0}, 0, s_h))|}{\|(\mathbf{v}_h, \mathbf{0}, 0, s_h)\|_s} \quad (3.27)$$

where C_2, C_1 are given according to

$$\begin{aligned} C_1 &\sim C_2 \left(\max_{M \in \mathcal{M}_h} \left(\frac{\sqrt{\tau_{u,SU,M}} \|\mathbf{a}\|_{L^\infty(M)^d}}{\sqrt{\nu}} \right) + \max_{M \in \mathcal{M}_h} \left(\frac{\sqrt{\tau_{u,gd,M}}}{\sqrt{\nu}} \right) \right. \\ &\quad \left. + \max_{M \in \mathcal{M}_h} \left(\frac{\|\mathbf{d}\|_{L^\infty(M)^d} \sqrt{\tilde{\tau}_{u,Lor,M}}}{\sqrt{\nu}} \right) + \max_{M \in \mathcal{M}_h} \left(\frac{\sqrt{\tau_{r,PSPG,M}} \sqrt{\lambda}}{L_0} \right) \right), \\ C_2 &\sim \max_{M \in \mathcal{M}_h} \left(\frac{\|\mathbf{a}\|_{\infty, M} h_M}{\nu} \right) + \max_{M \in \mathcal{M}_h} \left(\frac{\|\mathbf{d}\|_{\infty, M} h_M}{\sqrt{\nu \lambda}} \right) + \max_{M \in \mathcal{M}_h} \left(\sqrt{\frac{\nu}{\tau_{u,gd,M}}} \right) \\ &\quad + \max_{M \in \mathcal{M}_h} \left(\frac{L_0}{\sqrt{\lambda \tau_{r,PSPG,M}}} \right) + \max_{M \in \mathcal{M}_h} \left(\frac{\|\mathbf{d}\|_{\infty, M}}{\sqrt{\nu \lambda}} \right) + \max_{M \in \mathcal{M}_h} \left(\frac{\sqrt{\lambda} h_M}{\sqrt{\tau_{b,gd,M} L_0}} \right). \end{aligned}$$

Proof. [WAL15, Theorem 4.10] □

Remark 3.4.5. The above estimate is a stability result provided the requirements

$$c\nu \leq \tau_{u,gd,M} \leq C, \quad c \frac{L_0^2}{\lambda} \leq \tau_{r,PSPG,M} \leq C, \quad c \frac{\lambda h_M^2}{L_0^2} \leq \tau_{b,gd,M} \leq C$$

are fulfilled.

3.4.2 Quasi-Optimal Error Estimates

Now, we are in position to state estimates for the discretization error. We start with estimates for sufficiently smooth solutions without a special choice of coarse spaces and try to cure the arising mesh width restrictions in case the LPS compatibility condition 3.1.13 holds. Finally, we are interested in the case $\mathbf{b} \in H^{curl}(\Omega) \setminus H^1(\Omega)$.

For shortening the notation we define for the splitting of the total error

$$\mathcal{H} := (\eta_u, \eta_b, \eta_p, \eta_r), \quad \mathbf{E}_h := (e_u, e_b, e_p, e_r).$$

Then we can state a common bound for a considered cases.

Lemma 3.4.6.

The total discretization error is bounded by

$$\|\mathbf{E}_h\|_{Gal}^2 + \|\mathbf{E}_h\|_{Stab}^2 \leq S_1^2 + S_2^2$$

where S_1 and S_2 are defined by

$$\begin{aligned} S_1 &:= \|\mathcal{H}\|_{Gal} + \left(\sum_{M \in \mathcal{M}_h} \frac{1}{\nu} \|\mathbf{a}\|_{\infty, M}^2 \|\boldsymbol{\eta}_u\|_{0, M}^2 \right)^{\frac{1}{2}} + \left(\sum_{M \in \mathcal{M}_h} \frac{1}{\lambda} \|\mathbf{d}\|_{\infty, M}^2 \|\boldsymbol{\eta}_u\|_{0, M}^2 \right)^{\frac{1}{2}} \\ &\quad + \left(\sum_{M \in \mathcal{M}_h} \nu^{-1} (1 + \sqrt{d})^2 (\|\mathbf{d}\|_{\infty, M} + \|\nabla \mathbf{d}\|_{\infty, M})^2 \|\boldsymbol{\eta}_b\|_{0, M}^2 \right)^{\frac{1}{2}}, \\ S_2 &:= \|\mathcal{H}\|_{Stab} + \|\mathcal{U}\|_{Stab} + \left(\sum_{M \in \mathcal{M}_h} \frac{1}{\tau_{u, gd, M}} \|\boldsymbol{\eta}_p\|_{0, M}^2 \right)^{\frac{1}{2}} + \left(\sum_{M \in \mathcal{M}_h} \frac{1}{\tau_{b, gd, M}} \|\boldsymbol{\eta}_b\|_{0, M}^2 \right)^{\frac{1}{2}} \end{aligned}$$

Proof. [WAL15, Lemma 5.1] □

Error Estimates for Smooth Solutions without LPS-Compatibility

If we now consider sufficiently smooth solutions, we can estimate the remaining terms in S_1 and S_2 and achieve:

Theorem 3.4.7.

The approximation properties of the FE spaces and the local L^2 -projector yield in case $\mathcal{U} \in [H^{k+1}(\Omega)]^d \times [H^{k+1}(\Omega)]^d \times H^k(\Omega) \times H^k(\Omega)$ for the total discretization error the bound

$$\|\mathbf{E}_h\|_{Gal}^2 + \|\mathbf{E}_h\|_{Stab}^2 \leq S_1^2 + S_2^2$$

where S_1 and S_2 can be bounded by

$$\begin{aligned} S_1^2 &\leq C \sum_{M \in \mathcal{M}_h} h_M^{2k} \left[\left(\nu (1 + \frac{\|\mathbf{a}\|_{\infty, M}^2 h_M^2}{\nu^2}) + \lambda \frac{\|\mathbf{d}\|_{\infty, M}^2 h_M^2}{\lambda^2} \right) |\mathbf{u}|_{k+1, 2, M}^2 \right. \\ &\quad \left. + \left(\lambda + \frac{h_M^2}{\nu} (\|\mathbf{d}\|_{\infty, M} + \|\nabla \mathbf{d}\|_{\infty, M})^2 \right) |\mathbf{b}|_{k+1, 2, M}^2 \right], \\ S_2^2 &\leq C \sum_{M \in \mathcal{M}_h} h_M^{2k} \left[\tau_{u, gd, M} |\mathbf{u}|_{k+1, 2, M}^2 + h_M^{2(s-k)} (\tau_{u, SU, M} |\mathbf{a}_M|^2 + \tau_{b, Ind, M} |\mathbf{d}_M|^2) |\mathbf{u}|_{s+1, 2, M}^2 \right. \\ &\quad \left. + \frac{1}{\tau_{u, gd, M}} |p|_{k, 2, M}^2 + h_M^{2(s-k)} \tilde{\tau}_{u, Lor, M} |\mathbf{d}_M|^2 |\mathbf{b}|_{s+1, 2, M}^2 \right. \\ &\quad \left. + (\tau_{r, PSPG, M} + \frac{h_M^2}{\tau_{b, gd, M}}) |\mathbf{b}|_{k+1, 2, M}^2 \right]. \end{aligned}$$

Proof. [WAL15, Theorem 5.2] □

Denote the local fluid and magnetic Reynolds numbers by

$$Re_{f,M} := \|\mathbf{a}\|_{\infty,M} h_M / \nu, \quad Re_{m,M} := \|\mathbf{d}\|_{\infty,M} h_M / \lambda$$

respectively.

An equilibration of the terms in S_1^2 according to

$$\begin{aligned} \nu \left(1 + \frac{\|\mathbf{a}\|_{\infty,M}^2 h_M^2}{\nu^2} \right) + \lambda \frac{\|\mathbf{d}\|_{\infty,M}^2 h_M^2}{\lambda^2} &\sim 1, \\ \lambda + \frac{h_M^2}{\nu} (\|\mathbf{d}\|_{\infty,M} + \|\nabla \mathbf{d}\|_{\infty,M})^2 &\sim 1 \end{aligned}$$

leads to the following (mild) restrictions on the local mesh width h_M :

$$\sqrt{\nu} Re_{f,M} \leq C, \quad \sqrt{\lambda} Re_{m,M} \leq C, \quad h_M (\|\mathbf{d}\|_{\infty,M} + \|\nabla \mathbf{d}\|_{\infty,M}) \leq C \sqrt{\nu}. \quad (3.28)$$

Equilibration of terms in S_2^2 and comparison to S_1^2 yields

$$\begin{aligned} \tau_{u,SU,M} |\mathbf{a}_M|^2 + \tau_{b,Ind,M} |\mathbf{d}_M|^2 &\sim h_M^{2(k-s)}, & \tau_{u,gd,M} &\sim 1, \\ \tilde{\tau}_{u,Lor,M} |\mathbf{d}_M|^2 &\sim h_M^{2(k-s)}, & \tau_{r,PSPG,M} + \frac{h_M^2}{\tau_{b,gd,M}} &\sim 1. \end{aligned} \quad (3.29)$$

This leads to the following bounds on the stabilization parameters:

$$\begin{aligned} 0 \leq \tau_{u,SU,M} \leq C \frac{h_M^{2(k-s)}}{|\mathbf{a}_M|^2}, & \quad \tau_{u,gd,M} \sim 1, & \quad 0 \leq \tilde{\tau}_{u,Lor,M}, \tau_{b,Ind,M} \leq C \frac{h_M^{2(k-s)}}{|\mathbf{d}_M|^2}, \\ \tau_{b,gd,M} \sim \frac{L_0^2}{\lambda}, & \quad \tau_{r,PSPG,M} \sim \frac{h_M^2 \lambda}{L_0^2}. \end{aligned} \quad (3.30)$$

Remark 3.4.8. Provided the magnetic field satisfies at least $\mathbf{b} \in [H^1(\Omega)]^d$, it is possible to come up with a slightly different analysis that does not require PSPG stabilization for the magnetic pseudo-pressure. In this case, the grad-div stabilization parameter has to satisfy $\tau_{b,gd} \lesssim 1$. This gives the possibility to obtain much more control over the divergence constraint. We will consider this approach for the analysis of the fully discretized problem.

Error Estimates for Smooth Solutions with LPS-Compatibility

Similar to the Navier-Stokes equations, we want here to remove the mesh width restriction by carefully choosing ansatz spaces that satisfy the LPS compatibility condition 3.1.13 for the velocity ansatz spaces and the ansatz spaces for the magnetic field. For technical reasons, we assume here elementwise constant fields $\mathbf{a}|_M = \mathbf{a}_M$ and $\mathbf{d}|_M = \mathbf{b}_M$.

With modified estimates for S_1 and S_2 we can then improve the previous error estimate:

Theorem 3.4.9.

The approximation properties of the FE spaces, and the local L^2 -projector yield in case $\mathbf{u} \in [H^{k+1}(\Omega)]^d \times [H^{k+1}(\Omega)]^d \times H^k(\Omega) \times H^k(\Omega)$ for the total discretization error the bound

$$\|\mathbf{E}_h\|_{Gal}^2 + \|\mathbf{E}_h\|_{Stab}^2 \leq S_1^2 + S_2^2$$

with the bounds

$$S_1^2 \lesssim \sum_{M \in \mathcal{M}_h} h_M^{2k} \left[\left(\nu + \frac{h_M^2}{\tau_{u,SU,M}} + \frac{h_M^2}{\tilde{\tau}_{u,Lor,M}} \right) |\mathbf{u}|_{k+1,2,M}^2 + \left(\lambda + \frac{h_M^2}{\tau_{b,Ind,M}} \right) |\mathbf{b}|_{k+1,2,M}^2 \right] \quad (3.31)$$

on S_1 and it still holds

$$\begin{aligned} S_2^2 \lesssim \sum_{M \in \mathcal{M}_h} h_M^{2k} & \left[\tau_{u,gd,M} |\mathbf{u}|_{k+1,2,\omega_M}^2 + h_M^{2(s-k)} (\tau_{u,SU,M} |\mathbf{a}_M|^2 + \tau_{b,Ind,M} |\mathbf{d}_M|^2) |\mathbf{u}|_{s+1,2,\omega_M}^2 \right. \\ & + \frac{1}{\tau_{u,gd,M}} |p|_{k,2,\omega_M}^2 + \left(\tau_{r,PSPG,M} + \frac{h_M^2}{\tau_{b,gd,M}} \right) |\mathbf{b}|_{k+1,2,\omega_M}^2 \\ & \left. + h_M^{2(s-k)} \tilde{\tau}_{u,Lor,M} |\mathbf{d}_M|^2 |\mathbf{b}|_{s+1,2,\omega_M}^2 \right]. \end{aligned} \quad (3.32)$$

Proof. [WAL15, Theorem 5.5] □

A calibration of the parameters in (3.31) and (3.32) gives the new parameter bounds

$$\begin{aligned} ch_M^2 \leq \tau_{u,SU,M} & \leq C \frac{h_M^{2(k-s)}}{|\mathbf{a}_M|^2}, \quad \tau_{u,gd,M} \sim 1, \\ ch_M^2 \leq \tilde{\tau}_{u,Lor,M} & \leq C \frac{h_M^{2(k-s)}}{|\mathbf{d}_M|^2}, \quad ch_M^2 \leq \tau_{b,Ind,M} \leq C \frac{h_M^{2(k-s)}}{|\mathbf{d}_M|^2} \end{aligned} \quad (3.33)$$

and as before

$$\tau_{b,gd,M} \sim \frac{L_0^2}{\lambda}, \quad \tau_{r,PSPG,M} \sim \frac{h_M^2 \lambda}{L_0^2}. \quad (3.34)$$

Error Estimates for Singular Solutions

So far, we always considered solutions with $\mathbf{b} \in [H^1(\Omega)]^d$. Since the natural regularity of the Maxwell problem only requires $\mathbf{b} \in H^{curl}$, it is relevant to consider solutions with $\mathbf{b} \in H^{curl} \setminus [H^1(\Omega)]^d$ as well. This might happen if the domain is non-convex. For simplicity,

we here restrict ourselves to the stationary Maxwell problem with $\mathbf{u} \equiv 0, p \equiv 0$. Following Badia/Codina in [BC12], we introduce the Maxwell norm

$$|||(\mathbf{b}, r)||| := \|\mathbf{b}\|_C + \|r\|_S.$$

A different estimate of the term $\sum_{M \in \mathcal{M}_h} \tau_{r, PSPG, M} (\nabla \cdot (\mathbf{b} - j_b \mathbf{b}), \nabla \cdot \mathbf{c}_h)_M$ with an appropriate interpolation operator j_b is given in [BC12], leading to

$$|||(\mathbf{b}_h - \mathbf{b}, r_h - r)||| \lesssim \inf_{\substack{\mathbf{w}_h \in \mathbf{C}_h \\ s_h \in S_h}} \left[|||(\mathbf{b} - \mathbf{w}_h, r - s_h)||| + \left(\sum_{M \in \mathcal{M}_h} \frac{\lambda h_M}{L_0^2} \|\mathbf{b} - \mathbf{w}_h\|_{0, \partial M}^2 \right)^{\frac{1}{2}} \right].$$

According to Lemma 3.11 in [BC12], a solution $\mathbf{b} \in H_0^{curl}(\Omega) \cap H^{div}(\Omega)$ can be written as $\mathbf{b} = \mathbf{b}_0 + \nabla \phi$ with $\mathbf{b}_0 \in [W^{1+r, 2}(\Omega)]^d \cap H_0^{curl}(\Omega)$ and $\phi \in W_0^{1, 2}(\Omega) \cap W^{r, 2}(\Omega)$ for some $r > \frac{1}{2}$. Moreover, the following condition is assumed.

Assumption 3.4.10.

There exists a FE space G_h defined on \mathcal{T}_h such that $\nabla \phi_h \in \mathbf{C}_h$ for any $\phi_h \in G_h$ and that

$$\inf_{\phi_h \in G_h} \|\phi - \phi_h\|_{H^s(M)} \leq Ch_M^{t-s} \|\phi\|_{H^t(M)}$$

for all $M \in \mathcal{T}_h$, for $\phi \in W^{t, 2}(M)$ and $0 \leq s \leq t \leq k + 1$.

This leads to

$$|||(\mathbf{b} - \mathbf{b}_h, r - r_h)||| \leq C \sum_{M \in \mathcal{T}_h} \left(\sqrt{\lambda} h_M^t \|\mathbf{b}_0\|_{1, 2, M} + \frac{\sqrt{\lambda}}{L_0^{1-\varepsilon}} h_M^{t-\varepsilon} \|\phi\|_{1+t, 2, M} \right).$$

Some variants of simplicial and quadrilateral/hexahedral elements fulfilling Assumption 3.4.10 are discussed in [BC12] and [CD02].

The analysis in the present paper shows that the approach in [BC12] for the pure Maxwell problem is compatible with the analysis of the LPS method for the stationary linearized MHD problem. In particular, the so-called cross-box elements can be handled as a two-level LPS method where the LPS-compatibility condition 3.1.13 is valid.

3.5 Summary

The analytical findings for the semi-discretizations can be summarized as follows:

In all cases we achieve quasi-robust error estimates provided the stabilization parameters are sufficiently chosen. While grad-div stabilization proved to be essential, all parameters due to local projection stabilization are in most cases negligible with respect to quasi-

optimal convergence results. On the other hand, unphysical oscillations in the numerical solutions often occur due to vanishing control over terms the stabilizations are designed for. Due to the wide range of parameter bounds that we obtain, we are able to recover control while still obtaining convergence. Hence, we are in a good position to achieve physically sensible numerical results for a suitable parameter design.

Furthermore, the presented analysis offers various ways to avoid mesh width restrictions; either by assuming stronger stability of the numerical solutions such as $\tilde{\mathbf{u}}_h \in L^\infty(t_0, T; L^\infty(\Omega))$ or by a special choice of fine and coarse ansatz spaces. In the latter case, even superconvergent discretization errors could be proven. Apart from these special cases, the analysis does not require special ansatz spaces as long as the velocity and kinematic pressure ansatz spaces are inf-sup stable.

4 Error Estimates for the Fully Discretized Equations

After summarizing the estimates for the semi-discretized quantities, now the fully discretized scheme used in the implementation is considered. The results in this chapter are based on the error estimates for the fully discretized Navier-Stokes equations in [ADL15b].

4.1 Description of the Time Discretization

In the continuous Navier-Stokes problem, \mathbf{u} and p are coupled through the incompressibility constraint. The idea for pressure-correction projection methods is to define an auxiliary variable $\tilde{\mathbf{u}}$ and solve for $\tilde{\mathbf{u}}$ and p in two different steps such that the original velocity can be recovered from these two quantities. Such an approach was first considered by Chorin [Cho69] and Temam [Tem69].

An overview of different projection methods is given in [GMS06]. Badia and Codina [BC07] analyzed the incremental pressure-correction algorithm with BDF1 time discretization. The incremental pressure-correction algorithm with BDF2 time discretization is discussed by Guermond in [Gue99] for the unstabilized Navier-Stokes equations with $\nu = 1$. Shen considered a different second order time discretization scheme in [She96]. It turns out that this technique suffers from unphysical boundary conditions for the kinematic pressure that lead to reduced rates of convergence. To prevent this, Timmermans proposed in [TMV96] the rotational pressure-correction projection method that uses a divergence correction for the kinematic pressure. A thorough analysis for this has first been performed in [GS04] for the Stokes problem.

Here, the incremental pressure-correction approach is extended to cover also time discretizations for the temperature, magnetic field and magnetic pseudo-pressure.

Before describing the scheme, we need some abbreviations that will simplify the equations.

Definition 4.1.1 (Notation).

Let f^n describe the state of a quantity f at time $t_0 + n\Delta t$.

- The time propagation δ_t is defined as $\delta_t f^n = f^n - f^{n-1}$.

- The discrete time derivative D_t is defined as

$$D_t f^n = \frac{3f^n - 4f^{n-1} + f^{n-2}}{2\Delta t} = \frac{3\delta_t f^n - \delta_t f^{n-1}}{2\Delta t}.$$

- The time extrapolation is defined as

$$f^{*,n} := 2f^{n-1} - f^{n-2} \quad , \quad f(t_n)^* := 2f(t_{n-1}) - f(t_{n-2})$$

and we notice

$$f^n - f^{*,n} = \delta_{tt} f^n, \quad f(t_n) - f(t_n)^* = \delta_{tt} f(t_n).$$

For the time-discretization of the weak stabilized formulation (2.23)-(2.25), the stabilizations $s_{r,PSPG}$ and $\tilde{s}_{u,Lor}$ are neglected. Furthermore, we consider equidistant time steps of size Δt such that $t_n := t_0 + n\Delta t$. Then for each $n \in [2, \dots, N]$ the following sequence of problems is solved:

In the incremental pressure-correction scheme [GMS06], first an auxiliary velocity vector is introduced that solves the following problem with explicit treatment of the kinematic pressure:

Find $\tilde{\mathbf{u}}_{ht}^n \in \mathbf{V}_h$ such that

$$\begin{aligned} & \left(\frac{3\tilde{\mathbf{u}}_{ht}^n - 4\mathbf{u}_{ht}^{n-1} + \mathbf{u}_{ht}^{n-2}}{2\Delta t}, \mathbf{v}_h \right) + (2\boldsymbol{\omega}^n \times \tilde{\mathbf{u}}_{ht}^n, \mathbf{v}_h) + \nu(\nabla \tilde{\mathbf{u}}_{ht}^n, \nabla \mathbf{v}_h) + c_u(\tilde{\mathbf{u}}_{ht}^n; \tilde{\mathbf{u}}_{ht}^n, \mathbf{v}_h) \\ & + \sum_{M \in \mathcal{M}_h} \left(\tau_{u,SU,M}^n (\kappa_M^u((\tilde{\mathbf{u}}_M^n \cdot \nabla) \tilde{\mathbf{u}}_{ht}^n), \kappa_M^u((\tilde{\mathbf{u}}_M^n \cdot \nabla) \mathbf{v}_h))_M \right. \\ & \quad \left. + \tau_{u,Cor}^n (\kappa_M^u(\boldsymbol{\omega}^n \times \tilde{\mathbf{u}}_{ht}^n), \kappa_M^u(\boldsymbol{\omega}^n \times \mathbf{v}_h))_M + \tau_{u,gd}^n (\nabla \cdot \tilde{\mathbf{u}}_{ht}^n, \nabla \cdot \mathbf{v}_h)_M \right) \\ & = (\mathbf{f}_u^n, \mathbf{v}_h) - (\nabla p_{ht}^{n-1}, \mathbf{v}_h) + ((\nabla \times \mathbf{b}_{ht}^{*,n}) \times \mathbf{b}_{ht}^{*,n}, \mathbf{v}_h) - \beta(\mathbf{g}^n \theta_{ht}^{*,n}, \mathbf{v}_h) \end{aligned} \quad (4.1)$$

for all $\mathbf{v}_h \in \mathbf{V}_h$.

Afterwards, we solve for the kinematic pressure while projecting the auxiliary velocity into the space of weakly solenoidal solutions:

Find $(\mathbf{u}_{ht}^n, \phi_{ht}^n) \in \mathbf{V}_h \times Q_h$ such that for all $\mathbf{y}_h \in \nabla Q_h \oplus \mathbf{V}_h^{div}$ and $q_h \in Q_h$

$$\begin{aligned} \left(\frac{3\mathbf{u}_{ht}^n - 3\tilde{\mathbf{u}}_{ht}^n}{2\Delta t} + \nabla \phi_{ht}^n, \mathbf{y}_h \right) &= 0, \\ (\nabla \cdot \mathbf{u}_{ht}^n, q_h) &= 0. \end{aligned} \quad (4.2)$$

Then set the new kinematic pressure according to

$$(p_{ht}^n, q_h) = (\phi_{ht}^n + p_{ht}^{n-1} - \chi \nu \nabla \cdot \tilde{\mathbf{u}}_{ht}^n, q_h) \quad \forall q_h \in Q_h$$

where $\chi \in \{0, 1\}$.

For the magnetic part, again the standard incremental scheme is applied: We first solve for the magnetic field and treat the magnetic pseudo-pressure explicitly.

Find $\tilde{\mathbf{b}}_{ht}^n \in \mathbf{C}_h$ satisfying

$$\begin{aligned} & \left(\frac{3\tilde{\mathbf{b}}_{ht}^n - 4\mathbf{b}_{ht}^{n-1} + \mathbf{b}_{ht}^{n-2}}{2\Delta t}, \mathbf{c}_h \right) + \lambda (\nabla \times \mathbf{b}_{ht}^n, \nabla \times \mathbf{c}_h) - (\nabla \times (\tilde{\mathbf{u}}_{ht}^n \times \mathbf{b}_{ht}^n), \mathbf{c}_h) \\ & + \sum_{M \in \mathcal{M}_h} \left(\tau_{b,Lor,M}^n \left(\kappa_M^b (\nabla \times (\tilde{\mathbf{u}}_M^n \times \tilde{\mathbf{b}}_{ht}^n)), \kappa_M^b (\nabla \times (\tilde{\mathbf{u}}_M^n \times \mathbf{c}_h)) \right)_M \right. \\ & \quad \left. + \tau_{b,Ind,M}^n \left(\kappa_M^b ((\nabla \times \mathbf{b}_{ht}^n) \times \mathbf{b}_M^n), \kappa_M^b ((\nabla \times \mathbf{c}_h) \times \mathbf{b}_M^n) \right)_M \right. \\ & \quad \left. + \tau_{b,gd}^n (\nabla \cdot \mathbf{b}_{ht}^n, \nabla \cdot \mathbf{c}_h)_M \right) \\ & = (\mathbf{f}_b^n, \mathbf{c}_h) - (\nabla r_{ht}^{n-1}, \mathbf{c}_h) \end{aligned} \tag{4.3}$$

for all $\mathbf{c}_h \in \mathbf{C}_h$.

The projection onto the divergence-free constraint is achieved by solving the problem

Find $(\mathbf{b}_{ht}^n, r_{ht}^n) \in \mathbf{C}_h \times S_h$ such that

$$\begin{aligned} & \left(\frac{3\mathbf{b}_{ht}^n - 3\tilde{\mathbf{b}}_{ht}^n}{2\Delta t} + \nabla(r_{ht}^n - r_{ht}^{n-1}), \mathbf{z}_h \right) = 0, \\ & (\nabla \cdot \mathbf{b}_{ht}^n, s_h) = 0 \end{aligned}$$

holds for all $s_h \in S_h$ and $\mathbf{z}_h \in \nabla S_h \oplus \mathbf{C}_h^{div}$.

Finally, for the temperature a convection-diffusion problem is solved:

Find $\theta_{ht}^n \in \Theta_h$ such that

$$\begin{aligned} & \left(\frac{3\theta_{ht}^n - 4\theta_{ht}^{n-1} + \theta_{ht}^{n-2}}{2\Delta t}, \psi_h \right) + \alpha (\nabla \theta_{ht}^n, \nabla \psi_h) + c_\theta (\tilde{\mathbf{u}}_{ht}^n; \theta_{ht}^n, \psi_h) \\ & + \sum_{M \in \mathcal{M}_h} \tau_{\theta,SU,M}^n \left(\kappa_M^\theta ((\tilde{\mathbf{u}}_M^n \cdot \nabla) \theta_{ht}^n), \kappa_M^\theta ((\tilde{\mathbf{u}}_M^n \cdot \nabla) \psi_h) \right)_M \\ & = (\mathbf{f}_\theta^n, \psi_h) \end{aligned} \tag{4.4}$$

for all $\psi_h \in \Theta_h$.

For $\chi = 0$ the approach for the velocity is called standard incremental pressure-correction and in case of $\chi = 1$ rotational incremental pressure correction. The latter one attempts

to remove some artificial boundary conditions for the kinematic pressure and Guermond could prove in [GS04] that this yields improved error estimates in the Stokes case. Here, we will carry out the analysis for $\chi = 0$ only and consider for simplicity the boundary conditions

$$\mathbf{u}_{ht}^n|_{\partial\Omega} = \tilde{\mathbf{u}}_{ht}^n|_{\partial\Omega} = \mathbf{0}, \quad \mathbf{n} \times \mathbf{b}|_{\partial\Omega} = \mathbf{0}, \quad \theta|_{\partial\Omega} = 0. \quad (4.5)$$

For simplification of the presentation, globally constant grad-div parameter $\tau_{b,gd,M}^n \equiv \tau_{b,gd}^n, \tau_{u,gd,M}^n \equiv \tau_{u,gd}^n$ are assumed.

Definition 4.1.2 (Notation).

We remind of the splittings of the total errors into interpolation and discretization errors

$$\begin{aligned} \eta_u^n &= \mathbf{u}(t_n) - j_u \mathbf{u}(t_n), & e_u^n &= j_u \mathbf{u}(t_n) - \mathbf{u}_{ht}^n, & \xi_u^n &= \mathbf{u}(t_n) - \mathbf{u}_{ht}^n = \eta_u^n + e_u^n, \\ \tilde{\eta}_u^n &= j_u \mathbf{u}(t_n) - \tilde{\mathbf{u}}_{ht}^n, & \tilde{e}_u^n &= j_u \mathbf{u}(t_n) - \tilde{\mathbf{u}}_{ht}^n, & \tilde{\xi}_u^n &= \mathbf{u}(t_n) - \tilde{\mathbf{u}}_{ht}^n = \eta_u^n + \tilde{e}_u^n, \\ \eta_b^n &= \mathbf{b}(t_n) - j_b \mathbf{b}(t_n), & e_b^n &= j_b \mathbf{b}(t_n) - \mathbf{b}_{ht}^n, & \xi_b^n &= \mathbf{b}(t_n) - \mathbf{b}_{ht}^n = \eta_b^n + e_b^n, \\ \tilde{\eta}_b^n &= j_b \mathbf{b}(t_n) - \tilde{\mathbf{b}}_{ht}^n, & \tilde{e}_b^n &= j_b \mathbf{b}(t_n) - \tilde{\mathbf{b}}_{ht}^n, & \tilde{\xi}_b^n &= \mathbf{b}(t_n) - \tilde{\mathbf{b}}_{ht}^n = \eta_b^n + \tilde{e}_b^n, \\ \eta_p^n &= p(t_n) - j_p p(t_n), & e_p^n &= j_p p(t_n) - p_{ht}^n, & \xi_p^n &= p(t_n) - p_{ht}^n = \eta_p^n + e_p^n, \\ \eta_r^n &= r(t_n) - j_r r(t_n), & e_r^n &= j_r r(t_n) - r_{ht}^n, & \xi_r^n &= r(t_n) - r_{ht}^n = \eta_r^n + e_r^n, \\ \eta_\theta^n &= \theta(t_n) - j_\theta \theta(t_n), & e_\theta^n &= j_\theta \theta(t_n) - \theta_{ht}^n, & \xi_\theta^n &= \theta(t_n) - \theta_{ht}^n = \eta_\theta^n + e_\theta^n. \end{aligned}$$

4.2 On the Regularity of the Maxwell Problem

In contrast to the semi-discretized case, the PSPG stabilization for the magnetic pseudo-pressure is neglected in this approach. This needs justification that is given in this section. For $\mathbf{u} = \mathbf{0}$ the weak formulation of the induction equation (2.10) reduces in the stationary case to:

Find $\mathbf{b} \in H_0^{curl}(\Omega)$ such that

$$\begin{aligned} \lambda(\nabla \times \mathbf{b}, \nabla \times \mathbf{c}) - (r, \nabla \cdot \mathbf{c}) &= (\mathbf{f}_b, \mathbf{c}), \\ (\mathbf{b}, \nabla s) &= 0 \end{aligned} \quad (4.6)$$

holds for all $(\mathbf{c}, s) \in H_0^{curl}(\Omega) \times W_0^{1,2}(\Omega)$.

It can be shown that the corresponding bilinear form is coercive with respect to the natural norms on $H^{curl}(\Omega)$ and $W^{1,2}(\Omega)$ as defined in (2.7). Hence, this problem is well-posed. On the other hand, an uniform coercivity result for the respective discretization using nodal finite elements (with or without grad-div stabilization) is not known according to [BC12].

In [Haz02] it is shown that the above so-called *curl* formulation is equivalent to the following so-called *curl-div* formulation:

Find $\mathbf{b} \in H_0^{curl}(\Omega) \cap H^{div}(\Omega)$ such that

$$\begin{aligned} \lambda(\nabla \times \mathbf{b}, \nabla \times \mathbf{c}) + (\nabla r, \mathbf{c}) &= (\mathbf{f}_b, \mathbf{c}), \\ (\nabla \cdot \mathbf{b}, s) &= 0 \end{aligned} \tag{4.7}$$

holds for all $(\mathbf{c}, s) \in H_0^{curl}(\Omega) \cap H^{div}(\Omega) \times L_0^2(\Omega)$.

In particular, also this problem is well-posed. The discretization in time for the induction equation (4.3) corresponds to this latter formulation.

We now consider solutions \mathbf{b} for the Maxwell problem satisfying the stricter regularity assumption $\mathbf{b} \in H_0^{curl}(\Omega) \cap H^1(\Omega)$ and define the unit normal and the tangential parts of \mathbf{b} by:

Definition 4.2.1.

For an unit normal vector \mathbf{n} the normal part of a vector \mathbf{u} is given by

$$u_n = \mathbf{u} \cdot \mathbf{n}$$

and the tangential part by

$$\mathbf{u}_t = \mathbf{u} - u_n \mathbf{n}.$$

With this preparations, it can be shown that for a solenoidal \mathbf{b} the $H^{curl}(\Omega)$ semi-norm and the $H^1(\Omega)$ semi-norm are equivalent:

Lemma 4.2.2.

For a polyhedral domain Ω with boundary Γ and $\mathbf{u}, \mathbf{v} \in H^1(\Omega)$, the identity

$$(\nabla \times \mathbf{u}, \nabla \times \mathbf{v}) + (\nabla \cdot \mathbf{u}, \nabla \cdot \mathbf{v}) - (\nabla \mathbf{u}, \nabla \mathbf{v}) = (\nabla \cdot \mathbf{u}_t, v_n)|_\Gamma - (\nabla u_n, \mathbf{v}_t)_\Gamma$$

is fulfilled. In particular,

$$\|\nabla \times \mathbf{u}\|_0^2 + \|\nabla \cdot \mathbf{u}\|_0^2 = \|\nabla \mathbf{u}\|_0^2$$

if we prescribe homogeneous normal ($\mathbf{u} \cdot \mathbf{n} = 0$) or homogeneous tangential ($\mathbf{u} \times \mathbf{n} = 0$) boundary conditions on Γ .

Proof. [Cos91]

□

In particular, a discretization using inf-sup stable conforming elements in combination with $\tau_{b,gd}^n \leq \lambda$ is coercive with respect to the *curl-div* formulation. Due to the fact that for deriving convergence results we always need the solution to be sufficiently smooth, this result justifies omitting the PSPG stabilization for the magnetic pseudo-pressure.

Remark 4.2.3. If the reference solution has just regularity according to $\mathbf{b} \in H^{curl}(\Omega) \setminus [H^1(\Omega)]^d$, the discrete solution cannot converge in the above described framework: A solution \mathbf{b}_h to the discretized Maxwell equation satisfies the stability result

$$\begin{aligned} \lambda \|\nabla \mathbf{b}_h\|_0^2 &= \lambda \|\nabla \times \mathbf{b}_h\|_0^2 + \lambda \|\nabla \cdot \mathbf{b}_h\|_0^2 \\ &\leq \lambda \|\nabla \times \mathbf{b}_h\|_0^2 + \lambda \|\nabla \cdot \mathbf{b}_h\|_0^2 + s_{b,Ind}(\mathbf{b}_h; \mathbf{b}_h, \mathbf{b}_h) = (\mathbf{f}_b, \mathbf{b}_h) \\ &\leq \|\mathbf{f}_b\|_{-1} \|\nabla \mathbf{b}_h\|_0. \\ \Rightarrow \lambda \|\nabla \mathbf{b}_h\|_0 &\leq \|\mathbf{f}_b\|_{-1} \end{aligned}$$

and is hence uniformly bounded with respect to the $H^1(\Omega)$ semi-norm. Convergence to \mathbf{b} would however imply that $\lambda \|\nabla \mathbf{b}_h\|_0^2$ is unbounded in the limit. This case is not artificial: Provided Ω is not convex, Costabel proved in [Cos91] that $H_0^{curl}(\Omega) \cap [H^1(\Omega)]^d$ is a closed proper subspace of $H_0^{curl}(\Omega) \cap H^{div}(\Omega)$.

That is the reason why we still consider PSPG stabilization and a parameter design as in (3.30) in case of solutions with reduced regularity in the numerical examples.

4.3 Stability Estimates

After the justification of reduced set of stabilization parameters, we now proceed to stability results. The discrete error norms that we are interested in are given by:

Definition 4.3.1.

Consider sequences $\mathbf{u} = (\mathbf{u}^1, \dots, \mathbf{u}^N) \in \mathbf{A}^N$ of vector-valued and $p = (p^1, \dots, p^N) \in B^N$ of scalar-valued quantities, where \mathbf{A} and B are normed spaces and $1 \leq n \leq N$. Then discrete error norms are defined by

$$\begin{aligned} \|\mathbf{u}\|_{l^2(t_0, T; \mathbf{A})}^2 &:= \Delta t \sum_{n=1}^N \|\mathbf{u}^n\|_{\mathbf{A}}^2, & \|p\|_{l^2(t_0, T; B)}^2 &:= \Delta t \sum_{n=1}^N \|p^n\|_B^2, \\ \|\mathbf{u}\|_{l^\infty(t_0, T; \mathbf{A})} &:= \max_{1 \leq n \leq N} \|\mathbf{u}^n\|_{\mathbf{A}}, & \|p\|_{l^\infty(t_0, T; B)} &:= \max_{1 \leq n \leq N} \|p^n\|_B. \end{aligned}$$

Furthermore, we define similar to the semi-discrete case for the errors with respect to stabilization and the natural semi-norm:

$$\|\mathbf{v}^n\|_{LPS_u}^2 := \nu \|\nabla \mathbf{v}^n\|_0^2 + s_{u,gd}(\mathbf{v}^n, \mathbf{v}^n) + s_{u,SU}(\tilde{\mathbf{u}}_{ht}^n; \mathbf{v}^n, \mathbf{v}^n),$$

$$\begin{aligned}
\|\mathbf{v}^n\|_{l^2(t_0, T; LPS_u)}^2 &:= \Delta t \sum_{n=1}^N \|\mathbf{v}^n\|_{LPS_u}^2, \\
\|\mathbf{c}^n\|_{LPS_b}^2 &:= \lambda \|\nabla \times \mathbf{c}^n\|_0^2 + s_{b,gd}(\mathbf{v}^n, \mathbf{v}^n) + s_{b,Lor}(\tilde{\mathbf{u}}_{ht}^n; \mathbf{c}^n, \mathbf{c}^n) + s_{b,Ind}(\tilde{\mathbf{b}}_{ht}^n; \mathbf{c}^n, \mathbf{c}^n), \\
\|\mathbf{c}^n\|_{l^2(t_0, T; LPS_b)}^2 &:= \Delta t \sum_{n=1}^N \|\mathbf{c}^n\|_{LPS_b}^2, \\
\|\psi^n\|_{LPS_\theta}^2 &:= \alpha \|\nabla \psi^n\|_0^2 + s_{\theta,SU}(\tilde{\mathbf{u}}_{ht}^n; \psi^n, \psi^n), \\
\|\psi^n\|_{l^2(t_0, T; LPS_\theta)}^2 &:= \Delta t \sum_{n=1}^N \|\psi^n\|_{LPS_\theta}^2
\end{aligned}$$

for all $(\mathbf{v}, \mathbf{c}, \theta) \in \mathbf{V}^N \times \mathbf{C}^N \times \Theta^N$.

For quantities r that are continuous in time we identify r by its evaluation at the discrete points in time $(r(t_1), \dots, r(t_N))^T$.

Now, a stability result can be stated in case the magnetic coupling is treated implicitly in the momentum equation:

Lemma 4.3.2 (Stability).

Assume an implicit treatment of the magnetic coupling in the momentum equation, i.e. $(\nabla \times \tilde{\mathbf{b}}_{ht}^{n,*}) \times \tilde{\mathbf{b}}_{ht}^{n,*} := (\nabla \times \tilde{\mathbf{b}}_{ht}^n) \times \tilde{\mathbf{b}}_{ht}^n$, and $\mathbf{f}_u \in l^2(t_0, T; [L^2(\Omega)]^d)$, $\mathbf{f}_b \in l^2(t_0, T; [L^2(\Omega)]^d)$, $f_\theta \in l^2(t_0, T; L^2(\Omega))$, $\mathbf{g} \in l^\infty(t_0, T; [L^\infty(\Omega)]^d)$. Then it holds

$$\begin{aligned}
&\|\tilde{\mathbf{u}}_{ht}\|_{l^\infty(t_0, T; L^2(\Omega))}^2 + \|\tilde{\mathbf{u}}_{ht}\|_{l^2(t_0, T; LPS)}^2 + \|\tilde{\mathbf{b}}_{ht}\|_{l^\infty(t_0, T; L^2(\Omega))}^2 \\
&\quad + \|\tilde{\mathbf{b}}_{ht}\|_{l^2(t_0, T; LPS)}^2 + \|\theta_{ht}\|_{l^\infty(t_0, T; L^2(\Omega))}^2 + \|\theta_{ht}\|_{l^2(t_0, T; LPS)}^2 \\
&\quad + (\Delta t)^2 \|\nabla p_{ht}\|_{l^\infty(t_0, T; L^2(\Omega))}^2 + (\Delta t)^2 \|\nabla r_{ht}\|_{l^\infty(t_0, T; L^2(\Omega))}^2 \\
&\leq e^{C_G(T-t_0)} \left(\|\tilde{\mathbf{u}}_{ht}^1\|_0^2 + \|2\mathbf{u}_{ht}^1 - \mathbf{u}_{ht}^0\|_0^2 + \frac{4(\Delta t)^2}{3} \|\nabla p_{ht}^1\|_0^2 + \|\tilde{\mathbf{b}}_{ht}^1\|_0^2 \right. \\
&\quad \left. + \|2\mathbf{b}_{ht}^1 - \mathbf{b}_{ht}^0\|_0^2 + \frac{4(\Delta t)^2}{3} \|\nabla r_{ht}^1\|_0^2 + \|\theta_{ht}^1\|_0^2 + \|2\theta_{ht}^1 - \theta_{ht}^0\|_0^2 \right. \\
&\quad \left. + \sum_{n=2}^m \left(4\Delta t \|\mathbf{f}_u^n\|_0^2 + 4\Delta t \|\mathbf{f}_b^n\|_0^2 + \frac{\Delta t}{4\beta^2 \|\mathbf{g}^n\|_\infty^2} \|f_\theta^n\|_0^2 \right) \right) \tag{4.8}
\end{aligned}$$

where the Gronwall constant C_G is given by

$$C_G \sim (1 - K)^{-1}, \quad K := \frac{\Delta t}{2} + 4\Delta t \beta^2 \|\mathbf{g}^n\|_{l^\infty(t_0, T; L^\infty(\Omega))}^2 \stackrel{!}{<} 1.$$

Proof. Symmetric testing in the momentum equation (4.1) and (4.2) yields

$$\frac{(3\tilde{\mathbf{u}}_{ht}^n - 4\mathbf{u}_{ht}^{n-1} + \mathbf{u}_{ht}^{n-2}, \tilde{\mathbf{u}}_{ht}^n)}{\Delta t} + \nu \|\nabla \tilde{\mathbf{u}}_{ht}^n\|_0^2 + s_{u,gd}(\tilde{\mathbf{u}}_{ht}^n, \tilde{\mathbf{u}}_{ht}^n) + s_{u,SU}(\tilde{\mathbf{u}}_{ht}^n; \tilde{\mathbf{u}}_{ht}^n, \tilde{\mathbf{u}}_{ht}^n)$$

$$\begin{aligned}
&= (\mathbf{f}_u^n, \tilde{\mathbf{u}}_{ht}^n) + (p_{ht}^{n-1}, \nabla \cdot \tilde{\mathbf{u}}_{ht}^n) - ((\nabla \times \tilde{\mathbf{b}}_{ht}^{*,n}) \times \tilde{\mathbf{b}}_{ht}^{*,n}, \tilde{\mathbf{u}}_{ht}^n) - \beta(\mathbf{g}^n \theta_{ht}^{*,n}, \tilde{\mathbf{u}}_{ht}^n) \\
&\frac{(3\mathbf{u}_{ht}^n - 3\tilde{\mathbf{u}}_{ht}^n, \nabla p_{ht}^{n-1})}{2\Delta t} = \frac{3}{2\Delta t} (\nabla \cdot \tilde{\mathbf{u}}_{ht}^n, p_{ht}^{n-1}) = (\nabla(p_{ht}^{n-1} - p_{ht}^n), \nabla p_{ht}^{n-1}).
\end{aligned}$$

For the first term, we have the splitting

$$\begin{aligned}
&2(3\tilde{\mathbf{u}}_{ht}^n - 4\mathbf{u}_{ht}^{n-1} + \mathbf{u}_{ht}^{n-2}, \tilde{\mathbf{u}}_{ht}^n) \\
&= 3\|\tilde{\mathbf{u}}_{ht}^n\|_0^2 - 3\|\tilde{\mathbf{u}}_{ht}^n - \mathbf{u}_{ht}^n\|_0^2 - 2\|\mathbf{u}_{ht}^n\|_0^2 + 2(3\mathbf{u}_{ht}^n - 4\mathbf{u}_{ht}^{n-1} + \mathbf{u}_{ht}^{n-2}, \tilde{\mathbf{u}}_{ht}^n - \mathbf{u}_{ht}^n) \\
&\quad + \|2\mathbf{u}_{ht}^n - \mathbf{u}_{ht}^{n-1}\|_0^2 + \|\delta_{tt}\mathbf{u}_{ht}^n\|_0^2 - \|\tilde{\mathbf{u}}_{ht}^{n-1}\|_0^2 - \|2\mathbf{u}_{ht}^{n-1} - \mathbf{u}_{ht}^{n-2}\|_0^2
\end{aligned}$$

where the term $2(3\mathbf{u}_{ht}^n - 4\mathbf{u}_{ht}^{n-1} + \mathbf{u}_{ht}^{n-2}, \tilde{\mathbf{u}}_{ht}^n)$ vanishes due to the fact that \mathbf{u}_{ht}^n is the orthogonal projection of $\tilde{\mathbf{u}}_{ht}^n$ in the space of discretely solenoidal functions.

For the second equation, we notice

$$\begin{aligned}
\|\nabla \delta_t p_{ht}^n\|_0^2 &= \frac{9}{4(\Delta t)^2} \|\mathbf{u}_{ht}^n - \tilde{\mathbf{u}}_{ht}^n\|_0^2 \\
(\nabla(p_{ht}^{n-1} - p_{ht}^n), \nabla p_{ht}^{n-1}) &= \frac{1}{2} (\|\nabla p_{ht}^{n-1}\|_0^2 + \|\nabla \delta_t p_{ht}^n\|_0^2 - \|\nabla p_{ht}^n\|_0^2) \\
&= \frac{1}{2} (\|\nabla p_{ht}^{n-1}\|_0^2 - \|\nabla p_{ht}^n\|_0^2) + \frac{9}{8(\Delta t)^2} \|\mathbf{u}_{ht}^n - \tilde{\mathbf{u}}_{ht}^n\|_0^2.
\end{aligned}$$

In combination, this gives by multiplying the first equation with $4\Delta t$

$$\begin{aligned}
&\|\tilde{\mathbf{u}}_{ht}^n\|_0^2 + \|2\mathbf{u}_{ht}^n - \mathbf{u}_{ht}^{n-1}\|_0^2 + \|\delta_{tt}\mathbf{u}_{ht}^n\|_0^2 + \frac{4(\Delta t)^2}{3} \|\nabla p_{ht}^n\|_0^2 + 4\Delta t\nu \|\nabla \tilde{\mathbf{u}}_{ht}^n\|_0^2 \\
&\quad + 4\Delta t s_{u,gd}(\tilde{\mathbf{u}}_{ht}^n, \tilde{\mathbf{u}}_{ht}^n) + 4\Delta t s_{u,SU}(\tilde{\mathbf{u}}_{ht}^n; \tilde{\mathbf{u}}_{ht}^n, \tilde{\mathbf{u}}_{ht}^n) + 4\Delta t s_{u,Cor}(\boldsymbol{\omega}^n; \tilde{\mathbf{u}}_{ht}^n, \tilde{\mathbf{u}}_{ht}^n) \\
&\leq 3\|\tilde{\mathbf{u}}_{ht}^n\|_0^2 - 2\|\mathbf{u}_{ht}^n\|_0^2 + \|2\mathbf{u}_{ht}^n - \mathbf{u}_{ht}^{n-1}\|_0^2 + \|\delta_{tt}\mathbf{u}_{ht}^n\|_0^2 + \frac{4(\Delta t)^2}{3} \|\nabla p_{ht}^n\|_0^2 + 4\Delta t\nu \|\nabla \tilde{\mathbf{u}}_{ht}^n\|_0^2 \\
&\quad + 4\Delta t s_{u,gd}(\tilde{\mathbf{u}}_{ht}^n, \tilde{\mathbf{u}}_{ht}^n) + 4\Delta t s_{u,SU}(\tilde{\mathbf{u}}_{ht}^n; \tilde{\mathbf{u}}_{ht}^n, \tilde{\mathbf{u}}_{ht}^n) + 4\Delta t s_{u,Cor}(\boldsymbol{\omega}^n; \tilde{\mathbf{u}}_{ht}^n, \tilde{\mathbf{u}}_{ht}^n) \\
&= \|\mathbf{u}_{ht}^{n-1}\|_0^2 + \|2\mathbf{u}_{ht}^{n-1} - \mathbf{u}_{ht}^{n-2}\|_0^2 + \frac{4(\Delta t)^2}{3} \|\nabla p_{ht}^{n-1}\|_0^2 \tag{4.9} \\
&\quad + 4\Delta t(\mathbf{f}_u^n, \tilde{\mathbf{u}}_{ht}^n) - 4\Delta t((\nabla \times \tilde{\mathbf{b}}_{ht}^{*,n}) \times \tilde{\mathbf{b}}_{ht}^{*,n}, \tilde{\mathbf{u}}_{ht}^n) - 4\Delta t\beta(\mathbf{g}^n \theta_{ht}^{*,n}, \tilde{\mathbf{u}}_{ht}^n).
\end{aligned}$$

For the first estimate, we additionally used $\|\mathbf{u}_{ht}^n\|_0^2 = \|\pi_{\mathbf{V}_h^{div}} \tilde{\mathbf{u}}_{ht}^n\|_0^2 \leq \|\tilde{\mathbf{u}}_{ht}^n\|_0^2$.

An analogous estimate for the magnetic field yields

$$\begin{aligned}
&\|\tilde{\mathbf{b}}_{ht}^n\|_0^2 + \|2\mathbf{b}_{ht}^n - \mathbf{b}_{ht}^{n-1}\|_0^2 + \|\delta_{tt}\mathbf{b}_{ht}^n\|_0^2 + \frac{4(\Delta t)^2}{3} \|\nabla r_{ht}^n\|_0^2 + 4\Delta t\lambda \|\nabla \tilde{\mathbf{b}}_{ht}^n\|_0^2 \\
&\quad + 4\Delta t s_{b,gd}(\tilde{\mathbf{b}}_{ht}^n, \tilde{\mathbf{b}}_{ht}^n) + 4\Delta t s_{b,Lor}(\tilde{\mathbf{u}}_{ht}^n; \tilde{\mathbf{b}}_{ht}^n, \tilde{\mathbf{b}}_{ht}^n) + 4\Delta t s_{b,Ind}(\tilde{\mathbf{b}}_{ht}^n; \tilde{\mathbf{b}}_{ht}^n, \tilde{\mathbf{b}}_{ht}^n) \\
&\leq \|\mathbf{b}_{ht}^{n-1}\|_0^2 + \|2\mathbf{b}_{ht}^{n-1} - \mathbf{b}_{ht}^{n-2}\|_0^2 + \frac{4(\Delta t)^2}{3} \|\nabla r_{ht}^{n-1}\|_0^2 \\
&\quad + 4\Delta t(\mathbf{f}_b^n, \tilde{\mathbf{b}}_{ht}^n) + 4\Delta t(\nabla \times (\tilde{\mathbf{u}}_{ht}^n \times \tilde{\mathbf{b}}_{ht}^n), \tilde{\mathbf{b}}_{ht}^n).
\end{aligned} \tag{4.10}$$

Finally, we also test the advection-diffusion equation for the temperature symmetrically and obtain

$$\frac{(3\theta_{ht}^n - 4\theta_{ht}^{n-1} + \theta_{ht}^{n-2}, \theta_{ht}^n)}{2\Delta t} + \alpha \|\nabla \theta_{ht}^n\|_0^2 + s_{\theta, SU}(\tilde{\mathbf{u}}_{ht}^n; \theta_{ht}^n, \theta_{ht}^n) = (f_\theta^n, \theta_{ht}^n).$$

The first term can in an analogous manner to the discrete time derivative of the velocity be rewritten as

$$\begin{aligned} & 2(3\theta_{ht}^n - 4\theta_{ht}^{n-1} + \theta_{ht}^{n-2}, \theta_{ht}^n) \\ &= \|\theta_{ht}^n\|_0^2 + \|2\theta_{ht}^n - \theta_{ht}^{n-1}\|_0^2 + \|\delta_{tt}\theta_{ht}^n\|_0^2 - \|\theta_{ht}^{n-1}\|_0^2 - \|2\theta_{ht}^{n-1} - \theta_{ht}^{n-2}\|_0^2. \end{aligned}$$

Therefore, for the discrete temperature we obtain

$$\begin{aligned} & \|\theta_{ht}^n\|_0^2 + \|2\theta_{ht}^n - \theta_{ht}^{n-1}\|_0^2 + \|\delta_{tt}\theta_{ht}^n\|_0^2 + 4\Delta t\alpha \|\nabla \theta_{ht}^n\|_0^2 + 4\Delta t s_{\theta, SU}(\tilde{\mathbf{u}}_{ht}^n; \theta_{ht}^n, \theta_{ht}^n) \\ &= 4\Delta t(f_\theta^n, \theta_{ht}^n) - \|\theta_{ht}^{n-1}\|_0^2 + \|2\theta_{ht}^{n-1} - \theta_{ht}^{n-2}\|_0^2. \end{aligned} \quad (4.11)$$

A combination of the estimates (4.9)-(4.11) gives

$$\begin{aligned} & \|\tilde{\mathbf{u}}_{ht}^n\|_0^2 + \|2\mathbf{u}_{ht}^n - \mathbf{u}_{ht}^{n-1}\|_0^2 + \|\delta_{tt}\mathbf{u}_{ht}^n\|_0^2 + \frac{4(\Delta t)^2}{3} \|\nabla p_{ht}^n\|_0^2 + 4\Delta t\nu \|\nabla \tilde{\mathbf{u}}_{ht}^n\|_0^2 \\ &+ \|\tilde{\mathbf{b}}_{ht}^n\|_0^2 + \|2\mathbf{b}_{ht}^n - \mathbf{b}_{ht}^{n-1}\|_0^2 + \|\delta_{tt}\mathbf{b}_{ht}^n\|_0^2 + \frac{4(\Delta t)^2}{3} \|\nabla r_{ht}^n\|_0^2 + 4\Delta t\lambda \|\nabla \tilde{\mathbf{b}}_{ht}^n\|_0^2 \\ &+ \|\theta_{ht}^n\|_0^2 + \|2\theta_{ht}^n - \theta_{ht}^{n-1}\|_0^2 + \|\delta_{tt}\theta_{ht}^n\|_0^2 + 4\Delta t\alpha \|\nabla \theta_{ht}^n\|_0^2 + 4\Delta t s_{\theta, SU}(\tilde{\mathbf{u}}_{ht}^n; \theta_{ht}^n, \theta_{ht}^n) \\ &+ 4\Delta t s_{u, gd}(\tilde{\mathbf{u}}_{ht}^n, \tilde{\mathbf{u}}_{ht}^n) + 4\Delta t s_{u, SU}(\tilde{\mathbf{u}}_{ht}^n; \tilde{\mathbf{u}}_{ht}^n, \tilde{\mathbf{u}}_{ht}^n) + 4\Delta t s_{u, Cor}(\omega^n; \tilde{\mathbf{u}}_{ht}^n, \tilde{\mathbf{u}}_{ht}^n) \\ &+ 4\Delta t s_{b, gd}(\tilde{\mathbf{b}}_{ht}^n, \tilde{\mathbf{b}}_{ht}^n) + 4\Delta t s_{b, Lor}(\tilde{\mathbf{u}}_{ht}^n; \tilde{\mathbf{b}}_{ht}^n, \tilde{\mathbf{b}}_{ht}^n) + 4\Delta t s_{b, Ind}(\tilde{\mathbf{b}}_{ht}^n; \tilde{\mathbf{b}}_{ht}^n, \tilde{\mathbf{b}}_{ht}^n) \\ &\leq \|\mathbf{u}_{ht}^{n-1}\|_0^2 + \|2\mathbf{u}_{ht}^{n-1} - \mathbf{u}_{ht}^{n-2}\|_0^2 + \frac{4(\Delta t)^2}{3} \|\nabla p_{ht}^{n-1}\|_0^2 + \|\mathbf{b}_{ht}^{n-1}\|_0^2 + \|2\mathbf{b}_{ht}^{n-1} - \mathbf{b}_{ht}^{n-2}\|_0^2 \\ &+ \frac{4(\Delta t)^2}{3} \|\nabla r_{ht}^{n-1}\|_0^2 - \|\theta_{ht}^{n-1}\|_0^2 + \|2\theta_{ht}^{n-1} - \theta_{ht}^{n-2}\|_0^2 \\ &+ 4\Delta t(\mathbf{f}_u^n, \tilde{\mathbf{u}}_{ht}^n) - 4\Delta t((\nabla \times \tilde{\mathbf{b}}_{ht}^{*,n}) \times \tilde{\mathbf{b}}_{ht}^{*,n}, \tilde{\mathbf{u}}_{ht}^n) - 4\Delta t\beta(\mathbf{g}^n \theta_{ht}^{*,n}, \tilde{\mathbf{u}}_{ht}^n) \\ &+ 4\Delta t(\mathbf{f}_b^n, \tilde{\mathbf{b}}_{ht}^n) + 4\Delta t(\nabla \times (\tilde{\mathbf{u}}_{ht}^n \times \tilde{\mathbf{b}}_{ht}^n), \tilde{\mathbf{b}}_{ht}^n) + 4\Delta t(f_\theta^n, \theta_{ht}^n). \end{aligned} \quad (4.12)$$

Now, we estimate the last terms on the right-hand side according to

$$\begin{aligned} 4\Delta t(\mathbf{f}_u^n, \tilde{\mathbf{u}}_{ht}^n) &\leq \frac{\Delta t}{4} \|\tilde{\mathbf{u}}_{ht}^n\|_0^2 + 4\Delta t \|\mathbf{f}_u^n\|_0^2, \\ 4\Delta t(\mathbf{f}_b^n, \tilde{\mathbf{b}}_{ht}^n) &\leq \frac{\Delta t}{2} \|\tilde{\mathbf{b}}_{ht}^n\|_0^2 + 4\Delta t \|\mathbf{f}_b^n\|_0^2, \\ 4\Delta t(f_\theta^n, \theta_{ht}^n) &\leq 4\Delta t\beta^2 \|\mathbf{g}^n\|_\infty^2 \|\theta_{ht}^n\|_0^2 + \frac{\Delta t}{4\beta^2 \|\mathbf{g}^n\|_\infty^2} \|f_\theta^n\|_0^2, \\ 4\Delta t\beta(\mathbf{g}^n \theta_{ht}^{*,n}, \tilde{\mathbf{u}}_{ht}^n) &\leq 4\Delta t\beta^2 \|\mathbf{g}^n\|_\infty^2 \|\theta_{ht}^{*,n}\|_0^2 + \frac{\Delta t}{4} \|\tilde{\mathbf{u}}_{ht}^n\|_0^2 \end{aligned}$$

and note

$$\begin{aligned} & (\nabla \times (\tilde{\mathbf{u}}_{ht}^n \times \tilde{\mathbf{b}}_{ht}^n), \tilde{\mathbf{b}}_{ht}^n) - ((\nabla \times \tilde{\mathbf{b}}_{ht}^{*,n}) \times \tilde{\mathbf{b}}_{ht}^{*,n}, \tilde{\mathbf{u}}_{ht}^n) \\ & = ((\nabla \times \tilde{\mathbf{b}}_{ht}^n) \times \tilde{\mathbf{b}}_{ht}^n - (\nabla \times \tilde{\mathbf{b}}_{ht}^{*,n}) \times \tilde{\mathbf{b}}_{ht}^{*,n}, \tilde{\mathbf{u}}_{ht}^n) = \mathbf{0} \end{aligned}$$

due to the implicit treatment of the magnetic coupling.

Using these observations, (4.12) states after summing up for all $2 \leq m \leq N$

$$\begin{aligned} & \|\tilde{\mathbf{u}}_{ht}^m\|_0^2 + \|2\mathbf{u}_{ht}^m - \mathbf{u}_{ht}^{m-1}\|_0^2 + \frac{4(\Delta t)^2}{3} \|\nabla p_{ht}^m\|_0^2 + \|\tilde{\mathbf{b}}_{ht}^m\|_0^2 + \|2\mathbf{b}_{ht}^m - \mathbf{b}_{ht}^{m-1}\|_0^2 \\ & + \frac{4(\Delta t)^2}{3} \|\nabla r_{ht}^m\|_0^2 + \|\theta_{ht}^m\|_0^2 + \|2\theta_{ht}^m - \theta_{ht}^{m-1}\|_0^2 \\ & + \sum_{n=2}^m \left(\|\delta_{tt} \mathbf{u}_{ht}^n\|_0^2 + 4\Delta t \nu \|\nabla \tilde{\mathbf{u}}_{ht}^n\|_0^2 + \|\delta_{tt} \mathbf{b}_{ht}^n\|_0^2 + 4\Delta t \lambda \|\nabla \tilde{\mathbf{b}}_{ht}^n\|_0^2 + \|\delta_{tt} \theta_{ht}^n\|_0^2 \right. \\ & \quad + 4\Delta t \alpha \|\nabla \theta_{ht}^n\|_0^2 + 4\Delta t s_{\theta, SU}(\tilde{\mathbf{u}}_{ht}^n; \theta_{ht}^n, \theta_{ht}^n) + 4\Delta t s_{u, gd}(\tilde{\mathbf{u}}_{ht}^n, \tilde{\mathbf{u}}_{ht}^n) \\ & \quad + 4\Delta t s_{u, SU}(\tilde{\mathbf{u}}_{ht}^n; \tilde{\mathbf{u}}_{ht}^n, \tilde{\mathbf{u}}_{ht}^n) + 4\Delta t s_{u, Cor}(\boldsymbol{\omega}^n; \tilde{\mathbf{u}}_{ht}^n, \tilde{\mathbf{u}}_{ht}^n) + 4\Delta t s_{b, gd}(\tilde{\mathbf{b}}_{ht}^n, \tilde{\mathbf{b}}_{ht}^n) \\ & \quad \left. + 4\Delta t s_{b, Lor}(\tilde{\mathbf{u}}_{ht}^n; \tilde{\mathbf{b}}_{ht}^n, \tilde{\mathbf{b}}_{ht}^n) + 4\Delta t s_{b, Ind}(\tilde{\mathbf{b}}_{ht}^n; \tilde{\mathbf{b}}_{ht}^n, \tilde{\mathbf{b}}_{ht}^n) \right) \\ & \leq \|\tilde{\mathbf{u}}_{ht}^1\|_0^2 + \|2\mathbf{u}_{ht}^1 - \mathbf{u}_{ht}^0\|_0^2 + \frac{4(\Delta t)^2}{3} \|\nabla p_{ht}^1\|_0^2 + \|\tilde{\mathbf{b}}_{ht}^1\|_0^2 + \|2\mathbf{b}_{ht}^1 - \mathbf{b}_{ht}^0\|_0^2 \\ & \quad + \frac{4(\Delta t)^2}{3} \|\nabla r_{ht}^1\|_0^2 + \|\theta_{ht}^1\|_0^2 + \|2\theta_{ht}^1 - \theta_{ht}^0\|_0^2 \\ & \quad + \sum_{n=2}^m \left(4\Delta t (\mathbf{f}_u^n, \tilde{\mathbf{u}}_{ht}^n) - 4\Delta t \beta (\mathbf{g}^n \theta_{ht}^{*,n}, \tilde{\mathbf{u}}_{ht}^n) + 4\Delta t (\mathbf{f}_b^n, \tilde{\mathbf{b}}_{ht}^n) + 4\Delta t (f_\theta^n, \theta_{ht}^n) \right) \\ & \leq \|\tilde{\mathbf{u}}_{ht}^1\|_0^2 + \|2\mathbf{u}_{ht}^1 - \mathbf{u}_{ht}^0\|_0^2 + \frac{4(\Delta t)^2}{3} \|\nabla p_{ht}^1\|_0^2 + \|\tilde{\mathbf{b}}_{ht}^1\|_0^2 + \|2\mathbf{b}_{ht}^1 - \mathbf{b}_{ht}^0\|_0^2 \\ & \quad + \frac{4(\Delta t)^2}{3} \|\nabla r_{ht}^1\|_0^2 + \|\theta_{ht}^1\|_0^2 + \|2\theta_{ht}^1 - \theta_{ht}^0\|_0^2 \\ & \quad + \sum_{n=2}^m \left(\frac{\Delta t}{2} \|\tilde{\mathbf{u}}_{ht}^n\|_0^2 + 4\Delta t \|\mathbf{f}_u^n\|_0^2 + \frac{\Delta t}{2} \|\tilde{\mathbf{b}}_{ht}^n\|_0^2 + 4\Delta t \|\mathbf{f}_b^n\|_0^2 + 4\Delta t \beta^2 \|\mathbf{g}^n\|_\infty^2 \|\theta_{ht}^n\|_0^2 \right. \\ & \quad \left. + \frac{\Delta t}{4\beta^2 \|\mathbf{g}^n\|_\infty^2} \|f_\theta^n\|_0^2 + 4\Delta t \beta^2 \|\mathbf{g}^n\|_\infty^2 \|\theta_{ht}^{*,n}\|_0^2 \right). \end{aligned}$$

With application of a discrete Gronwall lemma for

$$\frac{\Delta t}{2} \|\tilde{\mathbf{u}}_{ht}^n\|_0^2 + \frac{\Delta t}{2} \|\tilde{\mathbf{b}}_{ht}^n\|_0^2 + 4\Delta t \beta^2 \|\mathbf{g}^n\|_\infty^2 \|\theta_{ht}^n\|_0^2 + 4\Delta t \beta^2 \|\mathbf{g}^n\|_\infty^2 \|\theta_{ht}^{*,n}\|_0^2,$$

we arrive at the final estimate

$$\begin{aligned} & \|\tilde{\mathbf{u}}_{ht}^m\|_0^2 + \|2\mathbf{u}_{ht}^m - \mathbf{u}_{ht}^{m-1}\|_0^2 + \frac{4(\Delta t)^2}{3} \|\nabla p_{ht}^m\|_0^2 + \|\tilde{\mathbf{b}}_{ht}^m\|_0^2 + \|2\mathbf{b}_{ht}^m - \mathbf{b}_{ht}^{m-1}\|_0^2 \\ & + \frac{4(\Delta t)^2}{3} \|\nabla r_{ht}^m\|_0^2 + \|\theta_{ht}^m\|_0^2 + \|2\theta_{ht}^m - \theta_{ht}^{m-1}\|_0^2 \end{aligned}$$

$$\begin{aligned}
& + \sum_{n=2}^m \left(\|\delta_{tt} \mathbf{u}_{ht}^n\|_0^2 + 4\Delta t \nu \|\nabla \tilde{\mathbf{u}}_{ht}^n\|_0^2 + \|\delta_{tt} \mathbf{b}_{ht}^n\|_0^2 + 4\Delta t \lambda \|\nabla \tilde{\mathbf{b}}_{ht}^n\|_0^2 + \|\delta_{tt} \theta_{ht}^n\|_0^2 \right. \\
& \quad + 4\Delta t \alpha \|\nabla \theta_{ht}^n\|_0^2 + 4\Delta t s_{\theta, SU}(\tilde{\mathbf{u}}_{ht}^n; \theta_{ht}^n, \theta_{ht}^n) + 4\Delta t s_{u, gd}(\tilde{\mathbf{u}}_{ht}^n, \tilde{\mathbf{u}}_{ht}^n) \\
& \quad + 4\Delta t s_{u, SU}(\tilde{\mathbf{u}}_{ht}^n; \tilde{\mathbf{u}}_{ht}^n, \tilde{\mathbf{u}}_{ht}^n) + 4\Delta t s_{u, Cor}(\boldsymbol{\omega}^n; \tilde{\mathbf{u}}_{ht}^n, \tilde{\mathbf{u}}_{ht}^n) + 4\Delta t s_{b, gd}(\tilde{\mathbf{b}}_{ht}^n, \tilde{\mathbf{b}}_{ht}^n) \\
& \quad \left. + 4\Delta t s_{b, Lor}(\tilde{\mathbf{u}}_{ht}^n; \tilde{\mathbf{b}}_{ht}^n, \tilde{\mathbf{b}}_{ht}^n) + 4\Delta t s_{b, Ind}(\tilde{\mathbf{b}}_{ht}^n; \tilde{\mathbf{b}}_{ht}^n, \tilde{\mathbf{b}}_{ht}^n) \right) \quad (4.13) \\
& \leq e^{C_G(T-t_0)} \left(\|\tilde{\mathbf{u}}_{ht}^1\|_0^2 + \|2\mathbf{u}_{ht}^1 - \mathbf{u}_{ht}^0\|_0^2 + \frac{4(\Delta t)^2}{3} \|\nabla p_{ht}^1\|_0^2 + \|\tilde{\mathbf{b}}_{ht}^1\|_0^2 \right. \\
& \quad + \|2\mathbf{b}_{ht}^1 - \mathbf{b}_{ht}^0\|_0^2 + \frac{4(\Delta t)^2}{3} \|\nabla r_{ht}^1\|_0^2 + \|\theta_{ht}^1\|_0^2 + \|2\theta_{ht}^1 - \theta_{ht}^0\|_0^2 \\
& \quad \left. + \sum_{n=2}^m \left(4\Delta t \|\mathbf{f}_u^n\|_0^2 + 4\Delta t \|\mathbf{f}_b^n\|_0^2 + \frac{\Delta t}{4\beta^2 \|\mathbf{g}^n\|_\infty^2} \|f_\theta^n\|_0^2 \right) \right)
\end{aligned}$$

where the Gronwall constant C_G is given by

$$C_G \sim (1 - K)^{-1} \quad K := \frac{\Delta t}{2} + 4\Delta t, \beta^2 \|\mathbf{g}^n\|_{l^\infty(t_0, T; L^\infty(\Omega))}^2 \stackrel{!}{<} 1.$$

This gives the claim. \square

Remark 4.3.3. In case of an electrically insulating fluid in an inertial frame of reference, this stability estimate reduces to a variant of the result in [Dal15].

4.4 Estimates of the Discretization Errors

In this section, first error estimates for each quantity separately are derived and in the end combined for an estimate on the total discretization error. In conjunction with the assumptions on the interpolation errors, this leads to convergence results for all considered quantities.

In the following approach, extensive use of previous results for individual equations or terms is made to shorten the presentation adequately. The estimates of the coupling terms are stressed here.

4.4.1 The Momentum Equation

For the momentum equation, the choice of an adequate interpolant is crucial. As in [ADL15b], we consider interpolants $(j_u \mathbf{u}(t_n), j_p p(t_n)) := (\mathbf{w}_{ht}^n, \hat{p}_{ht}^n)$ that preserve the discrete divergence as solution of the grad-div stabilized Stokes problem

Find $\mathbf{w}_{ht}^n \in \mathbf{V}_h$ and $\hat{p}_{ht}^n \in Q_h$ such that

$$\begin{aligned} & \nu(\nabla \mathbf{w}_{ht}^n, \nabla \mathbf{v}_h) + s_{u,gd}(\mathbf{w}_{ht}^n, \mathbf{v}_h) - (\hat{p}_{ht}^n, \nabla \cdot \mathbf{v}_h) \\ &= \nu(\nabla \mathbf{u}(t_n), \nabla \mathbf{v}_h) + s_{u,gd}(\mathbf{u}(t_n), \mathbf{v}_h) - (p(t_n), \nabla \cdot \mathbf{v}_h), \\ & (\nabla \cdot \mathbf{w}_{ht}^n, q_h) = (\nabla \cdot \mathbf{u}(t_n), q_h) = 0 \end{aligned} \quad (4.14)$$

holds for all $\mathbf{v}_h \in \mathbf{V}_h$ and $q_h \in Q_h$.

An extension of the result according to [JLLR13, Theorem 1] gives for the interpolation error the bound

$$\begin{aligned} & \nu \|\nabla \boldsymbol{\eta}_u^n\|_0^2 + \tau_{u,gd}^n \|\nabla \cdot \boldsymbol{\eta}_u^n\|_0^2 + \|e_p^n\|_0^2 \\ & \leq C \left(\inf_{\mathbf{w}_h \in \mathbf{V}_h^{div}} (\nu + \tau_{u,gd}^n) \|\nabla(\mathbf{u}(t_n) - \mathbf{w}_h)\|_0^2 + \frac{1}{\tau_{u,gd}^n} \inf_{q_h \in Q_h} \|p(t_n) - q_h\|_0^2 \right). \end{aligned}$$

Using Assumption 2.5.3 for the interpolation and the local inverse inequality (Assumption 2.5.1) results in

$$\begin{aligned} & \nu \|\boldsymbol{\eta}_u^n\|_1^2 + \tau_{u,gd}^n \|\nabla \cdot \boldsymbol{\eta}_u^n\|_0^2 + \|\eta_p^n\|_0^2 + h^2 \|\nabla \eta_p^n\|_0^2 \\ & \leq C(\nu + \tau_{u,gd}^n) h^{2k_u} \|\mathbf{u}(t_n)\|_{H^{k_u+1}}^2 + C(\tau_{u,gd}^n)^{-1} h^{2k_p+2} \|p(t_n)\|_{H^{k_p+1}}^2 \end{aligned} \quad (4.15)$$

and application of the Aubin-Nitsche trick for $k_u \geq 1$ finally yields

$$\begin{aligned} \|\boldsymbol{\eta}_u^n\|_0^2 & \leq Ch^2(\nu \|\boldsymbol{\eta}_u^n\|_1^2 + \tau_{u,gd}^n \|\nabla \cdot \boldsymbol{\eta}_u^n\|_0^2) \\ & \leq C((\nu + \tau_{u,gd}^n) h^{2k_u+2} \|\mathbf{u}(t_n)\|_{H^{k_u+1}}^2 + (\tau_{u,gd}^n)^{-1} h^{2k_p+4} \|p(t_n)\|_{H^{k_p+1}}^2). \end{aligned} \quad (4.16)$$

Discretization Error

With these preparations, the results in [ADL15b] state for the Navier-Stokes case:

Lemma 4.4.1.

For all $1 \leq m \leq N$ the discretization error for the uncoupled problem can be estimated according to

$$\begin{aligned} & \|\tilde{\mathbf{e}}_u^m\|_0^2 + \|2\mathbf{e}_u^m - \mathbf{e}_u^{m-1}\|_0^2 + \frac{4}{3}(\Delta t)^2 \|\nabla e_p^m\|_0^2 \\ & + \sum_{n=2}^m \left(2\Delta t \nu \|\nabla \tilde{\mathbf{e}}_u^n\|_0^2 + 4\Delta t \tau_{u,gd}^n \|\nabla \cdot \tilde{\mathbf{e}}_u^n\|_0^2 + \|\delta_{tt} \mathbf{e}_u^n\|_0^2 \right. \\ & \quad \left. + 3\Delta t \sum_{M \in \mathcal{M}_h} \tau_{u,SU,M}^n \|\kappa_M^u((\tilde{\mathbf{u}}_M^n \cdot \nabla) \tilde{\mathbf{e}}_u^n)\|_{0,M}^2 \right) \\ & \leq \|\tilde{\mathbf{e}}_u^1\|_0^2 + \|2\mathbf{e}_u^1 - \mathbf{e}_u^0\|_0^2 + \frac{4}{3}(\Delta t)^2 \|\nabla e_p^1\|_0^2 \end{aligned}$$

$$\begin{aligned}
& + \sum_{n=2}^m \left\{ \widetilde{K}_u^n \|\widetilde{\mathbf{e}}_u^n\|_0^2 + \frac{4(\Delta t)^3}{3} \|\nabla e_p^n\|_0^2 + \frac{4(\Delta t)^2}{3} \left(1 + \frac{1}{2\Delta t}\right) \|\nabla(\hat{p}_{ht}^{n-1} - \hat{p}_{ht}^n)\|_0^2 \right. \\
& \quad + C(\Delta t)^2 \|D_t \boldsymbol{\eta}_u^n\|_0^2 + C(\Delta t)^2 \|D_t \mathbf{u}(t_n) - \partial_t \mathbf{u}(t_n)\|_0^2 \\
& \quad + Ch^{-2z} \Delta t \|\boldsymbol{\eta}_u^n\|_0^2 + 3C\Delta th^{2-2z} \|\boldsymbol{\eta}_u^n\|_{LPS_u}^2 \\
& \quad \left. + C \frac{\Delta t}{\nu} \max_{M \in \mathcal{M}_h} \{\tau_{u,SU,M}^n |\widetilde{\mathbf{u}}_M^n|^2\} (\nu \|\boldsymbol{\eta}_u^n\|_1^2 + \nu \|\kappa_M^u(\nabla \mathbf{u}(t_n))\|_0^2) \right\}
\end{aligned}$$

where $z \in \{0, 1\}$ and with

$$\begin{aligned}
\widetilde{K}_u^n := & \left(\frac{1}{4} + C\Delta t \left[|\mathbf{u}(t_n)|_{W^{1,\infty}(\Omega)} + h^{2z} |\mathbf{u}(t_n)|_{W^{1,\infty}(\Omega)}^2 + \frac{h^{2z}}{\tau_{u,gd}^n} |\mathbf{u}(t_n)|_{W^{1,\infty}(\Omega)}^2 \right. \right. \\
& \left. \left. + \frac{h^{2z-2}}{\tau_{u,gd}^n} \|\mathbf{u}(t_n)\|_\infty^2 + h^{2z-2} \|\widetilde{\mathbf{u}}_{ht}^n\|_\infty^2 \right] \right) \stackrel{!}{<} 1.
\end{aligned}$$

The temperature coupling in the momentum equation can be estimated as

$$\begin{aligned}
(\theta(t_n) - \theta_{ht}^{*,n}, \widetilde{\mathbf{e}}_u^n) & = (\theta(t_n) - \theta(t_n)^*, \widetilde{\mathbf{e}}_u^n) + (\theta(t_n)^* - \theta_{ht}^{*,n}, \widetilde{\mathbf{e}}_u^n) \\
& \leq C \|\delta_{tt} \theta(t_n)\|_0^2 + \|\widetilde{\mathbf{e}}_u^n\|_0^2 + C \|e_\theta^{*,n}\|_0^2.
\end{aligned}$$

This gives essentially no restriction on the time step size.

We treat the coupling term due to the induction equation according to

$$\begin{aligned}
& ((\nabla \times \mathbf{b}(t_n)) \times \mathbf{b}(t_n) - (\nabla \times \widetilde{\mathbf{b}}_{ht}^{*,n}) \times \widetilde{\mathbf{b}}_{ht}^{*,n}, \widetilde{\mathbf{e}}_u^n) \\
& = \underbrace{((\nabla \times \mathbf{b}(t_n)) \times \mathbf{b}(t_n) - (\nabla \times \mathbf{b}(t_n)^*) \times \mathbf{b}(t_n)^*, \widetilde{\mathbf{e}}_u^n)}_I \\
& \quad + \underbrace{((\nabla \times \mathbf{b}(t_n)^*) \times \mathbf{b}(t_n)^* - (\nabla \times \widetilde{\mathbf{b}}_{ht}^{*,n}) \times \widetilde{\mathbf{b}}_{ht}^{*,n}, \widetilde{\mathbf{e}}_u^n)}_{II}
\end{aligned}$$

and bound the two terms using Young's inequality:

$$\begin{aligned}
I & = ((\nabla \times \delta_{tt} \mathbf{b}(t_n)) \times \mathbf{b}(t_n), \widetilde{\mathbf{e}}_u^n) + ((\nabla \times \mathbf{b}(t_n)^*) \times \delta_{tt} \mathbf{b}(t_n), \widetilde{\mathbf{e}}_u^n) \\
& \leq \|\nabla \times \delta_{tt} \mathbf{b}(t_n)\|_0 \|\mathbf{b}(t_n)\|_\infty \|\widetilde{\mathbf{e}}_u^n\|_0 + \|\nabla \times \mathbf{b}(t_n)^*\|_\infty \|\delta_{tt} \mathbf{b}(t_n)\|_0 \|\widetilde{\mathbf{e}}_u^n\|_0 \\
& \leq \|\nabla \times \delta_{tt} \mathbf{b}(t_n)\|_0^2 \|\mathbf{b}(t_n)\|_\infty^2 + \|\nabla \times \mathbf{b}(t_n)^*\|_\infty^2 \|\delta_{tt} \mathbf{b}(t_n)\|_0^2 + C \|\widetilde{\mathbf{e}}_u^n\|_0^2
\end{aligned}$$

$$\begin{aligned}
II & = ((\nabla \times (\mathbf{b}(t_n)^* - \widetilde{\mathbf{b}}_{ht}^{*,n})) \times \widetilde{\mathbf{b}}_{ht}^{*,n}, \widetilde{\mathbf{e}}_u^n) + ((\nabla \times \mathbf{b}(t_n)^*) \times (\mathbf{b}(t_n)^* - \widetilde{\mathbf{b}}_{ht}^{*,n}), \widetilde{\mathbf{e}}_u^n) \\
& = ((\nabla \times \widetilde{\mathbf{e}}_b^{*,n}) \times \widetilde{\mathbf{b}}_{ht}^{*,n}, \widetilde{\mathbf{e}}_u^n) + ((\nabla \times \mathbf{b}(t_n)^*) \times (\widetilde{\mathbf{e}}_b^{*,n}), \widetilde{\mathbf{e}}_u^n) \\
& \quad + ((\nabla \times \boldsymbol{\eta}_b^{*,n}) \times \widetilde{\mathbf{b}}_{ht}^{*,n}, \widetilde{\mathbf{e}}_u^n) + ((\nabla \times \mathbf{b}(t_n)^*) \times (\boldsymbol{\eta}_b^{*,n}), \widetilde{\mathbf{e}}_u^n)
\end{aligned}$$

$$\begin{aligned}
&\leq \|\nabla \times \tilde{\mathbf{e}}_b^{*,n}\|_0 \|\tilde{\mathbf{b}}_{ht}^{*,n}\|_\infty \|\tilde{\mathbf{e}}_u^n\|_0 + \|\nabla \times \mathbf{b}(t_n)^*\|_\infty \|\tilde{\mathbf{e}}_b^{*,n}\|_0 \|\tilde{\mathbf{e}}_u^n\|_0 \\
&\quad + \|\nabla \times \boldsymbol{\eta}_b^{*,n}\|_0 \|\tilde{\mathbf{b}}_{ht}^{*,n}\|_\infty \|\tilde{\mathbf{e}}_u^n\|_0 + \|\nabla \times \mathbf{b}(t_n)^*\|_\infty \|\boldsymbol{\eta}_b^{*,n}\|_0 \|\tilde{\mathbf{e}}_u^n\|_0 \\
&\leq \frac{C}{h} \|\tilde{\mathbf{e}}_b^{*,n}\|_0^2 \|\tilde{\mathbf{b}}_{ht}^{*,n}\|_\infty^2 + \frac{C}{h} \|\tilde{\mathbf{e}}_u^n\|_0^2 + \|\nabla \times \mathbf{b}(t_n)^*\|_\infty^2 \|\tilde{\mathbf{e}}_b^{*,n}\|_0^2 + C \|\tilde{\mathbf{e}}_u^n\|_0^2 \\
&\quad + \lambda \|\nabla \times \boldsymbol{\eta}_b^{*,n}\|_0^2 \|\tilde{\mathbf{b}}_{ht}^{*,n}\|_\infty^2 + \frac{C}{\lambda} \|\tilde{\mathbf{e}}_u^n\|_0^2 + \|\nabla \times \mathbf{b}(t_n)^*\|_\infty^2 \|\boldsymbol{\eta}_b^{*,n}\|_0^2 + C \|\tilde{\mathbf{e}}_u^n\|_0^2
\end{aligned}$$

In the last estimate, the local inverse inequality (Assumption 2.5.1) is used. This gives a time step size restriction according to $\Delta t \lesssim \min\{h, \lambda\}$. If we used $\mathbf{b}_{ht}^{*,n}$ instead of the approximation $\mathbf{b}_{ht}^{*,n}$, term I would vanish and the extrapolations in II would be replaced by the values at time t_n . Hence, we would not have to use the inverse inequality and could remove the restriction $\Delta t \leq h$.

Incorporating the above results for the coupling terms and the Coriolis force and Coriolis stabilization from [AL15], we achieve:

Lemma 4.4.2 (Discretization Error for the Momentum Equation).

For all $1 \leq m \leq N$ the discretization error for the coupled problem can be bounded as

$$\begin{aligned}
&\|\tilde{\mathbf{e}}_u^m\|_0^2 + \|2\mathbf{e}_u^m - \mathbf{e}_u^{m-1}\|_0^2 + \frac{4}{3}(\Delta t)^2 \|\nabla \mathbf{e}_p^m\|_0^2 \\
&\quad + \sum_{n=2}^m \left(2\Delta t \nu \|\nabla \tilde{\mathbf{e}}_u^n\|_0^2 + 4\Delta t \tau_{u,gd}^n \|\nabla \cdot \tilde{\mathbf{e}}_u^n\|_0^2 + \|\delta_{tt} \mathbf{e}_u^n\|_0^2 \right. \\
&\quad \quad \left. + 3\Delta t \sum_{M \in \mathcal{M}_h} \left(\tau_{u,SU,M}^n \|\kappa_M^u((\tilde{\mathbf{u}}_M^n \cdot \nabla) \tilde{\mathbf{e}}_u^n)\|_{0,M}^2 \right) + \tau_{u,Cor}^n \|\kappa_M^u(\boldsymbol{\omega}^n \times \tilde{\mathbf{e}}_u^n)\|_{0,M}^2 \right) \\
&\leq \|\tilde{\mathbf{e}}_u^1\|_0^2 + \|2\mathbf{e}_u^1 - \mathbf{e}_u^0\|_0^2 + \frac{4}{3}(\Delta t)^2 \|\nabla \mathbf{e}_p^1\|_0^2 \\
&\quad + \sum_{n=2}^m \left\{ K_u^n \|\tilde{\mathbf{e}}_u^n\|_0^2 + \frac{4(\Delta t)^3}{3} \|\nabla \mathbf{e}_p^n\|_0^2 + \frac{4(\Delta t)^2}{3} \left(1 + \frac{1}{2\Delta t} \right) \|\nabla(\hat{p}_{ht}^{n-1} - \hat{p}_{ht}^n)\|_0^2 \right. \\
&\quad \quad + C(\Delta t)^2 \|D_t \boldsymbol{\eta}_u^n\|_0^2 + C(\Delta t)^2 \|D_t \mathbf{u}(t_n) - \partial_t \mathbf{u}(t_n)\|_0^2 \\
&\quad \quad + Ch^{-2z} \Delta t \|\boldsymbol{\eta}_u^n\|_0^2 + 3C\Delta th^{2-2z} \|\boldsymbol{\eta}_u^n\|_{LPS_u}^2 \\
&\quad \quad + C \frac{\Delta t}{\nu} \max_{M \in \mathcal{M}_h} \{ \tau_{u,SU,M}^n |\tilde{\mathbf{u}}_M^n|^2 \} (\nu \|\boldsymbol{\eta}_u^n\|_1^2 + \nu \|\kappa_M^u(\nabla \mathbf{u}(t_n))\|_0^2) \\
&\quad \quad + C\Delta t \tau_{u,Cor}^n |\boldsymbol{\omega}^n|^2 (\|\boldsymbol{\eta}_u^n\|_0^2 + \|\kappa_M^u(\mathbf{u}(t_n))\|_0^2) \\
&\quad \quad + C\Delta t \|\delta_{tt} \theta(t_n)\|_0^2 + C\Delta t \|e_\theta^{*,n}\|_0^2 \\
&\quad \quad + \Delta t \|\nabla \times \delta_{tt} \mathbf{b}(t_n)\|_0^2 \|\mathbf{b}(t_n)\|_\infty^2 + \Delta t \|\nabla \times \mathbf{b}(t_n)^*\|_\infty^2 \|\delta_{tt} \mathbf{b}(t_n)\|_0^2 \\
&\quad \quad + C \frac{\Delta t}{h} \|\tilde{\mathbf{e}}_b^{*,n}\|_0^2 \|\tilde{\mathbf{b}}_{ht}^{*,n}\|_\infty^2 + \Delta t \|\nabla \times \mathbf{b}(t_n)^*\|_\infty^2 \|\tilde{\mathbf{e}}_b^{*,n}\|_0^2 \\
&\quad \quad \left. + \Delta t \lambda \|\nabla \times \boldsymbol{\eta}_b^{*,n}\|_0^2 \|\tilde{\mathbf{b}}_{ht}^{*,n}\|_\infty^2 + \Delta t \|\nabla \times \mathbf{b}(t_n)^*\|_\infty^2 \|\boldsymbol{\eta}_b^{*,n}\|_0^2 \right\}
\end{aligned}$$

where $z \in \{0, 1\}$ and with

$$K_u^n := \left(\frac{1}{4} + C\Delta t \left[1 + \frac{1}{h} + \frac{1}{\lambda} + |\mathbf{u}(t_n)|_{W^{1,\infty}(\Omega)} + h^{2z} |\mathbf{u}(t_n)|_{W^{1,\infty}(\Omega)}^2 + \frac{h^{2z}}{\tau_{u,gd}^n} |\mathbf{u}(t_n)|_{W^{1,\infty}(\Omega)}^2 + \frac{h^{2z-2}}{\tau_{u,gd}^n} \|\mathbf{u}(t_n)\|_\infty^2 + h^{2z-2} \|\tilde{\mathbf{u}}_{ht}^n\|_\infty^2 + |\boldsymbol{\omega}^n|^2 \right] \right) \stackrel{!}{<} 1.$$

4.4.2 The Fourier Equation

For the temperature, we choose the interpolation $j_\theta \theta(t_n) := \hat{\theta}_{ht}^n$ as solution of the Poisson problem

$$\alpha(\nabla \hat{\theta}_{ht}^n, \nabla \psi_h) = \alpha(\nabla \theta(t_n), \nabla \psi_h) \quad \forall \psi_h \in \Theta_h.$$

Using standard results (and the Aubin-Nitsche trick), this gives us the estimate

$$\frac{1}{h^2} \|\eta_\theta^n\|_0^2 + \alpha \|\eta_\theta^n\|_1^2 \leq C\alpha \inf_{\psi_h \in \Theta_h} \|\theta(t_n) - \psi_h\|_1^2.$$

In combination with Assumption 2.5.5, the interpolation error can be bounded by

$$\frac{1}{h^2} \|\eta_\theta^n\|_0^2 + \alpha \|\eta_\theta^n\|_1^2 \leq C\alpha h^{2k_\theta} \|\theta(t_n)\|_{H^{k_\theta+1}(\Omega)}.$$

Discretization Error

For the convective terms, we can modify the estimate from [DA15] analogously to the treatment in [ADL15b] and achieve:

Lemma 4.4.3.

Let $\varepsilon > 0$ and $(\mathbf{u}, \theta) \in \mathbf{V}^{div} \times \Theta$, $(\tilde{\mathbf{u}}_{ht}^n, \theta_h) \in \mathbf{V}_h^{div} \times \Theta_h$ be solutions of (2.9), (2.11) and (4.1), (4.4) satisfying $\mathbf{u}(t_n) \in [W^{1,\infty}(\Omega)]^d$, $\theta(t_n) \in W^{1,\infty}(\Omega)$ and $\tilde{\mathbf{u}}_{ht}^n \in [L^\infty(\Omega)]^d$. If Assumptions 2.5.1, 2.5.3 and 2.5.5 hold, the difference of the convective terms in the Fourier equation can be estimated as

$$\begin{aligned} & c_\theta(\mathbf{u}(t_n); \theta(t_n), e_\theta^n) - c_\theta(\tilde{\mathbf{u}}_{ht}^n; \theta_{ht}, e_\theta^n) \\ & \leq \frac{1}{2} |\theta(t_n)|_{W^{1,\infty}(\Omega)} \|\tilde{\mathbf{e}}_u^n\|_0^2 + \frac{C}{\varepsilon} h^{-2z} \|\eta_\theta(t_n)\|_0^2 \\ & \quad + \|e_\theta^n\|_0^2 \left(\frac{1}{2} |\theta(t_n)|_{W^{1,\infty}(\Omega)} + \varepsilon h^{2z-2} \|\tilde{\mathbf{u}}_{ht}^n\|_\infty^2 + \varepsilon h^{2z} |\theta(t_n)|_{W^{1,\infty}(\Omega)}^2 \right. \\ & \quad \left. + \frac{C}{\varepsilon} \frac{h^{2z}}{\tau_{u,gd}^n} |\theta(t_n)|_{W^{1,\infty}(\Omega)}^2 + \frac{C}{\varepsilon} \frac{h^{2z-2}}{\tau_{u,gd}^n} \|\theta(t_n)\|_\infty^2 \right) \end{aligned}$$

$$+ \frac{C}{\varepsilon} h^{-2z} \|\boldsymbol{\eta}_u^n\|_0^2 + 3\varepsilon \|\|\boldsymbol{\eta}_u^n\|_{LPS_u}^2 + 3\varepsilon \|\|\tilde{\boldsymbol{e}}_u^n\|_{LPS_u}^2$$

with $C > 0$ independent of the problem parameters, h , the solutions and $z \in \{0, 1\}$.

With this we can state the discretization error result for this quantity:

Lemma 4.4.4 (Discretization Error for the Fourier Equation).

For all $1 \leq m \leq N$ the discretization error stemming from the temperature equation can be bounded by

$$\begin{aligned} & \|e_\theta^m\|_0^2 + \|2e_\theta^m - e_\theta^{m-1}\|_0^2 + \sum_{n=2}^m \left(\|\delta_{tt}e_\theta^n\|_0^2 + 4\Delta t\alpha \|\nabla e_\theta^n\|_0^2 + s_\theta(\tilde{\boldsymbol{u}}_{ht}^n, e_\theta^n, \tilde{\boldsymbol{u}}_{ht}^n, e_\theta^n) \right) \\ & \lesssim \|e_\theta^1\|_0^2 + \|2e_\theta^1 - e_\theta^0\|_0^2 \\ & + \sum_{n=2}^m \left\{ K_\theta^n \|e_\theta^n\|_0^2 + (\Delta t)^2 \|D_t \eta_\theta^n\|_0^2 + C(\Delta t)^2 \|D_t \theta(t_n) - \partial_t \theta(t_n)\|_0^2 \right. \\ & \quad + C\Delta t |\theta(t_n)|_{W^{1,\infty}(\Omega)} \|\tilde{\boldsymbol{e}}_u^n\|_0^2 + C\Delta t h^{-2z} \|\eta_\theta(t_n)\|_0^2 \\ & \quad + C\Delta t h^{-2z} \|\boldsymbol{\eta}_u^n\|_0^2 + 3\varepsilon \Delta t h^{2-2z} \|\|\boldsymbol{\eta}_u^n\|_{LPS_u}^2 + 3\varepsilon \Delta t h^{2-2z} \|\|\tilde{\boldsymbol{e}}_u^n\|_{LPS_u}^2 \\ & \quad \left. + \Delta t \max_{M \in \mathcal{M}_h} \{\tau_{\theta, SU, M}^n |\tilde{\boldsymbol{u}}_M^n|^2\} (\|\kappa_M^\theta(\nabla \theta(t_n))\|_0^2 + \|\nabla \eta_\theta^n\|_0^2) \right\} \end{aligned}$$

where K_θ^n is defined according to

$$\begin{aligned} K_\theta^n := & \left(\frac{1}{4} + \Delta t \left(\frac{1}{2} |\theta(t_n)|_{W^{1,\infty}(\Omega)} + \varepsilon h^{2z-2} \|\tilde{\boldsymbol{u}}_{ht}^n\|_\infty^2 + \varepsilon h^{2z} |\theta(t_n)|_{W^{1,\infty}(\Omega)}^2 \right. \right. \\ & \left. \left. + \frac{C}{\varepsilon} \frac{h^{2z}}{\tau_{u, gd}^n} |\theta(t_n)|_{W^{1,\infty}(\Omega)}^2 + \frac{C}{\varepsilon} \frac{h^{2z-2}}{\tau_{u, gd}^n} \|\theta(t_n)\|_\infty^2 \right) \right) \stackrel{!}{<} 1. \end{aligned}$$

Proof. Similar to the previous approaches, the error equation for the temperature reads

$$\begin{aligned} & \|e_\theta^n\|_0^2 + \|2e_\theta^n - e_\theta^{n-1}\|_0^2 + \|\delta_{tt}e_\theta^n\|_0^2 + 4\Delta t\alpha \|\nabla e_\theta^n\|_0^2 + 4\Delta t s_\theta(\tilde{\boldsymbol{u}}_{ht}^n, e_\theta^n, \tilde{\boldsymbol{u}}_{ht}^n, e_\theta^n) \\ & \lesssim \|e_\theta^{n-1}\|_0^2 + \|2e_\theta^{n-1} - e_\theta^{n-2}\|_0^2 + (\Delta t)^2 \|D_t \eta_\theta^n\|_0^2 + C(\Delta t)^2 \|D_t \theta(t_n) - \partial_t \theta(t_n)\|_0^2 \\ & \quad + 4\Delta t c_\theta(\boldsymbol{u}(t_n); \theta(t_n), e_\theta^n) - 4\Delta t c_\theta(\tilde{\boldsymbol{u}}_{ht}^n; \theta_{ht}, e_\theta^n) \\ & \quad + \Delta t s_\theta(\tilde{\boldsymbol{u}}_{ht}^n, e_\theta^n, \tilde{\boldsymbol{u}}_{ht}^n, e_\theta^n) + \Delta t s_\theta(\tilde{\boldsymbol{u}}_{ht}^n, \theta_{ht}^n, \tilde{\boldsymbol{u}}_{ht}^n, e_\theta^n) \\ & \lesssim \|e_\theta^{n-1}\|_0^2 + \|2e_\theta^{n-1} - e_\theta^{n-2}\|_0^2 + (\Delta t)^2 \|D_t \eta_\theta^n\|_0^2 + C(\Delta t)^2 \|D_t \theta(t_n) - \partial_t \theta(t_n)\|_0^2 \\ & \quad + \frac{\Delta t}{2} |\theta(t_n)|_{W^{1,\infty}(\Omega)} \|\tilde{\boldsymbol{e}}_u^n\|_0^2 + \frac{C}{\varepsilon} \Delta t h^{-2z} \|\eta_\theta(t_n)\|_0^2 \\ & \quad + \Delta t \|e_\theta^n\|_0^2 \left(\frac{1}{2} |\theta(t_n)|_{W^{1,\infty}(\Omega)} + \varepsilon h^{2z-2} \|\tilde{\boldsymbol{u}}_{ht}^n\|_\infty^2 + \varepsilon h^{2z} |\theta(t_n)|_{W^{1,\infty}(\Omega)}^2 \right) \end{aligned}$$

$$\begin{aligned}
& + \frac{C}{\varepsilon} \frac{h^{2z}}{\tau_{u,gd}^n} |\theta(t_n)|_{W^{1,\infty}(\Omega)}^2 + \frac{C}{\varepsilon} \frac{h^{2z-2}}{\tau_{u,gd}^n} \|\theta(t_n)\|_{\infty}^2 \Big) \\
& + \frac{C}{\varepsilon} \Delta t h^{-2z} \|\boldsymbol{\eta}_u^n\|_0^2 + 3\varepsilon \Delta t \|\boldsymbol{\eta}_u^n\|_{LPS_u}^2 + 3\varepsilon \Delta t h^{2-2z} \|\tilde{\boldsymbol{e}}_u^n\|_{LPS_u}^2 \\
& + \Delta t s_{\theta}(\tilde{\boldsymbol{u}}_{ht}^n, j_{\theta}\theta(t_n), \tilde{\boldsymbol{u}}_{ht}^n, e_{\theta}^n).
\end{aligned}$$

Note that the interpolation error term $\alpha \|\nabla \eta_{\theta}^n\|_0^2$ does not appear due to the special choice of the interpolant.

Due to

$$\begin{aligned}
s_{\theta}(\tilde{\boldsymbol{u}}_{ht}^n, j_{\theta}\theta(t_n), \tilde{\boldsymbol{u}}_{ht}^n, e_{\theta}^n) & = s_{\theta}(\tilde{\boldsymbol{u}}_{ht}^n, \theta(t_n), \tilde{\boldsymbol{u}}_{ht}^n, e_{\theta}^n) - s_{\theta}(\tilde{\boldsymbol{u}}_{ht}^n, \eta_{\theta}^n, \tilde{\boldsymbol{u}}_{ht}^n, e_{\theta}^n) \\
& \lesssim \max_{M \in \mathcal{M}_h} \{\tau_{\theta, SU, M}^n\} |\tilde{\boldsymbol{u}}_M^n|^2 (\|\kappa_M^{\theta}(\nabla \theta(t_n))\|_0^2 + \|\nabla \eta_{\theta}^n\|_0^2) + \frac{1}{4} s_{\theta}(\tilde{\boldsymbol{u}}_{ht}^n, e_{\theta}^n, \tilde{\boldsymbol{u}}_{ht}^n, e_{\theta}^n)
\end{aligned}$$

we arrive at

$$\begin{aligned}
& \|e_{\theta}^m\|_0^2 + \|2e_{\theta}^m - e_{\theta}^{m-1}\|_0^2 + \sum_{n=2}^m \left(\|\delta_{tt} e_{\theta}^n\|_0^2 + 4\Delta t \alpha \|\nabla e_{\theta}^n\|_0^2 + 4\Delta t s_{\theta}(\tilde{\boldsymbol{u}}_{ht}^n, e_{\theta}^n, \tilde{\boldsymbol{u}}_{ht}^n, e_{\theta}^n) \right) \\
& \lesssim \|e_{\theta}^1\|_0^2 + \|2e_{\theta}^1 - e_{\theta}^0\|_0^2 \\
& + \sum_{n=2}^m \left\{ K_{\theta}^n \|e_{\theta}^n\|_0^2 + (\Delta t)^2 \|D_t \eta_{\theta}^n\|_0^2 + C(\Delta t)^2 \|D_t \theta(t_n) - \partial_t \theta(t_n)\|_0^2 \right. \\
& \quad + C\Delta t |\theta(t_n)|_{W^{1,\infty}(\Omega)} \|\tilde{\boldsymbol{e}}_u^n\|_0^2 + C\Delta t h^{-2z} \|\eta_{\theta}(t_n)\|_0^2 \\
& \quad + C\Delta t h^{-2z} \|\boldsymbol{\eta}_u^n\|_0^2 + 3\varepsilon \Delta t h^{2-2z} \|\boldsymbol{\eta}_u^n\|_{LPS_u}^2 + 3\varepsilon \Delta t h^{2-2z} \|\tilde{\boldsymbol{e}}_u^n\|_{LPS_u}^2 \\
& \quad \left. + \Delta t \max_{M \in \mathcal{M}_h} \{\tau_{\theta, SU, M}^n\} |\tilde{\boldsymbol{u}}_M^n|^2 (\|\kappa_M^{\theta}(\nabla \theta(t_n))\|_0^2 + \|\nabla \eta_{\theta}^n\|_0^2) \right\}
\end{aligned}$$

where K_{θ}^n is defined according to

$$\begin{aligned}
K_{\theta}^n & := \frac{1}{4} + \Delta t \left(\frac{1}{2} |\theta(t_n)|_{W^{1,\infty}(\Omega)} + \varepsilon h^{2z-2} \|\tilde{\boldsymbol{u}}_{ht}^n\|_{\infty}^2 + \varepsilon h^{2z} |\theta(t_n)|_{W^{1,\infty}(\Omega)}^2 \right. \\
& \quad \left. + \frac{C}{\varepsilon} \frac{h^{2z}}{\tau_{u,gd}^n} |\theta(t_n)|_{W^{1,\infty}(\Omega)}^2 + \frac{C}{\varepsilon} \frac{h^{2z-2}}{\tau_{u,gd}^n} \|\theta(t_n)\|_{\infty}^2 \right) \stackrel{!}{>} 1.
\end{aligned}$$

□

4.4.3 The Induction Equation

For the magnetic field, we assume again a divergence-preserving interpolant j_b that satisfies the Assumption 2.5.4 and sufficient regularity $\boldsymbol{b} \in H^1(\Omega)$ for the magnetic field. For the magnetic pseudo-pressure $j_r \equiv 0$ is used.

Remark 4.4.5. In principle, the interpolant could also be chosen as solution to a Maxwell problem similar to the approach for the momentum equation. However, it turns out that the term $\lambda \|\nabla \times \boldsymbol{\eta}_b^{*,n}\|_0^2 \|\mathbf{b}_{ht}^{*,n}\|_\infty^2$ in the estimate of the magnetic coupling term in the momentum equation prevents obtaining improved results for the discretization error with respect to spatial discretization. Therefore, we stick to the above simpler choice.

Discretization Error

We first estimate the coupling term by

$$\begin{aligned}
& (\nabla \times (\mathbf{u}(t_n) \times \mathbf{b}(t_n)) - \nabla \times (\tilde{\mathbf{u}}_{ht}^n \times \tilde{\mathbf{b}}_{ht}^n), \tilde{\mathbf{e}}_b^n) \\
&= (\mathbf{u}(t_n) \times \mathbf{b}(t_n) - \tilde{\mathbf{u}}_{ht}^n \times \tilde{\mathbf{b}}_{ht}^n, \nabla \times \tilde{\mathbf{e}}_b^n) \\
&= ((\mathbf{u}(t_n) - \tilde{\mathbf{u}}_{ht}^n) \times \mathbf{b}(t_n), \nabla \times \tilde{\mathbf{e}}_b^n) + (\tilde{\mathbf{u}}_{ht}^n \times (\mathbf{b}(t_n) - \tilde{\mathbf{b}}_{ht}^n), \nabla \times \tilde{\mathbf{e}}_b^n) \\
&\leq \frac{C}{\lambda} (\|\mathbf{e}_u^n\|_0^2 + \|\boldsymbol{\eta}_u^n\|_0^2) \|\mathbf{b}(t_n)\|_\infty^2 + \frac{\lambda}{4} \|\nabla \times \tilde{\mathbf{e}}_b^n\|_0^2 + \frac{C}{\lambda} \|\tilde{\mathbf{u}}_{ht}^n\|_\infty^2 (\|\boldsymbol{\eta}_b^n\|_0^2 + \|\tilde{\mathbf{e}}_b^n\|_0^2).
\end{aligned} \tag{4.17}$$

As we see later, this again gives a time step size restriction as $\Delta t \leq \lambda$.

For the LPS induction stabilization we achieve

$$\begin{aligned}
& s_{b,Ind}(\tilde{\mathbf{b}}_{ht}^n; j_b \mathbf{b}(t_n), \tilde{\mathbf{e}}_b^n) = s_{b,Ind}(\tilde{\mathbf{b}}_{ht}^n; \mathbf{b}(t_n), \tilde{\mathbf{e}}_b^n) - s_{b,Ind}(\tilde{\mathbf{b}}_{ht}^n; \boldsymbol{\eta}_b^n, \tilde{\mathbf{e}}_b^n) \\
&\leq \frac{1}{4} s_{b,Ind}(\tilde{\mathbf{b}}_{ht}^n; \tilde{\mathbf{e}}_b^n, \tilde{\mathbf{e}}_b^n) + \max_{M \in \mathcal{M}_h} \{\tau_{b,Ind,M}^n |\tilde{\mathbf{b}}_M^n|^2\} (\|\kappa_M^b(\nabla \times \mathbf{b}(t_n))\|_0^2 + \|\nabla \times \boldsymbol{\eta}_b^n\|_0^2).
\end{aligned} \tag{4.18}$$

With respect to the Lorentz stabilization, we first note

$$\nabla \times (\mathbf{a} \times \mathbf{b}) = \mathbf{a}(\nabla \cdot \mathbf{b}) - (\mathbf{a} \cdot \nabla) \mathbf{b} - \mathbf{b}(\nabla \cdot \mathbf{a}) + (\mathbf{b} \cdot \nabla) \mathbf{a}.$$

and for constant \mathbf{a}

$$\nabla \times (\mathbf{a} \times \mathbf{b}) = \mathbf{a}(\nabla \cdot \mathbf{b}) - (\mathbf{a} \cdot \nabla) \mathbf{b}.$$

Hence, we get

$$\begin{aligned}
& s_{b,Lor}(\tilde{\mathbf{u}}_{ht}^n; j_b \mathbf{b}(t_n), \tilde{\mathbf{e}}_b^n) = s_{b,Lor}(\tilde{\mathbf{u}}_{ht}^n; \mathbf{b}(t_n), \tilde{\mathbf{e}}_b^n) - s_{b,Lor}(\tilde{\mathbf{u}}_{ht}^n; \boldsymbol{\eta}_b^n, \tilde{\mathbf{e}}_b^n) \\
&\leq \frac{1}{4} s_{b,Lor}(\tilde{\mathbf{u}}_{ht}^n; \tilde{\mathbf{e}}_b^n, \tilde{\mathbf{e}}_b^n) + \max_{M \in \mathcal{M}_h} \{\tau_{b,Lor,M}^n |\tilde{\mathbf{u}}_M^n|^2\} (\|\kappa_M^b(\nabla \mathbf{b}(t_n))\|_0^2 + \|\nabla \boldsymbol{\eta}_b^n\|_0^2).
\end{aligned} \tag{4.19}$$

Now, we are in position to bound the discretization error:

Lemma 4.4.6 (Discretization Error for the Induction Equation).

For all $1 \leq m \leq N$ the discretization error due to the induction equation can be bounded by

$$\begin{aligned}
& \|\tilde{\mathbf{e}}_b^m\|_0^2 + \|2\mathbf{e}_b^m - \mathbf{e}_b^{m-1}\|_0^2 + \frac{4}{3}(\Delta t)^2 \|\nabla e_r^m\|_0^2 \\
& + \sum_{n=2}^m \left(2\Delta t \lambda \|\nabla \times \tilde{\mathbf{e}}_b^n\|_0^2 + 4\Delta t \tau_{b,gd}^n \|\nabla \cdot \tilde{\mathbf{e}}_b^n\|_0^2 + \|\delta_{tt} \mathbf{e}_b^n\|_0^2 \right. \\
& \quad \left. + 3\Delta t \sum_{M \in \mathcal{M}_h} \left(\tau_{b,Ind,M}^n \|\kappa_M^b((\nabla \times \tilde{\mathbf{e}}_b^n) \times \tilde{\mathbf{b}}_M^n)\|_{0,M}^2 \right. \right. \\
& \quad \quad \left. \left. + \tau_{b,Lor,M}^n \|\kappa_M^b(\nabla \times (\tilde{\mathbf{u}}_M^n \times \tilde{\mathbf{e}}_b^n))\|_{0,M}^2 \right) \right) \\
& \leq \|\tilde{\mathbf{e}}_b^1\|_0^2 + \|2\mathbf{e}_b^1 - \mathbf{e}_b^0\|_0^2 + \frac{4}{3}(\Delta t)^2 \|\nabla e_r^1\|_0^2 \\
& + \sum_{n=2}^m \left\{ K_b^n \|\tilde{\mathbf{e}}_b^n\|_0^2 + C\Delta t \lambda \|\nabla \times \boldsymbol{\eta}_b^n\|_0^2 + C\Delta t \tau_{b,gd}^n \|\nabla \cdot \boldsymbol{\eta}_b^n\|_0^2 + \frac{4(\Delta t)^3}{3} \|\nabla e_r^n\|_0^2 \right. \\
& \quad + C(\Delta t)^2 \|D_t \boldsymbol{\eta}_b^n\|_0^2 + C(\Delta t)^2 \|D_t \mathbf{b}(t_n) - \partial_t \mathbf{b}(t_n)\|_0^2 \\
& \quad + C \frac{\Delta t}{\lambda} \|\boldsymbol{\eta}_u^n\|_0^2 \|\mathbf{b}(t_n)\|_\infty^2 + C \frac{\Delta t}{\lambda} \|\tilde{\mathbf{u}}_{ht}^n\|_\infty^2 \|\boldsymbol{\eta}_b^n\|_0^2 \\
& \quad + \Delta t \max_{M \in \mathcal{M}_h} \{ \tau_{b,Ind,M}^n |\tilde{\mathbf{b}}_M^n|^2 \} (\|\kappa_M^b(\nabla \times \mathbf{b}(t_n))\|_0^2 + \|\nabla \times \boldsymbol{\eta}_b^n\|_0^2) \\
& \quad \left. + \Delta t \max_{M \in \mathcal{M}_h} \{ \tau_{b,Lor,M}^n |\tilde{\mathbf{u}}_M^n|^2 \} (\|\kappa_M^b(\nabla \mathbf{b}(t_n))\|_0^2 + \|\nabla \boldsymbol{\eta}_b^n\|_0^2) \right\}
\end{aligned}$$

where K_b^n is defined by

$$K_b^n := \left(\frac{1}{4} + \Delta t \left[\frac{C}{\lambda} \|\mathbf{b}(t_n)\|_\infty^2 + \frac{C}{\lambda} \|\tilde{\mathbf{u}}_{ht}^n\|_\infty^2 \right] \right) \stackrel{!}{<} 1.$$

Proof. The error equation reads

$$\begin{aligned}
& \left(\frac{3\tilde{\mathbf{e}}_b^n - 4\mathbf{e}_b^{n-1} + \mathbf{e}_b^{n-2}}{2\Delta t}, \mathbf{c}_h \right) + \lambda(\nabla \times \tilde{\mathbf{e}}_b^n, \nabla \times \mathbf{c}_h) + \tau_{b,gd}^n (\nabla \cdot \tilde{\mathbf{e}}_b^n, \nabla \cdot \mathbf{c}_h) \\
& + s_{b,Ind}(\tilde{\mathbf{b}}_{ht}^n; \tilde{\mathbf{e}}_b^n, \mathbf{c}_h) + s_{b,Lor}(\tilde{\mathbf{u}}_{ht}^n; \tilde{\mathbf{e}}_b^n, \mathbf{c}_h) \\
& = \underbrace{-(D_t \boldsymbol{\eta}_b^n, \mathbf{c}_h)}_I + \underbrace{(D_t \mathbf{b}(t_n), \mathbf{c}_h) - (\partial_t \mathbf{b}(t_n), \mathbf{c}_h)}_{II} + \underbrace{c_b(\tilde{\mathbf{u}}_{ht}^n, \tilde{\mathbf{b}}_{ht}^n, \mathbf{c}_h) - c_b(\mathbf{u}(t_n), \mathbf{b}(t_n), \mathbf{c}_h)}_{III} \\
& + \underbrace{s_{b,Ind}(\tilde{\mathbf{b}}_{ht}^n; \tilde{\mathbf{e}}_b^n, \mathbf{c}_h) + s_{b,Ind}(\tilde{\mathbf{b}}_{ht}^n; \tilde{\mathbf{b}}_{ht}^n, \mathbf{c}_h)}_{IV} + \underbrace{r(t_n) - r_{ht}^{n-1}, \nabla \cdot \mathbf{c}_h}_V \\
& + \underbrace{s_{b,Lor}(\tilde{\mathbf{u}}_{ht}^n; \tilde{\mathbf{e}}_b^n, \mathbf{c}_h) + s_{b,Lor}(\tilde{\mathbf{u}}_{ht}^n; \tilde{\mathbf{b}}_{ht}^n, \mathbf{c}_h)}_{VI} + \underbrace{-\lambda(\nabla \times \boldsymbol{\eta}_b^n, \nabla \times \mathbf{c}_h)}_{VII} - \underbrace{\tau_{b,gd}^n (\nabla \cdot \boldsymbol{\eta}_b^n, \nabla \cdot \mathbf{c}_h)}_{VIII}
\end{aligned}$$

due to the fact that the pair $(\mathbf{b}(t_n), r(t_n))$ fulfills the (continuous) induction equation.

Testing this equation with $\mathbf{c}_h = \tilde{\mathbf{e}}_b^n$ gives:

$$\begin{aligned} I &= -(D_t \boldsymbol{\eta}_b^n, \tilde{\mathbf{e}}_b^n) \leq C \|\tilde{\mathbf{e}}_b^n\|_0 \|D_t \boldsymbol{\eta}_b^n\|_0 \leq \frac{1}{32\Delta t} \|\tilde{\mathbf{e}}_b^n\|_0^2 + C\Delta t \|D_t \boldsymbol{\eta}_b^n\|_0^2, \\ II &= (D_t \mathbf{b}(t_n) - \partial_t \mathbf{b}(t_n), \tilde{\mathbf{e}}_b^n) \leq C\Delta t \|D_t \mathbf{b}(t_n) - \partial_t \mathbf{b}(t_n)\|_0^2 + \frac{1}{32\Delta t} \|\tilde{\mathbf{e}}_b^n\|_0^2. \end{aligned} \quad (4.20)$$

Noticing that the error equation for the projection step reads

$$\begin{aligned} -\left(\frac{3\mathbf{e}_b^n - 3\tilde{\mathbf{e}}_b^n}{2\Delta t}, \nabla s_h\right) &= (\nabla(r_{ht}^{n-1} - r_{ht}^n), \nabla s_h), \\ -\left(\frac{3\nabla \cdot \tilde{\mathbf{e}}_b^n}{2\Delta t}, s_h\right) &= (\nabla(r_{ht}^{n-1} - r_{ht}^n), \nabla s_h), \end{aligned}$$

we may write V by choosing $s_h = r(t_n) - r_{ht}^{n-1} = -r_{ht}^{n-1}$ as

$$\begin{aligned} -V &= (r_{ht}^{n-1}, \nabla \cdot \tilde{\mathbf{e}}_b^n) = -\frac{2\Delta t}{3} (\nabla(r_{ht}^{n-1} - r_{ht}^n), \nabla r_{ht}^{n-1}) \\ &= \frac{\Delta t}{3} (\|r_{ht}^n\|_0^2 - \|\nabla r_{ht}^{n-1}\|_0^2 - \|\nabla \delta_t r_{ht}^n\|_0^2) \\ &= \frac{\Delta t}{3} (\|\nabla e_r^n\|_0^2 - \|\nabla e_r^n\|_0^2) - \frac{3}{4\Delta t} \|\tilde{\mathbf{e}}_b^n - \mathbf{e}_b^n\|_0^2. \end{aligned}$$

For III, IV and VI the above derived bounds (4.17), (4.19) and (4.18) are used:

$$\begin{aligned} III &\leq \frac{C}{\lambda} (\|\mathbf{e}_u^n\|_0^2 + \|\boldsymbol{\eta}_u^n\|_0^2) \|\mathbf{b}(t_n)\|_\infty^2 + \lambda \|\nabla \times \tilde{\mathbf{e}}_b^n\|_0^2 + \frac{C}{\lambda} \|\tilde{\mathbf{u}}_{ht}^n\|_\infty^2 (\|\boldsymbol{\eta}_b^n\|_0^2 + \|\tilde{\mathbf{e}}_b^n\|_0^2), \\ IV &\leq \frac{1}{4} s_{b,Ind}(\tilde{\mathbf{b}}_{ht}^n; \tilde{\mathbf{e}}_b^n, \tilde{\mathbf{e}}_b^n) + \max_{M \in \mathcal{M}_h} \{\tau_{b,Ind,M}^n |\tilde{\mathbf{b}}_M^n|^2\} (\|\kappa_M^b(\nabla \times \mathbf{b}(t_n))\|_0^2 + \|\nabla \times \boldsymbol{\eta}_b^n\|_0^2), \\ VI &\leq \frac{1}{4} s_{b,Lor}(\tilde{\mathbf{u}}_{ht}^n; \tilde{\mathbf{e}}_b^n, \tilde{\mathbf{e}}_b^n) + \max_{M \in \mathcal{M}_h} \{\tau_{b,Lor,M}^n |\tilde{\mathbf{u}}_M^n|^2\} (\|\kappa_M^b(\nabla \mathbf{b}(t_n))\|_0^2 + \|\nabla \boldsymbol{\eta}_b^n\|_0^2). \end{aligned}$$

Finally, we have for the remaining two terms

$$\begin{aligned} -VII &= \lambda (\nabla \times \boldsymbol{\eta}_b^n, \nabla \times \tilde{\mathbf{e}}_b) \leq C\lambda \|\nabla \times \boldsymbol{\eta}_b^n\|_0^2 + \frac{1}{4} \lambda \|\nabla \times \tilde{\mathbf{e}}_b\|_0^2, \\ -VIII &= \tau_{b,gd}^n (\nabla \cdot \boldsymbol{\eta}_b^n, \nabla \cdot \tilde{\mathbf{e}}_b) \leq C\tau_{b,gd}^n \|\nabla \cdot \boldsymbol{\eta}_b^n\|_0^2 + \frac{1}{4} \tau_{b,gd}^n \|\nabla \cdot \tilde{\mathbf{e}}_b\|_0^2. \end{aligned}$$

For the discrete time derivative, we use the splitting

$$\begin{aligned} &2(3\tilde{\mathbf{e}}_b^n - 4\mathbf{e}_b^{n-1} + \mathbf{e}_b^{n-2}, \tilde{\mathbf{e}}_b^n) \\ &= 3\|\tilde{\mathbf{e}}_b^n\|_0^2 - 3\|\tilde{\mathbf{e}}_b^n - \mathbf{e}_b^n\|_0^2 - 2\|\mathbf{e}_b^n\|_0^2 + \underbrace{2(3\mathbf{e}_b^n - 4\mathbf{e}_b^{n-1} + \mathbf{e}_b^{n-2}, \tilde{\mathbf{e}}_b^n - \mathbf{e}_b^n)}_{=0} \\ &\quad + \|2\mathbf{e}_b^n - \mathbf{e}_b^{n-1}\|_0^2 + \|\delta_{tt} \mathbf{e}_b^n\|_0^2 - \|\tilde{\mathbf{e}}_b^{n-1}\|_0^2 - \|2\mathbf{e}_b^{n-1} - \mathbf{e}_b^{n-2}\|_0^2 \\ &\geq \|\tilde{\mathbf{e}}_b^n\|_0^2 - 3\|\tilde{\mathbf{e}}_b^n - \mathbf{e}_b^n\|_0^2 + \|2\mathbf{e}_b^n - \mathbf{e}_b^{n-1}\|_0^2 + \|\delta_{tt} \mathbf{e}_b^n\|_0^2 - \|\tilde{\mathbf{e}}_b^{n-1}\|_0^2 - \|2\mathbf{e}_b^{n-1} - \mathbf{e}_b^{n-2}\|_0^2 \end{aligned}$$

where the term $2(3\mathbf{e}_b^n - 4\mathbf{e}_b^{n-1} + \mathbf{e}_b^{n-2}, \tilde{\mathbf{e}}_b^n)$ vanishes due to the projection equation and the fact that \mathbf{e}_b^n is discretely divergence-free. In the last estimate $\|\mathbf{e}_b^n\|_0^2 = \|\pi_{\mathcal{C}_h^{div}} \tilde{\mathbf{e}}_b^n\|_0^2 \leq \|\tilde{\mathbf{e}}_b^n\|_0^2$ is used.

Now, we can summarize the above estimates to obtain

$$\begin{aligned}
& \|\tilde{\mathbf{e}}_b^m\|_0^2 + \|2\mathbf{e}_b^m - \mathbf{e}_b^{m-1}\|_0^2 + \frac{4}{3}(\Delta t)^2 \|\nabla e_r^m\|_0^2 \\
& + \sum_{n=2}^m \left(2\Delta t \lambda \|\nabla \times \tilde{\mathbf{e}}_b^n\|_0^2 + 4\Delta t \tau_{b,gd}^n \|\nabla \cdot \tilde{\mathbf{e}}_b^n\|_0^2 + \|\delta_{tt} \mathbf{e}_b^n\|_0^2 \right. \\
& \quad \left. + 3\Delta t \sum_{M \in \mathcal{M}_h} \left(\tau_{b,Ind,M}^n \|\kappa_M^b((\nabla \times \tilde{\mathbf{e}}_b^n) \times \tilde{\mathbf{b}}_M^n)\|_{0,M}^2 \right. \right. \\
& \quad \quad \left. \left. + \tau_{b,Lor,M}^n \|\kappa_M^b(\nabla \times (\tilde{\mathbf{u}}_M^n \times \tilde{\mathbf{e}}_b^n))\|_{0,M}^2 \right) \right) \\
& \leq \|\tilde{\mathbf{e}}_b^1\|_0^2 + \|2\mathbf{e}_b^1 - \mathbf{e}_b^0\|_0^2 + \frac{4}{3}(\Delta t)^2 \|\nabla e_r^1\|_0^2 \\
& + \sum_{n=2}^m \left\{ K_b^n \|\tilde{\mathbf{e}}_b^n\|_0^2 + C\Delta t \lambda \|\nabla \times \boldsymbol{\eta}_b^n\|_0^2 + C\Delta t \tau_{b,gd}^n \|\nabla \cdot \boldsymbol{\eta}_b^n\|_0^2 + C(\Delta t)^2 \|D_t \boldsymbol{\eta}_b^n\|_0^2 \right. \\
& \quad \left. + C(\Delta t)^2 \|D_t \mathbf{b}(t_n) - \partial_t \mathbf{b}(t_n)\|_0^2 \right. \\
& \quad \left. + C \frac{\Delta t}{\lambda} \|\boldsymbol{\eta}_u^n\|_0^2 \|\mathbf{b}(t_n)\|_\infty^2 + C \frac{\Delta t}{\lambda} \|\tilde{\mathbf{u}}_{ht}^n\|_\infty^2 \|\boldsymbol{\eta}_b^n\|_0^2 \right. \\
& \quad \left. + \Delta t \max_{M \in \mathcal{M}_h} \{ \tau_{b,Ind,M}^n |\tilde{\mathbf{b}}_M^n|^2 \} (\|\kappa_M^b(\nabla \times \mathbf{b}(t_n))\|_0^2 + \|\nabla \times \boldsymbol{\eta}_b^n\|_0^2) \right. \\
& \quad \left. + \Delta t \max_{M \in \mathcal{M}_h} \{ \tau_{b,Lor,M}^n |\tilde{\mathbf{u}}_M^n|^2 \} (\|\kappa_M^b(\nabla \mathbf{b}(t_n))\|_0^2 + \|\nabla \boldsymbol{\eta}_b^n\|_0^2) \right\}
\end{aligned}$$

where K_b^n is defined by

$$K_b^n := \left(\frac{1}{4} + \Delta t \left[\frac{C}{\lambda} \|\mathbf{b}(t_n)\|_\infty^2 + \frac{C}{\lambda} \|\tilde{\mathbf{u}}_{ht}^n\|_\infty^2 \right] \right) \stackrel{!}{<} 1.$$

□

Remark 4.4.7. In summary, we see that the discretization error equations are strongly coupled. From the momentum equation (without coupling), convergence in time is restricted to first order due to the estimate for the kinematic pressure gradient. This means that we can not expect more than that for the coupled equations although all the other error equations provide estimates of second order in time.

In space, the estimates of the Lorentz coupling in the momentum equation prevents achieving superconvergence for the discretization error. In consequence, quasi-optimal error estimates with respect to spatial discretization can just be expected for the H^1 and LPS errors, but not for the L^2 errors.

However, for an electrically non-conducting fluid, i.e. the Oberbeck-Boussinesq case, the error estimates give quasi-optimal and semi-robust results without mesh size restriction.

4.4.4 Summary

After deriving all the individual discretization error equations, they are now combined to get a bound depending only on the time step size, the interpolation errors and the continuous solutions.

Lemma 4.4.8.

The total discretization error can be bounded according to

$$E_{ht}(\tilde{\mathbf{e}}_u, \tilde{\mathbf{e}}_b, e_p, e_r, e_\theta) \leq RHS$$

where $E_{ht}(\tilde{\mathbf{e}}_u, \tilde{\mathbf{e}}_b, e_p, e_r, e_\theta)$ and RHS are defined below.

Proof. We first collect all the terms on the left-hand side of the equations:

$$\begin{aligned} E_{ht}(\tilde{\mathbf{e}}_u, \tilde{\mathbf{e}}_b, e_p, e_r, e_\theta) := & \|\tilde{\mathbf{e}}_u^m\|_0^2 + \|2\mathbf{e}_u^m - \mathbf{e}_u^{m-1}\|_0^2 + \frac{4}{3}(\Delta t)^2 \|\nabla e_p^m\|_0^2 + \|e_\theta^m\|_0^2 \\ & + \|2e_\theta^m - e_\theta^{m-1}\|_0^2 + \|\tilde{\mathbf{e}}_b^m\|_0^2 + \|2\mathbf{e}_b^m - \mathbf{e}_b^{m-1}\|_0^2 + \frac{4}{3}(\Delta t)^2 \|\nabla e_r^m\|_0^2 \\ & + \sum_{n=2}^m \left\{ 2\Delta t \nu \|\nabla \tilde{\mathbf{e}}_u^n\|_0^2 + 4\Delta t \tau_{u,gd}^n \|\nabla \cdot \tilde{\mathbf{e}}_u^n\|_0^2 + \|\delta_{tt} e_u^n\|_0^2 + \|\delta_{tt} e_\theta^n\|_0^2 \right. \\ & \quad + 4\Delta t \alpha \|\nabla e_\theta^n\|_0^2 + 2\Delta t \lambda \|\nabla \times \tilde{\mathbf{e}}_b^n\|_0^2 \\ & \quad + 4\Delta t \tau_{b,gd}^n \|\nabla \cdot \tilde{\mathbf{e}}_b^n\|_0^2 + \|\delta_{tt} \mathbf{e}_b^n\|_0^2 \\ & \quad + 3\Delta t \sum_{M \in \mathcal{M}_h} \left(\tau_{u,SU,M}^n \|\kappa_M^u((\tilde{\mathbf{u}}_M^n \cdot \nabla) \tilde{\mathbf{e}}_u^n)\|_{0,M}^2 \right. \\ & \quad \quad + \tau_{u,Cor}^n \|\kappa_M^u(\boldsymbol{\omega}^n \times \tilde{\mathbf{e}}_u^n)\|_{0,M}^2 \\ & \quad \quad + \tau_{\theta,SU,M}^n \|\kappa_M^u((\tilde{\mathbf{u}}_M^n \cdot \nabla) e_\theta^n)\|_{0,M}^2 \\ & \quad \quad + \tau_{b,Ind,M}^n \|\kappa_M^b((\nabla \times \tilde{\mathbf{e}}_b^n) \times \tilde{\mathbf{b}}_M^n)\|_{0,M}^2 \\ & \quad \quad \left. + \tau_{b,Lor,M}^n \|\kappa_M^b(\nabla \times (\tilde{\mathbf{u}}_M^n \times \tilde{\mathbf{e}}_b^n))\|_{0,M}^2 \right) \left. \right\}. \end{aligned}$$

The combined right-hand side reads:

$$\begin{aligned} \widetilde{RHS} = & \|\tilde{\mathbf{e}}_u^1\|_0^2 + \|2\mathbf{e}_u^1 - \mathbf{e}_u^0\|_0^2 + \frac{4}{3}(\Delta t)^2 \|\nabla e_p^1\|_0^2 + \|e_\theta^1\|_0^2 + \|2e_\theta^1 - e_\theta^0\|_0^2 \\ & + \|\tilde{\mathbf{e}}_b^1\|_0^2 + \|2\mathbf{e}_b^1 - \mathbf{e}_b^0\|_0^2 + \frac{4}{3}(\Delta t)^2 \|\nabla e_r^1\|_0^2 \\ & + \sum_{n=2}^m \left\{ K_u^n \|\tilde{\mathbf{e}}_u^n\|_0^2 + K_b^n \|\tilde{\mathbf{e}}_b^n\|_0^2 + K_\theta^n \|e_\theta^n\|_0^2 \right. \\ & \quad \left. + \frac{4(\Delta t)^3}{3} \|\nabla e_p^n\|_0^2 + \underbrace{C \Delta t |\theta(t_n)|_{W^{1,\infty}(\Omega)}}_{\text{wavy line}} \|\tilde{\mathbf{e}}_u^n\|_0^2 + \frac{4(\Delta t)^3}{3} \|\nabla e_r^n\|_0^2 \right\} \end{aligned}$$

$$\begin{aligned}
& + C \frac{\Delta t}{h} \|\tilde{\mathbf{e}}_b^{*,n}\|_0^2 \|\tilde{\mathbf{b}}_{ht}^{*,n}\|_\infty^2 + C \Delta t \|e_\theta^{*,n}\|_0^2 + \Delta t \|\nabla \times \mathbf{b}(t_n)^*\|_\infty^2 \|\tilde{\mathbf{e}}_b^{*,n}\|_0^2 \\
& + \underline{3\varepsilon \Delta t h^{2-2z} \|\tilde{\mathbf{e}}_u^n\|_{LPS_u}^2} \\
& \frac{4(\Delta t)^2}{3} \left(1 + \frac{1}{2\Delta t}\right) \|\nabla(\hat{p}_{ht}^{n-1} - \hat{p}_{ht}^n)\|_0^2 + C(\Delta t)^2 \|D_t \boldsymbol{\eta}_u^n\|_0^2 \\
& + C(\Delta t)^2 \|D_t \mathbf{u}(t_n) - \partial_t \mathbf{u}(t_n)\|_0^2 + Ch^{-2z} \Delta t \|\boldsymbol{\eta}_u^n\|_0^2 \\
& + \underline{3C \Delta t h^{2-2z} \|\boldsymbol{\eta}_u^n\|_{LPS_u}^2} \\
& + C \frac{\Delta t}{\nu} \max_{M \in \mathcal{M}_h} \{\tau_{u,SU,M}^n |\tilde{\mathbf{u}}_M^n|^2\} (\nu \|\boldsymbol{\eta}_u^n\|_1^2 + \nu \|\kappa_M^u(\nabla \mathbf{u}(t_n))\|_0^2) \\
& + C \Delta t \tau_{u,Cor}^n |\boldsymbol{\omega}^n|^2 (\|\boldsymbol{\eta}_u^n\|_0^2 + \|\kappa_M^u(\mathbf{u}(t_n))\|_0^2) \\
& + C \Delta t \|\delta_{tt} \theta(t_n)\|_0^2 \\
& + \Delta t \|\nabla \times \delta_{tt} \mathbf{b}(t_n)\|_0^2 \|\mathbf{b}(t_n)\|_\infty^2 + \Delta t \|\nabla \times \mathbf{b}(t_n)^*\|_\infty^2 \|\delta_{tt} \mathbf{b}(t_n)\|_0^2 \\
& + \Delta t \lambda \|\nabla \times \boldsymbol{\eta}_b^{*,n}\|_0^2 \|\tilde{\mathbf{b}}_{ht}^{*,n}\|_\infty^2 + \Delta t \|\nabla \times \mathbf{b}(t_n)^*\|_\infty^2 \|\boldsymbol{\eta}_b^{*,n}\|_0^2 \\
& + (\Delta t)^2 \|D_t \boldsymbol{\eta}_\theta^n\|_0^2 + C(\Delta t)^2 \|D_t \theta(t_n) - \partial_t \theta(t_n)\|_0^2 \\
& + C \Delta t h^{-2z} \|\boldsymbol{\eta}_\theta(t_n)\|_0^2 \\
& + C \Delta t h^{-2z} \|\boldsymbol{\eta}_u^n\|_0^2 + \underline{3\varepsilon \Delta t h^{2-2z} \|\boldsymbol{\eta}_u^n\|_{LPS_u}^2} \\
& + \Delta t \max_{M \in \mathcal{M}_h} \{\tau_{\theta,SU,M}^n |\tilde{\mathbf{u}}_M^n|^2\} (\|\kappa_M^\theta(\nabla \theta(t_n))\|_0^2 + \|\nabla \boldsymbol{\eta}_\theta^n\|_0^2) \\
& + C \Delta t \lambda \|\nabla \times \boldsymbol{\eta}_b^n\|_0^2 + C \Delta t \tau_{b,gd}^n \|\nabla \cdot \boldsymbol{\eta}_b^n\|_0^2 + C(\Delta t)^2 \|D_t \boldsymbol{\eta}_b^n\|_0^2 \\
& + C(\Delta t)^2 \|D_t \mathbf{b}(t_n) - \partial_t \mathbf{b}(t_n)\|_0^2 \\
& + C \frac{\Delta t}{\lambda} \|\boldsymbol{\eta}_u^n\|_0^2 \|\mathbf{b}(t_n)\|_\infty^2 + C \frac{\Delta t}{\lambda} \|\tilde{\mathbf{u}}_{ht}^n\|_\infty^2 \|\boldsymbol{\eta}_b^n\|_0^2 \\
& + \Delta t \max_{M \in \mathcal{M}_h} \{\tau_{b,Ind,M}^n |\tilde{\mathbf{b}}_M^n|^2\} (\|\kappa_M^b(\nabla \times \mathbf{b}(t_n))\|_0^2 + \|\nabla \times \boldsymbol{\eta}_b^n\|_0^2) \\
& + \Delta t \max_{M \in \mathcal{M}_h} \{\tau_{b,Lor,M}^n |\tilde{\mathbf{u}}_M^n|^2\} (\|\kappa_M^b(\nabla \mathbf{b}(t_n))\|_0^2 + \|\nabla \boldsymbol{\eta}_b^n\|_0^2) \}.
\end{aligned}$$

Provided Δt is sufficiently small, the underlined block can be hidden in the left-hand side.

For the first block (marked by \sim), a discrete Gronwall lemma is used. This gives

$$E_{ht}(\tilde{\mathbf{e}}_u, \tilde{\mathbf{e}}_b, e_p, e_r, e_\theta)$$

$$\begin{aligned}
& \lesssim RHS := C_G \left\{ \|\tilde{\mathbf{e}}_u^1\|_0^2 + \|2\mathbf{e}_u^1 - \mathbf{e}_u^0\|_0^2 + \frac{4}{3}(\Delta t)^2 \|\nabla e_p^1\|_0^2 + \|e_\theta^1\|_0^2 + \|2e_\theta^1 - e_\theta^0\|_0^2 \right. \\
& \quad + \|\tilde{\mathbf{e}}_b^1\|_0^2 + \|2\mathbf{e}_b^1 - \mathbf{e}_b^0\|_0^2 + \frac{4}{3}(\Delta t)^2 \|\nabla e_r^1\|_0^2 \\
& \quad + \sum_{n=2}^m \left\{ \frac{4(\Delta t)^2}{3} \left(1 + \frac{1}{2\Delta t}\right) \|\nabla(\hat{p}_{ht}^{n-1} - \hat{p}_{ht}^n)\|_0^2 + C(\Delta t)^2 \|D_t \boldsymbol{\eta}_u^n\|_0^2 \right. \\
& \quad \quad \left. + C(\Delta t)^2 \|D_t \mathbf{u}(t_n) - \partial_t \mathbf{u}(t_n)\|_0^2 + Ch^{-2z} \Delta t \|\boldsymbol{\eta}_u^n\|_0^2 \right.
\end{aligned}$$

$$\begin{aligned}
& + 3C\Delta th^{2-2z} \|\boldsymbol{\eta}_u^n\|_{LPS_u}^2 \\
& + C\frac{\Delta t}{\nu} \max_{M \in \mathcal{M}_h} \{\tau_{u,SU,M}^n |\tilde{\mathbf{u}}_M^n|^2\} (\nu \|\boldsymbol{\eta}_u^n\|_1^2 + \nu \|\kappa_M^u(\nabla \mathbf{u}(t_n))\|_0^2) \\
& + C\Delta t \tau_{u,Cor}^n |\boldsymbol{\omega}^n|^2 (\|\boldsymbol{\eta}_u^n\|^2 + \|\kappa_M^u(\mathbf{u}(t_n))\|_0^2) \\
& + C\Delta t \|\delta_{tt}\theta(t_n)\|_0^2 \\
& + \Delta t \|\nabla \times \delta_{tt}\mathbf{b}(t_n)\|_0^2 \|\mathbf{b}(t_n)\|_\infty^2 + \Delta t \|\nabla \times \mathbf{b}(t_n)^*\|_\infty^2 \|\delta_{tt}\mathbf{b}(t_n)\|_0^2 \\
& + \Delta t \lambda \|\nabla \times \boldsymbol{\eta}_b^{*,n}\|_0^2 \|\tilde{\mathbf{b}}_{ht}^{*,n}\|_\infty^2 + \Delta t \|\nabla \times \mathbf{b}(t_n)^*\|_\infty^2 \|\boldsymbol{\eta}_b^{*,n}\|_0^2 \\
& + (\Delta t)^2 \|D_t \eta_\theta^n\|_0^2 + C(\Delta t)^2 \|D_t \theta(t_n) - \partial_t \theta(t_n)\|_0^2 \\
& + C\Delta th^{-2z} \|\eta_\theta(t_n)\|_0^2 \\
& + C\Delta th^{-2z} \|\boldsymbol{\eta}_u^n\|_0^2 + 3\varepsilon \Delta th^{2-2z} \|\boldsymbol{\eta}_u^n\|_{LPS_u}^2 \\
& + \Delta t \max_{M \in \mathcal{M}_h} \{\tau_{\theta,SU,M}^n |\tilde{\mathbf{u}}_M^n|^2\} (\|\kappa_M^\theta(\nabla \theta(t_n))\|_0^2 + \|\nabla \eta_\theta^n\|_0^2) \\
& + C\Delta t \lambda \|\nabla \times \boldsymbol{\eta}_b^n\|_0^2 + C\Delta t \tau_{b,gd}^n \|\nabla \cdot \boldsymbol{\eta}_b^n\|_0^2 + C(\Delta t)^2 \|D_t \boldsymbol{\eta}_b^n\|_0^2 \\
& + C(\Delta t)^2 \|D_t \mathbf{b}(t_n) - \partial_t \mathbf{b}(t_n)\|_0^2 \\
& + C\frac{\Delta t}{\lambda} \|\boldsymbol{\eta}_u^n\|_0^2 \|\mathbf{b}(t_n)\|_\infty^2 + C\frac{\Delta t}{\lambda} \|\tilde{\mathbf{u}}_{ht}^n\|_\infty^2 \|\boldsymbol{\eta}_b^n\|_0^2 \\
& + \Delta t \max_{M \in \mathcal{M}_h} \{\tau_{b,Ind,M}^n |\tilde{\mathbf{b}}_M^n|^2\} (\|\kappa_M^b(\nabla \times \mathbf{b}(t_n))\|_0^2 + \|\nabla \times \boldsymbol{\eta}_b^n\|_0^2) \\
& + \Delta t \max_{M \in \mathcal{M}_h} \{\tau_{b,Lor,M}^n |\tilde{\mathbf{u}}_M^n|^2\} (\|\kappa_M^b(\nabla \mathbf{b}(t_n))\|_0^2 + \|\nabla \boldsymbol{\eta}_b^n\|_0^2) \} \}
\end{aligned}$$

where the Gronwall term C_G is given according to

$$\begin{aligned}
C_G & \sim \exp\left(\frac{T}{1-K}\right), \\
K & \sim \max_{2 \leq n \leq m} \{K_u^n + K_b^n + K_\theta^n + \Delta t |\theta(t_n)|_{W^{1,\infty}(\Omega)}\} \stackrel{!}{<} 1.
\end{aligned}$$

□

4.5 Convergence Results

With this combined estimate at hand we can proceed to a convergence result by using Assumptions 2.5.3, 2.5.4, 2.5.5 for the interpolation errors in the right-hand side.

Theorem 4.5.1.

Assume that the continuous solutions satisfy the regularity assumptions

$$\begin{aligned}
\mathbf{u} & \in W^{1,\infty}(t_0, T; H^{k_u+1}(\Omega)) \cap W^{2,\infty}(t_0, T; L^2(\Omega)), \\
p & \in W^{1,\infty}(t_0, T; H^{k_p+1}(\Omega)), \\
\mathbf{b} & \in W^{2,\infty}(t_0, T; H^1(\Omega)) \cap W^{1,\infty}(t_0, T; H^{k_b+1}(\Omega)) \cap L^\infty(t_0, T; W^{1,\infty}(\Omega)),
\end{aligned}$$

$$\theta \in W^{2,\infty}(t_0, T; L^2(\Omega)) \cap W^{1,\infty}(t_0, T; H^{k_\theta+1}(\Omega)),$$

that the discrete solutions fulfill the additional bound $\tilde{\mathbf{u}}_{ht}, \tilde{\mathbf{b}}_{ht} \in L^\infty(t_0, T; L^\infty(\Omega))$ and that the initial errors are sufficiently small.

1. The total error with respect to the LPS-norms can be bounded by

$$\begin{aligned} & \|\tilde{\boldsymbol{\xi}}_u\|_{l^\infty(t_0, T; L^2(\Omega))}^2 + \|\tilde{\boldsymbol{\xi}}_b\|_{l^\infty(t_0, T; L^2(\Omega))}^2 + \|\tilde{\boldsymbol{\xi}}_\theta\|_{l^\infty(t_0, T; L^2(\Omega))}^2 \\ & + \|\tilde{\boldsymbol{\xi}}_u\|_{l^\infty(t_0, T; LPS_u)}^2 + \|\tilde{\boldsymbol{\xi}}_b\|_{l^\infty(t_0, T; LPS_b)}^2 + \|\tilde{\boldsymbol{\xi}}_\theta\|_{l^\infty(t_0, T; LPS_\theta)}^2 \\ & \lesssim \Delta t^2 + h^{2k_u} + h^{2k_p+2} + h^{2k_\theta} + h^{2k_b} \end{aligned}$$

provided

$$\begin{aligned} \max_{M \in \mathcal{M}_h} \{\tau_{u, SU, M}^n |\tilde{\mathbf{u}}_M^n|^2\} &\lesssim \nu h^{2k_u - 2s_u}, & \tau_{u, gd}^n &\sim 1, \\ \tau_{u, Cor}^n |\boldsymbol{\omega}^n|^2 &\lesssim h^{2k_u - 2 - 2s_u}, & Re_{b, M} &\lesssim \frac{1}{\sqrt{\lambda}}, \\ \max_{M \in \mathcal{M}_h} \{\tau_{\theta, SU, M}^n |\tilde{\mathbf{u}}_M^n|^2\} &\lesssim h^{2k_\theta - 2s_\theta}, & \tau_{b, gd} &\lesssim 1, \\ \max_{M \in \mathcal{M}_h} \{\tau_{b, Ind, M}^n |\tilde{\mathbf{b}}_M^n|^2\} &\lesssim h^{2k_b - 2s_b}, & Re_{u, M} &\lesssim \frac{\sqrt{\lambda}}{\nu}, \\ \max_{M \in \mathcal{M}_h} \{\tau_{b, Lor, M}^n |\tilde{\mathbf{u}}_M^n|^2\} &\lesssim h^{2k_b - 2s_b} \end{aligned} \quad (4.21)$$

and $\Delta t \lesssim \min\{h, \lambda\}$ where

$$Re_{b, M} := \frac{h \|\mathbf{b}(t_n)\|_\infty}{\lambda}, \quad Re_{u, M} := \frac{h \|\tilde{\mathbf{u}}_{ht}^n\|_\infty}{\nu}.$$

are the local magnetic and fluid Reynolds number.

2. Neglecting the magnetic field, we can get an improved bound for the L^2 -errors

$$\|\tilde{\boldsymbol{\xi}}_u\|_{l^\infty(t_0, T; L^2(\Omega))}^2 + \|\tilde{\boldsymbol{\xi}}_\theta\|_{l^\infty(t_0, T; L^2(\Omega))}^2 \lesssim (\Delta t)^2 + h^{2k_u+2} + h^{2k_p+4} + h^{2k_\theta+2}$$

provided

$$\begin{aligned} \tau_{u, gd}^n &\sim 1, & \max_{M \in \mathcal{M}_h} \{\tau_{u, SU, M}^n |\tilde{\mathbf{u}}_M^n|^2\} &\lesssim \nu h^{2+2k_u-2s_u}, \\ \tau_{u, Cor}^n |\boldsymbol{\omega}^n|^2 &\lesssim h^{2k_u-2s_u}, & \max_{M \in \mathcal{M}_h} \{\tau_{\theta, SU, M}^n |\tilde{\mathbf{u}}_M^n|^2\} &\lesssim h^{2+2k_\theta-2s_\theta} \end{aligned} \quad (4.22)$$

and $\Delta t \lesssim h^2$.

Proof. For the total error with respect to the first result, we consider the splitting

$$\begin{aligned}
& \|\tilde{\boldsymbol{\xi}}_u\|_{l^\infty(t_0, T; L^2(\Omega))}^2 + \|\tilde{\boldsymbol{\xi}}_b\|_{l^\infty(t_0, T; L^2(\Omega))}^2 + \|\tilde{\boldsymbol{\xi}}_\theta\|_{l^\infty(t_0, T; L^2(\Omega))}^2 \\
& \quad + \|\tilde{\boldsymbol{\xi}}_u\|_{l^\infty(t_0, T; LPS_u)}^2 + \|\tilde{\boldsymbol{\xi}}_b\|_{l^\infty(t_0, T; LPS_b)}^2 + \|\tilde{\boldsymbol{\xi}}_\theta\|_{l^\infty(t_0, T; LPS_\theta)}^2 \\
& \lesssim RHS + \|\boldsymbol{\eta}_u\|_{l^\infty(t_0, T; L^2(\Omega))}^2 + \|\boldsymbol{\eta}_b\|_{l^\infty(t_0, T; L^2(\Omega))}^2 + \|\boldsymbol{\eta}_\theta\|_{l^\infty(t_0, T; L^2(\Omega))}^2 \\
& \quad + \|\boldsymbol{\eta}_u\|_{l^\infty(t_0, T; LPS_u)}^2 + \|\boldsymbol{\eta}_b\|_{l^\infty(t_0, T; LPS_b)}^2 + \|\boldsymbol{\eta}_\theta\|_{l^\infty(t_0, T; LPS_\theta)}^2
\end{aligned}$$

and the assumptions on the interpolations immediately give the expected rate of convergence for the interpolation errors apart from the nonlinear stabilizations. For those we estimate

$$\begin{aligned}
\tau_{u, SU, M}^n \|\kappa_M^u((\tilde{\mathbf{u}}_M^n \cdot \nabla) \boldsymbol{\eta}_u^n)\|_{0, M}^2 &\leq \tau_{u, SU, M}^n |\tilde{\mathbf{u}}_M^n|^2 \|\nabla \boldsymbol{\eta}_u^n\|_{0, M}^2, \\
\tau_{u, Cor}^n \|\kappa_M^u(\boldsymbol{\omega}^n \times \boldsymbol{\eta}_u^n)\|_{0, M}^2 &\leq \tau_{u, Cor}^n |\boldsymbol{\omega}^n|^2 \|\boldsymbol{\eta}_u^n\|_{0, M}^2, \\
\tau_{\theta, SU, M}^n \|\kappa_M^u((\tilde{\mathbf{u}}_M^n \cdot \nabla) \boldsymbol{\eta}_\theta^n)\|_{0, M}^2 &\leq \tau_{\theta, SU, M}^n |\tilde{\mathbf{u}}_M^n|^2 \|\nabla \boldsymbol{\eta}_\theta^n\|_{0, M}^2, \\
\tau_{b, Ind, M}^n \|\kappa_M^b((\nabla \times \boldsymbol{\eta}_b^n) \times \tilde{\mathbf{b}}_M^n)\|_{0, M}^2 &\leq \tau_{b, Ind, M}^n |\tilde{\mathbf{b}}_M^n|^2 \|\nabla \times \boldsymbol{\eta}_b^n\|_{0, M}^2, \\
\tau_{b, Lor, M}^n \|\kappa_M^b(\nabla \times (\tilde{\mathbf{u}}_M^n \times \boldsymbol{\eta}_b^n))\|_{0, M}^2 &\leq \tau_{b, Lor, M}^n |\tilde{\mathbf{u}}_M^n| \|\nabla \boldsymbol{\eta}_b^n\|_{0, M}^2
\end{aligned}$$

and notice that these terms already appear in *RHS*.

For the second result, we observe

$$\|\tilde{\boldsymbol{\xi}}_u\|_{l^\infty(t_0, T; L^2(\Omega))}^2 + \|\tilde{\boldsymbol{\xi}}_\theta\|_{l^\infty(t_0, T; L^2(\Omega))}^2 \lesssim RHS + \|\boldsymbol{\eta}_u\|_{l^\infty(t_0, T; L^2(\Omega))}^2 + \|\boldsymbol{\eta}_\theta\|_{l^\infty(t_0, T; L^2(\Omega))}^2$$

and again the interpolation results give the expected rate of convergence.

All that is left is an estimate of *RHS*.

We first bound the terms that give us the temporal order of convergence:

$$\begin{aligned}
& \frac{4(\Delta t)^2}{3} \left(1 + \frac{1}{2\Delta t}\right) \|\nabla \delta_t \hat{p}_{ht}^n\|_0^2 \leq C \Delta t^3 (\|\mathbf{u}\|_{W^{1, \infty}(t_0, T; H^{k_u+1}(\Omega))}^2 + \|p\|_{W^{1, \infty}(t_0, T; H^{k_p+1}(\Omega))}^2), \\
& (\Delta t)^2 \|D_t \mathbf{u}(t_n) - \partial_t \mathbf{u}(t_n)\|_0^2 \leq C (\Delta t)^4 \|\mathbf{u}\|_{W^{2, \infty}(t_0, T; L^2(\Omega))}^2, \\
& (\Delta t)^2 \|D_t \mathbf{b}(t_n) - \partial_t \mathbf{b}(t_n)\|_0^2 \leq C (\Delta t)^4 \|\mathbf{b}\|_{W^{2, \infty}(t_0, T; L^2(\Omega))}^2, \\
& (\Delta t)^2 \|D_t \theta(t_n) - \partial_t \theta(t_n)\|_0^2 \leq C (\Delta t)^4 \|\theta\|_{W^{2, \infty}(t_0, T; L^2(\Omega))}^2, \\
& \Delta t \|\nabla \times \delta_{tt} \mathbf{b}(t_n)\|_0^2 \|\mathbf{b}(t_n)\|_\infty^2 \leq C (\Delta t)^3 \|\mathbf{b}\|_{W^{2, \infty}(t_0, T; H^1(\Omega))}^2 \|\mathbf{b}(t_n)\|_\infty^2, \\
& \Delta t \|\nabla \times \mathbf{b}(t_n)^*\|_\infty^2 \|\delta_{tt} \mathbf{b}(t_n)\|_0^2 \leq C (\Delta t)^3 \|\mathbf{b}\|_{W^{2, \infty}(t_0, T; L^2(\Omega))}^2 \|\nabla \times \mathbf{b}(t_n)^*\|_\infty^2, \\
& \Delta t \|\delta_{tt} \theta(t_n)\|_0^2 \leq C (\Delta t)^3 \|\theta\|_{W^{2, \infty}(t_0, T; L^2(\Omega))}^2.
\end{aligned}$$

Next, we consider the approximation with respect to the velocity and the kinematic pressure:

$$\begin{aligned}
& (\Delta t)^2 \|D_t \boldsymbol{\eta}_u^n\|_0^2 \\
& \leq C(\Delta t)^2 ((\nu + \tau_{u,gd}^n) h^{2k_u+2} \|\mathbf{u}\|_{W^{1,\infty}(t_0,T;H^{k_u+1}(\Omega))}^2 + \frac{h^{2k_p+4}}{\tau_{u,gd}^n} \|p\|_{W^{1,\infty}(t_0,T;H^{k_p+1}(\Omega))}^2), \\
& h^{-2z} \Delta t \|\boldsymbol{\eta}_u^n\|_0^2 + \Delta t h^{2-2z} \|\boldsymbol{\eta}_u^n\|_{LPS_u}^2 \\
& \leq C\Delta t ((\nu + \tau_{u,gd}^n) h^{2k_u+2-2z} \|\mathbf{u}\|_{L^\infty(t_0,T;H^{k_u+1}(\Omega))}^2 + \frac{h^{2k_p+4-2z}}{\tau_{u,gd}^n} \|p(t_n)\|_{L^\infty(t_0,T;H^{k_p+1}(\Omega))}^2), \\
& (\nu \|\boldsymbol{\eta}_u^n\|_1^2 + \nu \|\kappa_M^u(\nabla \mathbf{u}(t_n))\|_0^2) \\
& \leq C((\nu + \tau_{u,gd}^n) h^{2k_u} \|\mathbf{u}\|_{L^\infty(t_0,T;H^{k_u+1}(\Omega))}^2 + \frac{h^{2k_p+2}}{\tau_{u,gd}^n} \|p(t_n)\|_{L^\infty(t_0,T;H^{k_u+1}(\Omega))}^2 \\
& \quad + \nu h^{2s_u} \|\mathbf{u}\|_{L^\infty(t_0,T;H^{s_u+1}(\Omega))}^2), \\
& \Delta t \tau_{u,Cor}^n |\boldsymbol{\omega}^n|^2 (\|\boldsymbol{\eta}_u^n\|_0^2 + \|\kappa_M^u(\mathbf{u}(t_n))\|_0^2) \\
& \leq C\Delta t \tau_{u,Cor}^n |\boldsymbol{\omega}^n|^2 ((\nu + \tau_{u,gd}^n) h^{2k_u+2} \|\mathbf{u}\|_{L^\infty(t_0,T;H^{k_u+1}(\Omega))}^2 \\
& \quad + \frac{h^{2k_p+4}}{\tau_{u,gd}^n} \|p(t_n)\|_{L^\infty(t_0,T;H^{k_u+1}(\Omega))}^2 + \nu h^{2s_u+2} \|\mathbf{u}\|_{L^\infty(t_0,T;H^{s_u+1}(\Omega))}^2), \\
& \frac{\Delta t}{\lambda} \|\boldsymbol{\eta}_u^n\|_0^2 \|\mathbf{b}(t_n)\|_\infty^2 \\
& \leq C \frac{\Delta t}{\lambda} \|\mathbf{b}(t_n)\|_\infty^2 ((\nu + \tau_{u,gd}^n) h^{2k_u+2-2z} \|\mathbf{u}\|_{L^\infty(t_0,T;H^{k_u+1}(\Omega))}^2 \\
& \quad + \frac{h^{2k_p+4-2z}}{\tau_{u,gd}^n} \|p(t_n)\|_{L^\infty(t_0,T;H^{k_p+1}(\Omega))}^2).
\end{aligned}$$

For the magnetic field, we notice

$$\begin{aligned}
& (\Delta t)^2 \|D_t \boldsymbol{\eta}_b^n\|_0^2 \leq C(\Delta t)^2 h^{2k_b+2} \|\mathbf{b}\|_{W^{1,\infty}(t_0,T;H^{k_b+1}(\Omega))}^2, \\
& \lambda \|\nabla \times \boldsymbol{\eta}_b^n\|_0^2 + \tau_{b,gd}^n \|\nabla \cdot \boldsymbol{\eta}_b^n\|_0^2 \leq C(\lambda + \tau_{b,gd}^n) h^{2k_b} \|\mathbf{b}\|_{L^\infty(t_0,T;H^{k_b+1}(\Omega))}^2, \\
& \Delta t \lambda \|\nabla \times \boldsymbol{\eta}_b^{*,n}\|_0^2 \|\tilde{\boldsymbol{b}}_{ht}^{*,n}\|_\infty^2 \leq C\Delta t \|\tilde{\boldsymbol{b}}_{ht}^{*,n}\|_\infty^2 \lambda h^{2k_b} \|\mathbf{b}\|_{L^\infty(t_0,T;H^{k_b+1}(\Omega))}^2, \\
& \Delta t \|\nabla \times \mathbf{b}(t_n)^*\|_\infty \|\boldsymbol{\eta}_b^{*,n}\|_0^2 \leq C\Delta t \|\nabla \times \mathbf{b}(t_n)^*\|_\infty h^{2k_b+2} \|\mathbf{b}\|_{L^\infty(t_0,T;H^{k_b+1}(\Omega))}^2, \\
& \frac{\Delta t}{\lambda} \|\tilde{\boldsymbol{u}}_{ht}^n\|_\infty^2 \|\boldsymbol{\eta}_b^n\|_0^2 \leq C \frac{\Delta t}{\lambda} \|\tilde{\boldsymbol{u}}_{ht}^n\|_\infty^2 h^{2k_b+2} \|\mathbf{b}\|_{L^\infty(t_0,T;H^{k_b+1}(\Omega))}^2, \\
& \|\kappa_M^b(\nabla \times \mathbf{b}(t_n))\|_0^2 + \|\nabla \times \boldsymbol{\eta}_b^n\|_0^2 \leq C(h^{2k_b} \|\mathbf{b}\|_{L^\infty(t_0,T;H^{k_b+1}(\Omega))}^2 + h^{2s_b} \|\mathbf{b}\|_{L^\infty(t_0,T;H^{s_b+1}(\Omega))}^2),
\end{aligned}$$

$$\|\kappa_M^b(\nabla \mathbf{b}(t_n))\|_0^2 + \|\nabla \boldsymbol{\eta}_b^n\|_0^2 \leq C(h^{2k_b} \|\mathbf{b}\|_{L^\infty(t_0, T; H^{k_b+1}(\Omega))}^2 + h^{2s_b} \|\mathbf{b}\|_{L^\infty(t_0, T; H^{s_b+1}(\Omega))}^2).$$

Finally, we consider the approximation results for the temperature

$$\begin{aligned} (\Delta t)^2 \|D_t \boldsymbol{\eta}_\theta^n\|_0^2 &\leq C(\Delta t)^2 \alpha h^{2k_\theta+2} \|\theta\|_{W^{1,\infty}(t_0, T; H^{k_\theta+1}(\Omega))}^2, \\ \Delta t h^{-2z} \|\boldsymbol{\eta}_\theta(t_n)\|_0^2 &\leq C \Delta t \alpha h^{2k_\theta+2-2z} \|\theta\|_{W^{1,\infty}(t_0, T; H^{k_\theta+1}(\Omega))}^2, \\ (\|\kappa_M^\theta(\nabla \theta(t_n))\|_0^2 + \|\nabla \boldsymbol{\eta}_\theta^n\|_0^2) &\leq C(h^{2k_\theta} \|\theta\|_{L^\infty(t_0, T; H^{k_\theta+1}(\Omega))}^2 + h^{2s_\theta} \|\theta\|_{L^\infty(t_0, T; H^{s_\theta+1}(\Omega))}^2). \end{aligned}$$

Collecting all these estimates and ignoring the initial errors, the bound for the discretization errors can be summarized as

$$\begin{aligned} &\Delta t E_{ht}(\tilde{\mathbf{e}}_u, \tilde{\mathbf{e}}_b, e_p, e_r, e_\theta) \\ &\lesssim \max_{2 \leq n \leq m} \Delta t^3 (\|\mathbf{u}\|_{W^{1,\infty}(t_0, T; H^{k_u+1}(\Omega))}^2 + \|p\|_{W^{1,\infty}(t_0, T; H^{k_p+1}(\Omega))}^2 + \|\mathbf{u}\|_{W^{2,\infty}(t_0, T; L^2(\Omega))}^2 \\ &\quad + \|\mathbf{b}\|_{W^{2,\infty}(t_0, T; L^2(\Omega))}^2 + \|\theta\|_{W^{2,\infty}(t_0, T; L^2(\Omega))}^2 + \|\mathbf{b}\|_{W^{2,\infty}(t_0, T; H^1(\Omega))} \|\mathbf{b}(t_n)\|_\infty^2 \\ &\quad + \|\mathbf{b}\|_{W^{2,\infty}(t_0, T; L^2(\Omega))} \|\nabla \times \mathbf{b}(t_n)^*\|_\infty^2 + \|\theta\|_{W^{2,\infty}(t_0, T; L^2(\Omega))}^2) \\ &\quad + (\Delta t)^2 ((\nu + \tau_{u,gd}^n) h^{2k_u+2} \|\mathbf{u}\|_{W^{1,\infty}(t_0, T; H^{k_u+1}(\Omega))}^2 + \frac{h^{2k_p+4}}{\tau_{u,gd}^n} \|p\|_{W^{1,\infty}(t_0, T; H^{k_p+1}(\Omega))}^2) \\ &\quad + \Delta t ((\nu + \tau_{u,gd}^n) h^{2k_u+2-2z} \|\mathbf{u}\|_{L^\infty(t_0, T; H^{k_u+1}(\Omega))}^2 \\ &\quad + \frac{h^{2k_p+4-2z}}{\tau_{u,gd}^n} \|p(t_n)\|_{L^\infty(t_0, T; H^{k_p+1}(\Omega))}^2) \\ &\quad + \frac{\Delta t}{\nu} \max_{M \in \mathcal{M}_h} \{\tau_{u,SU,M}^n |\tilde{\mathbf{u}}_M^n|^2\} ((\nu + \tau_{u,gd}^n) h^{2k_u} \|\mathbf{u}\|_{L^\infty(t_0, T; H^{k_u+1}(\Omega))}^2 \\ &\quad + \frac{h^{2k_p+2}}{\tau_{u,gd}^n} \|p(t_n)\|_{L^\infty(t_0, T; H^{k_u+1}(\Omega))}^2 \\ &\quad + \nu h^{2s_u} \|\mathbf{u}\|_{L^\infty(t_0, T; H^{s_u+1}(\Omega))}^2) \\ &\quad + \Delta t \tau_{u,Cor}^n |\boldsymbol{\omega}^n|^2 ((\nu + \tau_{u,gd}^n) h^{2k_u+2} \|\mathbf{u}\|_{L^\infty(t_0, T; H^{k_u+1}(\Omega))}^2 \\ &\quad + \frac{h^{2k_p+4}}{\tau_{u,gd}^n} \|p(t_n)\|_{L^\infty(t_0, T; H^{k_u+1}(\Omega))}^2 \\ &\quad + \nu h^{2s_u+2} \|\mathbf{u}\|_{L^\infty(t_0, T; H^{s_u+1}(\Omega))}^2) \\ &\quad + \frac{\Delta t}{\lambda} \|\mathbf{b}(t_n)\|_\infty^2 ((\nu + \tau_{u,gd}^n) h^{2k_u+2-2z} \|\mathbf{u}\|_{L^\infty(t_0, T; H^{k_u+1}(\Omega))}^2 \\ &\quad + \frac{h^{2k_p+4-2z}}{\tau_{u,gd}^n} \|p(t_n)\|_{L^\infty(t_0, T; H^{k_p+1}(\Omega))}^2) \\ &\quad + (\Delta t)^2 \alpha h^{2k_\theta+2} \|\theta\|_{W^{1,\infty}(t_0, T; H^{k_\theta+1}(\Omega))}^2 + \Delta t \alpha h^{2k_\theta+2-2z} \|\theta\|_{W^{1,\infty}(t_0, T; H^{k_\theta+1}(\Omega))}^2 \\ &\quad + \Delta t \max_{M \in \mathcal{M}_h} \{\tau_{\theta,SU,M}^n |\tilde{\mathbf{u}}_M^n|^2\} (h^{2k_\theta} \|\theta\|_{W^{1,\infty}(t_0, T; H^{k_\theta+1}(\Omega))}^2 + h^{2s_\theta} \|\theta\|_{W^{1,\infty}(t_0, T; H^{s_\theta+1}(\Omega))}^2) \\ &\quad + (\Delta t)^2 h^{2k_b+2} \|\mathbf{b}\|_{W^{1,\infty}(t_0, T; H^{k_b+1}(\Omega))}^2 + \Delta t \|\nabla \times \mathbf{b}(t_n)^*\|_\infty^2 h^{2k_b+2} \|\mathbf{b}\|_{L^\infty(t_0, T; H^{k_b+1}(\Omega))}^2 \end{aligned}$$

$$\begin{aligned}
& + \Delta t \|\tilde{\mathbf{b}}_{ht}^{*,n}\|_{\infty}^2 \lambda h^{2k_b} \|\mathbf{b}\|_{L^\infty(t_0, T; H^{k_b+1}(\Omega))}^2 + \Delta t (\lambda + \tau_{b,gd}) h^{2k_b} \|\mathbf{b}\|_{L^\infty(t_0, T; H^{k_b+1}(\Omega))}^2 \\
& + \frac{\Delta t}{\lambda} \|\tilde{\mathbf{u}}_{ht}^n\|_{\infty}^2 h^{2k_b+2} \|\mathbf{b}\|_{L^\infty(t_0, T; H^{k_b+1}(\Omega))}^2 \\
& + \Delta t \max_{M \in \mathcal{M}_h} \{\tau_{b,Ind,M}^n |\tilde{\mathbf{b}}_M^n|^2\} (h^{2k_b} \|\mathbf{b}\|_{L^\infty(t_0, T; H^{k_b+1}(\Omega))}^2 + h^{2s_b} \|\mathbf{b}\|_{L^\infty(t_0, T; H^{s_b+1}(\Omega))}^2) \\
& + \Delta t \max_{M \in \mathcal{M}_h} \{\tau_{b,Lor,M}^n |\tilde{\mathbf{u}}_M^n|^2\} (h^{2k_b} \|\mathbf{b}\|_{L^\infty(t_0, T; H^{k_b+1}(\Omega))}^2 + h^{2s_b} \|\mathbf{b}\|_{L^\infty(t_0, T; H^{s_b+1}(\Omega))}^2).
\end{aligned}$$

For the estimates with respect to the LPS-errors, we take $z = 1$ in the above estimate. Bounding the coefficients in front of the powers of h and Δt then gives the parameter bounds (4.21). For the second estimate we proceed similarly and use $z = 0$. Since we are ignoring the errors stemming from the induction equation and the related couplings, we achieve the claimed convergence results. The parameter bounds (4.22) are then again a consequence of constant coefficients in front of powers of h and Δt .

The restrictions on the time step size are due to the requirement $K < 1$ in the Gronwall term. Note that for the second estimate the terms $\frac{1}{\lambda}$ and $\frac{1}{h}$ can be neglected since they come from the induction equations or the Lorentz force term. \square

Remark 4.5.2. By choosing different interpolation operators, the restriction with respect to ν for the SU-LPS parameter for the velocity in (4.21) can be lifted. On the other hand, this does not allow to get quasi-optimal L^2 error estimates and hence the restriction in (4.22) remains.

Remark 4.5.3. The above convergence results for the LPS errors are quasi-optimal and semi-robust with respect to temporal and spatial discretization. If we neglect the magnetic field, there are no mesh size restrictions.

For the L^2 estimates the estimates are at least semi-robust and quasi-optimal with respect to spatial discretization. We expect that the L^2 errors convergence of second order in time in fact but a proof is out of the scope of this thesis. In [ADL15b], we could achieve this for the Navier-Stokes problem by considering an incremental error equation.

If we consider the induction equation alone, the above estimates give second-order convergence with respect to time discretization for both the L^2 and the LPS error.

Remark 4.5.4. For a tensor product polynomial $f(\mathbf{x}) = \sum_{|\alpha|_{\infty} \leq k} c_{\alpha} \mathbf{x}^{\alpha}$ of degree k on a cell $M = [0, h]^d$ the estimate

$$\frac{\|f(\mathbf{x})\|_{\infty, M}^2}{\|f(\mathbf{x})\|_{0, M}^2} \leq \left(\frac{2k+1}{h} \right)^d$$

can be shown. Hence, we obtain

$$h^{2z-2} \|\tilde{\mathbf{u}}_{ht}^n\|_{\infty}^2 = \max_M h^{2z-2} \|\tilde{\mathbf{u}}_{ht}^n\|_{\infty, M}^2 \leq h^{2z-2} \left(\frac{2k+1}{h} \right)^d \max_M \|\tilde{\mathbf{u}}_{ht}^n\|_{0, M}^2 \lesssim h^{2z-2-2d} \|\tilde{\mathbf{u}}_{ht}^n\|_0^2$$

and can avoid the requirement $\tilde{\mathbf{u}}_{ht}^n \in L^\infty(t_0, T; L^\infty(\Omega))$. With respect to the Gronwall constant this leads to the restriction $\Delta t \leq h^{2d+2-2z}$.

After obtaining convergence results for velocity, temperature and the magnetic field, we can now proceed to estimates for the kinematic pressure and the magnetic pseudo-pressure in the L^2 -norm. These rely here heavily on the inf-sup stability of the chosen ansatz spaces for velocity and kinematic pressure and the magnetic field and the pseudo kinematic pressure.

Theorem 4.5.5.

The total error for the kinematic pressure and the magnetic pseudo-pressure can be bounded by

$$\begin{aligned} \|\xi_p^{n-1}\|_{l^2(t_0, T; L^2(\Omega))}^2 &\leq C \frac{\|\tilde{\xi}_u^n\|_{l^\infty(t_0, T; L^2(\Omega))}^2}{(\Delta t)^2} + C \|\tilde{\xi}_u^n\|_{l^2(t_0, T; LPS_u)}^2 + C \|\xi_\theta^n\|_{l^2(t_0, T; L^2(\Omega))}^2 \\ &\quad + C \|\nabla \times \xi_b^n\|_{l^2(t_0, T; L^2(\Omega))}^2 + C \|\xi_b^n\|_{l^\infty(t_0, T; L^2(\Omega))}^2 + C(\Delta t)^4, \\ \|\xi_r^{n-1}\|_{l^2(t_0, T; L^2(\Omega))}^2 &\leq C \frac{\|\tilde{\xi}_b^n\|_{l^\infty(t_0, T; L^2(\Omega))}^2}{(\Delta t)^2} + C \|\tilde{\xi}_b^n\|_{l^2(t_0, T; LPS_b)}^2 \\ &\quad + C \|\xi_u^n\|_{l^\infty(t_0, T; L^2(\Omega))}^2 + C(\Delta t)^4 \end{aligned}$$

if the assumptions in Theorem 4.5.1 for the LPS errors are fulfilled.

Proof. The inf-sup stability for the discrete velocity/kinematic pressure pair allows us to find $\mathbf{w}_h \in \mathbf{V}_h$ such that

$$\|\nabla \mathbf{w}_h\|_0 \leq \|\xi_p^n\|_0 / \beta_h, \quad -(\nabla \cdot \mathbf{w}_h, \xi_p^n) = \|\xi_p^n\|_0^2. \quad (4.23)$$

We test the advection-diffusion error equation with \mathbf{w}_h :

$$\begin{aligned} &\left(\frac{3\tilde{\xi}_u^n - 4\xi_u^{n-1} + \xi_u^{n-2}}{2\Delta t}, \mathbf{w}_h \right) + \nu(\nabla \tilde{\xi}_u^n, \nabla \mathbf{w}_h) + \tau_{u,gd}^n (\nabla \cdot \tilde{\xi}_u^n, \nabla \cdot \mathbf{w}_h) \\ &= -c_u(\mathbf{u}(t_n), \mathbf{u}(t_n), \mathbf{w}_h) + c_u(\tilde{\mathbf{u}}_{ht}^n; \tilde{\mathbf{u}}_{ht}^n, \mathbf{w}_h) + s_{u,SU}(\tilde{\mathbf{u}}_{ht}^n; \tilde{\mathbf{u}}_{ht}^n, \mathbf{w}_h) \\ &\quad + s_{u,Cor}(\boldsymbol{\omega}^n; \tilde{\mathbf{u}}_{ht}^n, \mathbf{w}_h) + (D_t \mathbf{u}(t_n) - \partial_t \mathbf{u}(t_n), \mathbf{w}_h) - (\nabla(p(t_n) - p_{ht}^{n-1}), \mathbf{w}_h) \\ &\quad - (\boldsymbol{\beta}^n \xi_\theta^n, \mathbf{w}_h) - ((\nabla \times \mathbf{b}(t_n)) \times \mathbf{b}(t_n), \mathbf{w}_h) + ((\nabla \times \tilde{\mathbf{b}}_{ht}^{n,*}) \times \tilde{\mathbf{b}}_{ht}^{n,*}, \mathbf{w}_h). \end{aligned} \quad (4.24)$$

Noticing $\|\mathbf{f}\|_{-1} \leq \|\mathbf{f}\|_0$, we obtain

$$\begin{aligned} &\|\nabla \mathbf{w}_h\|_0 \|\xi_p^{n-1}\|_0 \\ &\leq \frac{1}{\beta_h} \|\xi_p^{n-1}\|_0^2 = -(\nabla \xi_p^{n-1}, \mathbf{w}_h) \\ &\leq \left\| \frac{3\tilde{\xi}_u^n - 4\xi_u^{n-1} + \xi_u^{n-2}}{2\Delta t} \right\|_{-1} \|\nabla \mathbf{w}_h\|_0 + \nu \|\nabla \tilde{\xi}_u^n\|_0 \|\nabla \mathbf{w}_h\|_0 + \tau_{u,gd}^n \|\nabla \cdot \tilde{\xi}_u^n\|_0 \|\nabla \cdot \mathbf{w}_h\|_0 \end{aligned}$$

$$\begin{aligned}
& + c_u(\mathbf{u}(t_n), \mathbf{u}(t_n), \mathbf{w}_h) - c_u(\tilde{\mathbf{u}}_{ht}^n, \tilde{\mathbf{u}}_{ht}^n, \mathbf{w}_h) + s_{u,SU}(\tilde{\mathbf{u}}_{ht}^n; \tilde{\mathbf{u}}_{ht}^n, \mathbf{w}_h) \\
& + s_{u,Cor}(\boldsymbol{\omega}^n; \tilde{\mathbf{u}}_{ht}^n, \mathbf{w}_h) + \|D_t \mathbf{u}(t_n) - \partial_t \mathbf{u}(t_n)\|_{-1} \|\nabla \mathbf{w}_h\|_0 \\
& + \|p(t_n) - p(t_{n-1})\|_0 \|\nabla \cdot \mathbf{w}_h\|_0 + \|\beta \mathbf{g}^n \xi_\theta^n\|_{-1} \|\nabla \mathbf{w}_h^n\|_0 \\
& - ((\nabla \times \mathbf{b}(t_n)) \times (\mathbf{b}(t_n), \mathbf{w}_h)) + ((\nabla \times \tilde{\mathbf{b}}_{ht}^n) \times (\tilde{\mathbf{b}}_{ht}^{n,*}, \mathbf{w}_h)).
\end{aligned}$$

We calculate for the convective terms

$$\begin{aligned}
& |c_u(\mathbf{u}(t_n), \mathbf{u}(t_n), \mathbf{w}_h) - c_u(\tilde{\mathbf{u}}_{ht}^n, \tilde{\mathbf{u}}_{ht}^n, \mathbf{w}_h)| \\
& = c_u(\tilde{\boldsymbol{\xi}}_u^n, \mathbf{u}(t_n), \mathbf{w}_h) - c_u(\tilde{\mathbf{u}}_{ht}^n, \tilde{\boldsymbol{\xi}}_u^n, \mathbf{w}_h) \\
& = c_u(\tilde{\boldsymbol{\xi}}_u^n, \mathbf{u}(t_n), \mathbf{w}_h) - c_u(\mathbf{u}(t_n), \tilde{\boldsymbol{\xi}}_u^n, \mathbf{w}_h) - c_u(\tilde{\boldsymbol{\xi}}_u^n, \tilde{\boldsymbol{\xi}}_u^n, \mathbf{w}_h) \\
& \leq C \|\tilde{\boldsymbol{\xi}}_u^n\|_0 \|\mathbf{u}(t_n)\|_2 \|\mathbf{w}_h\|_1 + C \|\tilde{\boldsymbol{\xi}}_u^n\|_1^2 \|\mathbf{w}_h\|_1
\end{aligned}$$

and for the stabilization terms

$$\begin{aligned}
s_{u,SU}(\tilde{\mathbf{u}}_{ht}^n; \tilde{\mathbf{u}}_{ht}^n, \mathbf{w}_h) & = s_{u,SU}(\tilde{\mathbf{u}}_{ht}^n; \mathbf{u}(t_n) - \tilde{\boldsymbol{\xi}}_u^n, \mathbf{w}_h) \\
& \leq C \sum_{M \in \mathcal{M}_h} \tau_{u,SU,M}^n |\tilde{\mathbf{u}}_M^n|^2 \|\kappa_M^u(\nabla \mathbf{u}(t_n))\|_{0,M} \|\mathbf{w}_h\|_{1,M} \\
& \quad + C \sum_{M \in \mathcal{M}_h} \tau_{u,SU,M}^n \|\kappa_M^u((\tilde{\mathbf{u}}_M^n \cdot \nabla) \tilde{\boldsymbol{\xi}}_u^n)\|_{0,M} |\tilde{\mathbf{u}}_M^n| \|\mathbf{w}_h\|_{1,M} \\
& \leq C \left(\max_{M \in \mathcal{M}_h} \{ \tau_{u,SU,M}^n |\tilde{\mathbf{u}}_M^n|^2 \|\kappa_M^u(\nabla \mathbf{u}(t_n))\|_{0,M} \} \right. \\
& \quad \left. + \sum_{M \in \mathcal{M}_h} \tau_{u,SU,M}^n |\tilde{\mathbf{u}}_M^n| \|\kappa_M^u((\tilde{\mathbf{u}}_M^n \cdot \nabla) \tilde{\boldsymbol{\xi}}_u^n)\|_{0,M} \right) \|\nabla \mathbf{w}_h\|_0 \\
s_{u,Cor}(\boldsymbol{\omega}^n; \tilde{\mathbf{u}}_{ht}^n, \mathbf{w}_h) & = s_{u,Cor}(\boldsymbol{\omega}^n; \mathbf{u}(t_n) - \tilde{\boldsymbol{\xi}}_u^n, \mathbf{w}_h) \\
& \leq C \sum_{M \in \mathcal{M}_h} \tau_{u,Cor,M}^n |\boldsymbol{\omega}^n|^2 \|\kappa_M^u(\mathbf{u}(t_n))\|_{0,M} \|\mathbf{w}_h\|_{1,M} \\
& \quad + C \sum_{M \in \mathcal{M}_h} \tau_{u,Cor,M}^n \|\kappa_M^u(\boldsymbol{\omega}^n \times \tilde{\boldsymbol{\xi}}_u^n)\|_{0,M} |\boldsymbol{\omega}^n| \|\mathbf{w}_h\|_{1,M} \\
& \leq C \left(\max_{M \in \mathcal{M}_h} \{ \tau_{u,Cor,M}^n |\boldsymbol{\omega}^n|^2 \|\kappa_M^u(\mathbf{u}(t_n))\|_{0,M} \} \right. \\
& \quad \left. + \sum_{M \in \mathcal{M}_h} \tau_{u,Cor,M}^n |\boldsymbol{\omega}^n| \|\kappa_M^u(\boldsymbol{\omega}^n \times \tilde{\boldsymbol{\xi}}_u^n)\|_{0,M} \right) \|\nabla \mathbf{w}_h\|_{0,M}.
\end{aligned}$$

Finally, the magnetic coupling can be bounded by

$$\begin{aligned}
& ((\nabla \times \mathbf{b}(t_n)) \times \mathbf{b}(t_n) - (\nabla \times \tilde{\mathbf{b}}_{ht}^{*,n}) \times \tilde{\mathbf{b}}_{ht}^{*,n}, \mathbf{w}_h) \\
& = \underbrace{((\nabla \times \mathbf{b}(t_n)) \times \mathbf{b}(t_n) - (\nabla \times \mathbf{b}(t_n)^*) \times \mathbf{b}(t_n)^*)}_{I}, \mathbf{w}_h)
\end{aligned}$$

$$+ \underbrace{((\nabla \times \mathbf{b}(t_n)^*) \times \mathbf{b}(t_n)^* - (\nabla \times \tilde{\mathbf{b}}_{ht}^{*,n}) \times \tilde{\mathbf{b}}_{ht}^{*,n}, \mathbf{w}_h)}_{II},$$

$$\begin{aligned} |I| &= |((\nabla \times \delta_{tt} \mathbf{b}(t_n)) \times \mathbf{b}(t_n), \mathbf{w}_h) + ((\nabla \times \mathbf{b}(t_n)^*) \times \delta_{tt} \mathbf{b}(t_n), \mathbf{w}_h)| \\ &\leq \|\nabla \times \delta_{tt} \mathbf{b}(t_n)\|_0 \|\mathbf{b}(t_n)\|_\infty \|\mathbf{w}_h\|_1 + \|\nabla \times \mathbf{b}(t_n)^*\|_\infty \|\delta_{tt} \mathbf{b}(t_n)\|_0 \|\mathbf{w}_h\|_1, \end{aligned}$$

$$\begin{aligned} |II| &= |((\nabla \times (\mathbf{b}(t_n)^* - \tilde{\mathbf{b}}_{ht}^{*,n})) \times \tilde{\mathbf{b}}_{ht}^{*,n}, \mathbf{w}_h) + ((\nabla \times \mathbf{b}(t_n)^*) \times (\mathbf{b}(t_n)^* - \tilde{\mathbf{b}}_{ht}^{*,n}), \mathbf{w}_h)| \\ &\leq \|\nabla \times \tilde{\boldsymbol{\xi}}_b^{*,n}\|_0 \|\tilde{\mathbf{b}}_{ht}^{*,n}\|_\infty \|\mathbf{w}_h\|_1 + \|\nabla \times \mathbf{b}(t_n)^*\|_\infty \|\boldsymbol{\xi}_b^{*,n}\|_0 \|\mathbf{w}_h\|_1. \end{aligned}$$

We combine these results and obtain due to the approximation property of the fluctuation operators and the previous results for velocity, magnetic field and temperature:

$$\begin{aligned} &\Delta t \sum_{n=1}^N \|\xi_p^{n-1}\|_0^2 \\ &\leq C \left\{ \frac{1}{(\Delta t)^2} \|\tilde{\boldsymbol{\xi}}_u\|_{l^\infty(t_0, T; L^2(\Omega))}^2 + \nu^2 \|\nabla \tilde{\boldsymbol{\xi}}_u\|_{l^2(t_0, T; L^2(\Omega))}^2 \right. \\ &\quad + (\tau_{u, gd}^n)^2 \|\nabla \cdot \tilde{\boldsymbol{\xi}}_u\|_{l^2(t_0, T; L^2(\Omega))}^2 + \|\tilde{\boldsymbol{\xi}}_u\|_{l^\infty(t_0, T; L^2(\Omega))}^2 \|\mathbf{u}\|_{l^2(t_0, T; H^2)}^2 \\ &\quad + \|\tilde{\boldsymbol{\xi}}_u\|_{l^\infty(t_0, T; H^1(\Omega))}^2 \|\tilde{\boldsymbol{\xi}}_u\|_{l^2(t_0, T; H^1(\Omega))}^2 \\ &\quad + \max_{1 \leq n \leq N} \max_{M \in \mathcal{M}_h} \{\tau_{u, SU, M}^n |\tilde{\mathbf{u}}_M^n|^2\}^2 h^{2s_u} \|\mathbf{u}\|_{l^2(t_0, T; H^{k_u+1}(\Omega))}^2 \\ &\quad + \max_{1 \leq n \leq N} \max_{M \in \mathcal{M}_h} \{\tau_{u, SU, M}^n\} \Delta t \sum_{n=1}^N \sum_{M \in \mathcal{M}_h} \tau_{u, SU, M}^n |\tilde{\mathbf{u}}_M^n|^2 \|\kappa_M^u ((\tilde{\mathbf{u}}_M^n \cdot \nabla) \tilde{\boldsymbol{\xi}}_u^n)\|_{0, M}^2 \\ &\quad + \max_{1 \leq n \leq N} \max_{M \in \mathcal{M}_h} \{\tau_{u, Cor, M}^n |\boldsymbol{\omega}^n|^2\}^2 h^{2s_u+2} \|\mathbf{u}\|_{l^2(t_0, T; H^{k_u+1}(\Omega))}^2 \\ &\quad + \max_{1 \leq n \leq N} \max_{M \in \mathcal{M}_h} \{\tau_{u, Cor, M}^n\} \Delta t \sum_{n=1}^N \sum_{M \in \mathcal{M}_h} \tau_{u, Cor, M}^n |\boldsymbol{\omega}^n|^2 \|\kappa_M^u (\boldsymbol{\omega}^n \times \tilde{\boldsymbol{\xi}}_u^n)\|_{0, M}^2 \\ &\quad + \max_{1 \leq n \leq N} \{\|\beta \mathbf{g}^n\|^2\} \|\xi_\theta^n\|_{l^2(t_0, T; L^2(\Omega))}^2 + \|\tilde{\mathbf{b}}_{ht}^n\|_{l^\infty(t_0, T; L^\infty)}^2 \|\nabla \times \boldsymbol{\xi}_b^n\|_{l^2(t_0, T; L^2(\Omega))}^2 \\ &\quad \left. + \|\nabla \times \mathbf{b}(t_n)\|_{l^\infty(t_0, T; L^\infty)}^2 \|\boldsymbol{\xi}_b^n\|_{l^\infty(t_0, T; L^2(\Omega))}^2 + C(\Delta t)^4 \right\} \\ &\leq C \left(\frac{1}{(\Delta t)^2} + \|\mathbf{u}\|_{l^2(t_0, T; H^2)}^2 \right) \|\tilde{\boldsymbol{\xi}}_u^n\|_{l^\infty(t_0, T; L^2(\Omega))}^2 \\ &\quad + C \left(\nu + \tau_{u, gd}^n + \max_{1 \leq n \leq N} \max_{M \in \mathcal{M}_h} \{\tau_{u, SU, M}^n |\tilde{\mathbf{u}}_M^n|^2\} \right. \\ &\quad \left. + \max_{1 \leq n \leq N} \max_{M \in \mathcal{M}_h} \{\tau_{u, Cor, M}^n |\boldsymbol{\omega}_M^n|^2\} + \frac{\|\tilde{\boldsymbol{\xi}}_u^n\|_{l^2(t_0, T; LPS_u)}}{\nu^2 \Delta t} \right) \|\tilde{\boldsymbol{\xi}}_u^n\|_{l^2(t_0, T; LPS_u)}^2 \\ &\quad + C \max_{1 \leq n \leq N} \{\|\beta \mathbf{g}^n\|^2\} \|\xi_\theta^n\|_{l^2(t_0, T; L^2(\Omega))}^2 \end{aligned}$$

$$\begin{aligned}
& + C \|\tilde{\mathbf{b}}_{ht}^n\|_{l^\infty(t_0, T; L^\infty)}^2 \|\nabla \times \boldsymbol{\xi}_b^n\|_{l^2(t_0, T; L^2(\Omega))}^2 \\
& + C \|\nabla \times \mathbf{b}(t_n)\|_{l^\infty(t_0, T; L^\infty)}^2 \|\boldsymbol{\xi}_b^n\|_{l^\infty(t_0, T; L^2(\Omega))}^2 \\
& + C \max_{1 \leq n \leq N} \max_{M \in \mathcal{M}_h} \{\tau_{u, SU, M}^n |\tilde{\mathbf{u}}_M^n|^2\}^2 h^{2k_u} \|\mathbf{u}\|_{l^2(t_0, T; H^{k_u+1}(\Omega))}^2 \\
& + C \max_{1 \leq n \leq N} \max_{M \in \mathcal{M}_h} \{\tau_{u, Cor, M}^n |\boldsymbol{\omega}_M^n|^2\}^2 h^{2k_u+2} \|\mathbf{u}\|_{l^2(t_0, T; H^{k_u+1}(\Omega))}^2 \\
& + C(\Delta t)^4.
\end{aligned}$$

Provided all the assumptions on the regularity and the parameter choice are satisfied, this can be shortened as

$$\begin{aligned}
\|\xi_p^{n-1}\|_{l^2(t_0, T; L^2(\Omega))}^2 & \leq C \frac{\|\tilde{\boldsymbol{\xi}}_u^n\|_{l^\infty(t_0, T; L^2(\Omega))}^2}{(\Delta t)^2} + C \|\tilde{\boldsymbol{\xi}}_u^n\|_{l^2(t_0, T; LPS_u)}^2 + C \|\xi_\theta^n\|_{l^2(t_0, T; L^2(\Omega))}^2 \\
& + C \|\nabla \times \boldsymbol{\xi}_b^n\|_{l^2(t_0, T; L^2(\Omega))}^2 + C \|\boldsymbol{\xi}_b^n\|_{l^\infty(t_0, T; L^2(\Omega))}^2 + C(\Delta t)^4.
\end{aligned}$$

For the magnetic pseudo-pressure, we proceed similarly: Due to the inf-sup stability of the discrete ansatz pair, there exists $\mathbf{d}_h \in \mathbf{C}_h$ such that

$$\|\nabla \mathbf{d}_h\|_0 \leq \|\xi_r^n\|_0 / \beta_h, \quad -(\nabla \cdot \mathbf{d}_h, \xi_r^n) = \|\xi_r^n\|_0^2. \quad (4.25)$$

and we test the induction error equation with \mathbf{d}_h :

$$\begin{aligned}
& \left(\frac{3\tilde{\boldsymbol{\xi}}_b^n - 4\boldsymbol{\xi}_b^{n-1} + \boldsymbol{\xi}_b^{n-2}}{2\Delta t}, \mathbf{d}_h \right) + \lambda(\nabla \times \tilde{\boldsymbol{\xi}}_b^n, \nabla \times \mathbf{d}_h) + \tau_{b, gd}^n (\nabla \cdot \tilde{\boldsymbol{\xi}}_b^n, \nabla \cdot \mathbf{d}_h) \\
& = +s_{b, Lor}(\tilde{\mathbf{u}}_{ht}^n; \tilde{\mathbf{b}}_{ht}^n, \mathbf{d}_h) + s_{u, Ind}(\tilde{\mathbf{b}}_{ht}^n; \tilde{\mathbf{b}}_{ht}^n, \mathbf{d}_h) + (D_t \mathbf{u}(t_n) - \partial_t \mathbf{u}(t_n), \mathbf{d}_h) \\
& \quad - (\nabla \times (\mathbf{u}(t_n) \times \mathbf{b}(t_n)), \mathbf{d}_h) + (\nabla \times (\tilde{\mathbf{u}}_{ht}^n \times \tilde{\mathbf{b}}_{ht}^n), \mathbf{d}_h).
\end{aligned} \quad (4.26)$$

Therefore, the term coupling magnetic pseudo-pressure and magnetic field in the above equation can be bounded according to

$$\begin{aligned}
\|\nabla \mathbf{d}_h\|_0 \|\xi_r^{n-1}\|_0 & \leq \frac{1}{\beta_h} \|\xi_r^{n-1}\|_0^2 = -(\nabla \xi_r^{n-1}, \mathbf{d}_h) \\
& \leq \left\| \frac{3\tilde{\boldsymbol{\xi}}_b^n - 4\boldsymbol{\xi}_b^{n-1} + \boldsymbol{\xi}_b^{n-2}}{2\Delta t} \right\|_{-1} \|\nabla \mathbf{d}_h\|_0 + \lambda \|\nabla \times \tilde{\boldsymbol{\xi}}_b^n\|_0 \|\nabla \times \mathbf{d}_h\|_0 + \tau_{b, gd}^n \|\nabla \cdot \tilde{\boldsymbol{\xi}}_b^n\|_0 \|\nabla \cdot \mathbf{d}_h\|_0 \\
& \quad + s_{b, Lor}(\tilde{\mathbf{b}}_{ht}^n; \tilde{\mathbf{b}}_{ht}^n, \mathbf{d}_h) + s_{u, Ind}(\tilde{\mathbf{b}}_{ht}^n; \tilde{\mathbf{b}}_{ht}^n, \mathbf{d}_h) + \|D_t \mathbf{b}(t_n) - \partial_t \mathbf{b}(t_n)\|_{-1} \|\nabla \mathbf{d}_h\|_0 \\
& \quad - (\nabla (\mathbf{u}(t_n) \times \mathbf{b}(t_n)), \mathbf{d}_h) + (\nabla (\tilde{\mathbf{u}}_{ht}^n \times \tilde{\mathbf{b}}_{ht}^n), \mathbf{d}_h).
\end{aligned}$$

First, we estimate the stabilization terms:

$$s_{b, Lor}(\tilde{\mathbf{u}}_{ht}^n; \tilde{\mathbf{b}}_{ht}^n, \mathbf{d}_h) = s_{b, Lor}(\tilde{\mathbf{u}}_{ht}^n; \mathbf{b}(t_n) - \tilde{\boldsymbol{\xi}}_b^n, \mathbf{d}_h)$$

$$\begin{aligned}
&\leq C \sum_{M \in \mathcal{M}_h} \tau_{b,Lor,M}^n |\tilde{\mathbf{u}}_M^n|^2 \|\kappa_M^b(\nabla \mathbf{b}(t_n))\|_{0,M} \|\mathbf{d}_h\|_{1,M} \\
&\quad + C \sum_{M \in \mathcal{M}_h} \tau_{b,Lor,M}^n \|\kappa_M^u(\nabla \times (\tilde{\mathbf{u}}_M^n \times \tilde{\boldsymbol{\xi}}_b^n))\|_{0,M} |\tilde{\mathbf{u}}_M^n| \|\mathbf{d}_h\|_{1,M} \\
&\leq C \left(\max_{M \in \mathcal{M}_h} \{ \tau_{b,Lor,M}^n |\tilde{\mathbf{u}}_M^n|^2 \|\kappa_M^b(\nabla \mathbf{b}(t_n))\|_{0,M} \} \right. \\
&\quad \left. + \sum_{M \in \mathcal{M}_h} \tau_{b,Lor,M}^n |\tilde{\mathbf{u}}_M^n| \|\kappa_M^u(\nabla \times (\tilde{\mathbf{u}}_M^n \times \tilde{\boldsymbol{\xi}}_b^n))\|_{0,M} \right) \|\nabla \mathbf{d}_h\|_0, \\
s_{b,Ind}(\tilde{\mathbf{b}}_{ht}^n; \tilde{\mathbf{b}}_{ht}^n, \mathbf{d}_h) &= s_{b,Ind}(\tilde{\mathbf{b}}_{ht}^n; \mathbf{b}(t_n) - \tilde{\boldsymbol{\xi}}_b^n, \mathbf{d}_h) \\
&\leq C \sum_{M \in \mathcal{M}_h} \tau_{b,Ind,M}^n |\tilde{\mathbf{b}}_M^n|^2 \|\kappa_M^b(\nabla \mathbf{b}(t_n))\|_{0,M} \|\mathbf{d}_h\|_{1,M} \\
&\quad + C \sum_{M \in \mathcal{M}_h} \tau_{b,Ind,M}^n \|\kappa_M^b(\tilde{\mathbf{b}}_{ht}^n \times \tilde{\boldsymbol{\xi}}_b^n)\|_{0,M} |\tilde{\mathbf{b}}_M^n| \|\mathbf{d}_h\|_{1,M} \\
&\leq C \left(\max_{M \in \mathcal{M}_h} \{ \tau_{b,Ind,M}^n |\tilde{\mathbf{b}}_M^n|^2 \|\kappa_M^b(\nabla \mathbf{b}(t_n))\|_{0,M} \} \right. \\
&\quad \left. + \sum_{M \in \mathcal{M}_h} \tau_{b,Ind,M}^n |\tilde{\mathbf{b}}_M^n| \|\kappa_M^b(\tilde{\mathbf{b}}_{ht}^n \times \tilde{\boldsymbol{\xi}}_b^n)\|_{0,M} \right) \|\nabla \mathbf{d}_h\|_{0,M}.
\end{aligned}$$

For the coupling term we obtain

$$\begin{aligned}
&(\nabla \times (\mathbf{u}(t_n) \times \mathbf{b}(t_n)) - \nabla \times (\tilde{\mathbf{u}}_{ht}^n \times \tilde{\mathbf{b}}_{ht}^n), \mathbf{d}_h^n) \\
&= (\mathbf{u}(t_n) \times \mathbf{b}(t_n) - \tilde{\mathbf{u}}_{ht}^n \times \tilde{\mathbf{b}}_{ht}^n, \nabla \times \mathbf{d}_h^n) \\
&= ((\mathbf{u}(t_n) - \tilde{\mathbf{u}}_{ht}^n) \times \mathbf{b}(t_n), \nabla \times \mathbf{d}_h^n) + (\tilde{\mathbf{u}}_{ht}^n \times (\mathbf{b}(t_n) - \tilde{\mathbf{b}}_{ht}^n), \nabla \times \mathbf{d}_h^n) \\
&\leq \|\tilde{\boldsymbol{\xi}}_u^n\|_0 \|\mathbf{b}(t_n)\|_\infty \|\nabla \mathbf{d}_h^n\|_0 + \|\tilde{\mathbf{u}}_{ht}^n\|_\infty \|\boldsymbol{\xi}_b^n\|_0 \|\nabla \mathbf{d}_h^n\|_0.
\end{aligned}$$

In combination, this gives with the approximation property of the fluctuation operators and the previous results for the velocity and the magnetic field:

$$\begin{aligned}
&\Delta t \sum_{n=1}^N \|\boldsymbol{\xi}_r^{n-1}\|_0^2 \\
&\leq C \left\{ \frac{\|\tilde{\boldsymbol{\xi}}_b\|_{l^\infty(t_0, T; L^2(\Omega))}^2}{(\Delta t)^2} + \lambda^2 \|\nabla \times \tilde{\boldsymbol{\xi}}_b\|_{l^2(t_0, T; L^2(\Omega))}^2 + (\tau_{b,gd}^n)^2 \|\nabla \cdot \tilde{\boldsymbol{\xi}}_b\|_{l^2(t_0, T; L^2(\Omega))}^2 \right. \\
&\quad + \max_{1 \leq n \leq N} \max_{M \in \mathcal{M}_h} \{ \tau_{u,Lor,M}^n |\tilde{\mathbf{u}}_M^n|^2 \}^2 h^{2s_b} \|\mathbf{b}\|_{l^2(t_0, T; H^{k_b+1}(\Omega))}^2 \\
&\quad + \max_{1 \leq n \leq N} \max_{M \in \mathcal{M}_h} \{ \tau_{u,Lor,M}^n \} \Delta t \sum_{n=1}^N \sum_{M \in \mathcal{M}_h} \tau_{u,Lor,M}^n |\tilde{\mathbf{u}}_M^n|^2 \|\kappa_M^u(\nabla \times (\tilde{\mathbf{u}}_M^n \times \tilde{\boldsymbol{\xi}}_b^n))\|_{0,M}^2 \\
&\quad \left. + \max_{1 \leq n \leq N} \max_{M \in \mathcal{M}_h} \{ \tau_{b,Ind,M}^n |\tilde{\mathbf{b}}_M^n|^2 \}^2 h^{2s_b} \|\mathbf{b}\|_{l^2(t_0, T; H^{k_b+1}(\Omega))}^2 \right)
\end{aligned}$$

$$\begin{aligned}
& + \max_{1 \leq n \leq N} \max_{M \in \mathcal{M}_h} \{\tau_{b,Ind,M}^n\} \Delta t \sum_{n=1}^N \sum_{M \in \mathcal{M}_h} \tau_{b,Ind,M}^n |\tilde{\mathbf{b}}_M^n|^2 \|\kappa_M^b ((\nabla \times \tilde{\mathbf{b}}_M^n) \times \tilde{\boldsymbol{\xi}}_b^n)\|_{0,M}^2 \\
& + \|\mathbf{b}(t_n)\|_{l^\infty(t_0, T; L^\infty)}^2 \|\tilde{\boldsymbol{\xi}}_u^n\|_{l^\infty(t_0, T; L^2(\Omega))}^2 \\
& + \|\tilde{\mathbf{u}}_{ht}^n\|_{l^\infty(t_0, T; L^\infty)}^2 \|\boldsymbol{\xi}_b^n\|_{l^\infty(t_0, T; L^2(\Omega))}^2 + C(\Delta t)^4 \Big\} \\
\leq & C \left(\frac{1}{(\Delta t)^2} + \|\tilde{\mathbf{u}}_{ht}^n\|_{l^\infty(t_0, T; L^\infty)}^2 \right) \|\tilde{\boldsymbol{\xi}}_b^n\|_{l^\infty(t_0, T; L^2(\Omega))}^2 \\
& + C \left(\lambda + \tau_{u,gd}^n + \max_{1 \leq n \leq N} \max_{M \in \mathcal{M}_h} \{\tau_{b,Lor,M}^n |\tilde{\mathbf{u}}_M^n|^2\} \right. \\
& \quad \left. + \max_{1 \leq n \leq N} \max_{M \in \mathcal{M}_h} \{\tau_{b,Ind,M}^n |\tilde{\mathbf{b}}_M^n|^2\} \right) \|\tilde{\boldsymbol{\xi}}_b^n\|_{l^2(t_0, T; LPS_u)}^2 \\
& + \|\mathbf{b}(t_n)\|_{l^\infty(t_0, T; L^\infty)}^2 \|\tilde{\boldsymbol{\xi}}_u^n\|_{l^\infty(t_0, T; L^2(\Omega))}^2 \\
& + C \max_{1 \leq n \leq N} \max_{M \in \mathcal{M}_h} \{\tau_{b,Lor,M}^n |\tilde{\mathbf{u}}_M^n|^2\}^2 h^{2s_b} \|\mathbf{b}\|_{l^2(t_0, T; H^{k_b+1}(\Omega))}^2 \\
& + C \max_{1 \leq n \leq N} \max_{M \in \mathcal{M}_h} \{\tau_{b,Ind,M}^n |\tilde{\mathbf{b}}_M^n|^2\}^2 h^{2s_b} \|\mathbf{b}\|_{l^2(t_0, T; H^{k_b+1}(\Omega))}^2 \\
& + C(\Delta t)^4.
\end{aligned}$$

Provided all our assumptions on the regularity and the parameter choice are satisfied, this can be shortened as

$$\begin{aligned}
\|\boldsymbol{\xi}_r^{n-1}\|_{l^2(t_0, T; L^2(\Omega))}^2 & \leq C \frac{\|\tilde{\boldsymbol{\xi}}_b^n\|_{l^\infty(t_0, T; L^2(\Omega))}^2}{(\Delta t)^2} + C \|\tilde{\boldsymbol{\xi}}_b^n\|_{l^2(t_0, T; LPS_b)}^2 \\
& + C \|\boldsymbol{\xi}_u^n\|_{l^\infty(t_0, T; L^2(\Omega))}^2 + C(\Delta t)^4.
\end{aligned}$$

□

Remark 4.5.6. The above estimates for kinematic pressure and magnetic pseudo-pressure are only slightly related to the chosen time discretization and stabilization. We see that (quasi-) optimal convergence results can only be achieved if the order of convergence for the L^2 errors is by one higher than for the LPS errors. Due to the fact that we have not proven more than first order convergence for the time discretization, the above results just show that the error remains bounded in time.

Furthermore, the terms $C \frac{\|\tilde{\boldsymbol{\xi}}_u^n\|_{l^\infty(t_0, T; L^2(\Omega))}^2}{(\Delta t)^2}$ and $C \frac{\|\tilde{\boldsymbol{\xi}}_b^n\|_{l^\infty(t_0, T; L^2(\Omega))}^2}{(\Delta t)^2}$ give a dependence on the mesh width h and the time step size Δt . For second order temporal convergence with respect to the $L^2(\Omega)$ error (as we proved in [ADL15b] for the Navier-Stokes equations), we would want to choose $\max\{h^{k_u+1}, h^{k_p+2}, h^{k_b+1}, h^{k_r+2}\} \lesssim (\Delta t)^2$.

5 Numerical Results

The analysis for the semi-discretizations and for the full-discretization gives parameter bounds that are quite wide. Using numerical examples, we want in this chapter to discuss what suitable choices of parameters within these bounds are and whether all of the considered stabilizations are really needed. In particular, we aim for a parameter design that is suited for a wide range of problems. Furthermore, we consider the performance of the implementation with respect to scalability and the sharpness of the convergence results. The presented examples are an extension of the publications this thesis is based on.

If not stated differently, the author's implementation based on the C++-FEM library `deal.II` [BHK07; BHH+15] is used. The development of a robust and scalable numerical solver within this framework has been an essential part of this PhD thesis for conducting the numerical experiments.

Due to the restriction of `deal.II` to linear, quadrilateral and hexahedral cells, in the following examples mainly those types of meshes appear.

In contrast to the analysis presented in the previous chapters, we investigate anisotropic meshes, too. Basic results for that case can be found in [Ape99]. In combination with the results presented below, this suggests that an extension of the analysis should be possible.

For the local projection stabilization always an one-level approach $\mathcal{M}_h = \mathcal{T}_h$ is used. If not stated differently, we choose the coarse space to be $\mathcal{D}_M = \mathbb{Q}^{-(k_u-1)}$.

The structure in this section is as follows:

First, in Section 5.1 the Navier-Stokes equations alone are considered. After validating the theoretical results for homogeneous Dirichlet boundary conditions and “directional-do-nothing conditions”, the influence of the grad-div and the LPS-SU stabilization is considered for more realistic types of flow.

In Section 5.2 we investigate the additional effects of the Fourier equations for the temperature. For a problem with known reference solution the rates of convergence, the choice of enriched ansatz spaces and the influence of SU stabilization for the temperature is investi-

gated. For Rayleigh-Bénard convection we try to find a setting that reproduces benchmark quantities for a wide spectrum of cases.

Afterwards, in Section 5.3, results for electrically conducting non-isothermal flows are considered. In particular, we are interested in how the regularity of the magnetic fields affects the choice of stabilization parameters and the achievable results.

Finally, in Section 5.4 the fully coupled setting is examined with respect to parallel scalability of the implementation.

5.1 Isothermal Insulating Flow

We first neglect all couplings and consider an isothermal, insulating fluid. In particular, the equations that describe our problem are the Navier-Stokes equations. The results presented here originate from [ADL15a; DAL15; LAD15] for an inertial frame of reference and from [AL15] for rotating frames of reference. In the first academic examples, the influence of grad-div stabilization is investigated. Due to the analytical results we expect that this term is crucial. Afterwards the behavior of the numerical model for more realistic types of flow, such as boundary layer behavior or turbulence, is considered. We expect that grad-div stabilization is not sufficient to suppress the arising spurious oscillations and that additional SU stabilization is necessary to resemble correct physical behavior.

5.1.1 The No-Flow Problem

We first consider the case in which the forcing term \mathbf{f}_u is a gradient field in the domain $\Omega = (0, 1)^3$. With $\mathbf{f}_u = (3x_1^2 + 1, 3x_2^2, 3x_3^2)^T$ and homogeneous Dirichlet boundary conditions the reference solution is given by $(\mathbf{u}, p)(x) = (\mathbf{0}, x_1^3 + x_1 + x_2^3 + x_3^3 - 1)$. For the discrete ansatz spaces we choose Taylor-Hood elements $\mathbf{V}_h/Q_h = [\mathbb{Q}_2]^3/Q_1$ and consider a randomly distorted Cartesian mesh. In this setup Theorem 3.1.6 tells us that the discretization error for the velocity can be bounded by

$$\min \left\{ \frac{d}{\nu}, \frac{1}{\tau_{u,gd,M}} \right\} \|\eta_p\|_{0,M}^2.$$

In particular, the velocity error strongly depends on the viscosity ν if no grad-div stabilization is applied.

Exactly this behavior can be observed in Figure 5.1: The error with respect to the $H^1(\Omega)$ -norm scales like ν^{-1} without and like $\nu^{-1/2}$ with a constant positive grad-div stabilization parameter $\tau_{u,gd,M} \equiv \gamma$. Interestingly, an influence on the kinematic pressure can not be observed. On the undistorted mesh, we further notice superconvergence. We conclude that Theorem 3.1.6 is sharp with respect to the dependence of the discretization error on $\tau_{u,gd,M}$. For this test case we observe no significant impact of $s_{u,SU}$. As the consideration

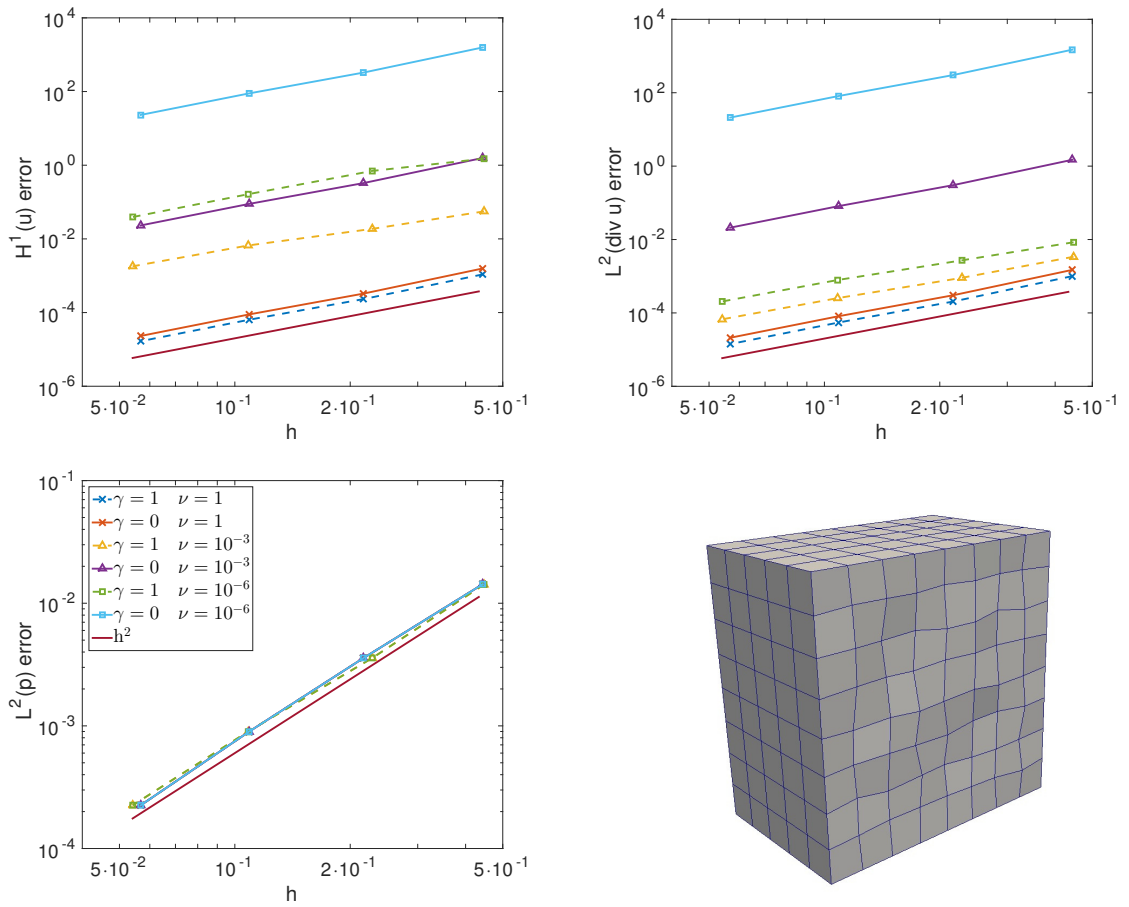


Figure 5.1: No-Flow test for $\mathbb{Q}_2/\mathbb{Q}_1$ and $\nu \in \{1, 10^{-3}, 10^{-6}\}$ with and without grad-div stabilization: (i) H^1 -velocity error, (ii) L^2 -divergence error, (iii) L^2 -kinematic pressure error, (iv) Cut through mesh

of non-isothermal or electrically conducting flow large external gradient forces are of great importance, we will in the following always consider $\tau_{u,gd,M} \sim 1$ as suggested in (3.8).

Remark 5.1.1. The above results do not depend on the fact that the reference solution is part of the ansatz space. Similar results for the two- and three-dimensional Couzy test problem [Cou95] can be observed in [DAL15] and for an extension to rotating frames of reference in [AL15]. The error strongly depends on the grad-div stabilization and local projection stabilization shows no considerable effect. In particular, it turned out that for these cases a grad-div stabilization parameter in the order of unity is best. Using bubble enriched ansatz spaces in general improves the results. Choosing inhomogeneous boundary conditions instead of homogeneous or periodic ones did not influence the errors significantly.

Remark 5.1.2. In [Lin14] Linke et al. modify inf-sup stable finite element pairs for incompressible flows in such a way that a pointwise divergence-free discrete velocity field can be obtained. The essential idea is to replace the test function \mathbf{v}_h in $(\mathbf{f}_u, \mathbf{v}_h)$ by $\Pi_h \mathbf{v}_h$ with a projector $\Pi_h : \mathbf{V} + \mathbf{V}_h \rightarrow \mathbf{X}_h$ to an appropriate finite element subspace of $H^{div}(\Omega)$. Potentially, this allows to omit the grad-div stabilization.

5.1.2 Outflow Boundary Conditions

After the investigation of the influence of the grad-div stabilization for homogeneous boundary conditions, we next want to verify the analytical results for the “directional-do-nothing condition”.

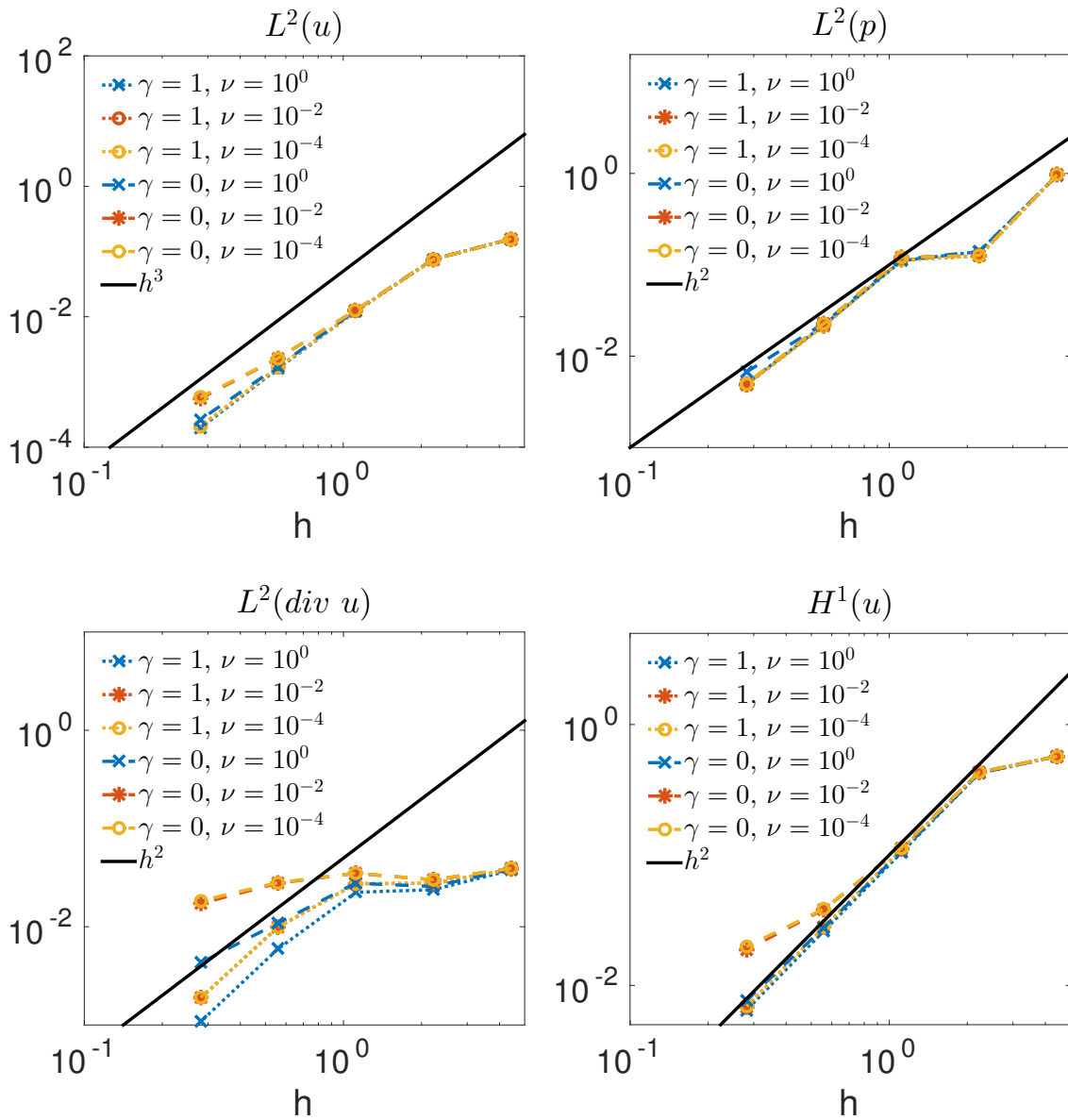
We consider the domain $\Omega := (0, 2\pi) \times (-\pi, \pi)$. and prescribe this outflow boundary condition at $S_1 := \{(2\pi, y) : -\pi \leq y \leq \pi\}$ with the parameter $\beta = 1$. For the remaining part of the boundary $S_0 := \partial\Omega \setminus S_1$ we use Dirichlet boundary conditions. Let $\chi : \mathbb{R} \rightarrow [0, 1]$ be defined as $\chi(y) = 1$ if $y < 0$, and $\chi(y) = 0$ for $y \geq 0$. The exact solution is in analytical form given by

$$\begin{aligned} \mathbf{u}(x, y) &:= (\sin(y) \cos(t)^2, 0)^T \\ p(x, y) &= -\frac{1}{2} \chi(y) \sin(y)^2 \cos(t)^4. \end{aligned}$$

The corresponding right-hand side then reads

$$\mathbf{f}(x, y) = (-2 \sin(t) \cos(t) \sin(y) + \cos(t)^2 \sin(y) \nu, -\chi(y) \cos(y) \sin(y) \cos(t)^4)^T.$$

Here, we want to neglect the error due to time discretization. Therefore, we choose $\Delta t = 10^{-4}$ and evaluate the error at $T = 10^{-2}$. We investigate the convergence behavior for the classical Taylor-Hood pair $\mathcal{Q}_2/\mathcal{Q}_1$.

Figure 5.2: Outflow Boundary Conditions: Errors for Taylor-Hood ($\mathcal{Q}_2/\mathcal{Q}_1$) elements

In Figure 5.2 we plotted the errors with respect to $\|p - p_h\|$, $\|\mathbf{u} - \mathbf{u}_h\|$, $|\mathbf{u} - \mathbf{u}_h|_1$, and $\|\operatorname{div}(\mathbf{u} - \mathbf{u}_h)\|$ in dependence of an uniform mesh size h for various viscosities ν and considered the effect of grad-div stabilization. The kinematic pressure error $\|p - p_h\|$ does essentially not depend on any of the parameters and we observe second order convergence. For the velocity energy error $\|\mathbf{u} - \mathbf{u}_h\|$ and the $H^1(\Omega)$ error the results deviate from the optimal rate of convergence (h^3 resp. h^2) if no grad-div stabilization is used. However, the biggest impact of the stabilization can be seen for the divergence error $\|\operatorname{div}(\mathbf{u} - \mathbf{u}_h)\|$. For sufficiently small viscosity the error stays nearly constant if no grad-div stabilization is used. Optimal rates of convergence can be recovered if grad-div stabilization is used. With respect to the LPS stabilization we did not observe any significant influence for the considered norms. In particular, the error does not blow up, even if there is inflow at the boundary S_1 .

5.1.3 Time Discretization

In this example we consider rates of convergence with respect to time discretization. In particular, we compare the rotational incremental form of the kinematic pressure segregation algorithm with the standard incremental one that we analyzed in Chapter 4.

The reference solution here is given as

$$\begin{aligned}\mathbf{u}(x, y, t) &:= (\sin(1-x) \sin(y+t), \cos(1-x) \cos(y+t))^T \\ p(x, y, t) &:= -\cos(1-x) \sin(y+t)\end{aligned}$$

and the forcing term \mathbf{f}_u is calculated accordingly such that (\mathbf{u}, p) is the solution to the time-dependent Navier-Stokes problem in the domain $\Omega = (-1, 1)^2$ and for $t \in [0, 1]$.

In [ADL15b] we considered three different Reynolds numbers $Re \in \{10^{-2}, 10^0, 10^2\}$. It turned out that, in contrast to the grad-div stabilization, the LPS-SU stabilization does not show any significant influence on the error in the considered parameter regime.

For $Re = 10^{-2}$ the effect of the rotational correction is clearly dominant compared to grad-div stabilization. This behavior is in good agreement with our analysis as the critical term in the velocity discretization error is

$$\min \left\{ \frac{d}{\nu}, \frac{1}{\tau_{u,gd,M}} \right\} \|\eta_p\|_{0,M}^2.$$

in our semi-discrete analysis. For $\nu \geq 1$ a grad-div stabilization as $\tau_{u,gd,M} \equiv 1$ has essentially no influence on this term.

In the chosen parameter regime, the velocity error is dominated by the spatial discretization. Hence, we observe quasi-optimal rates of convergence in space while the LPS error

only slightly depends on the time step size Δt .

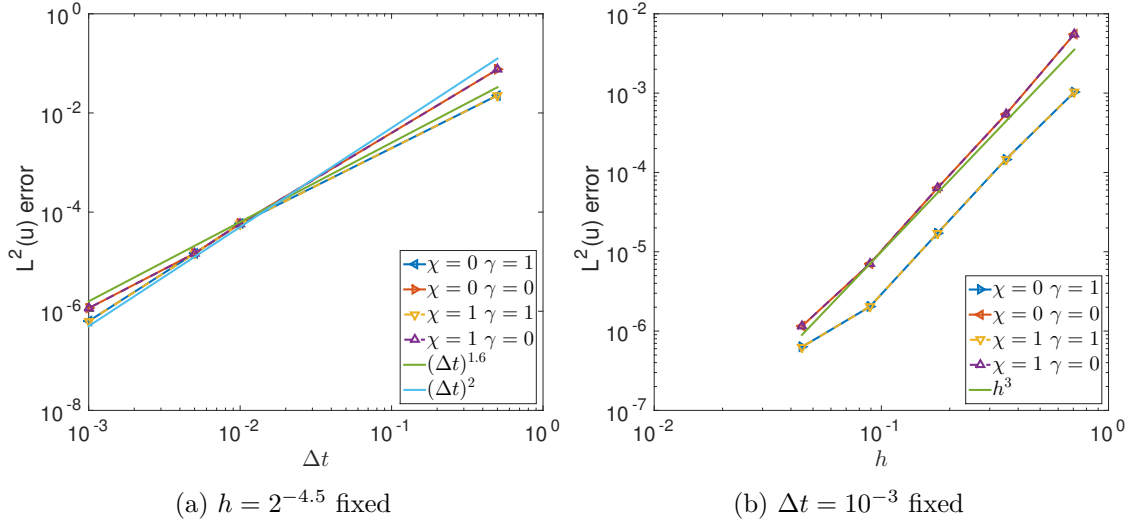


Figure 5.3: Time Discretization: $Re = 10^2$, errors for the velocity w.r.t $L^2(\mathbf{u})$

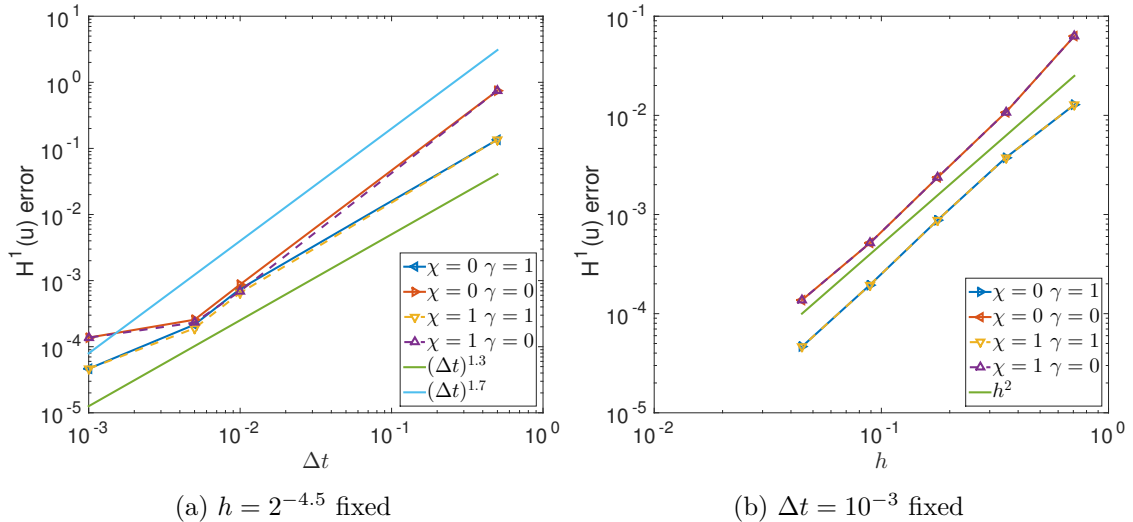


Figure 5.4: Time-Discretization: $Re = 10^2$, errors for the velocity w.r.t $H^1(\mathbf{u})$

Results for the case $Re = 10^2$ can be observed in Figures 5.3, 5.4, 5.5 and 5.6. In contrast to the previously discussed case, grad-div stabilization is dominant compared to the rotational correction. This is not too surprising as the correction scales with ν .

For the first three errors we get a clear picture with respect to spatial discretization. Grad-div stabilization diminishes the error by a fixed factor. This is exactly the behavior we have observed for the No-Flow test case.

With respect to the time discretization, grad-div stabilization improves the velocity errors.

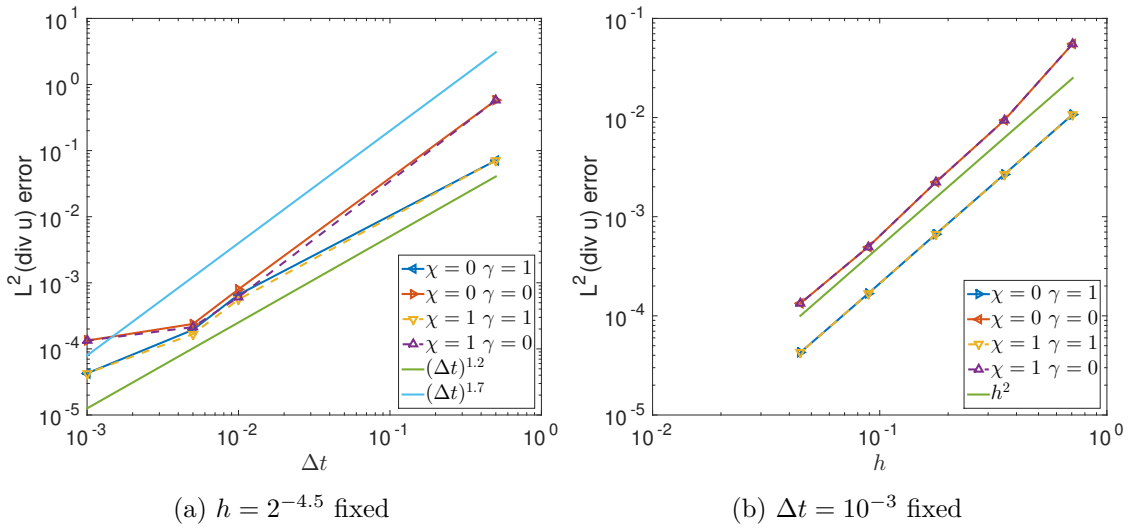


Figure 5.5: Time-Discretization: $Re = 10^2$, errors for the velocity w.r.t $L^2(\nabla \cdot \mathbf{u})$

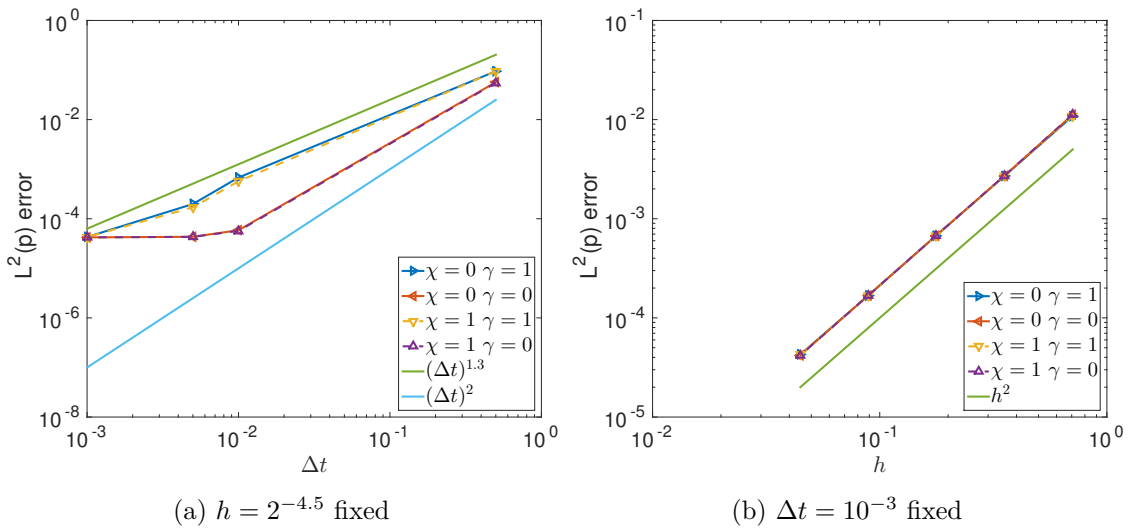


Figure 5.6: Time-Discretization: $Re = 10^2$, errors for the kinematic pressure w.r.t $L^2(p)$

In particular, we observe that the $L^2(u)$ error is convergent of second order and that the LPS error converges faster than linearly. Note that in view of the analysis carried out for these types of schemes the results are superconvergent.

Compared to the velocity, for the kinematic pressure error the behavior with respect to stabilization is the other way around: The error is best when no stabilization is used. This last case stresses that one really has to know which error one wants to control when choosing stabilization parameters. There is apparently no rule that is best for both velocity and kinematic pressure.

Experiments with higher Reynolds number show the same qualitative behavior of the errors.

In summary, one might say that the rotational correction never harms and even improves the results considerably if the viscosity ν is not too small. Grad-div stabilization however seems to be beneficial whenever the main interest is in the velocity solution. For the kinematic pressure the above example suggests that disabling the stabilization is the best option.

5.1.4 Flow Over a Horizontal Plate

For a slightly more realistic problem, we consider the flow over an infinitely thin, flat plate parallel to an outer constant velocity field of magnitude $u_\infty = 1$ for $\nu = 10^{-3}$. In a coordinate system in which the plate lies on the x -axis starting at the origin, the attached laminar boundary layer profile in the outer flow direction $u = u_\infty f'(\eta)$ developing along the plate can be well described by the Blasius profile as exact solution of Prandtl's boundary layer equations given by

$$\begin{aligned} 2f'''(\eta) + f(\eta)f''(\eta) &= 0, \\ f(0) = f'(0) &= 0, \quad f'(\infty) = 1, \end{aligned}$$

where $\eta = y\sqrt{u_\infty/(\nu x)}$ is a dimensionless variable.

Using a discretization with Taylor-Hood elements ($\mathbb{Q}_2/\mathbb{Q}_1$) on a structured rectangular mesh, we observe spurious modes of magnitude up to 10% of the velocity in front of the plate, see Figure 5.7 (left). On the other hand the boundary layer profile is in pretty good agreement with the reference data [How38], see Figure 5.7 (right).

These unphysical oscillations are exactly the kind of phenomenon for which we considered local projection stabilization. Using an empty coarse space or $D_M = \mathbb{Q}_0$ in conjunction with a constant LPS parameter $\tau_{u,SU,M} = 1$ approximation of the Blasius profile is perturbed. In addition to the thickening of the boundary layer, the oscillations are merely smeared than damped out (cf. Figure 5.8). Note that this choice is neither in agreement with the

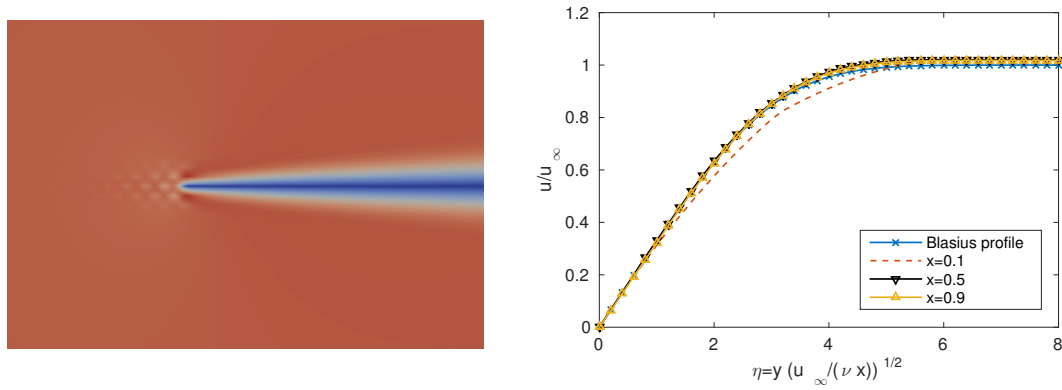


Figure 5.7: Flow over a horizontal plate for $\nu = 10^{-3}$, $\gamma = 1$, $\tau_{u,SU,M} = 0$, $h = 2^{-5}$

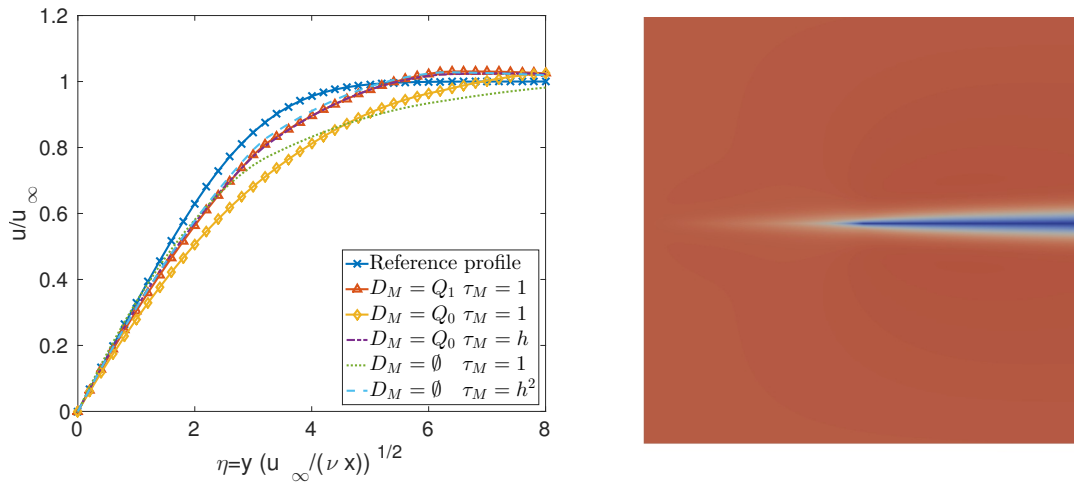


Figure 5.8: Blasius flow: Profiles for different coarse spaces D_M and stabilization parameters $\tau_{u,SU,M}$ at $x = 0.1$ (left) and velocity for $D_M = \emptyset$, $\tau_{u,SU,M} = 1$ (right)

parameter bounds (3.8) in the semi-discrete analysis nor with the bounds (4.21) in the fully discretized case. If the parameter is chosen in the magnitude $\mathcal{O}(h^2)$ (for $D_M = \emptyset$) respectively $\mathcal{O}(h)$ (for $D_M = \mathbb{Q}_0$), the boundary profile is nearly unaffected. For the finest possible coarse space $D_M = \mathbb{Q}_1$ we do not observe an influence of the stabilization with respect to the Blasius profile. As long as the parameter does not depend on h the spurious modes are damped out as effectively as with the previous choices for the coarse space even when $\tau_{u,SU,M} = u_{min,M}$.

In this example, the flow away from the plate is given by $(1, 0)$. In particular, this means that using any power of $u_{max,M}$ or $u_{min,M}$ changes the behavior in the boundary layer only. There the reference solution is of the form

$$f'(\eta) = \eta f''(0) - \frac{(f'')^2 \eta^4}{2 \cdot 4!} + \mathcal{O}(\eta^5)$$

and hence the streamline derivative is approximately linear away from the stagnation point. In particular, the velocity is well approximated in the coarse space D_M . Therefore it is not too surprising that the profile is just slightly influenced by the SU-LPS parameter, see Figure 5.9 (right).

If we use global refinement, a mesh size $h = 2^{-5}$ is necessary to approximate the boundary layer properly. This motivates the choice of a TVD-based refinement that controls

$$tol_K := \sum_{i=1}^d \left(\max_{\mathbf{x} \in K} \|u_i(\mathbf{x})\| - \min_{\mathbf{x} \in K} \|u_i(\mathbf{x})\| \right).$$

In this case we want to ensure $tol_K \approx 0.1$ on all elements $K \in \mathcal{T}_h$. Indeed, this criterion is sufficient to improve the approximation of the Blasius profile (Figure 5.9). Furthermore, this results in a rather coarse mesh away from the plate that removes the spurious modes without any further stabilization than grad-div. Increasing the Reynolds number to 10^4 , 10^5 and 10^6 shows that this criterion is stable with respect to the critical parameter and leads to convincing approximations of the reference Blasius profile with errors less than 1%, see Figure 5.9 (left) and 5.10.

In summary, we observe that local projection stabilization improves the numerical solution in all cases if the parameter is chosen within the bounds 3.8 derived in the semi-discrete analysis. However, choosing a suitable mesh that is sufficiently coarse in front of the obstacle has a similar effect. Mesh diffusion smoothens the unphysical solutions as well.

Remark 5.1.3. Further numerical results consider separation flow over a tilted plate and flow over a vertical plate (in [ADL15a]). In agreement with the observations above, LPS-SU was necessary to remove unphysical oscillations and capture important features of the flow such as the drag coefficient. In both cases a parameter choice as $\tau_{u,SU,M} = 1/\|\mathbf{u}_h\|_\infty^2$ proved to be useful to remove spurious modes and obtain correct physical behavior.

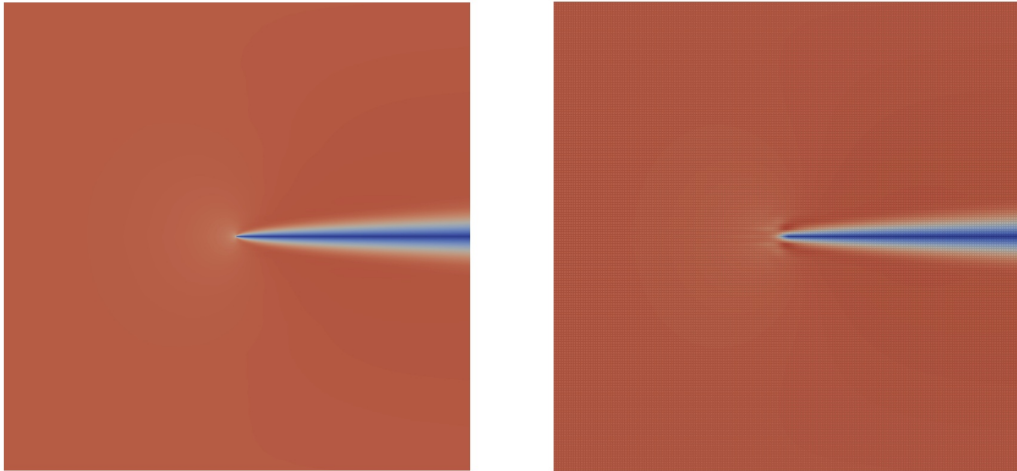


Figure 5.9: Blasius flow for $\nu = 10^{-3}$ on an adaptively refined mesh (left) and with global mesh size 2^{-5} for $D_M = \mathbb{Q}_1$ and $\tau_{u,SU,M} = 1$ (right)

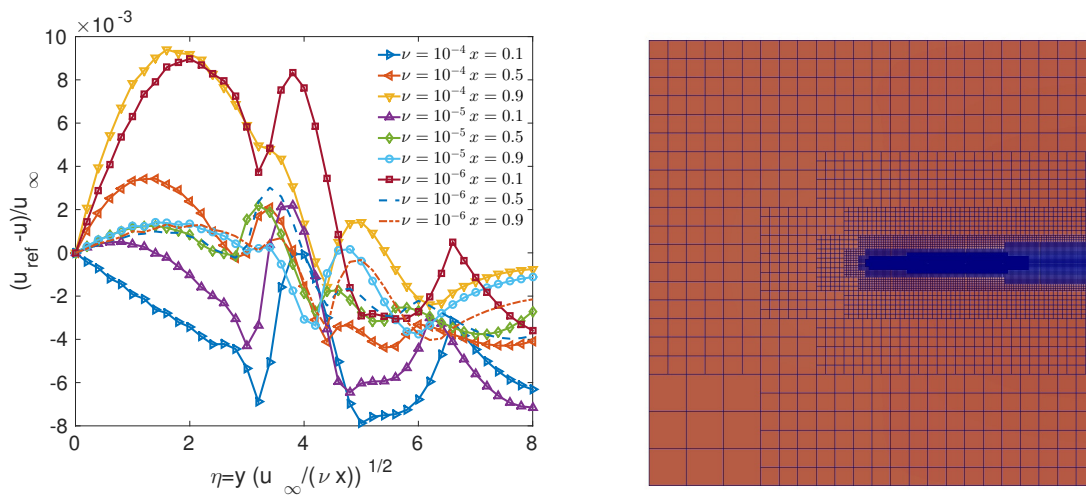


Figure 5.10: Blasius flow: Comparison of boundary layer approximation for different ν (left), mesh produced by the adaptive refinement criterion for $\nu = 10^{-3}$ (right)

5.1.5 Taylor-Green Vortex

In order to properly resolve turbulent flow considering the correct behavior on a large variety of scales is necessary. If not all these scales are properly resolved in a numerical simulation the distribution of energy with respect to different Fourier modes can not be resembled correctly. Hence, in all approaches apart from direct numerical simulations (DNS) diffusion on the smallest scales has to be modeled. There are many ideas for such large eddy simulations that only aim to resolve larger scales to to reduce computational costs. For an overview see [Sag06] or [Joh12].

In [MST07] it is argued that LPS terms can interpreted as artificial diffusion term for subscales. Hence, we are interested how the stabilization model performs as implicit subgrid model for a rather simple case of turbulence.

The setup of the flow is similar to the one in [CBCP15]: We consider a periodic box $\Omega = (0, a)^3$ with some $a > 0$ that we vary as needed. With $b > 0$, the initial values are

$$\mathbf{u}_0 = b \cdot \begin{pmatrix} \cos\left(\frac{2\pi}{a}x\right) \sin\left(\frac{2\pi}{a}y\right) \sin\left(\frac{2\pi}{a}z\right) \\ -\sin\left(\frac{2\pi}{a}x\right) \cos\left(\frac{2\pi}{a}y\right) \sin\left(\frac{2\pi}{a}z\right) \\ 0 \end{pmatrix},$$

$$p_0 = b \cdot \frac{1}{16} \left(\cos\left(\frac{4\pi}{a}x\right) + \cos\left(\frac{4\pi}{a}y\right) \right) \left(\cos\left(\frac{4\pi}{a}z\right) + 2 \right)$$

and we choose $a = 2\pi$, $b = 1$ for $\nu = 10^{-4}$ and $a = 8/\sqrt{3}$, $b = 1/10$ for $\nu = 10^{-5}$. The time interval is chosen according to $t \in [0, 10/b]$ and we use Taylor-Hood elements for the discretization. For the coarse space \mathbb{Q}_1 elements are used. According to [BMO+83] the flow is nearly isotropic for $Re \geq 10^3$.

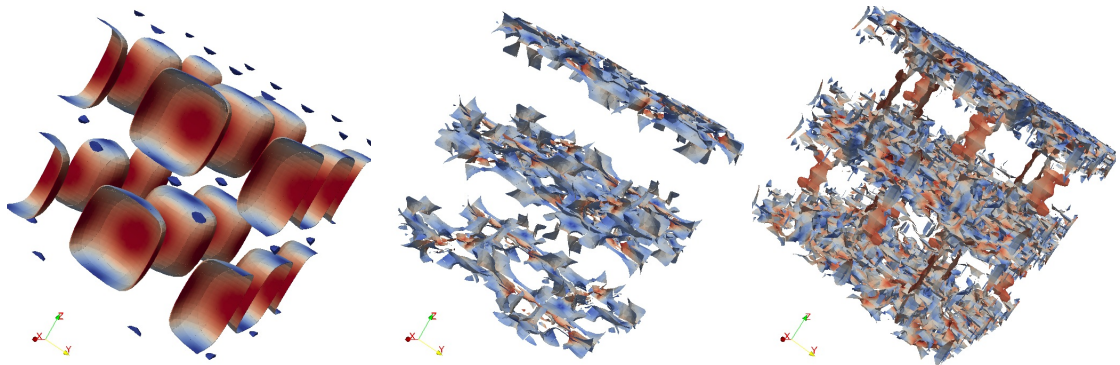


Figure 5.11: Taylor-Green Vortex: Isosurfaces for $|\omega| = 1$ at $t = 0$ (left), $|\omega| = 2.5$ at $t = 4$ (middle), $|\omega| = 4$ at $t = 9$ (right) with $h = \pi/8$, $\{a = 2\pi, b = 1\}$ and grad-div stabilization $\gamma_M = 1$.

In order to evaluate the numerical results, we are interested in the energy spectrum at time $T = 10/b$ given as

$$E(k, t) = \frac{1}{2} \sum_{k-\frac{1}{2} \leq |\mathbf{k}| \leq k+\frac{1}{2}} \hat{\mathbf{u}}(\mathbf{k}, t) \cdot \hat{\mathbf{u}}(\mathbf{k}, t)$$

with the Fourier transform $\hat{\mathbf{u}}(\mathbf{k}, t) = \int_{\Omega} \mathbf{u}(\mathbf{x}, t) \exp(-i\mathbf{k}\mathbf{x}) d\mathbf{x}$. For locally isotropic turbulence we expect in the inertial subrange the behavior (Kolmogorov's $-5/3$ -law)

$$E(k, t) \sim \varepsilon^{2/3} k^{-5/3},$$

where ε is the turbulent dissipation rate, see [Pop00] for the derivation and more details.

In Figure 5.11 we observe the time development of the flow: The large vortices in the initial solution decay into smaller eddies with increasing vorticity $|\omega|$. This is in good qualitative agreement with results in [CBCP15].

In a first attempt, we consider grad-div stabilization alone (cf. Figure 5.12(a)). The result clearly shows that the grad-div stabilization $\tau_{u,gd,M} \equiv 1$ does not produce enough dissipation as the smallest resolved scales carry too much energy. Additional LPS-SU stabilization cures this situation considerably but produces too much dissipation (Figure 5.12(b)).

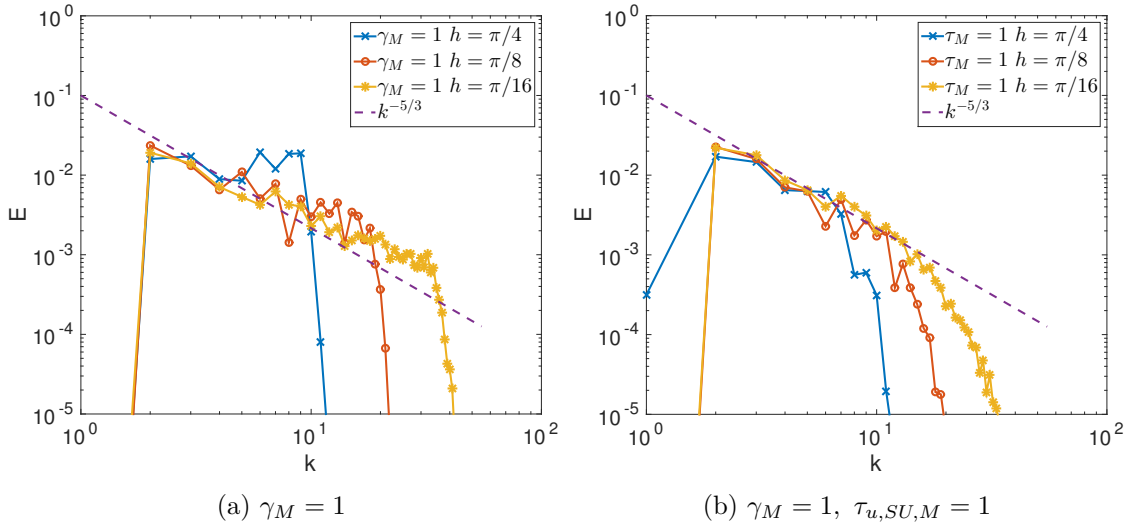


Figure 5.12: Taylor-Green Vortex: Energy spectra at $t = 9$ for different mesh widths; $a = 2\pi, b = 1$.

Figure 5.13(a) shows that the obtained results are comparable to those of the Smagorinsky model that is also known to be too dissipative. Dimensional analysis suggests to choose the parameter according to $\tau_{u,SU,M} = Ch/\|\mathbf{u}_h\|_{\infty,M}$. Interestingly, the choice $\tau_{u,SU,M} = h/(2\|\mathbf{u}_h\|_{\infty,M})$ performs as well as simply $\tau_{u,SU,M} = 1$ (cf. Figure 5.13(b)).

In summary, we observe that grad-div stabilization is not sufficient in this example. However, additional LPS SU stabilization performs considerably well as implicit subgrid model in this test case.

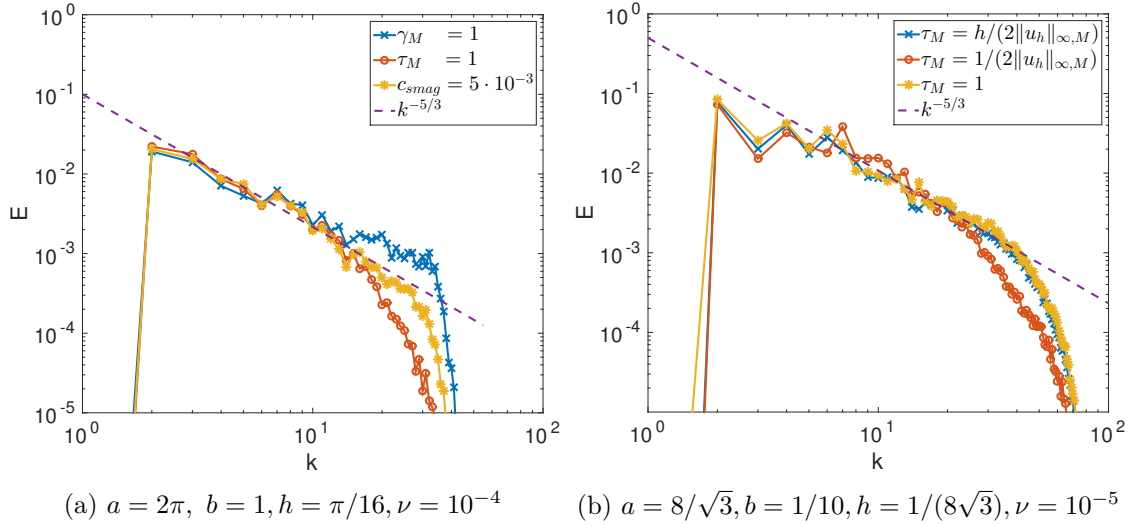


Figure 5.13: Taylor-Green Vortex: Energy spectra for different stabilization models

5.1.6 Rotating Poiseuille Flow

Next we are interested in the influence of the Coriolis stabilization in a fast rotating frame of reference. We consider a channel given by the domain $\Omega = (-2, 2) \times (-1, 1)$ which rotates around its midpoint and the inflow is given by a quadratic profile

$$\mathbf{u}(x, y) = \begin{cases} (1 - y^2, 0)^T, & x = -2 \\ (0, 0)^T, & |y| = 1 \end{cases},$$

$$p(x = 2, y) = 0,$$

$$\mathbf{u}_0 = 0, \quad p_0 = 0, \quad \mathbf{f} = 0.$$

Note again that the centrifugal force is absorbed in the pressure we consider here. In particular, $p = \tilde{p} - \frac{1}{2}|\boldsymbol{\omega} \times \mathbf{r}|^2$ if \tilde{p} is the pressure in an inertial frame of reference. For the critical parameters we choose $\boldsymbol{\omega} = (0, 0, 100)^T$ and $\nu = 10^{-3}$. The basic flow we expect is one where all outflow happens in a small area on the bottom left side. In particular, the streamlines are strongly curved at the outflow boundary and resolving the boundary layers there by stabilization or grid refinement is important to prevent oscillations from occurring.

For this example we use the stabilization parameters $\gamma = 1$, $\tau_{u,SU,M} = 1/|\mathbf{u}_M|^2$ and $\alpha = 1/h$. Using only grad-div stabilization leads to high oscillations that spread from

the outflow into the interior of the domain (Figure 5.14). This behavior improves when the mesh is refined adaptively (Figure 5.15), but nevertheless oscillations occur. Hence, grad-div stabilization is not sufficient in this example.

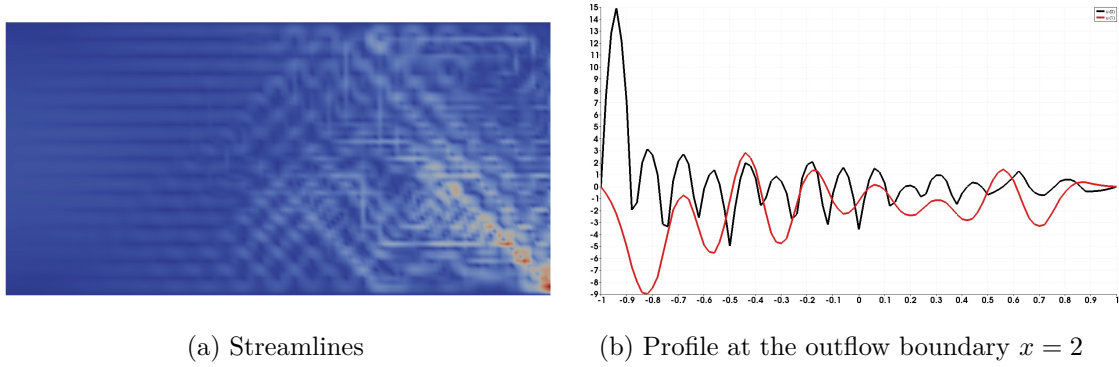


Figure 5.14: Rotating Poiseuille Flow: $\tau_{u,gd,M} \equiv 1$

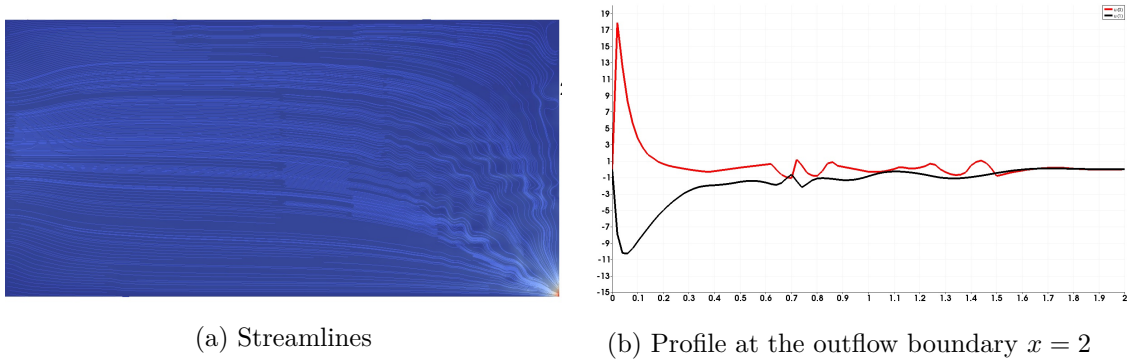


Figure 5.15: Rotating Poiseuille Flow: $\tau_{u,gd,M} \equiv 1$, adaptive mesh

Using LPS-Coriolis stabilization additionally improves the solution a lot. All the oscillation in the interior of the domain are damped away and only at the outflow boundary smaller oscillations occur (Figure 5.16). If we use the LPS-SUPG stabilization instead the situation is similar but there are oscillations that spread into the interior (Figure 5.17).

Finally, we combine all the considered stabilizations and use adaptive mesh refinement. This finally leads to a solution that has all the features (Figure 5.18) and we see that all these parts are necessary.

Remark 5.1.4. In [AL15] we additionally investigated the Proudman-Stewartson problem in which the fluid motion between two rotating spheres is considered. In accordance with the observations for the rotating Poiseuille flow, we observe that a combination of grad-div and Coriolis stabilization on an adaptively refined mesh is sufficient to capture the physical behavior correctly and achieve convincing results for a wide spectrum of problem parameters.

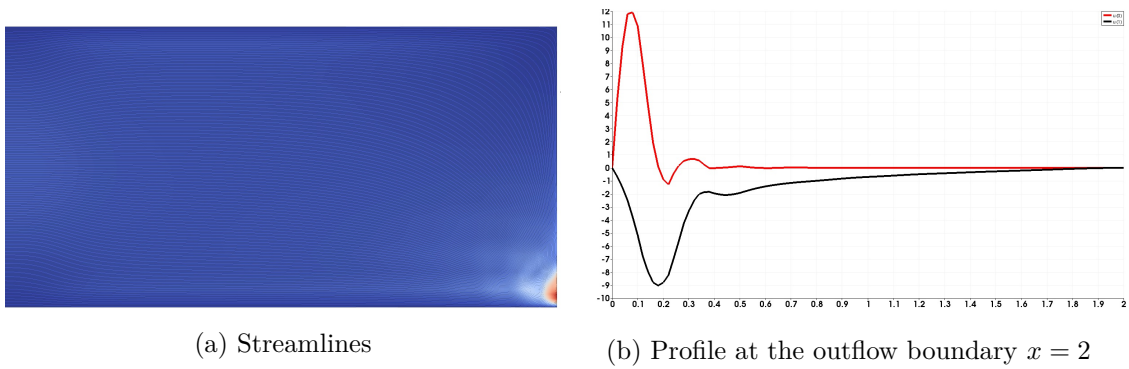


Figure 5.16: Rotating Poiseuille Flow: $\tau_{u,gd,M} \equiv 1$, $\tau_{u,Cor,M} \equiv 1/h$

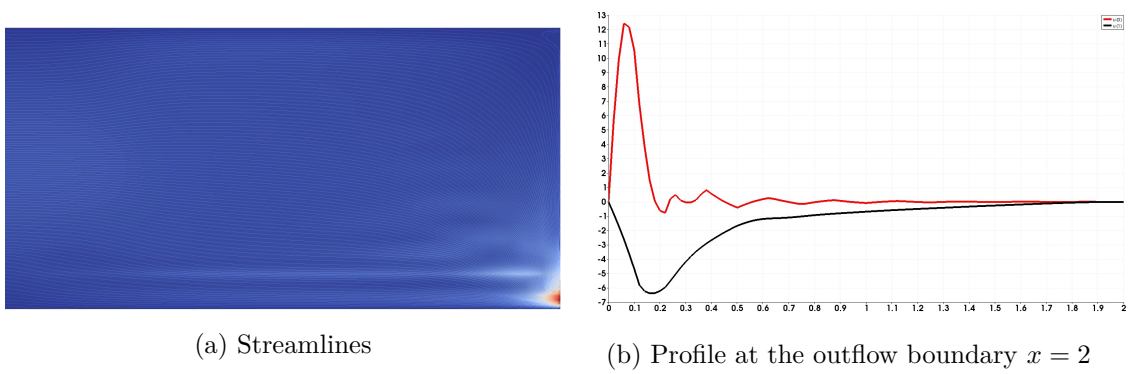


Figure 5.17: Rotating Poiseuille Flow: $\tau_{u,gd,M} \equiv 1$, $\tau_{u,SU,M} \equiv 1$

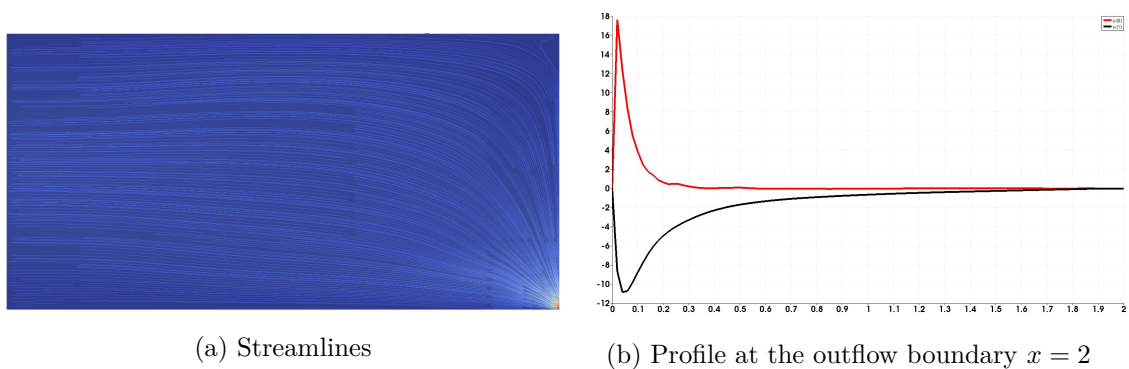


Figure 5.18: Rotating Poiseuille Flow: $\tau_{u,gd,M} \equiv 1$, $\tau_{u,SU,M} \equiv 1$, $\tau_{u,Cor,M} \equiv 1/h$, adaptive mesh

5.2 Non-Isothermal Insulating Flow

For non-isothermal flow two test cases are investigated. We first confirm the rates of convergence with respect to the temperature and consider the influence of the SU stabilization for the parameter in a case in which we prescribe a reference solution. The second example is Rayleigh-Bénard convection in a heated cylinder. We consider both the cases of a rotating and a non-rotating hull.

5.2.1 Traveling Wave

In this example we want to confirm the rates of convergence with respect to the temperature. Therefore we consider a time-dependent, two-dimensional solution of the Oberbeck-Boussinesq equations for different parameters $\nu, \alpha, \beta > 0$ in a box $\Omega = (0, 1)^2$ with $t \in [0, 6 \cdot 10^{-3}]$:

$$\begin{aligned} \mathbf{u}(x, y, t) &= (100, 0)^T, \quad p(x, y, t) = 0, \\ \theta(x, y, t) &= (1 + 3200\alpha t)^{-1/2} \exp\left(-\left(\frac{1}{2} + 100tx\right)^2 \left(\frac{1}{800} + 4\alpha t\right)^{-1}\right) \end{aligned}$$

with $\mathbf{g} \equiv (0, -1)^T$ and (time dependent) inhomogeneous Dirichlet boundary conditions for \mathbf{u} and θ . The right-hand sides \mathbf{f}_u, f_θ are calculated such that (\mathbf{u}, p, θ) solves the equations. Initially, the temperature peak is located at $x = \frac{1}{2}$ and moves in the x -direction until it finally hits the wall at $x = 1, t = 0.005$ and is transported out of the domain.

For the discretization, we consider a randomly distorted mesh and use $\mathbb{Q}_2/\mathbb{Q}_1/(\mathbb{Q}_2/\mathbb{Q}_1)$ or $\mathbb{Q}_2/\mathbb{Q}_1/(\mathbb{Q}_2^+/\mathbb{Q}_1)$ elements for velocity, kinematic pressure and fine and coarse temperature. Since only the temperature ansatz spaces are varied here, we write $\mathbb{Q}_2^{(+)}/\mathbb{Q}_1$ for convenience.

Figure 5.19 shows that the expected order of convergence for the stabilization error $|||\xi_u|||_{LPS_u} + |||\xi_\theta|||_{LPS_\theta} \sim h^2$ is obtained even without stabilization. For unenriched elements, an additional LPS stabilization for θ shows no significant influence. On the other hand, for $\mathbb{Q}_2^+/\mathbb{Q}_1$ elements the error clearly improves by using LPS stabilization for small α .

The temperature profile at $y = 0.5$ can be observed in Figure 5.20. The impression from the error results are confirmed here: For small α spurious modes appear in the solution. In case of a $\mathbb{Q}_2/\mathbb{Q}_1$ ansatz function for fine and coarse temperature space LPS stabilization is not able to damp these oscillations. On the other hand for $\mathbb{Q}_2^+/\mathbb{Q}_1$ ansatz spaces there is an obvious improvement.

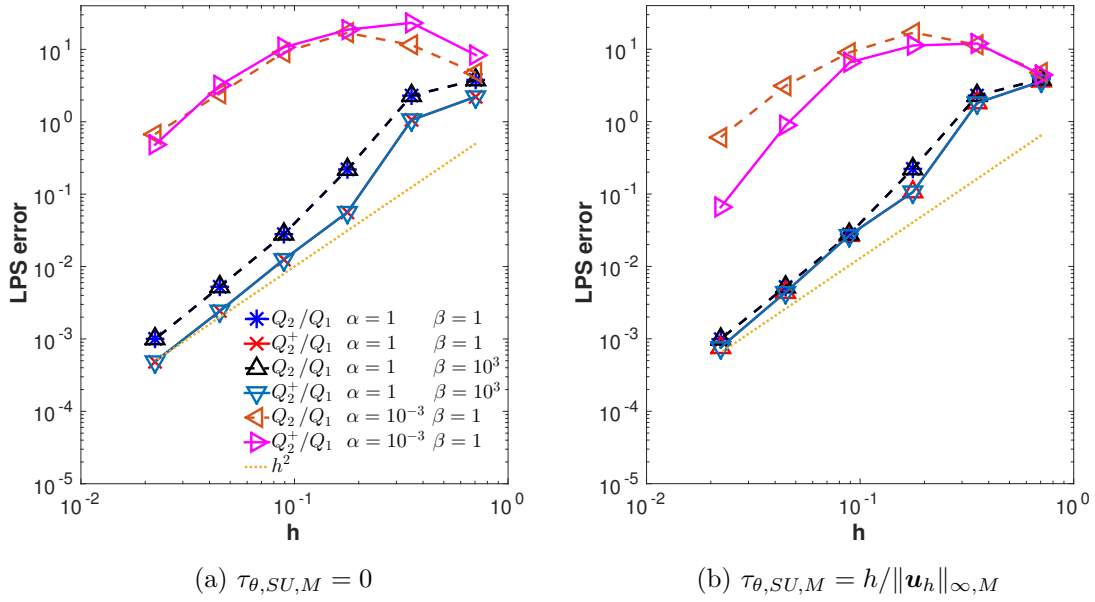


Figure 5.19: Traveling wave: LPS-errors for different finite elements and choices of α and β , $\nu = 1$

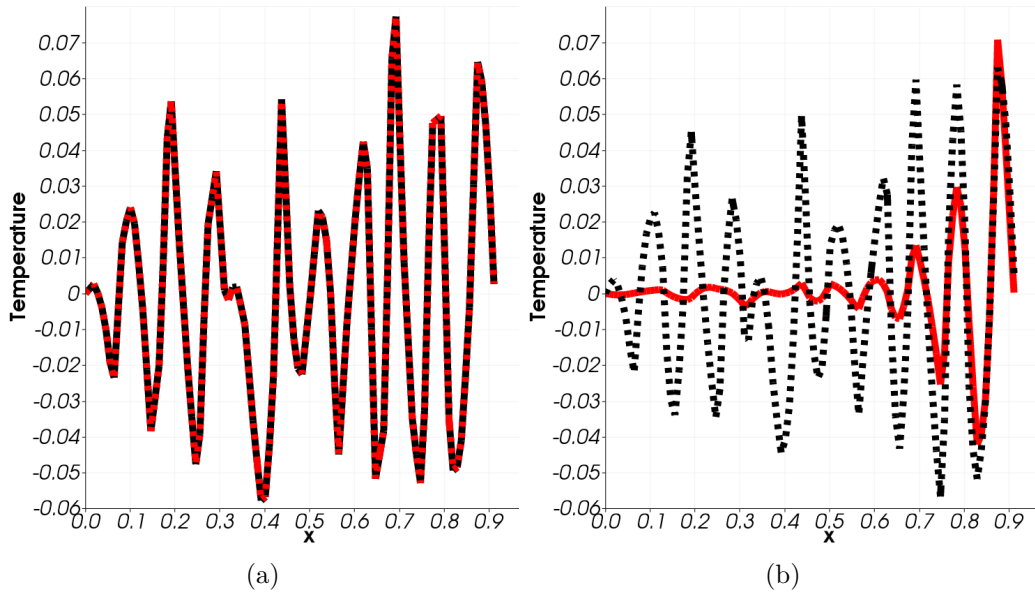


Figure 5.20: Traveling wave: Plot over temperature at $y = 0.5$ ($x \in [0, 0.9]$) at time $t = 0.005$ with $h = 1/16$ in case of (a) Q_2/Q_1 elements for $\tau_{\theta,SU,M} = 0$ (dotted line) and for $\tau_{\theta,SU,M} = \|\mathbf{u}_h\|_{\infty,M}^{-2}$ (solid line), (b) Q_2^+/Q_1 elements for $\tau_{\theta,SU,M} = 0$ (dotted line) and for $\tau_{\theta,SU,M} = \|\mathbf{u}_h\|_{\infty,M}^{-2}$ (solid line), $(\nu, \alpha, \beta) = (1, 10^{-3}, 1)$. The dotted and solid lines lie on top of each other in (a)

5.2.2 Rayleigh-Bénard Convection

We consider Rayleigh-Bénard convection in a three-dimensional cylindrical domain

$$\Omega := \left\{ (x, y, z) \in \left(-\frac{1}{2}, \frac{1}{2}\right)^3 \mid \sqrt{x^2 + y^2} \leq \frac{1}{2}, |z| \leq \frac{1}{2} \right\}$$

with aspect ratio $\Gamma = 1$ for different Prandtl numbers $Pr \in \{0.786, 6.4\}$, Rayleigh numbers $10^5 \leq Ra \leq 10^9$ and Rossby numbers $Ro \in \{0.09, 0.36, 1.08, \infty\}$. These critical parameters are defined by

$$Pr = \frac{\nu}{\alpha} \quad Ra = \frac{|\mathbf{g}| \beta \Delta \theta_{\text{ref}} L_{\text{ref}}^3}{\nu \alpha} \quad Ro = \frac{\sqrt{|\mathbf{g}| \beta \Delta T L}}{2|\boldsymbol{\omega}| L}.$$

In this test case the gravitational acceleration $\mathbf{g} \equiv (0, 0, -1)^T$ as well as the angular velocity $\boldsymbol{\omega}$ are (anti-)parallel to the z -axis. The temperature is fixed by Dirichlet boundary conditions at the (warm) bottom and (cold) top plate; the vertical wall is adiabatic with Neumann boundary conditions $\frac{\partial \theta}{\partial \mathbf{n}} = 0$. Homogeneous Dirichlet boundary data for the velocity are prescribed.

As a benchmark quantity, the Nusselt number Nu is used. For fixed z we consider the disc B_z defined by

$$B_z := \left\{ (x, y, z) \in \left(-\frac{1}{2}, \frac{1}{2}\right)^3 \mid \sqrt{x^2 + y^2} \leq \frac{1}{2} \right\}.$$

Then the Nusselt number Nu is calculated from the vertical heat flux $q_z = u_z \theta - \alpha \frac{\partial \theta}{\partial z}$ from the warm wall to the cold one by averaging over B_z and in time:

$$Nu(z) = \Gamma \left(\alpha |B| (T - t_0) |\theta_{\text{bottom}} - \theta_{\text{top}}| \right)^{-1} \int_{t_0}^T \int_B q_z(x, y, z, t) dx dy dt$$

with a suitable interval $[t_0, T]$. For the variation of the Nusselt number in z -direction we obtain

$$\frac{\partial Nu}{\partial z} = \int_0^{2\pi} \int_0^R -(Pr Ra)^{1/2} r \partial_t \theta dr d\varphi$$

due to the thermally insulating walls and the homogeneous Dirichlet conditions for the divergence-free velocity. This means that for a stationary temperature field there is no variation in z -direction. This also holds for the time averaged Nusselt number in any case in the limit

$$\frac{\partial}{\partial z} \left(\frac{1}{T - t_0} \int_{t_0}^T Nu dt \right) = \int_0^{2\pi} \int_0^R -(Pr Ra)^{1/2} r \frac{\theta(t_0) - \theta(T)}{T - t_0} dr d\varphi.$$

In the instationary convection-diffusion equation for the temperature there is no inlet boundary and hence a maximum principle shows that θ is bounded by $\theta(t_0)$. In particular, we get

$$\begin{aligned} \left| \frac{\partial}{\partial z} \left(\frac{1}{T - t_0} \int_{t_0}^T Nu \, dt \right) \right| &\leq \left| \int_0^{2\pi} \int_0^R -(PrRa)^{1/2} r \frac{\theta(t_0) - \theta(T)}{T - t_0} \, dr \, d\varphi \right| \\ &\leq \frac{2\pi R^2 \|\theta(t_0)\|_\infty}{T - t_0} \xrightarrow{T \rightarrow \infty} 0 \end{aligned}$$

In order to assess the quality of our simulations, we compute the Nusselt number for different $z \in \{-0.5, -0.25, 0, 0.25, 0.5\}$, where the heat transfer is integrated over a disk at fixed z . Then we compare these quantities with the Nusselt number Nu^{avg} calculated as the heat transfer averaged over the whole cylinder Ω and in time. The maximal deviation σ within the domain is evaluated according to

$$\sigma := \max\{|Nu^{\text{avg}} - Nu(z)|, z \in \{-0.5, -0.25, 0, 0.25, 0.5\}\}.$$

Non-Rotating Cylinder, $Pr = .78$

We first summarize results that we obtained for $Pr = 0.78$ in [DA15] by comparing with DNS simulations in [WSW12]. The used meshes are problem-adapted and obtained from an isotropic mesh by the transformation $T_{xyz}: \Omega \rightarrow \Omega$ defined by

$$T_{xyz}: (x, y, z)^T \mapsto \left(\frac{x}{r} \cdot \frac{\tanh(4r)}{2 \tanh(2)}, \frac{y}{r} \cdot \frac{\tanh(4r)}{2 \tanh(2)}, \frac{\tanh(4z)}{2 \tanh(2)} \right)^T \quad (5.1)$$

with $r := \sqrt{x^2 + y^2}$. With these grids the resulting isosurfaces for the temperature are depicted in Figure 5.21 and it is clearly visible how the increasing Rayleigh number Ra leads to increased mixing of the temperature and an enhanced transport from heat away from the wall. In all cases we observe for the large scale behavior one large convection cell (upflow of warm fluid and descent of cold fluid) while for larger Ra smaller structures and thin boundary layers occur. This is in good qualitative agreement with simulations run by [WSW12].

In Table 5.1 we compare the resulting Nusselt numbers for an optimal grad-div parameter and no grad-div stabilization at all. While the average Nusselt number is in both cases in good agreement with the reference value with up to $Ra = 10^7$, the deviation between Nusselt numbers at different z -positions quickly increases without grad-div stabilization. Despite this, for all $Ra \in \{10^5, 10^6, 10^7, 10^8\}$, the reference values Nu^{ref} obtained by DNS can be approximated surprisingly well with the help of grad-div stabilization on a mesh with only $N = 10 \cdot 8^3$ cells. We note that the optimal grad-div parameter only slightly depends on the Rayleigh number and with this choice the Nusselt number varies little

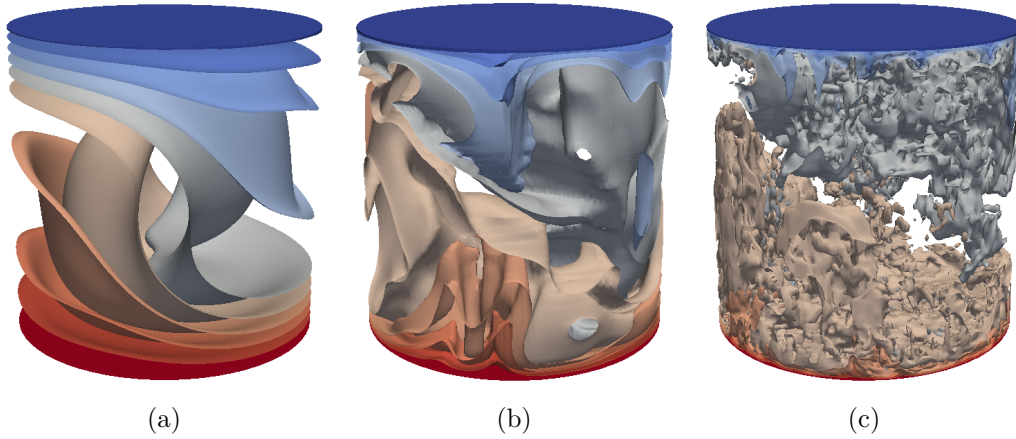


Figure 5.21: Temperature isosurfaces at $T = 1000$ for $Pr = 0.786$, (a) $Ra = 10^5$, (b) $Ra = 10^7$, (c) $Ra = 10^9$, $N = 10 \cdot 16^3$, $\gamma_M = 0.1$

Ra	10^5		10^6		10^7		10^8		10^9	
	Nu^{avg}	σ	Nu^{avg}	σ	Nu^{avg}	σ	Nu^{avg}	σ	Nu^{avg}	σ
nGD	3.84	0.04	8.65	0.34	16.41	1.83	37.70	29.5	118.8	137.6
GD	3.84	0.03	8.65	0.02	16.88	0.11	31.29	0.70	55.52	1.35
Nu^{ref}	3.83		8.6		16.9		31.9		63.1	

Table 5.1: Rayleigh-Bénard Convection: Averaged Nusselt numbers and maximal deviations σ for different Ra and different grad-div parameters $\tau_{u,gd,M}$, averaged over time $t \in [150, 1000]$, $N = 10 \cdot 8^3$, $\mathbb{Q}_2/\mathbb{Q}_1/\mathbb{Q}_1$ elements are used. nGD indicates that no stabilization is used (in particular, $\tau_{u,gd,M} = 0$), GD means that an optimal grad-div parameter is used: $\tau_{u,gd,M} = 0.1$ for $10^5 \leq Ra \leq 10^8$ and $\tau_{u,gd,M} = 0.01$ for $Ra = 10^9$. Nu^{ref} denotes DNS results from [WSW12]

with respect to different z . It turned out that this parameter design is independent of the considered refinement.

With respect to the LPS stabilization it turned out that for anisotropically refined meshes $\tau_{\theta, SU, M}$ produced the best results. In case of isotropic grids, that are not adapted to the problem, LPS SU stabilization for the temperature becomes necessary. Bubble enrichment enhances the accuracy on all grids.

Figure 5.22 gives an overview of the obtained results (using the respective optimal stabilization parameters and an anisotropic grid). We compare the reduced Nusselt numbers $Nu/Ra^{0.3}$ for different finite element spaces, indicated by th and bb as above, with DNS data from the literature. The Grossmann-Lohse theory from [GL00] suggests that there is a scaling law of the Nusselt number depending on Ra (at fixed Pr) that holds over wide parameter ranges. The reduced Nusselt number calculated in our experiments is nearly constant. However, one does not observe a global behavior of the Nusselt number as $Nu \propto Ra^{0.3}$. But as in [WSW12], a smooth transition between different Ra -regimes $Ra \leq 10^6$, $10^6 \leq Ra \leq 10^8$ and $Ra \geq 10^8$ can be expected. Note that the presented results on the finest grid ($N = 10 \cdot 32^3$) differ by only 0.1%.

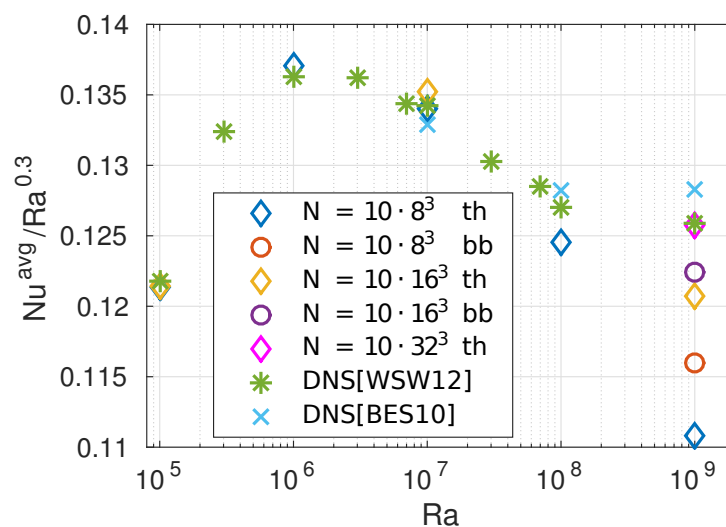


Figure 5.22: Rayleigh-Bénard Convection: $Nu/Ra^{0.3}$ ($\Gamma = 1$, $Pr = 0.786$) for an anisotropic grid with $N \in \{10 \cdot 8^3, 10 \cdot 16^3\}$ cells, compared with DNS data from [WSW12] ($\Gamma = 1$, $Pr = 0.786$) and [BES10] ($\Gamma = 1$, $Pr = 0.7$). The grid is transformed via T_{xyz} for $N \in \{10 \cdot 8^3, 10 \cdot 16^3\}$ and via T_z for $N = 10 \cdot 32^3$. The label th indicates that $(Q_2/Q_1)/Q_1/(Q_2/Q_1)$ elements are used and $(Q_2^+/Q_1)/Q_1/(Q_2^+/Q_1)$ are denoted by bb . For $10^5 \leq Ra \leq 10^8$, $(\tau_{u, gd, M}, \tau_M^u, \tau_M^\theta) = (0.1, 0, 0)$ is chosen; $(\tau_{u, gd, M}, \tau_M^u, \tau_M^\theta) = (0.01, \frac{1}{2}h/\|\mathbf{u}_h\|_{\infty, M}, 0)$ in case of $Ra = 10^9$

Table 5.2 validates that a grid transformed via T_{xyz} (together with grad-div stabilization) resolves the boundary layer: For a grid with $N = 10 \cdot 16^3$ cells, the dependence between

	$\langle \delta_\theta \rangle$			$\langle \delta_\theta \rangle \propto Ra^m$	
	$Ra = 10^5$	$Ra = 10^7$	$Ra = 10^9$	m	m^{ref}
top	0.1295	0.0311	0.0084	-0.2970	-0.285
bottom	0.1295	0.0293	0.0085	-0.2957	-0.285

Table 5.2: Rayleigh-Bénard Convection: Thermal boundary layer thicknesses at the top and bottom plates $\langle \delta_\theta \rangle^{\text{top/bottom}}$, averaged over $r = \sqrt{x^2 + y^2} \in [0, \frac{1}{2}]$, and slopes $m^{\text{top/bottom}}$ resulting from the fitting $\langle \delta_\theta \rangle \propto Ra^m$. The grid with $N = 10 \cdot 16^3$ cells is transformed via T_{xyz} ; $\mathbb{Q}_2/\mathbb{Q}_1/\mathbb{Q}_2$ elements are used. $\tau_{u,gd,M} = 0.1$ for $Ra \in \{10^5, 10^7\}$ and $\tau_{u,gd,M} = 0.01$ for $Ra = 10^9$. m^{ref} denotes the slope proposed by [WSW12]

Ra and the resulting thermal boundary layer thickness $\langle \delta_\theta \rangle$ is in good agreement with the law $\langle \delta_\theta \rangle \propto Ra^{-0.285}$ suggested by [WSW12]. Here, the thermal boundary layer thickness δ_θ is calculated via the so-called slope criterion as in [WSW12]. δ_θ is the distance from the boundary at which the linear approximation of temperature profile at the boundary crosses the line $\theta = 0$. $\langle \delta_\theta \rangle$ denotes the average over $r = \sqrt{x^2 + y^2} \in [0, \frac{1}{2}]$.

All in all, our simulations illustrate that we obtain surprisingly well approximated benchmark quantities even on relatively coarse meshes (compared with DNS from the reference data). For example, for the grid with $N = 10 \cdot 16^3$ cells, we have a total number of approximately 1,400,000 degrees of freedom (DoFs) in case of $(\mathbb{Q}_2/\mathbb{Q}_1)/\mathbb{Q}_1/(\mathbb{Q}_2/\mathbb{Q}_1)$ elements. Enriched $(\mathbb{Q}_2^+/\mathbb{Q}_1)/\mathbb{Q}_1/(\mathbb{Q}_2^+/\mathbb{Q}_1)$ elements result in 1,900,000 DoFs for $N = 10 \cdot 16^3$ cells. Refinement increases the number of DoFs roughly by a factor of 8. In comparison, the DNS in [WSW12] requires approximately 1,500,000,000 DoFs.

Rotating Cylinder, $Pr = 6.4$

Finally, the question arises whether these observations transfer to the case in which the cylinder is rotating. Therefore we consider the setup in [KBG15] where the Prandtl number is chosen as $Pr = 6.4$. For the anisotropically refined mesh with $N = 10 \cdot 8^3$ cells and $\tau_{u,gd,M} = 0.01$ we visualize for Rayleigh numbers $Ra \in \{10^6, 10^7, 10^8, 10^9\}$ the flow structures and isosurfaces of the temperature in Figures 5.23, 5.24, 5.25, 5.26. In accordance with the reference we observe that for $Ro = \infty$ the convection is dominated by large scale circulation. For strong steady rotation, i.e., $Ro = 0.09$, the flow structure is very different as now Taylor columns dominate the temperature and the velocity field. Hence, we see that this problem is quite similar to our considerations in [AL15] for the Taylor-Proudman problem. All in all we achieve comparable results to those in [KBG15].

Ra	Ro	Nu^{avg}	σ	$\tau_{u,gd,M}$	mesh	Nu^{ref}
10^6	0.09	5.2851	0.1014	0.1	iso	5.5 ± 0.2
10^6	∞	8.2327	0.8263	0	aniso	9.0 ± 0.1
10^7	0.09	15.7992	0.2971	0.1	aniso	16.1 ± 0.5
10^7	0.36	18.9784	0.1057	0.1	aniso	18.8 ± 0.4
10^7	1.08	17.3130	0.0620	0.1	aniso	17.4 ± 0.3
10^7	∞	16.4804	0.1806	0.1	aniso	16.5 ± 0.2
10^8	0.09	38.8861	0.6861	0.1	aniso	38.2 ± 0.8
10^8	∞	32.0387	0.5651	0.1	aniso	33.2 ± 0.4
10^9	0.09	64.8679	6.5222	0.1	aniso	73.8 ± 1.0
10^9	0.36	78.2142	5.9778	0.01	aniso	72.2 ± 0.9
10^9	1.08	71.8906	2.9568	0.01	aniso	67.0 ± 1.6
10^9	∞	66.2219	2.6035	0.01	aniso	66.5 ± 1.8

Table 5.3: Rotating Rayleigh-Bénard Convection: Averaged Nusselt numbers and maximal deviations σ for optimized grad-div parameter $\tau_{u,gd,M}$ with $Pr = 6.4$ and varying Rayleigh and Rossby numbers. Nu^{ref} denotes DNS results from [KBG15]

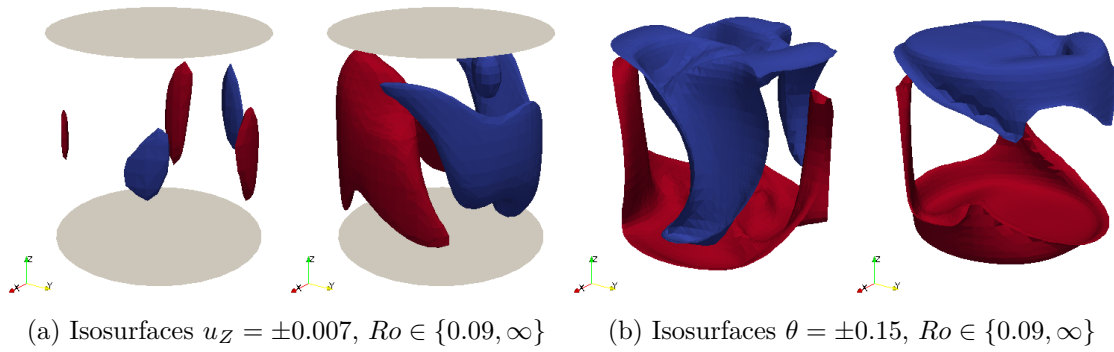
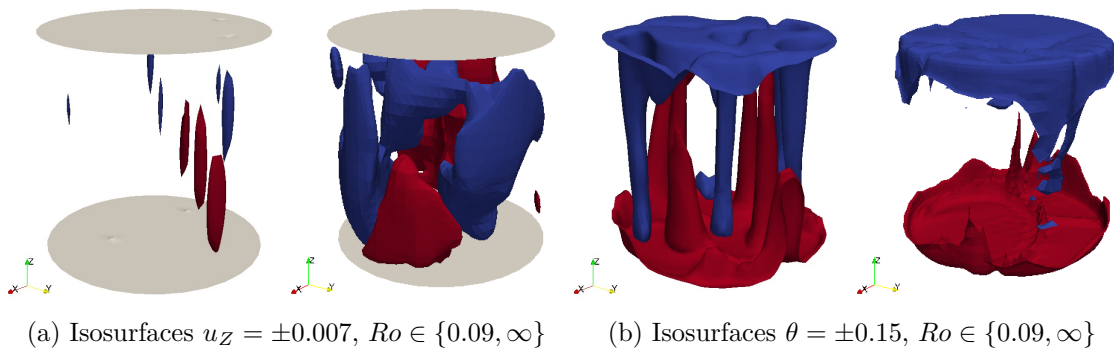
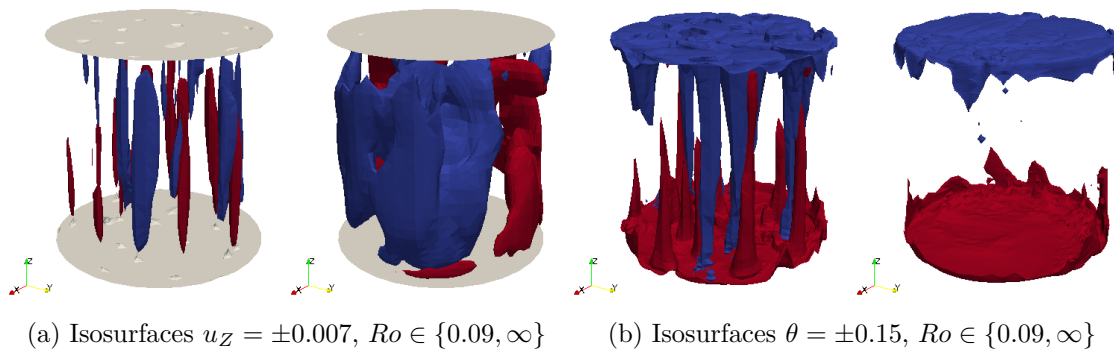
For the results with respect to the Nusselt number we only state here the best results for $N = 10 \cdot 8^3$ cells where we always tried $\tau_{u,gd,M} \in \{0, 0.01, 0.1, 1\}$ on an isotropic and anisotropic mesh.

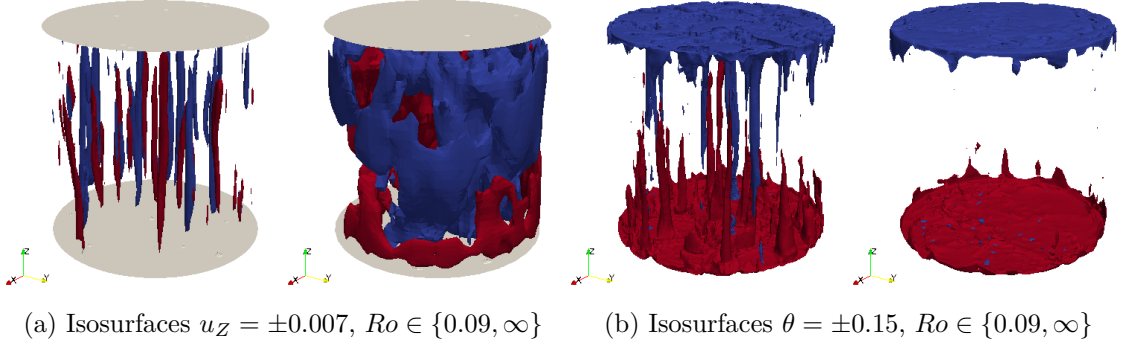
Table 5.3 shows that also in this case the reference Nusselt number can be approximated surprisingly well on the rather coarse mesh. The parameter design with respect to the grad-div $\tau_{u,gd,M}$ is confirmed. Up to $Ra = 10^8$ a parameter $\tau_{u,gd,M} = 0.1$ is best, only for $Ra = 10^9$ we gain from the smaller parameter $\tau_{u,gd,M} = 0.01$. Although the flow structure differs quite a lot, it turned out that the anisotropically transformed grid is still superior to the isotropic ones.

All in all, we conclude that for both the rotating and non-rotating case DNS results can be well approximated when a suitably transformed mesh and grad-div stabilization is used. In particular, local projection is only beneficial on the isotropic meshes.

5.3 Isothermal Electrically Conducting Flow

For the magnetic field we considered convergence results in [WAL15]. Here, we extend two examples that show typical features of the Maxwell equations. The first one describes a solution of reduced regularity and in the second one sharp inner boundary layers appear.

Figure 5.23: Rotating Rayleigh-Bénard Convection: $Ra = 10^6$ Figure 5.24: Rotating Rayleigh-Bénard Convection: $Ra = 10^7$ Figure 5.25: Rotating Rayleigh-Bénard Convection: $Ra = 10^8$

Figure 5.26: Rotating Rayleigh-Bénard Convection: $Ra = 10^9$

Both cases are challenging, although quite different as we will see in terms of a proper parameter design.

5.3.1 Singular Solution

The first example is one for which $\mathbf{b} \in H^{curl}(\Omega) \setminus [H^1(\Omega)]^2$ holds. In particular, we consider in the L-shaped domain $\Omega = (-1, 1)^2 \setminus \{[0, 1] \times [-1, 0]\}$ the reference solution (in polar coordinates (d, φ))

$$\begin{aligned} \mathbf{b}(d, \varphi) &:= d^{\frac{2}{3}} \sin\left(\frac{2\varphi}{3}\right) \in [H^{2/3}(\Omega)]^2 & r(d, \varphi) &:= 0. \\ \mathbf{u}(d, \varphi) &:= \mathbf{0} & p(d, \varphi) &:= 0. \end{aligned}$$

Due to $\nabla \cdot \mathbf{b} = 0$ and $\nabla \times \mathbf{b} = \mathbf{0}$ the right-hand side for velocity and magnetic field vanishes, i.e., $\mathbf{f}_u = \mathbf{f}_b = \mathbf{0}$. On the boundary, we choose homogeneous Dirichlet boundary conditions for \mathbf{u} and r and prescribe the tangential component of the magnetic field $\mathbf{n} \times \mathbf{b} = \mathbf{n} \times \mathbf{b}_D$ where \mathbf{b}_D is the exact solution on $\partial\Omega$.

In [WAL15] we solved the above presented problem for fixed $\mathbf{u} = \mathbf{0}$ by a stationary solver written in **FreeFEM++** [Hec12] and considered equal-order ansatz spaces $\mathbb{P}_1/\mathbb{P}_1$ as well as the Taylor-Hood pair $\mathbb{P}_2/\mathbb{P}_1$. The used meshes can be seen in Figure 5.27.

For the parameter design $\tau_{b,gd,M} = \lambda h^2$, $\tau_{r,PSPG,M} = 1/\lambda$, we received the following results with the rate of convergence in brackets.

In accordance with [BC12] the cross-box element works fine and achieves the expected rates of convergence. Furthermore, the Taylor-Hood approximation in $\mathbb{P}_2/\mathbb{P}_1$ reaches the asymptotically optimal rates of convergence as well in contrast to the equal order approximation in $\mathbb{P}_1/\mathbb{P}_1$ on the other given meshes.

Now, the question arises whether these results also hold in the framework we consider in this thesis and in the case of an instationary solver. Note that this kind of problem is not

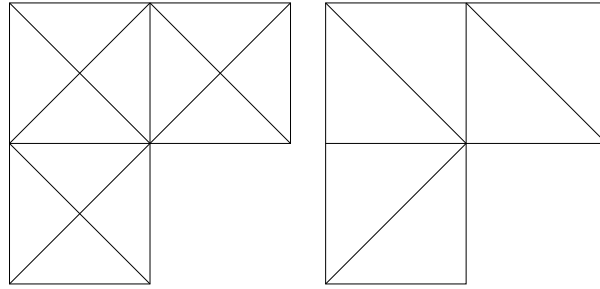


Figure 5.27: Different meshes for the calculations: (left) Cross-box, (right) \mathbb{P}_1 standard mesh

covered by the analysis for the fully discretized scheme considered in Chapter 4. We choose for both the pairs (\mathbf{u}, p) and (\mathbf{b}, r) the inf-sup stable Taylor-Hood ansatz spaces $[\mathbb{Q}_2]^2/\mathbb{Q}_1$. The resulting errors can be observed in Figure 5.28 for a Cartesian quadrilateral mesh.

In accordance with Section 4.2, we observe for the choice $\tau_{b,gd,M} = 1$, $\tau_{r,PSPG} = 0$ no convergence with respect to the total error magnetic field error that is locally given as sum of the $L^2(M)$ - $H^{curl}(M)$ - and the $H^{div}(M)$ -error scaled with $\sqrt{\tau_{b,gd,M}}$. Only for the $H^{div}(\Omega)$ -error are the results much better than for all the other parameter choices.

Decreasing the grad-div parameter and choosing $\tau_{PSPG} \leq 1$ improves the results in such a way that the total error is at least not increasing with mesh refinement. For a parameter choice according to $\tau_{b,gd,M} = h^2/L_0$, $\tau_{r,PSPG} = L_0$ with $L_0 \geq 10^4$ we finally achieve results comparable to those with the stationary solver above. Just the rate of convergence for the divergence is reduced since here only observe a scaling like $h^{-2/3}$. This choice is in agreement with the bounds (3.30) derived for the semi-discrete case.

If we now try to distort the mesh slightly, the results first improve for all considered errors, but then suddenly grow immensely. This clearly shows the sensitivity of this example with respect to a special choice of meshes.

In Figure 5.29 the numerical solution is depicted. Although we have seen that the parameter design for the left picture shows the best convergence behavior, unphysical oscillations only disappear when the grad-div parameter is increased.

5.3.2 Magnetic Field Expulsion

In this example we examine the influence of a rotating electrically conducting fluid rotating in an infinitely long cylinder on an uniform magnetic field. Therefore, we consider on the domain $\Omega = (-1, 1)^2$ with $R = \frac{1}{2}$ the prescribed velocity field

$$\mathbf{u} = \begin{cases} (-y, x)^T & \mathbf{x} \leq R \\ (0, 0)^T & \mathbf{x} > R \end{cases}.$$

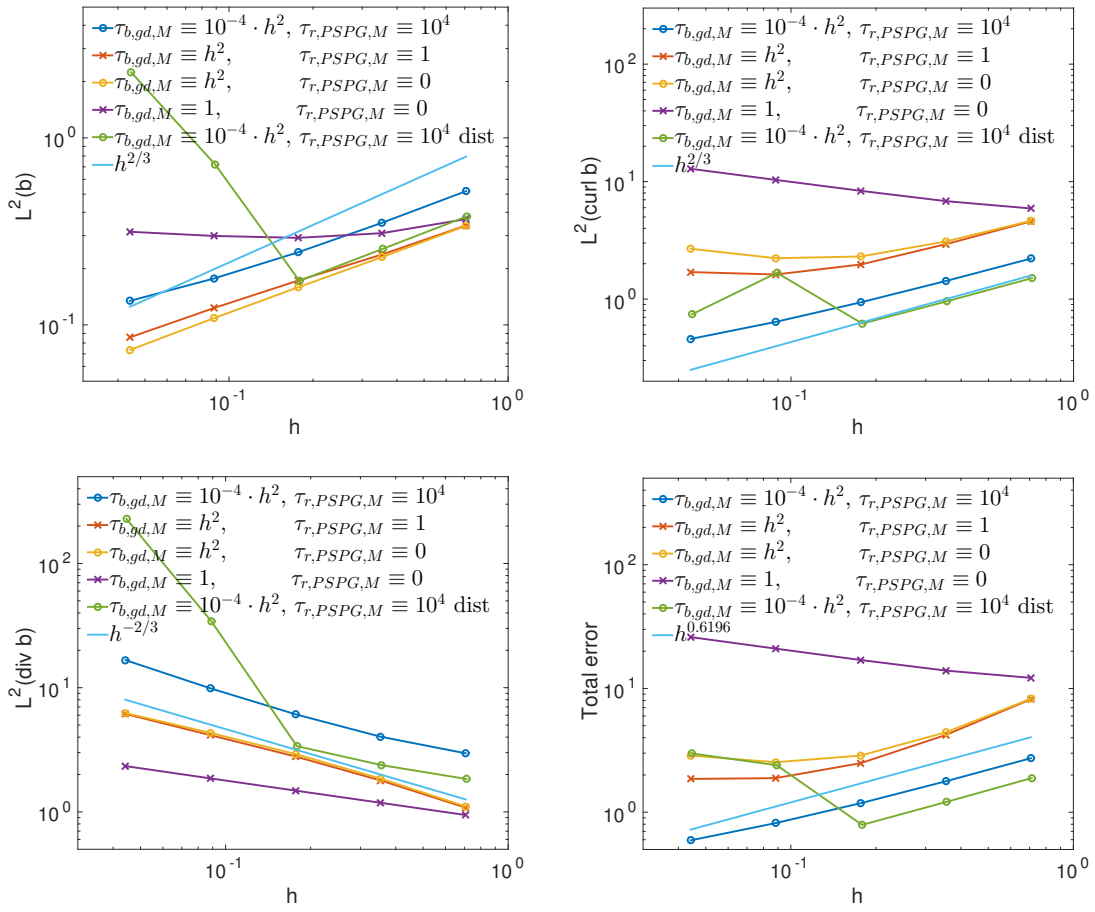


Figure 5.28: Error for the singular solution with Taylor-Hood $[Q_2]^2/Q_1$ elements



(a) $\tau_{b,gd,M} \equiv h^2 \cdot 10^{-4}, \tau_{r,PSPG,M} \equiv 10^4$

(b) $\tau_{b,gd,M} \equiv h^2, \tau_{r,PSPG,M} \equiv 1$

Figure 5.29: Magnitude of the singular solution

Cross-box, Equal-order				
h	2^{-4}	2^{-5}	2^{-6}	2^{-7}
$\ \mathbf{b} - \mathbf{b}_h\ _0$	$1.71E - 1$	$1.09E - 1$ (0.65)	$6.91E - 2$ (0.66)	$4.36E - 2$ (0.66)
$\ \nabla \times (\mathbf{b} - \mathbf{b}_h)\ _0$	$1.93E - 2$	$7.66E - 3$ (1.33)	$3.04E - 3$ (1.33)	$1.23E - 3$ (1.31)
$\ r - r_h\ _0$	$7.94E - 3$	$3.46E - 3$ (1.20)	$1.45E - 3$ (1.25)	$5.96E - 4$ (1.28)
$\ \nabla(r - r_h)\ _0$	$3.91E - 2$	$2.49E - 2$ (0.65)	$1.57E - 2$ (0.66)	$9.92E - 3$ (0.66)
$\ \nabla \cdot (\mathbf{b} - \mathbf{b}_h)\ _0$	3.65	4.57 (-0.32)	5.75 (-0.33)	7.23 (-0.33)
Cross-box, Taylor-Hood				
h	2^{-4}	2^{-5}	2^{-6}	2^{-7}
$\ \mathbf{b} - \mathbf{b}_h\ _0$	$1.60E - 1$	$1.02E - 1$ (0.65)	$6.45E - 2$ (0.66)	$4.07E - 2$ (0.66)
$\ \nabla \times (\mathbf{b} - \mathbf{b}_h)\ _0$	$1.55E - 2$	$6.13E - 3$ (1.34)	$2.42E - 3$ (1.34)	$9.61E - 4$ (1.33)
$\ r - r_h\ _0$	$6.25E - 3$	$2.74E - 3$ (1.19)	$1.15E - 3$ (1.25)	$4.71E - 4$ (1.29)
$\ \nabla(r - r_h)\ _0$	$3.04E - 2$	$1.94E - 2$ (0.65)	$1.23E - 2$ (0.66)	$7.74E - 3$ (0.67)
$\ \nabla \cdot (\mathbf{b} - \mathbf{b}_h)\ _0$	3.52	4.41 (-0.33)	5.54 (-0.33)	6.98 (-0.33)
\mathbb{P}_1 standard mesh, Equal-order				
h	2^{-4}	2^{-5}	2^{-6}	2^{-7}
$\ \mathbf{b} - \mathbf{b}_h\ _0$	$3.62E - 1$	$2.86E - 1$ (0.34)	$2.23E - 1$ (0.36)	$1.74E - 1$ (0.36)
$\ \nabla \times (\mathbf{b} - \mathbf{b}_h)\ _0$	$1.19E - 1$	$7.98E - 2$ (0.58)	$5.68E - 2$ (0.49)	$4.19E - 2$ (0.44)
$\ r - r_h\ _0$	$2.33E - 2$	$1.46E - 2$ (0.67)	$8.83E - 3$ (0.73)	$5.30E - 3$ (0.74)
$\ \nabla(r - r_h)\ _0$	$7.98E - 2$	$6.39E - 2$ (0.32)	$5.07E - 2$ (0.33)	$4.00E - 2$ (0.34)
$\ \nabla \cdot (\mathbf{b} - \mathbf{b}_h)\ _0$	3.06	3.94 (-0.36)	5.24 (-0.41)	7.12 (-0.44)
\mathbb{P}_1 standard mesh, Taylor-Hood				
h	2^{-4}	2^{-5}	2^{-6}	2^{-7}
$\ \mathbf{b} - \mathbf{b}_h\ _0$	$2.19E - 1$	$1.41E - 1$ (0.64)	$8.98E - 2$ (0.65)	$5.68E - 2$ (0.66)
$\ \nabla \times (\mathbf{b} - \mathbf{b}_h)\ _0$	$2.87E - 2$	$1.16E - 2$ (1.31)	$4.72E - 3$ (1.30)	$1.92E - 3$ (1.30)
$\ r - r_h\ _0$	$1.00E - 2$	$4.58E - 3$ (1.13)	$1.96E - 3$ (1.22)	$8.13E - 4$ (1.27)
$\ \nabla(r - r_h)\ _0$	$3.81E - 2$	$2.46E - 2$ (0.63)	$1.56E - 2$ (0.66)	$9.89E - 3$ (0.66)
$\ \nabla \cdot (\mathbf{b} - \mathbf{b}_h)\ _0$	3.18	3.99 (-0.33)	5.02 (-0.33)	6.32 (-0.33)

Table 5.4: Singular solution: Errors for simplicial meshes

In particular, we neglect the influence of the magnetic field on the velocity field. We assume that the boundary $\partial\Omega$ is electrically conducting and prescribe $\mathbf{b} \cdot \mathbf{n} = (0, 1)^T$.

For an infinite domain this problem admits an analytical solution [Mof78] that can be expressed in polar coordinates (d, φ) by

$$\mathbf{b}(d, \varphi) := \nabla \times \Re[f(d) \exp(i\varphi)] \quad f(d) := \begin{cases} d + C/d, & d > R \\ Dj_1(pr), & d \leq R \end{cases}$$

where $j_n(x)$ are the Bessel functions of first kind and the constants C , D and p are given by

$$C = \frac{R[2j_1(pR) - pRj_0(pR)]}{pj_0(pR)} \quad D = \frac{2}{pj_0(pR)} \quad p = (1 - i)\sqrt{2\lambda}.$$

For $\lambda \rightarrow \infty$ the initially described magnetic field is undistorted and $\mathbf{b}(x, y) = (0, 1)^T$. On the other hand, for vanishing magnetic diffusivity we obtain

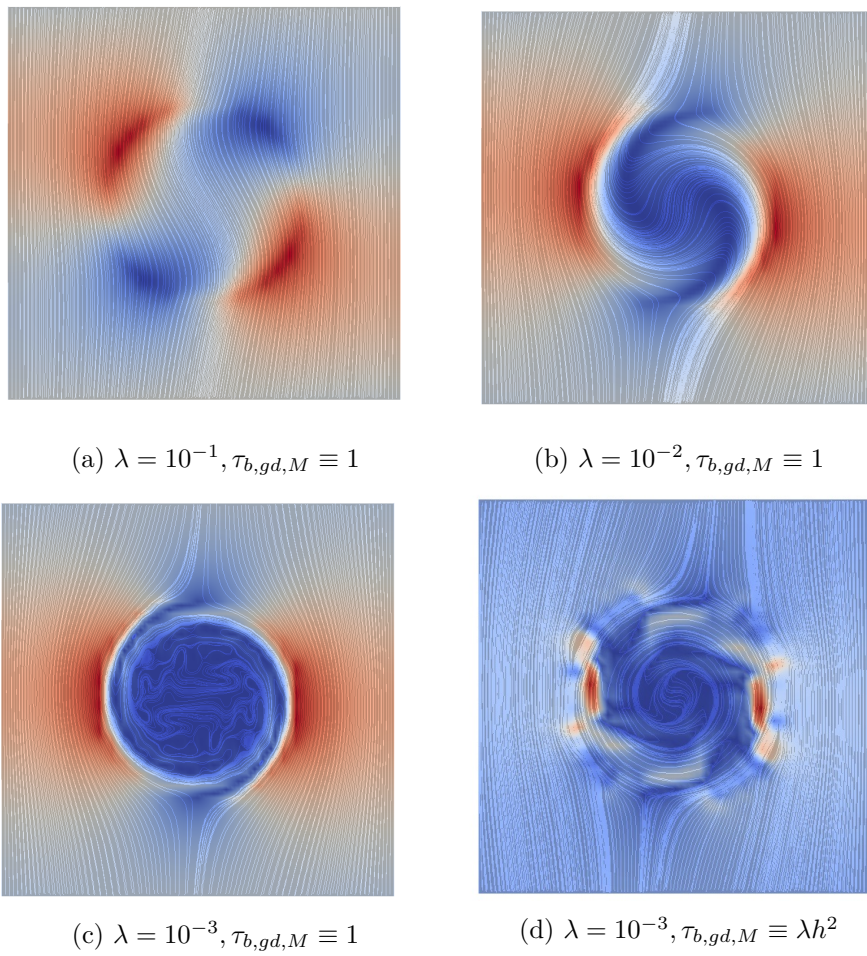
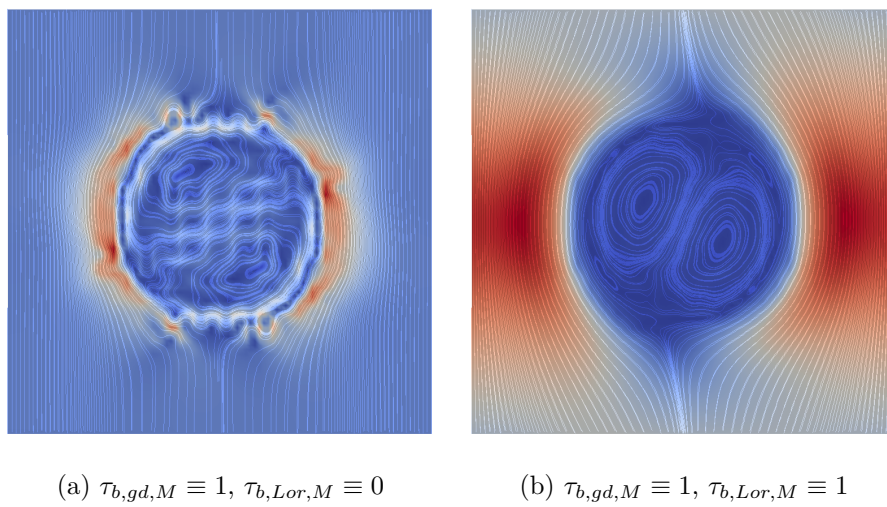
$$\lim_{\lambda \rightarrow 0} \mathbf{b} = \begin{cases} \mathbf{0}, & d < R \\ -\nabla \times \left(\left(d - \frac{R^2}{d} \right) \cos(\theta) \right), & d \geq R \end{cases} = \begin{cases} \mathbf{0} & d < R \\ \left(\frac{-xy}{2(x^2+y^2)^2}, 1 + \frac{x^2-y^2}{4(x^2+y^2)^2} \right)^T & d \geq R \end{cases}.$$

In particular, we observe that the magnetic field is expelled and a sharp inner boundary layer appears.

For moderately small λ the numerical solutions are depicted in Figure 5.30 for a constant grad-div stabilization parameter $\tau_{b,gd,M} \equiv 1$ and no PSPG or LPS stabilization. In all these cases, we achieve on this rather coarse mesh ($h = \sqrt{2}/16$) results that resemble the correct behavior of the solution. Just for the choice $\tau_{b,gd} \equiv \lambda h^2$ for $\lambda = 10^{-3}$ suggested in the semi-discrete approach (3.30) spurious oscillations introduced by the inner boundary layer occur.

If we decrease the magnetic diffusivity further, suddenly lots of unphysical oscillations occur (Figure 5.31(left)). These can be removed by using the stabilization $s_{b,Lor}$ with $\tau_{b,Lor,M} \equiv 1$ (Figure 5.31 right).

Comparing with the Blasius test case (Subsection 5.1.4) one might expect that further refinement should be sufficient to remove oscillations and to capture the correct behavior of the solution with grad-div stabilization alone. In Figure 5.32 we consider for the case $\lambda = 10^{-5}$ the influence of the Lorentz stabilization again for two different meshes ($h = \sqrt{2}/32$ and $h = \sqrt{2}/128$). While the magnetic field grows exponentially in time for the grad-div stabilized solution on the coarse mesh, the solution on the fine mesh stays bounded and no oscillations are visible. On the other hand, the magnitude is still too large by a factor of 10 and the streamlines away from the cylinder seem not to be influenced by the rotating fluid at all. However, for the Lorentz stabilized solution we obtain physically reasonable results. The magnitude of the solution is of the order of the analytical solution for vanishing magnetic diffusivity and infinite domain. Furthermore, the inner boundary layer is sufficiently resolved such that the expulsion of the magnetic field is clearly visible. On the coarse mesh a quite strong magnetic field in the inside of the domain is visible. This is due to the fact that the numerical simulation has been stopped after the magnetic

Figure 5.30: Magnetic field for moderately small magnetic diffusivity λ Figure 5.31: Effect of LPS stabilization for the Lorentz coupling $\lambda = 10^{-4}$

field outside of the cylinder became stationary. We expect that this inner magnetic field decays further in time due to diffusivity.

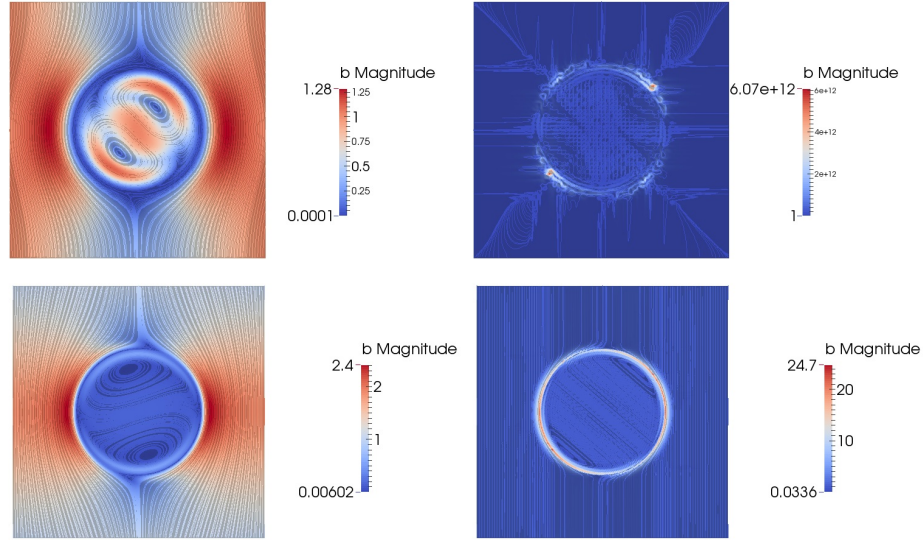


Figure 5.32: Magnetic field with (left) and without (right) LPS on coarse (top) and fine (bottom) meshes for $\lambda = 10^{-5}$

Finally, we consider in Figure 5.33 for the same λ different stabilizations on an adaptively refined mesh. The mesh width is in the range $h_M \in [\sqrt{2}/32, \sqrt{2}/512]$ and as error indicator the gradient jumps in normal direction over cell faces are used. We first observe that the results for the grad-div stabilized and the additionally Lorentz stabilized solutions are qualitatively comparable to those on the isotropic meshes. Using the induction stabilization $s_{b,Ind}$ leads to an improperly refined mesh: There is no sharp boundary layer and the position of the maximum is incorrect. A combination with the Lorentz stabilization clearly improves the situation, but compared to Lorentz stabilization alone the solution is blurred since too much diffusivity is introduced.

This example shows first that the parameter design for solutions with reduced regularity is not appropriate here. In case of small magnetic diffusivity grad-div stabilization is not sufficient for a proper resolution of the inner boundary layer but additional Lorentz stabilization is needed. With this combination we are able to remove unphysical oscillation even for small values of λ on coarse meshes. On the other hand the stabilization $s_{b,Ind}$ seems not to be appropriate for this problem. Using adaptive mesh refinement we can greatly diminish the number of degrees of freedom ($\sim 6 \cdot 10^5$ on the fine mesh in Figure 5.32 and $\sim 4 \cdot 10^4$ for the meshes in Figure 5.33) while preserving a comparably good solution.

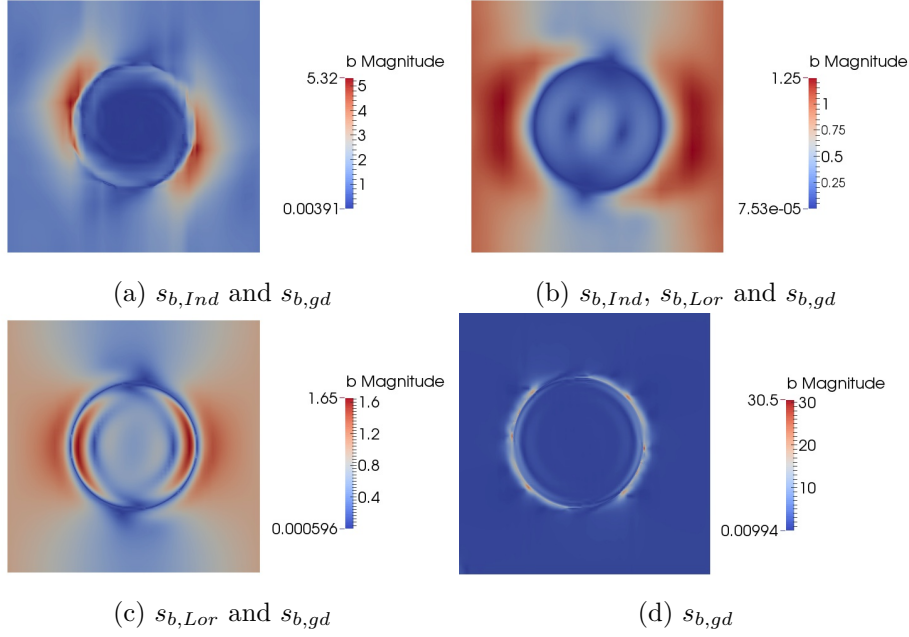


Figure 5.33: Different stabilizations on an adaptively refined mesh for $\lambda = 10^{-5}$

5.4 Non-Isothermal Electrically Conducting Flow

In the last example we consider the fully coupled model. On the domain $\Omega = (0, 10) \times (0, 1)$ we investigate the flow that develops in an infinite channel that is heated from below and cooled from above and possibly stabilized by a magnetic field in y -direction. In particular, we consider the boundary conditions

$$\begin{aligned}
 \mathbf{u}|_{y \in \{0,1\}} &= 0 & \mathbf{u}|_{x=0} &= \mathbf{u}|_{x=10} \\
 \mathbf{n} \cdot \mathbf{b}|_{y \in \{0,1\}} &= b_0 & \mathbf{b}|_{x=0} &= \mathbf{u}|_{x=10} \\
 \theta|_{y \in \{0,1\}} &= \left(y - \frac{1}{2}\right) Ra & \theta|_{x=0} &= \theta|_{x=10}.
 \end{aligned}$$

Above a critical Rayleigh number Ra flow is induced when the buoyancy effects dominate the stabilizing viscous forces. At fixed Rayleigh number this flow is damped out when the magnetic field is sufficiently strong [Cha13]. A typical stable state is depicted in Figure 5.34. In particular, stationary convection cells develop that transport temperature from the warm bottom to the cold top.

The main interest in this test case is the consideration of the parallel scaling behavior of the implemented numerical solver. For $Ra = 25000$ and $b_0 = 10$ we calculate with a time step size Δt the first 100 time steps of the numerical solution on successively refined meshes with $N = 1280 \cdot 4^k$, $k \in [0, 6]$ cells. Figure 5.35 shows that we obtain for all problem sizes convincing results. In particular, we obtain for $k \geq 3$ (nearly) linear weak scaling,

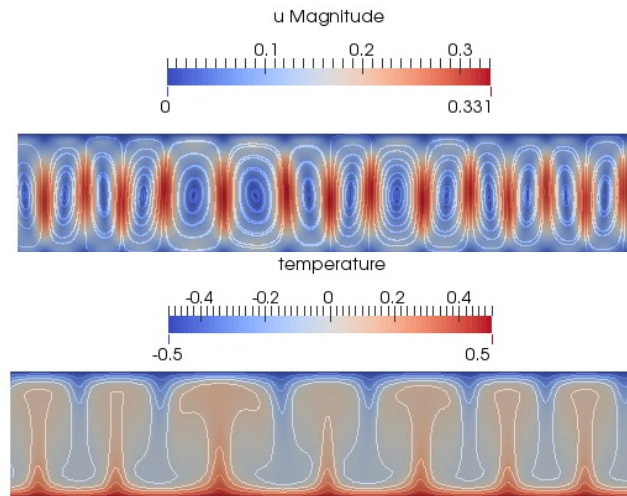


Figure 5.34: Flow structure for $Ra = 25000$ and b_0 in steady state

i.e., the run time halves when the number of used processes halves. Weak scaling on the other hand means that the run time stays the same when the size of the problem and the number of processes are doubled. We observe that this is approximately the case if the problem is sufficiently large. In Figure 5.36 we have a closer look on the scaling behavior of the major parts of the solver for a mesh with $N = 1280 \cdot 4^6 = 5,242,880$ cells. This means for that we have to solve for 115,417,095 unknowns in each time step for ansatz spaces according to $\mathbf{V}_h = \mathbb{Q}_2^2$, $\mathbf{C}_h = \mathbb{Q}_2^2$, $Q_h = \mathbb{Q}_1$, $S_h = \mathbb{Q}_1$. We observe that all assembling parts of the algorithm scale linearly. Just for solving for the kinematic pressure and the magnetic pseudo-pressure the scaling breaks quickly down. Since linear solvers typically need more than 10,000 unknowns to achieve convincing results, this is not too surprising. In sum these contributions clearly vanish when we consider the total run time.

All in all, we observe good scaling results for up to 1024 processes. This suggests that the chosen splitting in combination with the stabilizations is also well-suited with respect to numerical efficiency.

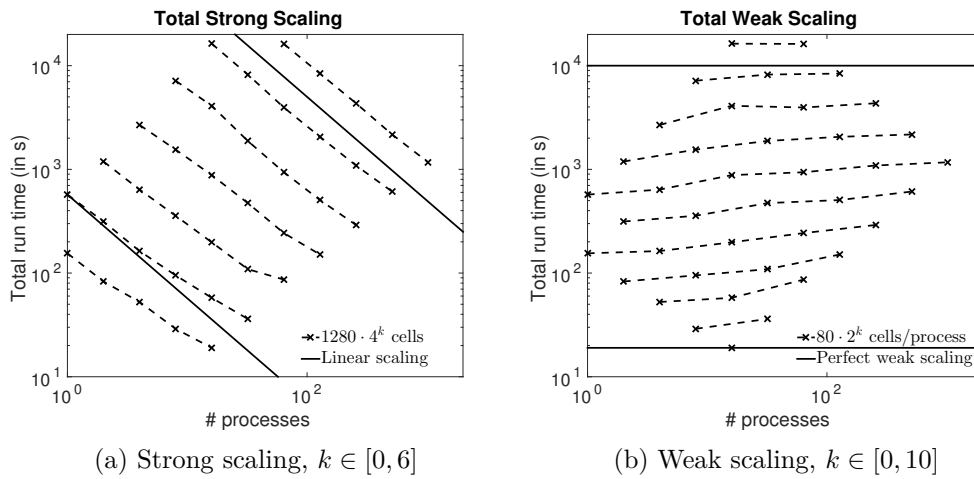


Figure 5.35: Scaling results

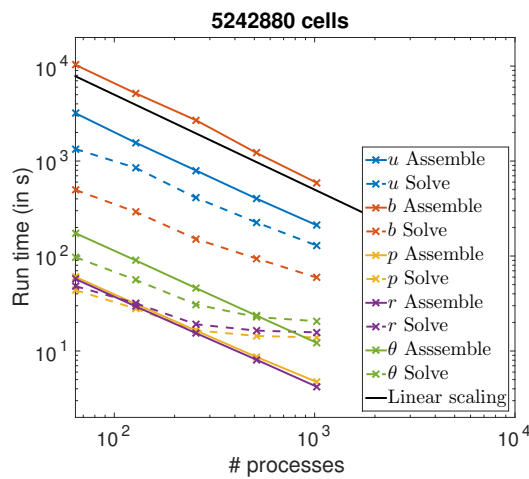


Figure 5.36: Detailed run times

6 Discussion and Conclusions

This thesis is concerned with the numerical solution of the incompressible Navier-Stokes equations for a non-isothermal, electrically conducting fluid in a rotating frame of reference. In particular, the goal has been to propose a suitable model and to investigate it both analytically and numerically. The mathematical description is based on the Oberbeck-Boussinesq approximation for the influence of temperature and for electrically conducting fluids resistive magnetohydrodynamics is considered.

With respect to the spatial discretization in Chapter 2 a finite element approach has been suggested that combines stabilizations of the incompressibility constraints with local projection stabilizes for various force terms to prevent unphysical numerical solutions and to model subgrid behavior appropriately.

The discretization in time is first considered in Chapter 4 and consists of a pressure-correction projection method based on BDF2 that we considered both in the standard incremental and the rotational incremental variant. Although projection methods have been considered for a long time (starting with Chorin [Cho69] and Temam [Tem69]), to the best of our knowledge, this is the first time that the approach has been applied to a model for non-isothermal and electrically conducting flow.

In the following, we summarize the findings with respect to theoretical (Chapter 3 and Chapter 4) and numerical investigation (Chapter 5).

6.1 Discussion of the Analytical Results

We first considered analytical results for the semi-discretized model in Chapter 3. The outcome can be summarized as follows: In most cases we were able to prove stability without any requirements on the stabilization parameters. Just for the linearized and stationary MHD model, stability depends on a proper choice of the grad-div parameters for velocity $\tau_{u,gd,M}$ and magnetic field $\tau_{b,gd,M}$ and on suitable parameter bounds for the magnetic pseudo-pressure $\tau_{r,PSPG,M}$. The reason for the different behavior for the electrically conducting case lies in the fact that for the discretized stationary problem the stability for the semi-norm not immediately extends to stability for the full $H^{curl}(\Omega)$ norm, cf. Theorem 3.4.4.

With respect to error estimates for the discretization error, always three cases can be considered.

In the first approach no particular assumption with respect to fine and coarse ansatz spaces is needed. We were able to derive semi-robust a priori estimates provided a certain local mesh restriction depending on critical non-dimensional quantities is satisfied. Essentially, we require in this case

$$\begin{aligned} Re_{u,M} &= \frac{h_M \|\mathbf{u}_h\|_{\infty,M}}{\nu} \leq \frac{1}{\sqrt{\nu}} & Pe_M &= \frac{h_M \|\mathbf{u}_h\|_{\infty,M}}{\alpha} \leq \frac{1}{\sqrt{\alpha}} \\ Re_{b,M} &= \frac{h_M \|\mathbf{b}_h\|_{\infty,M}}{\lambda} \leq \min\left\{\frac{1}{\sqrt{\lambda}}, \frac{\sqrt{\nu}}{\lambda}\right\}. \end{aligned}$$

Compared to the global condition

$$Re_{\Omega} := \frac{\|\mathbf{b}\|_{\infty} C_P}{\nu} \leq \frac{1}{\sqrt{\nu}}$$

in [MST07] not depending on the mesh width, these restrictions can be considered mild. Deriving semi-robust results in this case critically depends on the existence of a divergence-preserving interpolation operator. The construction in [GS03] is based on the inf-sup stability that we assume throughout this thesis. With respect to the interpolation errors the obtained estimates for the discretization errors are quasi-optimal for the LPS errors. In this approach the mesh width restrictions with respect to velocity and temperature can be circumvented by a modified estimate of the convective terms at the price of assuming $\mathbf{u}_h \in L^{\infty}(t_0, T; L^{\infty}(\Omega))$. This latter assumption might be removed by using bootstrapping techniques as considered in [GT99; AGN05].

With respect to the stabilization parameters there are upper and lower bounds for the fluid grad-div parameter suggesting for a feasible parameter design $\tau_{u,gd,M} \equiv \tau_{u,gd,0}$. Furthermore, the magnetic grad-div parameter and the PSPG parameter for the magnetic pseudo-pressure have in this analysis to be chosen as $\tau_{b,gd,M} \sim \lambda h_M^2$, $\tau_{r,PSPG,M} \sim 1/\lambda$. With respect to the LPS parameters there is no lower bound meaning that they do not contribute to the rate of convergence.

In a second approach special choices of fine and coarse spaces satisfying a compatibility condition are considered. This allows to avoid the mesh width restriction without additional assumptions for the discrete solutions. In this case a lower bound for the LPS parameter according to

$$\tau_{u,SU,M} \geq h_M^2, \quad \tau_{\theta,SU,M} \geq h_M^2, \quad \tilde{\tau}_{u,Lor,M} \geq h_M^2, \quad \tau_{b,Ind,M} \geq h_M^2$$

is needed (for results with respect to the Oberbeck-Boussinesq model alone in this setting refer to [Dal15]). The bounds on the grad-div parameters remain the same.

The third approach then aims to extend the second approach to obtain superconvergent estimates for the discretization error provided the viscosities are smaller than the mesh

width. This can be achieved using a much more restrictive choice of fine and coarse ansatz spaces and a clear design for the LPS parameters. In particular, local projection plays a major role in obtaining the discretization error estimates.

With respect to the “directional-do-nothing conditions” we observed that apart from an additional term in the Gronwall constant the error estimates do not change compared to homogeneous Dirichlet conditions. In particular, we were able to derive stability and quasi-optimal results for a suitable model of outflow boundary conditions.

For the fully discretized equations, we considered different approaches in [AD15]. In particular, we considered what restrictions arise when trying to extend spatial discretization results to the fully discretized case or discretization results for the temporal approximation to the fully discretized case. While both of these approaches are possible, we observed severe restrictions and suboptimal convergence results.

Finally, in [ADL15b] we were able to achieve quasi-optimal and semi-robust error estimates for the fully discretized Navier-Stokes equations. In comparison to the results in Chapter 3 even quasi-optimal results with respect to the $L^2(\Omega)$ were obtained. Chapter 4 aimed to transfer these estimates to the fully coupled set of equations. The analysis in this section combines ideas from the semi-discretization with ideas from [Gue99]. In particular, a proper estimate of the convective terms plays an important role in order to avoid time step size restriction like $\Delta t \leq \nu^3$ that would appear in a naive approach. In conjunction with problem suited interpolation operators, we were able to derive semi-robust estimates that are quasi-optimal with respect to the LPS errors with respect to temporal and spatial approximation. The coupling between velocity and magnetic field prevents the derivation of quasi-optimal results for the $L^2(\Omega)$ errors with respect to spatial discretization. However, for the Oberbeck-Boussinesq alone quasi-optimality in space can be achieved and we assume that the results from [AD15] with respect to temporal discretization can be extended to that model.

The necessary assumptions with respect to stabilization parameters and temporal and spatial resolution are similar to those in the first approach for the semi-discretization.

Although for the fully discretized a slightly different stabilization model for the magnetic field has been chosen, grad-div stabilization still proves to be essential for obtaining semi-robust results. In particular, we are able to neglect PSPG stabilization for the pseudo-pressure and choose the grad-div parameter $\tau_{b,gd,M}$ in the order of unity. For obtaining convergence results, LPS stabilizations can again be neglected. On the other hand, the analysis allows for a wide range for stabilization parameters that allow to control behavior of the numerical solution beyond convergence considerations.

With respect to mesh size restriction and LPS error estimates the coupling between magnetic field and velocity still requires a sufficiently fine mesh according to

$$Re_{b,M} \lesssim \frac{1}{\sqrt{\lambda}}, \quad Re_{u,M} \lesssim \frac{\sqrt{\lambda}}{\nu}.$$

and time step size restriction according to $\Delta t \lesssim \min\{h, \lambda\}$. Compared to a time step size restriction like $\Delta t \leq \nu^3$ this is still mild and comparable to results one would obtain without an improved error estimate for the convective terms. Although the $L^2(\Omega)$ error estimates require an even stricter bound for the LPS parameters, this need is never observed in the numerical results.

6.2 Discussion of the Numerical Results

In Chapter 5 we validated the analytical results and considered a suitable parameter design for different types of flow. We started with academic test cases that do not show any complex behavior but merely served for numerical validation for isothermal and isolating fluids. In accordance with the analytical results we observed that in these cases the total error essentially depends on the grad-div parameter. In particular, a constant grad-div parameter is crucial for semi-robust error estimates even in case the velocity vanishes. With respect to LPS stabilization we did not observe any significant influence. The obtained rates of convergence were in agreement with the analytical expectations. However, in none of these cases we observed any influence of a mesh width restriction.

In Section 5.1.4 with the Blasius profile the first example that exhibits instabilities due to arising boundary layers. We observed that grad-div stabilization is not sufficient to remove the spurious oscillations in front of the obstacle. With global refinement a rather fine mesh is needed to remove these spurious modes. However, with the help of the LPS-SU model these unphysical modes can be removed on rather coarse meshes. Another possibility is to use a problem-adapted mesh that is only refined near the obstacle. In this case mesh diffusivity is sufficient to remove the spurious modes, but additional SU stabilization does not harm either.

For investigating the behavior of LPS-SU stabilization as subgrid model for turbulent flow we considered in Section 5.1.5 the Taylor-Green vortex. In accordance with the expectations we observed that grad-div stabilization alone is not able to produce sufficiently dissipation to model the scaling of the energy spectrum correctly. Choosing the LPS-SU parameter as $\tau_{u,SU,M} = h_M/\mathbf{u}_h$ improved this behavior much and we observed results

similar to those of a Smagorinsky model. Therefore, we conclude that at least for simple types of turbulent flow the LPS-SU stabilization may serve as implicit LES model. Due to the fact that the LPS-SU acts in flow direction it might well be that for flow with a clear direction such as a turbulent channel results could be even better. This is subject to future research.

For non-isothermal flow, we started again with a prescribed reference solution that models a temperature peak moving through the domain and hitting a wall where $\mathbf{u} \cdot \mathbf{n} > 0$ and Dirichlet boundary conditions are prescribed. Similar to the analytical test cases for isothermal fluids we obtained for all choices of α and β the theoretical rates of convergence. However, in case of small α spurious oscillations occur that spread across the whole domain. Surprisingly, for $\mathbb{Q}_2/\mathbb{Q}_1$ elements a LPS-SU stabilization for the temperature does not show any significant influence. If the velocity ansatz space is enriched by bubble functions, the stabilization suddenly shows effect and diminishes the oscillations considerably.

A much more complex example is the Rayleigh-Bénard convection that we considered in Section 5.2.2. In all considered cases grad-div stabilization on anisotropically refined meshes is sufficient to reproduce DNS results from the literature. LPS SU stabilization for velocity or temperature improved the results only in case of isotropically refined meshes that were not problem-adapted. For the rotating case nearly no influence of the Coriolis stabilization could be observed.

For electrically conducting fluids two examples have been considered in Section 4.2. For the case of a solution with reduced regularity we observe that, in agreement with the considerations in 4.2, the parameter design derived in Chapter 4 for smooth solutions does not lead to convergence, but PSPG plays a major role. On the other hand, with the parameter design that is also suited for solutions of reduced regularity from Section 5.3 convergence results are obtained although still unphysical oscillations in the solution can be observed. In the second example the expulsion of the magnetic field by an electrically conducting fluid has been considered. In comparison to the singular solution it turned out that in this case grad-div stabilization for the magnetic field is crucial to obtain physically sensible solutions. As long as the magnetic diffusivity is sufficiently big, no additional LPS stabilization is needed. This changes as $\lambda = 10^{-4}$ is approached. Suddenly unphysical oscillations appear due to the developing sharp inner boundary layer. Adding LPS stabilization for the Lorentz coupling with a parameter in the order of magnitude cures this behavior considerably and convincing results for down to $\lambda = 10^{-5}$ are obtained. In contrast to the Blasius flow example it turns out that adaptive mesh refinement in this case is not sufficient, but additional LPS stabilization is still needed. Nevertheless, refining not globally is extremely beneficial for this example as numerical errors are confined to a rather small part of the domain.

In the last numerical problem we considered exemplarily the performance of the numerical solver that has been developed by the author for conducting the various numerical experiments in this thesis and the related publications. We observe good parallel scaling results for at least 1024 processes.

6.3 Conclusions

In this thesis we considered fully discretized model for non-isothermal, electrically conducting in compressible flow in a rotating frame of reference. For the spatial discretization we used a finite element methods and stabilizations for the incompressibility constraints, convective terms and force terms in the Navier-Stokes, Fourier and induction equation to circumvent numerical instabilities. For the discretization in time a projection pressure-correction approach based on BDF2 was considered that allows to solve for each quantity (velocity, kinematic pressure, magnetic field, magnetic pseudo-pressure and temperature) separately instead of solving for all quantities at the same time. With respect to efficiency such an approach appears useful especially due to the fact that good numerical solving strategies for each of the resulting smaller problems are known. In particular, we could validate good scaling results for the author's implementation.

With respect to analytical investigations results the semi-discrete and fully-discretized analysis draw a consistent picture: Using inf-sup stable ansatz spaces for the velocity and the kinematic pressure just grad-div stabilization is necessary to obtain quasi-optimal and semi-robust estimates for the discretization error. Unless certain compatibility conditions are considered, local projection stabilizations do not improve the rate of convergence of the considered scheme. For the magnetic field and the magnetic pseudo-pressure on the other hand no inf-sup stability is assumed in the semi-discrete analysis and hence an additional PSPG stabilization is necessary. Considering inf-sup stable pairs as in the fully discretized case, this stabilization can be neglected for sufficiently smooth solutions. Due to the fact that the continuous magnetic pseudo-pressure vanishes in this case, grad-div stabilization for the magnetic field can also be neglected with respect to quasi-optimal error estimates. This behavior is confirmed in the numerical examples: For academic examples neither the local projection stabilizations nor the PSPG stabilization or the magnetic grad-div stabilization are crucial. Just grad-div stabilization for the velocity has to be used in order to obtain quasi-robust results. On the other hand, for more complex flow with inner shear or boundary layers or turbulent flow applying local projection stabilizations is crucial to remove numerical instabilities. In summary, local projection stabilization (almost) never harms but is beneficial in many cases. In order to obtain best results a problem-adapted mesh in combination with grad-div and local projection stabilization in the order of unity one is recommended.

In case of solution for the magnetic field with reduced regularity, PSPG stabilization turns out to be crucial while all the other stabilization are not. In particular, convergence can only be achieved if the grad-div stabilization parameter for the magnetic field is sufficiently small. This can be verified analytically and numerically.

6.4 Outlook

Although the used error indicator based on the gradient jumps across element faces produced in all cases suitable indications for refinement, an a posteriori estimator for the suggested model could be interesting. Some indication on how to do this for splitting algorithms are given in [SLL12].

In [GMS05] Guermond et al. investigated outflow boundary conditions with respect to convergence behavior in time for splitting algorithms. It would be interesting to extend the analysis for the presented model as well, in particular with respect to the DDN condition. Furthermore, a higher order time discretization as recently suggested in [GM15] or adaptive time step sizes could be considered.

With respect to numerical results, we observed fairly broad results. However, the application to even more complex problems would be interesting to test the limits of this approach.

Problem-adapted meshes often require anisotropic meshes and it should be possible to extend the analysis to this case based on the consideration of Thomas Apel in [Ape99].

Bibliography

- [ABL15] D. Arndt, M. Braack, and G. Lube, “Finite elements for the Navier-Stokes problem with outflow condition”, in *Proceedings ENUMATH 2015*, submitted, 2015.
- [AD15] D. Arndt and H. Dallmann, “Error Estimates for the Fully Discretized Incompressible Navier-Stokes Problem with LPS Stabilization”, Institute for Numerical and Applied Mathematics, Tech. Rep., 2015, Nr. 2015-08.
- [ADL15a] D. Arndt, H. Dallmann, and G. Lube, “Local projection FEM stabilization for the time-dependent incompressible Navier–Stokes problem”, *Numerical Methods for Partial Differential Equations*, vol. 31, no. 4, pp. 1224–1250, 2015.
- [ADL15b] ———, “Quasi-Optimal Error Estimates for the Fully Discretized Stabilized Incompressible Navier-Stokes Problem”, *ESAIM: Mathematical Modelling and Numerical Analysis*, 2015, under review.
- [AGN05] B. Ayuso, B. García-Archilla, and J. Novo, “The Postprocessed Mixed Finite-Element Method for the Navier–Stokes Equations”, *SIAM Journal on Numerical Analysis*, vol. 43, no. 3, pp. 1091–1111, 2005.
- [AL15] D. Arndt and G. Lube, “FEM with Local Projection Stabilization for Incompressible Flows in Rotating Frames”, NAM-Preprint, 2015.
- [AM15] D. Arndt and M. Maier, *deal.II - step-45 tutorial program*, 2015. [Online]. Available: https://www.dealii.org/developer/doxygen/deal.II/step_45.html.
- [Ape99] T. Apel, *Anisotropic Finite Elements: Local Estimates and Applications*, ser. Advances in Numerical Mathematics. Stuttgart: Teubner, 1999, ISBN: 3-519-02744-5.
- [BC07] S. Badia and R. Codina, “Convergence analysis of the FEM approximation of the first order projection method for incompressible flows with and without the inf-sup condition”, *Numerische Mathematik*, vol. 107, no. 4, pp. 533–557, 2007.

- [BC12] S. Badia and R. Codina, “A nodal-based finite element approximation of the Maxwell problem suitable for singular solutions”, *SIAM Journal on Numerical Analysis*, vol. 50, no. 2, pp. 398–417, 2012.
- [BES10] J. Bailon-Cuba, M. Emran, and J. Schumacher, “Aspect ratio dependence of heat transfer and large-scale flow in turbulent convection”, *Journal of Fluid Mechanics*, vol. 655, pp. 152–173, 2010.
- [BHH+15] W. Bangerth, T. Heister, L. Heltai, G. Kanschat, M. Kronbichler, M. Maier, B. Turcksin, and T. D. Young, “The deal.II Library, Version 8.2”, *Archive of Numerical Software*, vol. 3, 2015.
- [BHK07] W. Bangerth, R. Hartmann, and G. Kanschat, “deal.II – a general purpose object oriented finite element library”, *ACM Transactions on Mathematical Software*, vol. 33, no. 4, pp. 24/1–24/27, 2007.
- [BMO+83] M. Brachet, D. Meiron, S. Orszag, B. Nickel, R. Morf, and U. Frisch, “Small-scale structure of the Taylor–Green vortex”, *Journal of Fluid Mechanics*, vol. 130, pp. 411–452, 1983.
- [BMZ14] M. Braack, P. B. Mucha, and W. M. Zajackowski, “Directional do-nothing condition for the Navier-Stokes equations”, *Journal of Computational Mathematics*, vol. 32, no. 5, pp. 507–521, 2014.
- [Bou03] J. Boussinesq, *Théorie analytique de la chaleur: mise en harmonie avec la thermodynamique et avec la théorie mécanique de la lumière*. Gauthier-Villars, 1903, vol. 2.
- [Bra15] M. Braack, “Outflow conditions for the Navier-Stokes equations with skew-symmetric formulation of the convective term”, in *Boundary and Interior Layers, Computational and Asymptotic Methods - BAIL 2014*, P. Knobloch, Ed., ser. Lecture Notes in Computational Science and Engineering, vol. 108, Springer International Publishing, 2015. DOI: [10.1007/978-3-319-25727-3](https://doi.org/10.1007/978-3-319-25727-3).
- [CBCP15] O. Colomés, S. Badia, R. Codina, and J. Principe, “Assessment of variational multiscale models for the large eddy simulation of turbulent incompressible flows”, *Computer Methods in Applied Mechanics and Engineering*, vol. 285, pp. 32–63, 2015.
- [CD02] M. Costabel and M. Dauge, “Weighted regularization of Maxwell equations in polyhedral domains”, *Numerische Mathematik*, vol. 93, no. 2, pp. 239–277, 2002.
- [Cha13] S. Chandrasekhar, *Hydrodynamic and hydromagnetic stability*. Courier Corporation, 2013.

- [Cho69] A. Chorin, “On the convergence of discrete approximations to the Navier-Stokes equations”, *Mathematics of Computation*, vol. 23, no. 106, pp. 341–353, 1969.
- [Cos91] M. Costabel, “A coercive bilinear form for Maxwell’s equations”, *Journal of mathematical analysis and applications*, vol. 157, no. 2, pp. 527–541, 1991.
- [Cou95] W. Couzy, “Spectral element discretization of the unsteady Navier-Stokes Equations and its iterative solution on parallel computers”, PhD thesis, EPFL Lausanne, 1995. [Online]. Available: http://infoscience.epfl.ch/record/31858/files/EPFL_TH1380.pdf.
- [DA15] H. Dallmann and D. Arndt, “Stabilized Finite Element Methods for the Oberbeck-Boussinesq Model”, *Journal of Scientific Computing*, 2015, in revision.
- [DAL15] H. Dallmann, D. Arndt, and G. Lube, “Local projection stabilization for the Oseen problem”, *IMA Journal of Numerical Analysis*, 2015. DOI: [10.1093/imanum/drv032](https://doi.org/10.1093/imanum/drv032).
- [Dal15] H. Dallmann, “Finite Element Methods with Local Projection Stabilization for Thermally Coupled Incompressible Flow”, PhD thesis, Georg-August Universität Göttingen, 2015.
- [Dav01] P. A. Davidson, *An introduction to magnetohydrodynamics*. Cambridge university press, 2001, vol. 25.
- [FN09] E. Feireisl and A. Novotny, *Singular limits in thermodynamics of viscous fluids*. Springer Science & Business Media, 2009.
- [GL00] S. Grossmann and D. Lohse, “Scaling in thermal convection: a unifying theory”, *Journal of Fluid Mechanics*, vol. 407, pp. 27–56, 2000.
- [GM15] J.-L. Guermond and P. Mineev, “High-Order Time Stepping for the Incompressible Navier–Stokes Equations”, *SIAM Journal on Scientific Computing*, vol. 37, no. 6, A2656–A2681, 2015.
- [GMS05] J.-L. Guermond, P. Mineev, and J. Shen, “Error analysis of pressure-correction schemes for the time-dependent Stokes equations with open boundary conditions”, *SIAM Journal on Numerical Analysis*, vol. 43, no. 1, pp. 239–258, 2005.
- [GMS06] —, “An overview of projection methods for incompressible flows”, *Computer Methods in Applied Mechanics and Engineering*, vol. 195, no. 44, pp. 6011–6045, 2006.
- [GS03] V. Girault and L. Scott, “A quasi-local interpolation operator preserving the discrete divergence”, *Calcolo*, vol. 40, no. 1, pp. 1–19, 2003.

- [GS04] J.-L. Guermond and J. Shen, “On the error estimates for the rotational pressure-correction projection methods”, *Mathematics of Computation*, vol. 73, no. 248, pp. 1719–1737, 2004.
- [GT99] B. García-Archilla and E. S. Titi, “Postprocessing the Galerkin method: The finite-element case”, *SIAM Journal on Numerical Analysis*, vol. 37, no. 2, pp. 470–499, 1999.
- [Gue99] J.-L. Guermond, “Un résultat de convergence d’ordre deux en temps pour l’approximation des équations de Navier–Stokes par une technique de projection incrémentale”, *ESAIM: Mathematical Modelling and Numerical Analysis*, vol. 33, no. 01, pp. 169–189, 1999.
- [Haz02] C. Hazard, “Numerical simulation of corner singularities: a paradox in Maxwell-like problems”, *Comptes Rendus Mécanique*, vol. 330, no. 1, pp. 57–68, 2002.
- [Hec12] F. Hecht, “New development in FreeFem++”, *Journal of Numerical Mathematics*, vol. 20, no. 3-4, pp. 251–266, 2012.
- [How38] L. Howarth, “On the solution of the laminar boundary layer equations”, in *Proceedings of the Royal Society of London A: Mathematical, Physical and Engineering Sciences*, The Royal Society, vol. 164, 1938, pp. 547–579.
- [HRT96] J. Heywood, R. Rannacher, and S. Turek, “Artificial boundaries and flux and pressure conditions for the incompressible Navier-Stokes equations”, *Int. J. Numer. Meth. Fluids.*, vol. 22, pp. 325–352, 1996.
- [JJLR13] E. Jenkins, V. John, A. Linke, and L. Rebholz, “On the parameter choice in grad-div stabilization for incompressible flow problems”, *Advances in Computational Mathematics*, 2013.
- [Joh12] V. John, *Large eddy simulation of turbulent incompressible flows: Analytical and numerical results for a class of LES models*. Springer Science & Business Media, 2012, vol. 34.
- [KBG15] G. Kooij, M. Botchev, and B. Geurts, “Direct numerical simulation of Nusselt number scaling in rotating Rayleigh–Bénard convection”, *International Journal of Heat and Fluid Flow*, vol. 55, pp. 26–33, 2015.
- [LAD15] G. Lube, D. Arndt, and H. Dallmann, “Understanding the limits of inf-sup stable Galerkin-FEM for incompressible flows”, in *Boundary and Interior Layers, Computational and Asymptotic Methods - BAIL 2014*, P. Knobloch, Ed., ser. Lecture Notes in Computational Science and Engineering, vol. 108, Springer International Publishing, 2015. DOI: [10.1007/978-3-319-25727-3](https://doi.org/10.1007/978-3-319-25727-3).

- [Lin14] A. Linke, “On the role of the Helmholtz decomposition in mixed methods for incompressible flows and a new variational crime”, *Computer Methods in Applied Mechanics and Engineering*, vol. 268, pp. 782–800, 2014.
- [Mof78] H. K. Moffatt, *Field Generation in Electrically Conducting Fluids*. Cambridge University Press, Cambridge, London, New York, Melbourne, 1978.
- [Mon03] P. Monk, *Finite element methods for Maxwell’s equations*. Oxford University Press, 2003.
- [MST07] G. Matthies, P. Skrzypacz, and L. Tobiska, “A unified convergence analysis for local projection stabilisations applied to the Oseen problem”, *ESAIM-Mathematical Modelling and Numerical Analysis*, vol. 41, no. 4, pp. 713–742, 2007.
- [MT15] G. Matthies and L. Tobiska, “Local projection type stabilization applied to inf-sup stable discretizations of the Oseen problem”, *IMA Journal of Numerical Analysis*, vol. 35, no. 1, pp. 239–269, 2015.
- [Obe79] A. Oberbeck, “Über die Wärmeleitung der Flüssigkeiten bei Berücksichtigung der Strömungen infolge von Temperaturdifferenzen”, *Annalen der Physik*, vol. 243, no. 6, pp. 271–292, 1879.
- [Pop00] S. Pope, *Turbulent flows*. Cambridge University Press, 2000.
- [RST08] H.-G. Roos, M. Stynes, and L. Tobiska, *Robust numerical methods for singularly perturbed differential equations: Convection-diffusion-reaction and flow problems*. Springer Science & Business Media, 2008, vol. 24.
- [Sag06] P. Sagaut, *Large eddy simulation for incompressible flows: An introduction*. Springer Science & Business Media, 2006.
- [She96] J. Shen, “On error estimates of the projection methods for the Navier-Stokes equations: second-order schemes”, *Mathematics of Computation of the American Mathematical Society*, vol. 65, no. 215, pp. 1039–1065, 1996.
- [SLL12] K. Selim, A. Logg, and M. G. Larson, “An adaptive finite element splitting method for the incompressible Navier–Stokes equations”, *Computer Methods in Applied Mechanics and Engineering*, vol. 209, pp. 54–65, 2012.
- [Tem69] R. Temam, “Sur l’approximation de la solution des équations de Navier-Stokes par la méthode des pas fractionnaires (II)”, *Archive for Rational Mechanics and Analysis*, vol. 33, no. 5, pp. 377–385, 1969.
- [TMV96] L. Timmermans, P. Mineev, and F. Van De Vosse, “An approximate projection scheme for incompressible flow using spectral elements”, *International journal for numerical methods in fluids*, vol. 22, no. 7, pp. 673–688, 1996.

- [Wac15] B. Wacker, “Stabilisierte Lagrange Finite-Elemente im Elektromagnetismus und in der inkompressiblen Magnetohydrodynamik”, PhD thesis, Georg-August Universität Göttingen, 2015.
- [WAL15] B. Wacker, D. Arndt, and G. Lube, “Nodal-based Finite Element Methods with Local Projection Stabilization for Linearized Incompressible Magneto-hydrodynamics”, *Computer Methods in Applied Mechanics and Engineering*, 2015, accepted for publication. DOI: [10.1016/j.cma.2016.01.004](https://doi.org/10.1016/j.cma.2016.01.004).
- [WSW12] S. Wagner, O. Shishkina, and C. Wagner, “Boundary layers and wind in cylindrical Rayleigh–Bénard cells”, *Journal of Fluid Mechanics*, vol. 697, pp. 336–366, 2012.

Curriculum Vitae

Daniel Arndt

University of Göttingen

Institute for Numerical and Applied Mathematics

Lotzestr. 16-18, D-37083 Göttingen, Germany

Phone: +49 551-39 4531
E-Mail: d.arndt@math.uni-goettingen.de
Homepage: <http://num/math.uni-goettingen.de/~d.arndt/>
Born: January 18th, 1988 in Hildesheim, Germany
Nationality: German

Education

04/2013 - now Ph.D. student in GAUSS at the University of Göttingen
10/2011 - 03/2013 Master of Science at the University of Göttingen,
passed with distinction,
“Augmented Taylor-Hood Elements for Incompressible Flow”
10/2008 - 09/2011 Bachelor of Science at the University of Göttingen,
passed with distinction,
“Ein adaptives Mehrschritt-IMEX-Verfahren”
07/1998 - 06/2007 Gymnasium Josephinum in Hildesheim, Abitur
07/1994 - 06/1998 St. Martinusschule in Himmelsthür, Primary School

Professional Experience

10/2013 - now Research Assistant, University of Göttingen
04/2011 - 09/2013 Student and Teaching Assistant, University of Göttingen
08/2012 - 10/2012 JSC Guest Student Programme 2012, Forschungszentrum Jülich

Presentations at Conferences

- 05/08/2015 *Application to Coupled Flow Problems*
deal.II Workshop 2015
- 27/02/2015 *Suitability of LPS for laminar and turbulent flow*
VMS 2015
- 24/07/2014 *Projection Methods for Rotating Flow*
ECFD VI 2014
- 20/08/2013 *$Q_k + Q_0$ -Elements in Incompressible Flows*
deal.II Workshop 2013
- 14/06/2013 *Augmented Taylor-Hood Elements for Incompressible Flow*
MAFELAP 2013

Publications

- [ABL15] D. Arndt, M. Braack, and G. Lube, “Finite elements for the Navier-Stokes problem with outflow condition”, in *Proceedings ENUMATH 2015*, submitted, 2015.
- [AD15] D. Arndt and H. Dallmann, “Error Estimates for the Fully Discretized Incompressible Navier-Stokes Problem with LPS Stabilization”, Institute for Numerical and Applied Mathematics, Tech. Rep., 2015, Nr. 2015-08.
- [ADL15a] D. Arndt, H. Dallmann, and G. Lube, “Local projection FEM stabilization for the time-dependent incompressible Navier–Stokes problem”, *Numerical Methods for Partial Differential Equations*, vol. 31, no. 4, pp. 1224–1250, 2015.
- [ADL15b] —, “Quasi-Optimal Error Estimates for the Fully Discretized Stabilized Incompressible Navier-Stokes Problem”, *ESAIM: Mathematical Modelling and Numerical Analysis*, 2015, under review.
- [AL15] D. Arndt and G. Lube, “FEM with Local Projection Stabilization for Incompressible Flows in Rotating Frames”, NAM-Preprint, 2015.
- [Arn12] D. Arndt, “Design and Implementation of an Experimental Finite Element Solver”, *JSC Guest Student Programme on Scientific Computing*, pp. 83–93, 2012.
- [DA15] H. Dallmann and D. Arndt, “Stabilized Finite Element Methods for the Oberbeck-Boussinesq Model”, *Journal of Scientific Computing*, 2015, in revision.

- [DAL15] H. Dallmann, D. Arndt, and G. Lube, “Local projection stabilization for the Oseen problem”, *IMA Journal of Numerical Analysis*, 2015. DOI: [10.1093/imanum/drv032](https://doi.org/10.1093/imanum/drv032).
- [LAD15] G. Lube, D. Arndt, and H. Dallmann, “Understanding the limits of inf-sup stable Galerkin-FEM for incompressible flows”, in *Boundary and Interior Layers, Computational and Asymptotic Methods - BAIL 2014*, P. Knobloch, Ed., ser. Lecture Notes in Computational Science and Engineering, vol. 108, Springer International Publishing, 2015. DOI: [10.1007/978-3-319-25727-3](https://doi.org/10.1007/978-3-319-25727-3).
- [WAL15] B. Wacker, D. Arndt, and G. Lube, “Nodal-based Finite Element Methods with Local Projection Stabilization for Linearized Incompressible Magneto-hydrodynamics”, *Computer Methods in Applied Mechanics and Engineering*, 2015, accepted for publication. DOI: [10.1016/j.cma.2016.01.004](https://doi.org/10.1016/j.cma.2016.01.004).